CODATA Recommended Values of the Fundamental Physical Constants: 2014*

Peter J. Mohr,[a] David B. Newell,[b] and Barry N. Taylor[c]
National Institute of Standards and Technology, Gaithersburg, Maryland 20899-8420, USA

(Received 28 April 2016; accepted 6 September 2016; published online 22 November 2016)

This paper gives the 2014 self-consistent set of values of the constants and conversion factors of physics and chemistry recommended by the Committee on Data for Science and Technology (CODATA). These values are based on a least-squares adjustment that takes into account all data available up to 31 December 2014. Details of the data selection and methodology of the adjustment are described. The recommended values may also be found at http://physics.nist.gov/constants. © *2016 AIP Publishing LLC for the National Institute of Standards and Technology.* [http://dx.doi.org/10.1063/1.4954402]

CONTENTS

*This review is being published simultaneously by Reviews of Modern Physics.

This report was prepared by the authors under the auspices of the CODATA Task Group on Fundamental Constants. The members of the task group are F. Cabiati, Istituto Nazionale di Ricerca Metrologica, Italy; J. Fischer, Physikalisch-Technische Bundesanstalt, Germany; J. Flowers (deceased), National Physical Laboratory, United Kingdom; K. Fujii, National Metrology Institute of Japan, Japan; S. G. Karshenboim, Pulkovo Observatory, Russian Federation and Max-Planck-Institut für Quantenoptik, Germany; E. de Mirandés, Bureau international des poids et mesures; P. J. Mohr, National Institute of Standards and Technology, United States of America; D. B. Newell, National Institute of Standards and Technology, United States of America; F. Nez, Laboratoire Kastler-Brossel, France; K. Pachucki, University of Warsaw, Poland; T. J. Quinn, Bureau international des poids et mesures; C. Thomas, Bureau international des poids et mesures; B. N. Taylor, National Institute of Standards and Technology, United States of America; B. M. Wood, National Research Council, Canada; and Z. Zhang, National Institute of Metrology, People's Republic of China.

[a]mohr@nist.gov
[b]dnewell@nist.gov
[c]barry.taylor@nist.gov

RIGHTSLINK

List of Tables

RIGHTSLINK

List of Figures

RIGHTSLINK

I. Introduction

This report describes work carried out under the auspices of the Task Group on Fundamental Constants, one of several task groups of the Committee on Data for Science and Technology (CODATA) founded in 1966 as an interdisciplinary committee of the International Council for Science (ICSU). It gives a detailed account of the 2014 CODATA multivariate least-squares adjustment of the values of the constants as well as the resulting 2014 set of over 300 self-consistent recommended values. The cutoff date for new data to be considered for possible inclusion in the 2014 adjustment was at the close of 31 December 2014, and the new set of values first became available on 25 June 2015 at http://physics.nist.gov/constants, part of the website of the Fundamental Constants Data Center of the National Institute of Standards and Technology (NIST), Gaithersburg, Maryland, USA.

A. Background

The compilation of a carefully reviewed set of values of the fundamental constants of physics and chemistry arguably began over 85 years ago with the paper of Birge (1929). In 1969, 40 years after the publication of Birge's paper, the CODATA Task Group on Fundamental Constants was established for the following purpose: to periodically provide the scientific and technological communities with a self-consistent set of internationally recommended values of the basic constants and conversion factors of physics and chemistry based on all the data available at a given point in time. The Task Group first met this responsibility with its 1973 multivariate least-squares adjustment of the values of the constants (Cohen and Taylor, 1973), which was followed 13 years later by the 1986 adjustment (Cohen and Taylor, 1987). Starting with its third adjustment in 1998 the Task Group has carried them out every 4 years; if the 1998 adjustment is counted as the first of the new 4-year cycle, the 2014 adjustment described in this report is the 5th of the cycle. Throughout this article we refer to the detailed reports describing the 1998, 2002, 2006, 2010, and 2014 adjustments, or sometimes the adjustments themselves, as CODATA-*XX*, where *XX* is 98, 02, 06, 10, or 14 (Mohr and Taylor, 2000, 2005; Mohr, Taylor, and Newell, 2008a, 2008b, 2012a, 2012b).

To help keep this report to a reasonable length, our data review focuses on the new results that became available between the 31 December 2010 and 31 December 2014 closing dates of the 2010 and 2014 adjustments (in this paper the term "past 4 years" means this time interval); our previous reports should be consulted for discussions of the older data. Indeed, only new data are given both in the text where they are first discussed and in the summary tables in Sec. XIII; data that have been considered for inclusion in one or more past adjustments are given only in those summary tables. Further, extensive descriptions of new experiments and theoretical calculations are generally omitted; comments are made on only their most relevant features.

Readers should also consult the earlier reports for discussions of the motivation for, and underlying philosophy of, CODATA adjustments, the treatment of numerical calculations and uncertainties, etc. With regard to uncertainties, as in past adjustments they are always given as "standard uncertainties," that is, 1 standard deviation estimates, either in the unit of the quantity being considered and thus absolute, or as a relative standard uncertainty, denoted u_r. As an aid to the reader, included near the end of this report is a comprehensive list of symbols and abbreviations.

Because of its importance, we do once again state that, as a working principle, the validity of the physical theory underlying the 2014 adjustment is assumed. This includes, as in previous adjustments, special and general relativity, quantum mechanics, quantum electrodynamics (QED), the standard model of particle physics, including *CPT* invariance, and for all practical purposes the exactness of the relations $K_J = 2e/h$ and $R_K = h/e^2$, where K_J and R_K are the Josephson and von Klitzing constants, respectively, and e is the elementary charge and h is the Planck constant.

There continues to be no observed time variation of the values of the constants relevant to the data used in adjustments carried out in our current era. Indeed, a recent summary based on frequency ratio measurements of various transitions in different atomic systems carried out over a number of years in several different laboratories gives $-0.7(2.1) \times 10^{-17}$ per year as the constraint on the time variation of the fine-structure constant α and $-0.2(1.1) \times 10^{-16}$ per year for the proton-to-electron mass ratio m_p/m_e (Godun *et al.*, 2014).

In general, a result considered for possible inclusion in a CODATA adjustment is identified by the institution where the work was primarily carried out and by the last two digits of the year in which it was published in an archival journal. Even if a result is labeled with a "15" identifier, it can be safely assumed that it was available by the 31 December 2014 closing date for new data. A new result was considered to have met this date if published, or if the Task Group received a preprint describing the work by that date and it had already been, or was

RIGHTSLINK

about to be, submitted for publication. However, this closing date does not apply to clarifying information requested from authors. The name of an institution is always given in full together with its abbreviation when first used, but for the convenience of the reader the abbreviations and full institutional names are also included in the aforementioned comprehensive list of symbols and abbreviations near the end of this report.

B. Highlights of the CODATA 2014 adjustment

We summarize here the most significant advances made, or lack thereof, in our knowledge of the values of the fundamental constants in the past 4 years and, where appropriate, their impact. The multivariate least-squares methodology employed in the four previous adjustments is employed in the 2014 adjustment but in this case with $N = 141$ items of input data, $M = 74$ variables or unknowns, and $\nu = N - M = 67$ degrees of freedom. The chi square statistic is $\chi^2 = 50.4$ with probability $p(50.4|67) = 0.93$ and the Birge ratio is $R_B = \sqrt{50.4/67} = 0.87$. This adjustment includes data for the Newtonian constant of gravitation G, although it is independent of the other constants.

1. Planck constant h, elementary charge e, Boltzmann constant k, Avogadro constant N_A, and the redefinition of the SI

It is planned that at its meeting in the fall of 2018, the 26th General Conference on Weights and Measures (CGPM) will adopt a resolution to revise the International System of Units (SI). This new SI, as it is sometimes called, will be defined by assigning exact values to the following seven defining constants: the ground-state hyperfine-splitting frequency of the ^{133}Cs atom $\Delta\nu_{Cs}$, the speed of light in vacuum c, the Planck constant h, the elementary charge e, the Boltzmann constant k, the Avogadro constant N_A, and the luminous efficacy of monochromatic radiation of frequency 540 THz, K_{cd}. As a result of the significant advances made since CODATA-10 in watt-balance measurements of h, x-ray-crystal-density (XRCD) measurements of N_A using silicon spheres composed of highly enriched silicon, and acoustic-gas-thermometry (AGT) measurements of the molar gas constant, the relative standard uncertainties of the four constants h, e, k, and N_A have been reduced (respectively, in parts in 10^8) from 4.4, 2.2, 91, and 4.4 in CODATA-10 to 1.2, 0.61, 57, and 1.2, in CODATA-14. (The defining constants $\Delta\nu_{Cs}$, c, and K_{cd} will retain their present values.)

This is a truly major development, because these uncertainties are now sufficiently small that the adoption of the new SI by the 26th CGPM is expected. It has been made possible to a large extent by the resolution of the disagreement between different watt-balance measurements of h and the disagreement of the value of h inferred from the XRCD value of N_A with one of the watt-balance values. These disagreements led the Task Group to increase the initial assigned uncertainties of the 2010 data that contributed to the determination of h by a factor of 2. Further, the reduction in the relative uncertainty of k from 9.1×10^{-7} to 5.7×10^{-7} is in large part a consequence of three new AGT determinations of the molar gas constant with relative uncertainties (in parts in 10^6) of 0.9, 1.0, and 1.4. The significant reductions in the uncertainties of h, e, k, and N_A have also led to the reduction of the uncertainties of many other constants and conversion factors.

The values of the constants to be adopted by the CGPM for the redefinition will be based on a special least-squares adjustment carried out by the Task Group during the summer of 2017. Data for this adjustment must be described in a paper that has been published or accepted for publication by 1 July 2017.

2. Relative atomic mass of the electron A_r(e)

The relative standard uncertainty of the 2014 recommended value of $A_r(e)$ is 2.9×10^{-11}, nearly 14 times smaller than that of the 2010 recommended value. It is based on extremely accurate measurements, using a specially designed triple Penning trap, of the ratio of the electron spin-precession (or spin-flip) frequency in hydrogenic carbon and silicon ions to the cyclotron frequency of the ions, together with the theory of the electron bound-state g-factor in the ions. The uncertainties of the measurements are so small that the data used to obtain the CODATA-10 value of $A_r(e)$ are no longer competitive and are excluded from the 2014 adjustment. Thus, there is no discussion of antiprotonic helium in this report. The new value of $A_r(e)$ will eliminate a potentially significant source of uncertainty in obtaining the fine-structure constant from anticipated high-accuracy atom-recoil measurements of h/m for an atom of mass m.

3. Proton magnetic moment in units of the nuclear magneton μ_p/μ_N

The CODATA-10 recommended value of the magnetic moment of the proton in nuclear magnetons μ_p/μ_N, where $\mu_N = e\hbar/2m_p$ and m_p is the proton mass, has a relative standard uncertainty of 8.2×10^{-9} and is calculated from other measured constants including the electron to proton mass ratio. However, because of the development of a unique double Penning trap similar to the triple Penning trap mentioned in the previous section, for the first time a value of μ_p/μ_N from direct measurements of the spin-flip and cyclotron frequencies of a single proton with an uncertainty of 3.3×10^{-9} has become available. As a consequence, the uncertainty of the 2014 recommended value is 3.0×10^{-9}, which is 2.7 times smaller than that of the 2010 value, and similar reductions in the uncertainties of other constants that depend on the μ_p/μ_N result.

4. Fine-structure constant α

Improved numerical calculations of the 8th- and 10th-order mass-independent coefficients of the theoretical expression for the electron magnetic-moment anomaly a_e have allowed full advantage to be taken of the 2.4×10^{-10} relative standard uncertainty of the experimental value of a_e for the determination of the fine-structure constant; the relative uncertainty of the 2014 recommended value of α is 2.3×10^{-10} compared with 3.2×10^{-10} for the CODATA-10 value. However, because of the somewhat unexpected large size of the 10th-order coefficient, the 2014 recommended value of α is fractionally smaller than the CODATA-10 value by 4.7 parts in 10^{10}.

RIGHTSLINK

5. Relative atomic masses

A new atomic mass evaluation, called AME2012, was completed and published by the Atomic Mass Data Center (now transferred from France to China), and its recommended values are generally used for the various relative atomic masses required for the 2014 adjustment, including that for the neutron. Because AME2012 is a self-consistent evaluation based on data included in CODATA-10, those data are neither discussed nor included in CODATA-14. However, two new, highly precise pairs of cyclotron frequency ratios relevant to the determination of the masses of the deuteron, triton, and helion (nucleus of the ^{3}He atom) were reported after the completion of AME2012 and are included in this adjustment. Yet, because the values of the relative atomic mass of ^{3}He implied by the relevant ratio in each pair disagree, the initial uncertainty of each of these ratios is multiplied by 2.8 to reduce the inconsistency to an acceptable level.

6. Newtonian constant of gravitation G

Three new values of G obtained by different methods have become available for CODATA-14 with relative standard uncertainties of 1.9×10^{-5}, 2.4×10^{-5}, and 15×10^{-5}, respectively, but have not resolved the considerable disagreements that have existed among the measurements of G for the past 20 years. These inconsistencies led the Task Group to apply an expansion factor of 14 to the initial uncertainty of each of the 11 values available for the 2010 adjustment and to adopt their weighted mean with its relative uncertainty of 12×10^{-5} as the 2010 recommended value. The expansion factor 14 was chosen so that the smallest and largest values would differ from the recommended value by about twice its uncertainty. For the 2014 adjustment the Task Group has decided that its usual practice in such cases, which is to choose an expansion factor that reduces the normalized residual of each datum to less than 2, should be followed instead. Thus an expansion factor of 6.3 is chosen and the weighted mean of the 14 values with its relative uncertainty 4.7×10^{-5} is adopted as the 2014 recommended value. Because of the three new values of G, the 2014 recommended value is larger than the 2010 value by 3.6 parts in 10^5.

7. Proton radius r_p and theory of the muon magnetic-moment anomaly a_μ

The very precise value of the root-mean-square charge radius of the proton r_p obtained from spectroscopic measurements of a Lamb-shift transition frequency in the muonic hydrogen atom μ-p was omitted from CODATA-10 because of its significant disagreement with the value from electron-proton elastic scattering and from spectroscopic measurements of hydrogen and deuterium. Although the originally measured Lamb-shift frequency has been reevaluated, the result from a second frequency that gives a value of r_p consistent with the first has been reported, and improvements were made to the theory required to extract r_p from the Lamb-shift frequencies, the disagreement persists. The Task group has, therefore, decided to omit the muonic hydrogen result for r_p from the 2014 adjustment.

Similarly, because the value of the muon magnetic-moment anomaly a_μ(th) predicted by the theoretical expression for the anomaly significantly disagreed with the value obtained from a seminal experiment at Brookhaven National Laboratory, USA, the theory was omitted from CODATA-10. Even though much effort has been devoted in the past 4 years to improving the theory, the disagreement and concerns about the theory remain. Thus the Task Group has also decided not to employ the theory of a_μ in the 2014 adjustment.

C. Outline of the paper

Some constants that have exact values in the International System of Units (SI) (BIPM, 2006), which is the unit system used in all CODATA adjustments, are recalled in Sec. II. Sections III through XII discuss the input data with an emphasis on the new results that have become available during the past 4 years. As discussed in Appendix E of CODATA-98, in a least-squares analysis of the values of the constants, the numerical data, both experimental and theoretical, also called observational data or input data, are expressed as functions of a set of independent variables or unknowns called adjusted constants. The functions themselves are called observational equations, and the least-squares methodology yields best estimates of the adjusted constants in the least-squares sense. Basically, the methodology provides the best estimate of each adjusted constant by automatically taking into account all possible ways its value can be determined from the input data. The best values of other constants are calculated from the best values of the adjusted constants.

The analysis of the input data is discussed in Sec. XIII. It is carried out by directly comparing measured values of the same quantity, by comparing measured values of different quantities through inferred values of α, h, and k, and by carrying out least-squares calculations. These investigations are the basis for the selection of the final input data used to determine the adjusted constants, and hence the entire 2014 CODATA set of recommended values.

Section XIV provides, in several tables, the set of over 300 CODATA-14 recommended values of the basic constants and conversion factors of physics and chemistry, including the covariance matrix of a selected group of constants. The report concludes with Sec. XV, which includes a comparison of a representative subset of 2014 recommended values with their 2010 counterparts, comments on some of the implications of CODATA-14 for metrology and physics, and some suggestions for future work, both experimental and theoretical, that could advance our knowledge of the values of the fundamental constants.

II. Special Quantities and Units

Table I gives the values of a number of exactly known constants of interest. The speed of light in vacuum c is exact as a consequence of the definition of the meter in the SI and the magnetic constant (vacuum permeability) μ_0 is exact because of the SI definition of the ampere (BIPM, 2006). Thus the electric constant (vacuum permittivity) $\epsilon_0 = 1/\mu_0 c^2$ is also exact. The molar mass of carbon 12, $M(^{12}\mathrm{C})$, is exact as a consequence of the SI definition of the mole, as is the molar

RIGHTSLINK

TABLE I. Some exact quantities relevant to the 2014 adjustment

Quantity	Symbol	Value
Speed of light in vacuum	c, c_0	299 792 458 $\mathrm{m\,s^{-1}}$
Magnetic constant	μ_0	$4\pi \times 10^{-7}$ $\mathrm{N\,A^{-2}} = 12.566\,370\,614\ldots \times 10^{-7}$ $\mathrm{N\,A^{-2}}$
Electric constant	ϵ_0	$(\mu_0 c^2)^{-1} = 8.854\,187\,817\ldots \times 10^{-12}$ $\mathrm{F\,m^{-1}}$
Molar mass of ^{12}C	$M(^{12}\mathrm{C})$	12×10^{-3} $\mathrm{kg\,mol^{-1}}$
Molar mass constant	M_u	$M(^{12}\mathrm{C})/12 = 10^{-3}$ $\mathrm{kg\,mol^{-1}}$
Relative atomic mass of ^{12}C	$A_r(^{12}\mathrm{C})$	12
Conventional value of Josephson constant	K_{J-90}	483 597.9 $\mathrm{GHz\,V^{-1}}$
Conventional value of von Klitzing constant	R_{K-90}	25 812.807 Ω

mass constant $M_u = M(^{12}\mathrm{C})/12$. By definition, the relative atomic mass of the carbon 12 atom $A_r(^{12}\mathrm{C}) = 12$ is exact. The quantities K_{J-90} and R_{K-90} are the exact, conventional values of the Josephson and von Klitzing constants adopted by the International Committee for Weights and Measures (CIPM) in 1989 for worldwide use starting 1 January 1990 for measurements of electrical quantities using the Josephson and quantum-Hall effects (BIPM, 2006). Quantities measured in terms of these conventional values are labeled with a subscript 90.

III. Relative Atomic Masses

The relative atomic masses of some particles and ions are used in the least-squares adjustment. These values are extracted from measured atom and ion masses by calculating the effect of the bound-electron masses and the binding energies, as discussed in the following sections.

A. Relative atomic masses of atoms

Results from the periodic atomic mass evaluations (AMEs) carried out by the Atomic Mass Data Center (AMDC), Centre de Spectrométrie Nucléaire et de Spectrométrie de Masse (CSNSM), Orsay, France, have long been used as input data in CODATA adjustments. Indeed, results from AME2003, the most recent evaluation at the time, were employed in the 2006 and 2010 CODATA adjustments. In 2008 a memorandum between the Institute of Modern Physics, Chinese Academy of Sciences (IMP), in Lanzhou, PRC, and CSNSM was signed that initiated the transfer of the AMDC from CSNMS to IMP. The transfer was concluded in 2013 after the completion of AME2012, which supersedes its immediate predecessor, AME2003. The results of the 2012 evaluation, which was a collaborative effort between IMP and CSNSM, are published (Audi *et al.*, 2012; Wang *et al.*, 2012) and are also available on the AMDC website at http://amdc.impcas.ac.cn/evaluation/data2012/ame.html.

The AME2012 relative atomic mass values of interest for the 2014 adjustment are given in Table II; additional digits were supplied in 2014 to the Task Group by M. Wang of the AMDC to reduce rounding errors. However, the AME2012 values for $A_r(^2\mathrm{H})$ and $A_r(^3\mathrm{He})$ from which the relative atomic masses of the deuteron d and helion h (nucleus of the ^{3}He atom) can be obtained are not included. This is because the AME2012 value for $A_r(^2\mathrm{H})$ is based to a large extent on preliminary data from the group of R. Van Dyck at the University of Washington (UWash), Seattle, Washington, USA, that have been superseded by recently reported final data (Zafonte and Van Dyck, 2015). Further, the AME2012 value for $A_r(^3\mathrm{He})$ is partially based on very old UWash data that have been superseded by newer and much more accurate data given in the paper that reports the final $A_r(^2\mathrm{H})$-related data. These new UWash results are discussed below in Sec. III.C together with new measurements related to the triton and helion from the group of E. Myers at Florida State University (FSU), Tallahassee, Florida, USA.

TABLE II. Relative atomic masses used in the least-squares adjustment as given in the 2012 atomic mass evaluation and the defined value for ^{12}C

Atom	Relative atomic mass $A_r(X)$	Relative standard uncertainty u_r
n	1.008 664 915 85(49)	4.9×10^{-10}
^{1}H	1.007 825 032 231(93)	9.3×10^{-11}
^{3}H	3.016 049 2779(24)	7.9×10^{-10}
^{4}He	4.002 603 254 130(63)	1.6×10^{-11}
^{12}C	12	(exact)
^{28}Si	27.976 926 534 65(44)	1.6×10^{-11}
^{36}Ar	35.967 545 105(29)	8.1×10^{-10}
^{38}Ar	37.962 732 11(21)	5.5×10^{-9}
^{40}Ar	39.962 383 1237(24)	6.0×10^{-11}
^{87}Rb	86.909 180 5319(65)	7.5×10^{-11}
^{107}Ag	106.905 0916(26)	2.4×10^{-8}
^{109}Ag	108.904 7553(14)	1.3×10^{-8}
^{133}Cs	132.905 451 9615(86)	6.5×10^{-11}

The covariances among the AME2012 values in Table II are taken from the file covariance.covar available at the AMDC website indicated above and are used as appropriate in our calculations. They are given in the form of correlation coefficients in Table XIX, Sec. XIII.

In the four previous CODATA adjustments, the recommended value of the relative atomic mass of the neutron $A_r(\mathrm{n})$ was based on the wavelength of the 2.2 MeV γ ray emitted in the reaction $\mathrm{n} + \mathrm{p} \rightarrow \mathrm{d} + \gamma$ as measured in the 1990s. In the current adjustment the AME2012 value in Table II is taken as an input datum and $A_r(\mathrm{n})$ as an adjusted constant, because the 2012 AME is an internally consistent evaluation that uses all available data relevant to the determination of $A_r(\mathrm{n})$.

B. Relative atomic masses of ions and nuclei

The mass of an atom or ion is the sum of the nuclear mass and the masses of the electrons minus the mass equivalent of the binding energy of the electrons. To produce an ion X^{n+} with net charge ne, the energy needed to remove n electrons from the neutral atom is the sum of the electron ionization energies $E_I(X^{i+})$:

$$\Delta E_B(X^{n+}) = \sum_{i=0}^{n-1} E_I(X^{i+}) . \quad (1)$$

RIGHTSLINK

For a neutral atom we have $n = 0$ and $\Delta E_B(X^{0+}) = 0$; for a bare nucleus $n = Z$. In the 2014 least-squares adjustment, we use the removal energies expressed in terms of wave numbers given by

$$\Delta E_B(^1H^+)/hc = 1.096\,787\,717\,4307(10) \times 10^7 \text{ m}^{-1},$$
$$\Delta E_B(^3H^+)/hc = 1.097\,185\,4390(13) \times 10^7 \text{ m}^{-1},$$
$$\Delta E_B(^4He^{2+})/hc = 6.372\,195\,4487(28) \times 10^7 \text{ m}^{-1},$$
$$\Delta E_B(^{12}C^{6+})/hc = 83.083\,962(72) \times 10^7 \text{ m}^{-1},$$
$$\Delta E_B(^{12}C^{5+})/hc = 43.563\,345(72) \times 10^7 \text{ m}^{-1},$$
$$\Delta E_B(^{28}Si^{13+})/hc = 420.608(19) \times 10^7 \text{ m}^{-1},$$

which follow from the data tabulated in Table III. In that table, the value for ^{1}H is from Jentschura *et al.* (2005), and the rest are from the NIST online Atomic Spectra Database (ASD, 2015), in which the value for ^{3}H is based on a calculation by Kotochigova (2006). In general, because of the relatively small size of the uncertainties of the ionization energies given in Table III, any correlations that might exist among them or with other data used in the CODATA-14 are unimportant. However, there is a significant covariance between the two carbon binding-energy values, because a large part of the uncertainty is due to common uncertainties in the lower ionization stages; this yields the correlation coefficient

$$r[E_B(^{12}C^{5+})/hc, E_B(^{12}C^{6+})/hc] = 0.999\,976. \quad (2)$$

The relative atomic mass of an atom, its ions, the relative atomic mass of the electron, and the relative atomic mass equivalent of the binding energy of the removed electrons are related according to

$$A_r(X) = A_r(X^{n+}) + nA_r(e) - \frac{\Delta E_B(X^{n+})}{m_u c^2}, \quad (3)$$

where $m_u = m(^{12}C)/12$ is the unified atomic mass constant. Equation (3) is the form of the observational equation for $A_r(X)$ used in previous adjustments with $A_r(X^{n+})$ and $A_r(e)$ taken as adjusted constants with the binding-energy term taken to be exact. However, because for ^{28}Si the binding-energy uncertainty is not negligible compared with the uncertainty of $A_r(^{28}Si)$, we adopt the following new approach for treating binding energies in all calculations in which they are required. Since the binding energies are known most accurately in terms of their wave number equivalents, and since $R_\infty = \alpha^2 m_e c/2h$ and $m_e = A_r(e)m_u$, one can write

$$\frac{\Delta E_B(X^{n+})}{m_u c^2} = \frac{\alpha^2 A_r(e)}{2R_\infty} \frac{\Delta E_B(X^{n+})}{hc}. \quad (4)$$

Thus, in the 2014 adjustment we replace the binding-energy term in Eq. (3) by Eq. (4) and take the binding energy $\Delta E_B(X^{n+})/hc$ as both an input datum and an adjusted constant, thereby obtaining a new form of observational equation for $A_r(X)$ expressed solely in terms of adjusted constants. Although this requires taking binding energies as input data rather than exactly known quantities, it allows all binding-energy uncertainties and covariances to be properly taken into account. This new form of observational equation is used for the AME2012 values of $A_r(^1H)$, $A_r(^3H)$, $A_r(^4He)$, and $A_r(^{28}Si)$, and the new way of treating binding energies is used in the observational equations for a number of frequency ratios; see Table XXIV, Sec. XIII.

TABLE III. Ionization energies for ^{1}H, ^{3}H, ^{3}He, ^{4}He, ^{12}C, and ^{28}Si

Atom or ion	E_I/hc (10^7 m^{-1})
^{1}H	1.096 787 717 4307(10)
^{3}H	1.097 185 4390(13)
^{3}He$^+$	4.388 891 936(3)
^{4}He	1.983 106 6637(20)
^{4}He$^+$	4.389 088 785(2)
^{12}C	0.908 2045(10)
^{12}C$^+$	1.966 74(7)
^{12}C^{2+}	3.862 410(10)
^{12}C^{3+}	5.201 758(15)
^{12}C^{4+}	31.624 233(2)
^{12}C^{5+}	39.520 616 7(5)
^{28}Si	0.657 4776(25)
^{28}Si$^+$	1.318 381(3)
^{28}Si^{2+}	2.701 393(7)
^{28}Si^{3+}	3.640 931(6)
^{28}Si^{4+}	13.450 7(2)
^{28}Si^{5+}	16.5559(15)
^{28}Si^{6+}	19.867(8)
^{28}Si^{7+}	24.492(14)
^{28}Si^{8+}	28.318(6)
^{28}Si^{9+}	32.374(3)
^{28}Si^{10+}	38.406(6)
^{28}Si^{11+}	42.216 3(6)
^{28}Si^{12+}	196.610 389(16)

C. Relative atomic mass of the deuteron, triton, and helion

We consider here the recent data of the University of Washington and Florida State University groups mentioned above relevant to the determination of the relative atomic masses of the nuclei of the ^{2}H (deuterium D), ^{3}H (tritium T), and ^{3}He atoms, or deuteron d, triton t, and helion h, respectively. The data are cyclotron frequency ratios obtained in a Penning trap and it is these ratios that are used as input data in the adjustment to determine $A_r(d)$, $A_r(t)$, and $A_r(h)$, which are taken as adjusted constants. These new results became available shortly before the 31 December 2014 closing date of the adjustment and were published in 2015.

The UWash group reports as the final values of the cyclotron frequency ratios d and h to $^{12}C^{6+}$ (Zafonte and Van Dyck, 2015)

$$\frac{\omega_c(d)}{\omega_c(^{12}C^{6+})} = 0.992\,996\,654\,743(20) \quad [2.0 \times 10^{-11}], \quad (5)$$

$$\frac{\omega_c(h)}{\omega_c(^{12}C^{6+})} = 1.326\,365\,862\,193(19) \quad [1.4 \times 10^{-11}]. \quad (6)$$

These ratios are correlated because of the image charge correction applied to each; based on the published uncertainty budgets and additional information provided by Van Dyck (2015), their correlation coefficient is

RIGHTSLINK

$$r[\omega_c(d)/\omega_c(^{12}C^{6+}), \omega_c(h)/\omega_c(C^{6+})] = 0.306. \quad (7)$$

The relative atomic masses follow from the relations

$$\frac{\omega_c(d)}{\omega_c(^{12}C^{6+})} = \frac{A_r(^{12}C^{6+})}{6A_r(d)}, \quad (8)$$

$$\frac{\omega_c(h)}{\omega_c(^{12}C^{6+})} = \frac{A_r(^{12}C^{6+})}{3A_r(h)}, \quad (9)$$

where

$$A_r(^{12}C^{6+}) = 12 - 6A_r(e) + \frac{\Delta E_B(^{12}C^{6+})}{m_u c^2}, \quad (10)$$

which takes into account the definition $A_r(^{12}C) = 12$.

An overview of the University of Washington Penning trap mass spectrometer (UW-PTMS), which was developed over several decades, is given by Zafonte and Van Dyck (2015); a discussion of the various experimental effects that can influence UW-PTMS cyclotron frequency measurements is given by Van Dyck, *et al.* (2006). The later paper also reports a preliminary value of $A_r(^2H)$ based on the analysis of $\omega_c(d)/\omega_c(^{12}C^{6+})$ data obtained in three early data runs. The final result of the UWash deuterium measurements given in Eq. (5) is based on 10 data runs, each of which yields one frequency ratio and lasted more than a month when the time required to check all experimental effects is included. Corrections for six significant experimental effects are applied to each of the 10 ratios before their weighted mean is calculated. The largest of these by far is that for image charge; its fractional magnitude is -245×10^{-12} for each ratio. Each correction has an uncertainty, but since the 9.9×10^{-12} relative standard uncertainty u_r of the image charge correction is the same for each ratio, it is omitted from the individual ratio uncertainties. Rather, Zafonte and Van Dyck (2015) take it into account by combining it with the uncertainty $u_r = 17.4 \times 10^{-12}$ of the weighted mean calculated without the image charge uncertainty, thereby obtaining the 20 parts in 10^{12} final uncertainty.

Although there were seven successful helion runs to determine $\omega_c(h)/\omega_c(^{12}C^{6+})$, Zafonte and Van Dyck (2015) decided to exclude runs three and four from their final analysis because they were found to contain two $^{12}C^{6+}$ ions instead of one. To avoid the problem of isolating a single $^{12}C^{6+}$ ion, they used a single $^{12}C^{5+}$ ion in the three other runs and scaled the results using the well-known values of $A_r(^{12}C^{5+})$ and $A_r(^{12}C^{6+})$ without adding any significant uncertainty to what they would have obtained if a $^{12}C^{6+}$ ion had been used. Zafonte and Van Dyck (2015) treat the five individual $\omega_c(h)/\omega_c(^{12}C^{6+})$ frequency ratios as they did the 10 $\omega_c(d)/\omega_c(^{12}C^{6+})$ ratios; the fractional image charge correction is -515×10^{-12} with $u_r = 8.9 \times 10^{-12}$, for the weighted mean of the five ratios $u_r = 11.2 \times 10^{-12}$, and for the final value $u_r = 14 \times 10^{-12}$.

The cyclotron frequency ratios of HD^+ to $^3He^+$ and to t reported by the FSU group are (Myers *et al.*, 2015)

$$\frac{\omega_c(HD^+)}{\omega_c(^3He^+)} = 0.998\,048\,085\,153(48) \quad [4.8 \times 10^{-11}], \quad (11)$$

$$\frac{\omega_c(HD^+)}{\omega_c(t)} = 0.998\,054\,687\,288(48) \quad [4.8 \times 10^{-11}]. \quad (12)$$

As for the two UWash ratios, these ratios are correlated, but in this case because of the correction to account for imbalance between the cyclotron radii of the two ions. Based on the published uncertainty budgets and additional information provided by Myers (2015), their correlation coefficient is

$$r[\omega_c(HD^+)/\omega_c(^3He^+), \omega_c(HD^+)/\omega_c(t)] = 0.875. \quad (13)$$

The relevant equations for these data are

$$\frac{\omega_c(HD^+)}{\omega_c(^3He^+)} = \frac{A_r(^3He^+)}{A_r(HD^+)}, \quad (14)$$

$$\frac{\omega_c(HD^+)}{\omega_c(t)} = \frac{A_r(t)}{A_r(HD^+)}, \quad (15)$$

where

$$A_r(^3He^+) = A_r(h) + A_r(e) - \frac{E_I(^3He^+)}{m_u c^2}, \quad (16)$$

$$E_I(^3He^+)/hc = 43\,888\,919.36(3)\ m^{-1}, \quad (17)$$

$$A_r(HD^+) = A_r(p) + A_r(d) + A_r(e) - \frac{E_I(HD^+)}{m_u c^2}, \quad (18)$$

$$E_I(HD^+)/hc = 13\,122\,468.415(6)\ m^{-1}. \quad (19)$$

The ionization wave number in Eq. (17) is from Table III, and the value in Eq. (19) is from Liu *et al.* (2010) and Sprecher *et al.* (2010).

In the FSU experiment pairs of individual ions, either HD^+ and $^3H^+$ or HD^+ and $^3He^+$, are confined at the same time in a Penning trap at 4.2 K with an applied magnetic flux density of 8.5 T. The cyclotron frequency of one ion centered in the trap in an orbit with a radius of about 45 μm is determined while the other ion is kept in an outer orbit with a radius of about 1.1 mm to reduce perturbations on the inner ion due to Coulomb interactions. The two ions are then interchanged. In a typical run lasting up to 10 h about 20 cyclotron frequency measurements are made on each ion. The temporal variation of the magnet flux density is accounted for by simultaneously fitting a fourth-order polynomial to the individual cyclotron frequencies as a function of time. In total 34 $HD^+/^3He^+$ and $HD^+/^3H^+$ runs were carried out over a 5 month period. For each frequency ratio the standard uncertainty of the mean of the individual values before correction for two systematic effects is 17×10^{-12}. The correction for cyclotron radius imbalance for each is $22(45) \times 10^{-12}$ and for the polarizability of the HD^+ ion, 94×10^{-12} with negligible uncertainty. These two uncertainty components lead to the final uncertainty for each of 48×10^{-12}.

Since the cyclotron frequencies in Eqs. (11) and (12) are both measured with reference to the same molecular ion HD^+ and there is a sizable correlation coefficient between the frequency ratio measurements, Myers *et al.* (2015) obtain a value for the ratio $\omega_c(^3H^+)/\omega_c(^3He^+)$ with only one-half the 4.8×10^{-11} uncertainty of that for either of the ratios determined with HD^+. They are thus able to deduce for the mass difference between the tritium and helium-3 atoms, $m(^3H) -$

RIGHTSLINK

$m(^3\mathrm{He}) = 1.995\,934\,(7) \times 10^{-5}$ u $= 18\,592.01\,(7)$ eV$/c^2$, which has a significantly smaller uncertainty than any other value.

The value of $A_r(^3\mathrm{He})$ deduced by Myers *et al.* (2015) from their data, 3.016 029 322 43(19), exceeds the value deduced by Zafonte and Van Dyck (2015) from their data, 3.016 029 321 675(43), by 3.9 times the standard uncertainty of their difference u_{diff} or 3.9σ. (Throughout the paper, σ as used here is the standard uncertainty u_{diff} of the difference between two values.) How this disagreement is treated in the 2014 adjustment is discussed in Sec. XIII. The THe-Trap experiment currently underway at the Max-Planck-Institut für Kernphysik (MPIK), Heidelberg, Germany, the aim of which is to determine the ratio $A_r(^3\mathrm{H})/A_r(^3\mathrm{He})$ in order to determine the Q-value of tritium, may clarify the cause of this discrepancy; see Diehl *et al.* (2011) and Streubel *et al.* (2014).

IV. Atomic Transition Frequencies

Comparison of theory and experiment for transition frequencies in hydrogen, deuterium, and muonic hydrogen provides information on the Rydberg constant, and on the charge radii of the proton and deuteron. Hyperfine splittings in hydrogen and fine-structure splittings in helium are also briefly considered.

A. Hydrogen and deuterium transition frequencies, the Rydberg constant R_∞, and the proton and deuteron charge radii r_p, r_d

The transition frequency between states i and i' with energy levels E_i and $E_{i'}$ in hydrogen or deuterium is given by

$$h\nu_{ii'} = E_{i'} - E_i\,. \tag{20}$$

The energy levels are given by

$$E_i = -\frac{\alpha^2 m_e c^2}{2n_i^2}(1+\delta_i) = -\frac{R_\infty hc}{n_i^2}(1+\delta_i)\,, \tag{21}$$

where R_∞ is the Rydberg constant, n_i is the principal quantum number of state i, and δ_i, where $|\delta_i| \ll 1$, contains the details of the theory of the energy level.

1. Theory of hydrogen and deuterium energy levels

References to the original works are generally omitted; these may be found in earlier detailed CODATA reports, in Eides, Grotch, and Shelyuto (2001, 2007), and in Sapirstein and Yennie (1990). Uncertainties we assign to the individual theoretical contributions are categorized as either correlated or uncorrelated. Correlations we consider arise in two forms. One case is where the uncertainties are mainly of the form C/n_i^3, where C is the same for all states with the same L and j. Such uncertainties are denoted by u_0, while the uncorrelated uncertainties are denoted by u_i. The other correlations we consider are those between corrections for the same state in different isotopes, where the correction only depends on the mass of the isotope. Calculations of the uncertainties of the energy levels and the corresponding correlation coefficients are described in Sec. IV.A.1.l.

a. Dirac eigenvalue. The Dirac eigenvalue for an electron bound to a stationary point nucleus is

$$E_D = f(n,j)m_e c^2\,, \tag{22}$$

where

$$f(n,j) = \left[1 + \frac{(Z\alpha)^2}{(n-\delta)^2}\right]^{-1/2}, \tag{23}$$

n and j are the principal and total angular-momentum quantum numbers of the bound state,

$$\delta = j + \frac{1}{2} - \left[\left(j+\frac{1}{2}\right)^2 - (Z\alpha)^2\right]^{1/2}, \tag{24}$$

and Z is the charge number of the nucleus.

For a nucleus with a finite mass m_N, we have

$$E_M(\mathrm{H}) = Mc^2 + [f(n,j)-1]m_r c^2 - [f(n,j)-1]^2\frac{m_r^2 c^2}{2M} + \frac{1-\delta_{\ell 0}}{\kappa(2\ell+1)}\frac{(Z\alpha)^4 m_r^3 c^2}{2n^3 m_N^2} + \cdots \tag{25}$$

for hydrogen or

$$E_M(\mathrm{D}) = Mc^2 + [f(n,j)-1]m_r c^2 - [f(n,j)-1]^2\frac{m_r^2 c^2}{2M} + \frac{1}{\kappa(2\ell+1)}\frac{(Z\alpha)^4 m_r^3 c^2}{2n^3 m_N^2} + \cdots \tag{26}$$

for deuterium, where ℓ is the nonrelativistic orbital angular-momentum quantum number, $\delta_{\ell 0}$ is the Kronecker delta, $\kappa = (-1)^{j-\ell+1/2}(j+\frac{1}{2})$ is the angular-momentum-parity quantum number, $M = m_e + m_N$, and $m_r = m_e m_N/(m_e+m_N)$ is the reduced mass.

b. Relativistic recoil. The leading relativistic-recoil correction, to lowest order in $Z\alpha$ and all orders in m_e/m_N, is (Erickson, 1977; Sapirstein and Yennie, 1990)

$$E_S = \frac{m_r^3}{m_e^2 m_N}\frac{(Z\alpha)^5}{\pi n^3}m_e c^2 \times\left\{\frac{1}{3}\delta_{\ell 0}\ln(Z\alpha)^{-2} - \frac{8}{3}\ln k_0(n,\ell) - \frac{1}{9}\delta_{\ell 0} - \frac{7}{3}a_n - \frac{2}{m_N^2 - m_e^2}\delta_{\ell 0}\left[m_N^2\ln\left(\frac{m_e}{m_r}\right) - m_e^2\ln\left(\frac{m_N}{m_r}\right)\right]\right\}, \tag{27}$$

where

$$a_n = -2\left[\ln\left(\frac{2}{n}\right) + \sum_{i=1}^{n}\frac{1}{i} + 1 - \frac{1}{2n}\right]\delta_{\ell 0} + \frac{1-\delta_{\ell 0}}{\ell(\ell+1)(2\ell+1)}. \tag{28}$$

Values we use for the Bethe logarithms $\ln k_0(n,\ell)$ in Eqs. (27), (38), and (65) are given in Table IV.

Additional contributions to lowest order in the mass ratio and of higher order in $Z\alpha$ are

$$E_R = \frac{m_e}{m_N}\frac{(Z\alpha)^6}{n^3}m_e c^2[D_{60} + D_{72}Z\alpha\ln^2(Z\alpha)^{-2} + \cdots], \tag{29}$$

where

RIGHTSLINK

TABLE IV. Relevant values of the Bethe logarithms $\ln k_0(n, \ell)$

n	S	P	D
1	2.984 128 556		
2	2.811 769 893	−0.030 016 709	
3	2.767 663 612		
4	2.749 811 840	−0.041 954 895	−0.006 740 939
6	2.735 664 207		−0.008 147 204
8	2.730 267 261		−0.008 785 043
12			−0.009 342 954

$$D_{60} = \left(4\ln 2 - \frac{7}{2}\right)\delta_{\ell 0} + \left[3 - \frac{\ell(\ell+1)}{n^2}\right]\frac{2(1-\delta_{\ell 0})}{(4\ell^2-1)(2\ell+3)}, \tag{30}$$

$$D_{72} = -\frac{11}{60\pi}\delta_{\ell 0}. \tag{31}$$

The uncertainty in the relativistic recoil correction is taken to be

$$[0.1\delta_{\ell 0} + 0.01(1-\delta_{\ell 0})]E_{\rm R}. \tag{32}$$

Covariances follow from the $(m_e/m_N)/n^3$ scaling of the uncertainty.

c. Nuclear polarizability. For the nuclear polarizability in hydrogen, we use

$$E_{\rm P}({\rm H}) = -0.070(13)h\frac{\delta_{\ell 0}}{n^3}\ {\rm kHz}, \tag{33}$$

and for deuterium

$$E_{\rm P}({\rm D}) = -21.37(8)h\frac{\delta_{\ell 0}}{n^3}\ {\rm kHz}. \tag{34}$$

Presumably the polarizability effect is negligible for states of higher ℓ in either hydrogen or deuterium.

d. Self energy. The one-photon self energy of an electron bound to a stationary point nucleus is

$$E^{(2)}_{\rm SE} = \frac{\alpha}{\pi}\frac{(Z\alpha)^4}{n^3}F(Z\alpha)m_e c^2, \tag{35}$$

where

$$F(Z\alpha) = A_{41}\ln(Z\alpha)^{-2} + A_{40} + A_{50}(Z\alpha) + A_{62}(Z\alpha)^2\ln^2(Z\alpha)^{-2} + A_{61}(Z\alpha)^2\ln(Z\alpha)^{-2} + G_{\rm SE}(Z\alpha)(Z\alpha)^2, \tag{36}$$

with

$$A_{41} = \frac{4}{3}\delta_{\ell 0}, \tag{37}$$

$$A_{40} = -\frac{4}{3}\ln k_0(n,\ell) + \frac{10}{9}\delta_{\ell 0} - \frac{1}{2\kappa(2\ell+1)}(1-\delta_{\ell 0}), \tag{38}$$

$$A_{50} = \left(\frac{139}{32} - 2\ln 2\right)\pi\delta_{\ell 0}, \tag{39}$$

$$A_{62} = -\delta_{\ell 0}, \tag{40}$$

$$A_{61} = \left[4\left(1 + \frac{1}{2} + \cdots + \frac{1}{n}\right) + \frac{28}{3}\ln 2 - 4\ln n - \frac{601}{180} - \frac{77}{45n^2}\right]\delta_{\ell 0} + \frac{n^2-1}{n^2}\left(\frac{2}{15} + \frac{1}{3}\delta_{j\frac{1}{2}}\right)\delta_{\ell 1} + \frac{[96n^2 - 32\ell(\ell+1)](1-\delta_{\ell 0})}{3n^2(2\ell-1)(2\ell)(2\ell+1)(2\ell+2)(2\ell+3)}. \tag{41}$$

Values for $G_{\rm SE}(\alpha)$ in Eq. (36) are listed in Table V. See CODATA-10 for details. The uncertainty of the self-energy contribution to a given level is due to the uncertainty of $G_{\rm SE}(\alpha)$ listed in that table and is taken to be type u_n.

Following convention, $F(Z\alpha)$ is multiplied by the reduced-mass factor $(m_r/m_e)^3$, except the magnetic-moment term $-1/[2\kappa(2\ell+1)]$ in A_{40} which is instead multiplied by the factor $(m_r/m_e)^2$, and the argument $(Z\alpha)^{-2}$ of the logarithms is replaced by $(m_e/m_r)(Z\alpha)^{-2}$.

e. Vacuum polarization. The stationary point nucleus second-order vacuum-polarization level shift is

$$E^{(2)}_{\rm VP} = \frac{\alpha}{\pi}\frac{(Z\alpha)^4}{n^3}H(Z\alpha)m_e c^2, \tag{42}$$

where $H(Z\alpha) = H^{(1)}(Z\alpha) + H^{(\rm R)}(Z\alpha)$,

$$H^{(1)}(Z\alpha) = V_{40} + V_{50}(Z\alpha) + V_{61}(Z\alpha)^2\ln(Z\alpha)^{-2} + G^{(1)}_{\rm VP}(Z\alpha)(Z\alpha)^2, \tag{43}$$

$$H^{(\rm R)}(Z\alpha) = G^{(\rm R)}_{\rm VP}(Z\alpha)(Z\alpha)^2, \tag{44}$$

with

$$V_{40} = -\frac{4}{15}\delta_{\ell 0}, \quad V_{50} = \frac{5}{48}\pi\delta_{\ell 0}, \quad V_{61} = -\frac{2}{15}\delta_{\ell 0}. \tag{45}$$

Values of $G^{(1)}_{\rm VP}(Z\alpha)$ are given in Table VI, and

TABLE V. Values of the function $G_{\rm SE}(\alpha)$

n	$S_{1/2}$	$P_{1/2}$	$P_{3/2}$	$D_{3/2}$	$D_{5/2}$
1	−30.290 240(20)				
2	−31.185 150(90)	−0.973 50(20)	−0.486 50(20)		
3	−31.047 70(90)				
4	−30.9120(40)	−1.1640(20)	−0.6090(20)		0.031 63(22)
6	−30.711(47)				0.034 17(26)
8	−30.606(47)			0.007 940(90)	0.034 84(22)
12				0.009 130(90)	0.035 12(22)

RIGHTSLINK

TABLE VI. Values of the function $G_{\rm VP}^{(1)}(\alpha)$

n	$S_{1/2}$	$P_{1/2}$	$P_{3/2}$	$D_{3/2}$	$D_{5/2}$
1	−0.618 724				
2	−0.808 872	−0.064 006	−0.014 132		
3	−0.814 530				
4	−0.806 579	−0.080 007	−0.017 666		−0.000 000
6	−0.791 450				−0.000 000
8	−0.781 197			−0.000 000	−0.000 000
12				−0.000 000	−0.000 000

$$G_{\rm VP}^{(\rm R)}(Z\alpha)=\left(\frac{19}{45}-\frac{\pi^2}{27}\right)\delta_{\ell 0}+\left(\frac{1}{16}-\frac{31\pi^2}{2880}\right)\pi(Z\alpha)\delta_{\ell 0}+\cdots. \tag{46}$$

Higher-order terms are negligible. We multiply Eq. (42) by $(m_{\rm r}/m_{\rm e})^3$ and include a factor of $(m_{\rm e}/m_{\rm r})$ in the argument of the logarithm in Eq. (43).

Vacuum polarization from $\mu^+\mu^-$ pairs is

$$E_{\mu\rm VP}^{(2)}=\frac{\alpha}{\pi}\frac{(Z\alpha)^4}{n^3}\left(-\frac{4}{15}\delta_{\ell 0}\right)\left(\frac{m_{\rm e}}{m_\mu}\right)^2\left(\frac{m_{\rm r}}{m_{\rm e}}\right)^3 m_{\rm e}c^2, \tag{47}$$

and hadronic vacuum polarization is given by

$$E_{\rm hadVP}^{(2)}=0.671(15)E_{\mu\rm VP}^{(2)}. \tag{48}$$

Uncertainties are of type u_0. The muonic and hadronic vacuum-polarization contributions are negligible for higher-ℓ states.

f. Two-photon corrections. The two-photon correction is

$$E^{(4)}=\left(\frac{\alpha}{\pi}\right)^2\frac{(Z\alpha)^4}{n^3}m_{\rm e}c^2F^{(4)}(Z\alpha), \tag{49}$$

where

$$\begin{aligned}F^{(4)}(Z\alpha)=&B_{40}+B_{50}(Z\alpha)+B_{63}(Z\alpha)^2\ln^3(Z\alpha)^{-2}\\&+B_{62}(Z\alpha)^2\ln^2(Z\alpha)^{-2}+B_{61}(Z\alpha)^2\ln(Z\alpha)^{-2}\\&+B_{60}(Z\alpha)^2+B_{72}(Z\alpha)^3\ln^2(Z\alpha)^{-2}\\&+B_{71}(Z\alpha)^3\ln(Z\alpha)^{-2}+B_{70}(Z\alpha)^3\\&+\cdots,\end{aligned} \tag{50}$$

with

$$\begin{aligned}B_{40}=&\left[\frac{3\pi^2}{2}\ln 2-\frac{10\pi^2}{27}-\frac{2179}{648}-\frac{9}{4}\zeta(3)\right]\delta_{\ell 0}\\&+\left[\frac{\pi^2\ln 2}{2}-\frac{\pi^2}{12}-\frac{197}{144}-\frac{3\zeta(3)}{4}\right]\frac{1-\delta_{\ell 0}}{\kappa(2\ell+1)},\end{aligned} \tag{51}$$

$$B_{50}=-21.554\,47(13)\delta_{\ell 0}, \tag{52}$$

$$B_{63}=-\frac{8}{27}\delta_{\ell 0}, \tag{53}$$

$$\begin{aligned}B_{62}=&\frac{16}{9}\left[\frac{71}{60}-\ln 2+\gamma+\psi(n)-\ln n-\frac{1}{n}+\frac{1}{4n^2}\right]\delta_{\ell 0}\\&+\frac{4}{27}\frac{n^2-1}{n^2}\delta_{\ell 1},\end{aligned} \tag{54}$$

$$\begin{aligned}B_{61}=&\left\{\frac{413\,581}{64\,800}+\frac{4N(n\rm S)}{3}+\frac{2027\pi^2}{864}-\frac{616\ln 2}{135}-\frac{2\pi^2\ln 2}{3}\right.\\&+\frac{40\ln^2 2}{9}+\zeta(3)\\&\left.+\left(\frac{304}{135}-\frac{32\ln 2}{9}\right)\left[\frac{3}{4}+\gamma+\psi(n)-\ln n-\frac{1}{n}+\frac{1}{4n^2}\right]\right\}\delta_{\ell 0}\\&+\left[\frac{4}{3}N(n\rm P)+\frac{n^2-1}{n^2}\left(\frac{31}{405}+\frac{1}{3}\delta_{j\frac{1}{2}}-\frac{8}{27}\ln 2\right)\right]\delta_{\ell 1}.\end{aligned} \tag{55}$$

Values for B_{61} used in the adjustment are listed in Table VII. In CODATA-10, the entries for states with $\ell=1$ in the corresponding Table IX are incorrect, which had negligible effect on the results. Corrected values are listed here in Table VII. The values of $N(n\rm L)$, which appear in Eq. (54), are listed in Table VIII. The uncertainties are negligible.

Values used in the adjustment for B_{60} and $\overline{B}_{60}$ are listed in Table IX. For the S-state values, the first number in parentheses is the state-dependent uncertainty $u_n(B_{60})$, and the second number in parentheses is the state-independent uncertainty $u_0(B_{60})$ that is common to all S-state values of B_{60}. For higher-ℓ states, the notation $\overline{B}_{60}$ indicates that the number listed in the table is the value of the line center shift for the level, in contrast to the total real part of the two-photon correction. See CODATA-10 for a complete explanation. For S states, the difference between B_{60} and $\overline{B}_{60}$ is negligible compared to the uncertainty of the value of B_{60}. The uncertainties of $\overline{B}_{60}$ for higher-ℓ states are taken to be independent.

For S states, the next term B_{72} is state independent, but its value is not known. However, the state dependence of the following term is

$$\begin{aligned}\Delta B_{71}(n\rm S)=&B_{71}(n\rm S)-B_{71}(1\rm S)=\pi\left(\frac{427}{36}-\frac{16}{3}\ln 2\right)\\&\times\left[\frac{3}{4}-\frac{1}{n}+\frac{1}{4n^2}+\gamma+\psi(n)-\ln n\right],\end{aligned} \tag{56}$$

TABLE VII. Values of B_{61} used in the 2014 adjustment

n	$B_{61}(n\rm S_{1/2})$	$B_{61}(n\rm P_{1/2})$	$B_{61}(n\rm P_{3/2})$	$B_{61}(n\rm D_{3/2})$	$B_{61}(n\rm D_{5/2})$
1	48.958 590 24(1)				
2	41.062 164 31(1)	0.157 775 547(1)	−0.092 224 453(1)		
3	38.904 222(1)				
4	37.909 514(1)	0.191 192 600(1)	−0.121 307 400(1)		0.0(0)
6	36.963 391(1)				0.0(0)
8	36.504 940(1)			0.0(0)	0.0(0)
12				0.0(0)	0.0(0)

RIGHTSLINK

TABLE VIII. Values of N used in the 2014 adjustment

n	$N(n\mathrm{S})$	$N(n\mathrm{P})$
1	17.855 672 03(1)	
2	12.032 141 58(1)	0.003 300 635(1)
3	10.449 809(1)	
4	9.722 413(1)	−0.000 394 332(1)
6	9.031 832(1)	
8	8.697 639(1)	

with a relative uncertainty of 50%. We include this difference, which is listed in Table IX, along with an estimated uncertainty of $u_n(\Delta B_{71}) = \Delta B_{71}/2$.

As with the one-photon correction, the two-photon correction is multiplied by the reduced-mass factor $(m_r/m_e)^3$, except the magnetic-moment term proportional to $1/[\kappa(2\ell+1)]$ in B_{40} which is multiplied by the factor $(m_r/m_e)^2$, and the argument $(Z\alpha)^{-2}$ of the logarithms is replaced by $(m_e/m_r)(Z\alpha)^{-2}$.

g. Three-photon corrections. The three-photon contribution in powers of $Z\alpha$ is

$$E^{(6)} = \left(\frac{\alpha}{\pi}\right)^3 \frac{(Z\alpha)^4}{n^3} m_e c^2 [C_{40} + C_{50}(Z\alpha) + \cdots]. \tag{57}$$

The leading term C_{40} is

$$C_{40} = \left[-\frac{568a_4}{9} + \frac{85\zeta(5)}{24} - \frac{121\pi^2\zeta(3)}{72} - \frac{84\,071\zeta(3)}{2304} - \frac{71\ln^4 2}{27} - \frac{239\pi^2\ln^2 2}{135} + \frac{4787\pi^2\ln 2}{108} + \frac{1591\pi^4}{3240} - \frac{252\,251\pi^2}{9720} + \frac{679\,441}{93\,312}\right]\delta_{\ell 0}$$
$$+ \left[-\frac{100a_4}{3} + \frac{215\zeta(5)}{24} - \frac{83\pi^2\zeta(3)}{72} - \frac{139\zeta(3)}{18} - \frac{25\ln^4 2}{18} + \frac{25\pi^2\ln^2 2}{18} + \frac{298\pi^2\ln 2}{9} + \frac{239\pi^4}{2160} - \frac{17\,101\pi^2}{810} - \frac{28\,259}{5184}\right]\frac{1-\delta_{\ell 0}}{\kappa(2\ell+1)}, \tag{58}$$

where $a_4 = \sum_{n=1}^{\infty} 1/(2^n n^4) = 0.517\,479\,061\ldots$. Partial results for C_{50} have been calculated by Eides and Shelyuto (2004, 2007). The uncertainty is taken to be $u_0(C_{50}) = 30\delta_{\ell 0}$ and $u_n(C_{63}) = 1$, where C_{63} would be the coefficient of $(Z\alpha)^2\ln^3(Z\alpha)^{-2}$ in the square brackets in Eq. (57). The dominant effect of the finite mass of the nucleus is taken into account by multiplying the term proportional to $\delta_{\ell 0}$ by the reduced-mass factor $(m_r/m_e)^3$ and the term proportional to $1/[\kappa(2\ell+1)]$, the magnetic-moment term, by the factor $(m_r/m_e)^2$.

The contribution from four photons is expected to be negligible at the level of uncertainty of current interest.

h. Finite nuclear size. For S states the leading and next-order correction to the level shift due to the finite size of the nucleus is given by

$$E_{\mathrm{NS}} = \mathcal{E}_{\mathrm{NS}}\left\{1 - C_\eta \frac{m_r}{m_e}\frac{r_N}{\lambda\!\!\!^{-}_C} Z\alpha - \left[\ln\left(\frac{m_r}{m_e}\frac{r_N}{\lambda\!\!\!^{-}_C}\frac{Z\alpha}{n}\right) + \psi(n) + \gamma - \frac{(5n+9)(n-1)}{4n^2} - C_\theta\right](Z\alpha)^2\right\}, \tag{59}$$

where

$$\mathcal{E}_{\mathrm{NS}} = \frac{2}{3}\left(\frac{m_r}{m_e}\right)^3 \frac{(Z\alpha)^2}{n^3} m_e c^2 \left(\frac{Z\alpha r_N}{\lambda\!\!\!^{-}_C}\right)^2, \tag{60}$$

r_N is the bound-state root-mean-square (rms) charge radius of the nucleus, $\lambda\!\!\!^{-}_C$ is the Compton wavelength of the electron divided by 2π, C_η and C_θ are constants that depend on the charge distribution in the nucleus with values $C_\eta = 1.7(1)$ and $C_\theta = 0.47(4)$ for hydrogen or $C_\eta = 2.0(1)$ and $C_\theta = 0.38(4)$ for deuterium.

For the $\mathrm{P}_{1/2}$ states in hydrogen the leading term is

$$E_{\mathrm{NS}} = \mathcal{E}_{\mathrm{NS}} \frac{(Z\alpha)^2(n^2-1)}{4n^2}. \tag{61}$$

For $\mathrm{P}_{3/2}$ states and higher-ℓ states the nuclear-size contribution is negligible.

i. Nuclear-size correction to self energy and vacuum polarization. For the lowest-order self energy and vacuum polarization the correction due to the finite size of the nucleus is

TABLE IX. Values of B_{60}, $\overline{B}_{60}$, or ΔB_{71} used in the 2014 adjustment. The uncertainties of B_{60} are explained in the text.

n	$B_{60}(n\mathrm{S}_{1/2})$	$\overline{B}_{60}(n\mathrm{P}_{1/2})$	$\overline{B}_{60}(n\mathrm{P}_{3/2})$	$\overline{B}_{60}(n\mathrm{D}_{3/2})$	$\overline{B}_{60}(n\mathrm{D}_{5/2})$	$\Delta B_{71}(n\mathrm{S}_{1/2})$
1	−81.3(0.3)(19.7)					
2	−66.2(0.3)(19.7)	−1.6(3)	−1.7(3)			16(8)
3	−63.0(0.6)(19.7)					22(11)
4	−61.3(0.8)(19.7)	−2.1(3)	−2.2(3)		−0.005(2)	25(12)
6	−59.3(0.8)(19.7)				−0.008(4)	28(14)
8	−58.3(2.0)(19.7)			0.015(5)	−0.009(5)	29(15)
12				0.014(7)	−0.010(7)	

RIGHTSLINK

$$E_{\rm NSE} = \left(4\ln 2 - \frac{23}{4}\right)\alpha(Z\alpha)\mathcal{E}_{\rm NS}\delta_{\ell 0}\,, \tag{62}$$

and

$$E_{\rm NVP} = \frac{3}{4}\alpha(Z\alpha)\mathcal{E}_{\rm NS}\delta_{\ell 0}\,, \tag{63}$$

respectively.

j. Radiative-recoil corrections. Corrections for radiative-recoil effects are

$$E_{\rm RR} = \frac{m_{\rm r}^3}{m_{\rm e}^2 m_{\rm N}}\frac{\alpha(Z\alpha)^5}{\pi^2 n^3} m_{\rm e}c^2\delta_{\ell 0} \times \left[6\zeta(3) - 2\pi^2\ln 2 + \frac{35\pi^2}{36} - \frac{448}{27} + \frac{2}{3}\pi(Z\alpha)\ln^2(Z\alpha)^{-2} + \cdots\right]. \tag{64}$$

The uncertainty is $(Z\alpha)\ln(Z\alpha)^{-2}$ relative to the square brackets with a factor of 10 for u_0 and 1 for u_n. Corrections for higher-ℓ states are negligible.

k. Nucleus self energy. The nucleus self energy correction for S states is

$$E_{\rm SEN} = \frac{4Z^2\alpha(Z\alpha)^4}{3\pi n^3}\frac{m_{\rm r}^3}{m_{\rm N}^2}c^2\left[\ln\left(\frac{m_{\rm N}}{m_{\rm r}(Z\alpha)^2}\right)\delta_{\ell 0} - \ln k_0(n,\ell)\right], \tag{65}$$

with an uncertainty u_0 given by Eq. (65) with the factor in the square brackets replaced by 0.5. For higher-ℓ states, the correction is negligible.

l. Total energy and uncertainty. The energy $E_X(n{\rm L}_j)$ of a level (where ${\rm L} = {\rm S}, {\rm P}, \ldots$ and $X = {\rm H}, {\rm D}$) is the sum of the various contributions listed above. Uncertainties in the fundamental constants that enter the theoretical expressions are taken into account through the formalism of the least-squares adjustment. To take uncertainties in the theory into account, a correction $\delta_X(n{\rm L}_j)$ that is zero with an uncertainty that is the rms sum of the uncertainties of the individual contributions

$$u^2[\delta_X(n{\rm L}_j)] = \sum_i [u_{0i}^2(Xn{\rm L}_j) + u_{ni}^2(Xn{\rm L}_j)], \tag{66}$$

where $u_{0i}(Xn{\rm L}_j)$ and $u_{ni}(Xn{\rm L}_j)$ are the components of uncertainty u_0 and u_n of contribution i, is added to the level. The corrections $\delta_X(n{\rm L}_j)$, which includes their uncertainties, are taken as input data in the least-squares adjustment. Covariances are taken into account by calculating all the covariances and including them in the input data for the adjustment.

Covariances of the δs for a given isotope are

$$u[\delta_X(n_1{\rm L}_j), \delta_X(n_2{\rm L}_j)] = \sum_i u_{0i}(Xn_2{\rm L}_j)u_{0i}(Xn_1{\rm L}_j)\,. \tag{67}$$

Covariances between δs for hydrogen and deuterium for states of the same n are

$$u[\delta_{\rm H}(n{\rm L}_j), \delta_{\rm D}(n{\rm L}_j)] = \sum_{i=\{i_{\rm c}\}} [u_{0i}({\rm H}n{\rm L}_j)u_{0i}({\rm D}n{\rm L}_j) + u_{ni}({\rm H}n{\rm L}_j)u_{ni}({\rm D}n{\rm L}_j)], \tag{68}$$

and for $n_1 \neq n_2$

$$u[\delta_{\rm H}(n_1{\rm L}_j), \delta_{\rm D}(n_2{\rm L}_j)] = \sum_{i=\{i_{\rm c}\}} u_{0i}({\rm H}n_1{\rm L}_j)u_{0i}({\rm D}n_2{\rm L}_j)\,, \tag{69}$$

where the summation is over the uncertainties common to hydrogen and deuterium.

Values of $u[\delta_X(n{\rm L}_j)]$ are given in Table XVI of Sec. XIII, and the non-negligible covariances of the δs are given as correlation coefficients in Table XVII.

m. Transition frequencies between levels with $n = 2$ and the fine-structure constant α. QED predictions for hydrogen transition frequencies between levels with $n = 2$ are obtained from a least-squares adjustment that does not include an experimental value for the transitions being calculated (items *A*39, *A*40.1, or *A*40.2 in Table XVI), where the constants $A_{\rm r}({\rm e})$, $A_{\rm r}({\rm p})$, $A_{\rm r}({\rm d})$, and α are assigned the 2014 values. The results are

$$\begin{aligned}
&\nu_{\rm H}(2{\rm P}_{1/2} - 2{\rm S}_{1/2}) = 1\,057\,843.7(2.1)\ {\rm kHz} \quad [2.0\times10^{-6}],\\
&\nu_{\rm H}(2{\rm S}_{1/2} - 2{\rm P}_{3/2}) = 9\,911\,197.8(2.1)\ {\rm kHz} \quad [2.1\times10^{-7}],\\
&\nu_{\rm H}(2{\rm P}_{1/2} - 2{\rm P}_{3/2}) = 10\,969\,041.530(41)\ {\rm kHz} \quad [3.7\times10^{-9}],
\end{aligned} \tag{70}$$

which are consistent with the experimental results given in Table XVI.

Data for the hydrogen and deuterium transitions yield a value for the fine-structure constant α, which follows from a least-squares adjustment that includes all the transition frequency data in Table XVI, the 2014 adjusted values of $A_{\rm r}({\rm e})$, $A_{\rm r}({\rm p})$, and $A_{\rm r}({\rm d})$, but no other input data for α. The result is

$$\alpha^{-1} = 137.035\,992(55) \quad [4.0\times10^{-7}], \tag{71}$$

and is also given in Table XX.

2. Experiments on hydrogen and deuterium

Table X gives the hydrogen and deuterium transition frequencies used to determine the Rydberg constant R_∞, items *A*26 to *A*48 in Table XVI, Sec. XIII. The only difference between this table and the corresponding Table XI in CODATA-10 is that the value for the $1{\rm S}_{1/2} - 2{\rm S}_{1/2}$ hydrogen transition frequency obtained by the group at the Max-Planck-Institut für Quantenoptik (MPQ), Garching, Germany, used in the 2010 adjustment is superseded by two new values obtained by the same group but with significantly smaller uncertainties (first two entries of Table X):

$$\nu_{\rm H}(1{\rm S}_{1/2} - 2{\rm S}_{1/2}) = 2\,466\,061\,413\,187.035(10)\ [4.2\times10^{-15}], \tag{72}$$

$$\nu_{\rm H}(1{\rm S}_{1/2} - 2{\rm S}_{1/2}) = 2\,466\,061\,413\,187.018(11)\ [4.4\times10^{-15}]. \tag{73}$$

RIGHTSLINK

TABLE X. Summary of measured transition frequencies ν considered in the present work for the determination of the Rydberg constant R_∞ (ν_H for hydrogen and ν_D for deuterium)

Authors	Laboratory[a]	Frequency interval(s)	Reported value ν/kHz	Rel. stand. uncert. u_r
Parthey *et al.* (2011)	MPQ	$\nu_H(1S_{1/2}-2S_{1/2})$	2 466 061 413 187.035(10)	4.2×10^{-15}
Matveev *et al.* (2013)	MPQ	$\nu_H(1S_{1/2}-2S_{1/2})$	2 466 061 413 187.018(11)	4.4×10^{-15}
Weitz *et al.* (1995)	MPQ	$\nu_H(2S_{1/2}-4S_{1/2})-\frac{1}{4}\nu_H(1S_{1/2}-2S_{1/2})$	4 797 338(10)	2.1×10^{-6}
		$\nu_H(2S_{1/2}-4D_{5/2})-\frac{1}{4}\nu_H(1S_{1/2}-2S_{1/2})$	6 490 144(24)	3.7×10^{-6}
		$\nu_D(2S_{1/2}-4S_{1/2})-\frac{1}{4}\nu_D(1S_{1/2}-2S_{1/2})$	4 801 693(20)	4.2×10^{-6}
		$\nu_D(2S_{1/2}-4D_{5/2})-\frac{1}{4}\nu_D(1S_{1/2}-2S_{1/2})$	6 494 841(41)	6.3×10^{-6}
Parthey *et al.* (2010)	MPQ	$\nu_D(1S_{1/2}-2S_{1/2})-\nu_H(1S_{1/2}-2S_{1/2})$	670 994 334.606(15)	2.2×10^{-11}
de Beauvoir *et al.* (1997)	LKB/SYRTE	$\nu_H(2S_{1/2}-8S_{1/2})$	770 649 350 012.0(8.6)	1.1×10^{-11}
		$\nu_H(2S_{1/2}-8D_{3/2})$	770 649 504 450.0(8.3)	1.1×10^{-11}
		$\nu_H(2S_{1/2}-8D_{5/2})$	770 649 561 584.2(6.4)	8.3×10^{-12}
		$\nu_D(2S_{1/2}-8S_{1/2})$	770 859 041 245.7(6.9)	8.9×10^{-12}
		$\nu_D(2S_{1/2}-8D_{3/2})$	770 859 195 701.8(6.3)	8.2×10^{-12}
		$\nu_D(2S_{1/2}-8D_{5/2})$	770 859 252 849.5(5.9)	7.7×10^{-12}
Schwob *et al.* (1999)	LKB/SYRTE	$\nu_H(2S_{1/2}-12D_{3/2})$	799 191 710 472.7(9.4)	1.2×10^{-11}
		$\nu_H(2S_{1/2}-12D_{5/2})$	799 191 727 403.7(7.0)	8.7×10^{-12}
		$\nu_D(2S_{1/2}-12D_{3/2})$	799 409 168 038.0(8.6)	1.1×10^{-11}
		$\nu_D(2S_{1/2}-12D_{5/2})$	799 409 184 966.8(6.8)	8.5×10^{-12}
Arnoult *et al.* (2010)	LKB	$\nu_H(1S_{1/2}-3S_{1/2})$	2 922 743 278 678(13)	4.4×10^{-12}
Bourzeix *et al.* (1996)	LKB	$\nu_H(2S_{1/2}-6S_{1/2})-\frac{1}{4}\nu_H(1S_{1/2}-3S_{1/2})$	4 197 604(21)	4.9×10^{-6}
		$\nu_H(2S_{1/2}-6D_{5/2})-\frac{1}{4}\nu_H(1S_{1/2}-3S_{1/2})$	4 699 099(10)	2.2×10^{-6}
Berkeland, Hinds, and Boshier (1995)	Yale	$\nu_H(2S_{1/2}-4P_{1/2})-\frac{1}{4}\nu_H(1S_{1/2}-2S_{1/2})$	4 664 269(15)	3.2×10^{-6}
		$\nu_H(2S_{1/2}-4P_{3/2})-\frac{1}{4}\nu_H(1S_{1/2}-2S_{1/2})$	6 035 373(10)	1.7×10^{-6}
Hagley and Pipkin (1994)	Harvard	$\nu_H(2S_{1/2}-2P_{3/2})$	9 911 200(12)	1.2×10^{-6}
Lundeen and Pipkin (1986)	Harvard	$\nu_H(2P_{1/2}-2S_{1/2})$	1 057 845.0(9.0)	8.5×10^{-6}
Newton, Andrews, and Unsworth (1979)	U. Sussex	$\nu_H(2P_{1/2}-2S_{1/2})$	1 057 862(20)	1.9×10^{-5}

[a]MPQ: Max-Planck-Institut für Quantenoptik, Garching, Germany. LKB: Laboratoire Kastler-Brossel, Paris, France. SYRTE: Systèmes de référence Temps Espace, Paris, France. Yale: Yale University, New Haven, Connecticut, USA. Harvard: Harvard University, Cambridge, Massachusetts, USA. U. Sussex: University of Sussex, Brighton, UK.

The result reported by Parthey *et al.* (2011) has a relative standard uncertainty $u_r = 4.2\times10^{-15}$, about one-third that of the value used in the 2010 adjustment. The reduction was achieved using a more stable spectroscopy laser and by reducing the uncertainties from the principal systematic effects, namely, the second-order Doppler shift and ac and dc Stark shifts.

The result reported by Matveev *et al.* (2013) has a relative standard uncertainty of 4.4×10^{-15}. In contrast to the 2011 measurement, which used an on-site transportable cesium fountain clock as the frequency reference, the 2013 measurement used the nonmovable cesium fountain clock at the Phyisikalisch-Technische Budesanstalt (PTB) in Braunschweig, Germany, by connecting the MPQ experiment in Garching to the PTB clock in Braunschweig via a 920 km fiber link. Another difference is the use of an improved detector of the Lyman-α photons emitted when the excited hydrogen atom beam is deexcited from the 2S state. The new results are consistent with each other and with that used in 2010. However, the 2011 and 2013 values are correlated, and based on the published uncertainty budgets and information provided by the researchers (Udem, 2014) the correlation coefficient is estimated to be 0.707. This correlation coefficient is included in Table XVII, Sec. XIII, together with the correlation coefficients of the other correlated frequencies in Table X as discussed in CODATA-98.

3. Nuclear radii

It follows from Eqs. (59) and (60) in Sec. IV.A.1.h that transition frequencies in hydrogen and deuterium atoms depend on the bound-state rms charge radius r_p and r_d of their respective nuclei, the proton p and deuteron d. Accurate values for these radii can be obtained if they are taken as adjusted constants in a least-squares adjustment together with experimental H and D transition frequency input data and theory. The values so determined are often referred to as the H-D spectroscopic values of r_p and r_d.

a. Electron scattering. Values of r_p and r_d are also available from electron-proton (e-p) and electron-deuteron (e-d) elastic scattering data. If these values are included as input data in an adjustment together with the H and D spectroscopic data and theory, a combined least-squares adjusted value for r_p and for r_d can be obtained. In the 2010 adjustment the value of r_d determined by Sick (2008) from an analysis of the available data on e-d elastic scattering was used as an input datum and it

RIGHTSLINK

is again used as an input datum in the 2014 adjustment. That value is $r_d = 2.130(10)$ fm.

The e-p scattering value of r_p is more problematic. Two such values were used in the 2010 adjustment: $r_p = 0.895(18)$ fm and $r_p = 0.8791(79)$ fm. The first is due to Sick (2008) based on his analysis of the data then available. The second is from a seminal experiment, described in detail by Bernauer *et al.* (2014), carried out at the Johannes Gutenberg Universität Mainz (or simply the University of Mainz), Mainz, Germany, with the Mainz microtron electron-beam accelerator MAMI. Both values are discussed in CODATA-10, as is the significant disagreement of the H-D spectroscopic and e-p scattering values of r_p with the value determined from spectroscopic measurements of the Lamb shift in muonic hydrogen. The cause of the disagreement remains unknown, and we review the current situation in the following section and in Sec. XIII.B.2.

To assist in deciding what scattering value or values of r_p to use in the 2014 adjustment, the Task Group invited a number of researchers active in the field to attend its annual meeting in November 2014. It also helped organize the Workshop on the Determination of the Fundamental Constants held in Eltville, Germany, in February 2015, the proceedings of which are published in J. Phys. Chem. Ref. Data **44**(3) (2015). A point of concern at these meetings was how best to extract r_p from the MAMI data and from the combination of the MAMI data with the remaining available data. As a result of the discussions at these meetings two pairs of knowledgeable researchers, J. Arrington and I. Sick, and J. C. Bernauer and M. O. Distler, provided the Task Group with their best estimate of r_p from all the available data. The Arrington-Sick value, $r_p = 0.879(11)$ fm, has been published (Arrington and Sick, 2015) but was initially transmitted to the Task Group as a private communication in 2015; the Bernauer-Distler value, $r_p = 0.880(11)$ fm, was also transmitted to the Task Group in 2015 as a private communication but has not been published. The two values are highly consistent even though different approaches and assumptions were used to obtain them. We therefore adopt as the e-p scattering-data input datum for r_p in the 2014 adjustment

$$r_p = 0.879(11) \quad [1.3 \times 10^{-2}] \text{ fm}, \tag{74}$$

which is the weighted mean of the two values, but the uncertainty is the average of their uncertainties since each value was based on essentially the same data.

The Task Group well recognizes that Eq. (74) is not the last word on the subject and that the topic remains one of active interest; see, for example, the papers by Kraus *et al.* (2014), Arrington (2015), Lorenz *et al.* (2015), and Sick (2015). Particularly noteworthy is the paper by Lee, Arrington, and Hill (2015), which did not become available until well after the 31 December closing date of the 2014 adjustment, that provides a new and improved analysis to obtain $r_p = 0.895(20)$ fm from the MAMI data, $r_p = 0.916(24)$ fm from the remaining available data but not including the MAMI data, and $r_p = 0.904(15)$ fm by combining these two values. Three recent papers by Griffioen, Carlson and Maddox (2016), Higinbotham *et al.* (2016), and Horbatsch and Hessels (2016) obtain results consistent with the smaller muonic hydrogen radius in Eq. (78). However, Bernauer and Distler (2016) point out a number of problems with the analyses in these papers.

b. Isotope shift and the deuteron-proton radius difference. From a comparison of experiment and theory for the hydrogen-deuterium isotope shift, one can extract a value for the difference of the squares of the charge radii for the deuteron and proton, based on the 2014 recommended values, given by

$$r_d^2 - r_p^2 = 3.819\,48(37) \text{ fm}^2. \tag{75}$$

The corresponding result based on the 2010 recommended values,

$$r_d^2 - r_p^2 = 3.819\,89(42) \text{ fm}^2, \tag{76}$$

differs from the current value due mainly to the change in the relative atomic mass of the electron used to evaluate the theoretical expression for the isotope shift. The electron mass appears as an overall factor as can be seen from the leading term (Jentschura *et al.*, 2011)

$$\Delta f_{1S-2S,d} - \Delta f_{1S-2S,p} \approx -\frac{3}{4} R_\infty c \left(\frac{m_e}{m_d} - \frac{m_e}{m_p} \right). \tag{77}$$

c. Muonic hydrogen. The first reported value of r_p from spectroscopic measurements of the Lamb shift in the muonic hydrogen atom μ-p obtained by the Charge Radius Experiment with Muonic Atoms (CREMA) collaboration (Pohl *et al.*, 2010) and the problem, now often called the "proton radius puzzle," that resulted from its significant disagreement with the scattering and spectroscopic values is discussed in CODATA-10. As a result of this inconsistency the Task Group decided that the initial μ-p value of r_p should be omitted from the 2010 adjustment and the 2010 recommended value should be based on only the two available e-p scattering values (see previous section) and the H-D spectroscopic data and theory. Consequently the disagreement of the μ-p value with the 2010 recommended value was 7σ and with the H-D spectroscopic value, 4.4σ.

The μ-p Lamb-shift experiment employs pulsed laser spectroscopy at a special muon beam line at the proton accelerator of the Paul Scherrer Institute (PSI), Villigen, Switzerland. Muonic atoms in the 2S state (lifetime 1 μs) are formed when muons from the beam strike a gaseous H_2 target, a 5 ns near-resonance laser pulse (tunable from 50 THz to 55 THz) induces transitions to the 2P state (lifetime 8.5 ps), the atoms decay to the 1S ground state by emitting 1.9 keV Kα x rays, and a resonance curve is obtained by counting the number of x rays as a function of laser frequency. (Because of the large electron vacuum-polarization effect in μ-p, the $2S_{1/2}$ level is far below both the $2P_{1/2}$ and $2P_{3/2}$ levels.)

The transition initially measured was $2S_{1/2}(F = 1) - 2P_{3/2}(F = 2)$ at 50 THz or 6 μm. More recently, the CREMA collaboration reported their result for the transition $2S_{1/2}(F = 0) - 2P_{3/2}(F = 1)$ at 55 THz or 5.5 μm, as well as their reevaluation of the 50 THz data (Antognini *et al.*, 2013b).

RIGHTSLINK

This reevaluation reduced the original frequency by 0.53 GHz and its uncertainty from 0.76 GHZ to 0.65 GHz. By comparison, the uncertainty of the 55 THz frequency is 1.05 GHz.

The theory that relates the muonic hydrogen Lamb-shift transition frequencies to r_p reflects the calculations and critical investigations of many researchers, and a number of issues have been resolved since the closing date of the 2010 adjustment; a detailed review is given by Antognini *et al.* (2013a). Using the theory in this paper the CREMA collaboration reports, in the same paper in which they give their two measured transition frequencies (Antognini *et al.*, 2013b), the following value as the best estimate of r_p from muonic hydrogen:

$$r_p = 0.840\,87(39)\ \text{fm}. \tag{78}$$

This may be compared with the muonic hydrogen value $r_p = 0.841\,69(66)$ fm available for consideration in the 2010 adjustment based on the $2S_{1/2}(F=1) - 2P_{3/2}(F=2)$ transition frequency before reevaluation and the theory as it existed at the time. Because the new result in Eq. (78) is smaller and has a smaller uncertainty than this value and that neither the H-D data nor theory have changed significantly, it is not surprising that the disagreement still persists and that the Task Group has decided to omit the μ-p result for r_p in the 2014 adjustment. Indeed, the disagreement of the value in Eq. (78) with the 2014 CODATA recommended value 0.8751(61) fm is 5.6σ and with the H-D spectroscopic value 0.8759(77) fm is 4.5σ.

The negative effect of including the value of r_p in Eq. (78) as an input datum in the 2014 adjustment and why the Task Group concluded that it should be excluded is discussed further in Sec. XIII.B.2. However, we do point out here the two following facts.

First, if the least-squares adjustment that leads to the value of α^{-1} given in Eq. (71) is carried out with the value in Eq. (78) included as an input datum, the result is $\alpha^{-1} = 137.035\,876(35)$ $[2.6 \times 10^{-7}]$, which differs from the 2014 recommended value by 3.5σ.

Second, Karshenboim (2014) has proposed a different approach to the calculation of the next-to-leading higher-order proton-size contribution to the theory of the muonic hydrogen Lamb shift than was used by Antognini *et al.* (2013b) to obtain the value of r_p in Eq. (78). The approach changes the value in Eq. (78) to $r_p = 0.840\,22(56)$ fm (Karshenboim, 2014), for which the disagreement with the 2014 CODATA recommended value is 5.7σ and with the H-D spectroscopic value is 4.6σ. [The slightly different value $r_p = 0.840\,29(55)$ fm was subsequently published after the closing date of the 2014 adjustment by Karshenboim *et al.* (2015).] Because this value of r_p is consistent with the value in Eq. (78), because the disagreement for the two values with the 2014 CODATA recommended value and H-D spectroscopic value are very nearly the same, and because the suggested approach has not yet been widely accepted, we have used the value of r_p in Eq. (78) for our discussion here and analysis in Sec. XIII.B.2.

A recent review of the proton radius puzzle is given by Carlson (2015).

B. Hyperfine structure and fine structure

In principle, together with theory, hyperfine-structure measurements other than in muonium, and fine-structure measurements other than in hydrogen and deuterium, could provide accurate values of some constants, most notably the fine-structure constant α. Indeed, it has long been the hope that a competitive value of α could be obtained from experimental measurements and theoretical calculations of ^{4}He fine-structure transition frequencies. However, as discussed in CODATA-10, no such data were available for the 2010 adjustment and this is also the case for the 2014 adjustment.

For completeness, we note that there have been significant improvements in both the theory and experimental determination of the hyperfine splitting in positronium [see Adkins *et al.* (2015), Eides and Shelyuto (2015), Ishida (2015), and Miyazaki *et al.* (2015) and the references cited therein]. Also, Marsman, Horbatsch, and Hessels (2015a, 2015b) have found that the measured values of helium fine-structure transition frequencies can be significantly influenced by quantum-mechanical interference between neighboring resonances even if separated by thousands of natural linewidths. The shifts they calculated for reported experimental values of the $2^3P_1 - 2^3P_2$ fine-structure interval in ^{4}He improve their agreement with theory.

V. Magnetic Moments and *g*-factors

The magnetic-moment vector of a charged lepton is

$$\boldsymbol{\mu}_\ell = g_\ell \frac{e}{2m_\ell}\boldsymbol{s}, \tag{79}$$

where ℓ = e, μ, or τ, g_ℓ is the g-factor, with the convention that it has the same sign as the charge of the particle, e is the (positive) unit charge, m_ℓ is the lepton mass, and $\boldsymbol{s}$ is its spin. Since the spin has projection eigenvalues of $s_z = \pm\hbar/2$, the magnetic moment is defined to be

$$\mu_\ell = \frac{g_\ell}{2}\frac{e\hbar}{2m_\ell}, \tag{80}$$

and the Bohr magneton is just

$$\mu_B = \frac{e\hbar}{2m_e}. \tag{81}$$

The g-factor differs from the Dirac value of 2 because of the lepton magnetic-moment anomaly a_ℓ defined by

$$|g_\ell| = 2(1 + a_\ell). \tag{82}$$

The theoretical value of the anomaly is given by QED, predominately electroweak, and predominantly strong-interaction effects denoted by

$$a_\ell(\text{th}) = a_\ell(\text{QED}) + a_\ell(\text{weak}) + a_\ell(\text{had}), \tag{83}$$

respectively.

RIGHTSLINK

A. Electron magnetic-moment anomaly a_e and the fine-structure constant α

A value for the fine-structure constant α is obtained by equating theory and experiment for the electron magnetic-moment anomaly.

1. Theory of a_e

The QED contribution to the electron anomaly is

$$a_e(\mathrm{QED}) = A_1 + A_2(m_e/m_\mu) + A_2(m_e/m_\tau) + A_3(m_e/m_\mu, m_e/m_\tau), \quad (84)$$

where the mass-dependent terms arise from vacuum-polarization loops. Each term may be expanded in powers of the fine-structure constant as

$$A_i = \sum_{n=1}^{\infty} A_i^{(2n)} \left(\frac{\alpha}{\pi}\right)^n, \quad (85)$$

where $A_2^{(2)} = A_3^{(2)} = A_3^{(4)} = 0$.

The mass-independent terms $A_1^{(2n)}$ are known accurately through sixth order:

$$A_1^{(2)} = \frac{1}{2}, \quad (86)$$

$$A_1^{(4)} = -0.328\,478\,965\,579\,193\ldots, \quad (87)$$

$$A_1^{(6)} = 1.181\,241\,456\ldots. \quad (88)$$

Recent numerical evaluations have yielded values for the eighth- and tenth-order coefficients (Aoyama *et al.*, 2014)

$$A_1^{(8)} = -1.912\,98(84), \quad (89)$$

$$A_1^{(10)} = 7.795(336). \quad (90)$$

Higher-order coefficients are assumed to be negligible.

Mass-dependent coefficients for the electron, based on the CODATA-14 values of the mass ratios, are

$$A_2^{(4)}(m_e/m_\mu) = 5.197\,386\,76(23) \times 10^{-7} \to 24.182 \times 10^{-10} a_e, \quad (91)$$

$$A_2^{(4)}(m_e/m_\tau) = 1.837\,98(33) \times 10^{-9} \to 0.086 \times 10^{-10} a_e, \quad (92)$$

$$A_2^{(6)}(m_e/m_\mu) = -7.373\,941\,71(24) \times 10^{-6} \to -0.797 \times 10^{-10} a_e, \quad (93)$$

$$A_2^{(6)}(m_e/m_\tau) = -6.5830(11) \times 10^{-8} \to -0.007 \times 10^{-10} a_e. \quad (94)$$

Additional series expansions in the mass ratios yield (Kurz *et al.*, 2014a)

$$A_2^{(8)}(m_e/m_\mu) = 9.161\,970\,83(33) \times 10^{-4} \to 0.230 \times 10^{-10} a_e, \quad (95)$$

$$A_2^{(8)}(m_e/m_\tau) = 7.4292(12) \times 10^{-6} \to 0.002 \times 10^{-10} a_e. \quad (96)$$

A numerical calculation gives the next term (Aoyama *et al.*, 2012b)

$$A_2^{(10)}(m_e/m_\mu) = -0.003\,82(39) \to -0.002 \times 10^{-10} a_e. \quad (97)$$

Additional terms have been calculated, but are negligible at the current level of accuracy; see, for example, Aoyama *et al.* (2014) and Kurz *et al.* (2014a).

All contributing terms of each order in α are combined to yield the total coefficients in the series

$$a_e(\mathrm{QED}) = \sum_{n=1}^{\infty} C_e^{(2n)} \left(\frac{\alpha}{\pi}\right)^n, \quad (98)$$

with

$$\begin{aligned} C_e^{(2)} &= 0.5, \\ C_e^{(4)} &= -0.328\,478\,444\,00\ldots, \\ C_e^{(6)} &= 1.181\,234\,017\ldots, \\ C_e^{(8)} &= -1.912\,06(84), \\ C_e^{(10)} &= 7.79(34), \end{aligned} \quad (99)$$

where higher-order coefficients are negligible.

The electroweak contribution, calculated as in CODATA-98 but with present values of G_F and $\sin^2\theta_W$ (see Sec. XII), is

$$a_e(\mathrm{weak}) = 0.029\,73(23) \times 10^{-12} = 0.2564(20) \times 10^{-10} a_e. \quad (100)$$

The hadronic contribution is the sum

$$a_e(\mathrm{had}) = a_e^{\mathrm{LO,VP}}(\mathrm{had}) + a_e^{\mathrm{NLO,VP}}(\mathrm{had}) + a_e^{\mathrm{LL}}(\mathrm{had}) + \cdots, \quad (101)$$

where $a_e^{\mathrm{LO,VP}}(\mathrm{had})$ and $a_e^{\mathrm{NLO,VP}}(\mathrm{had})$ are the leading order and next-to-leading order (with an additional photon or electron loop) hadronic vacuum-polarization corrections given by Nomura and Teubner (2013)

$$a_e^{\mathrm{LO,VP}}(\mathrm{had}) = 1.866(11) \times 10^{-12}, \quad (102)$$

$$a_e^{\mathrm{NLO,VP}}(\mathrm{had}) = -0.2234(14) \times 10^{-12}, \quad (103)$$

and $a_e^{\mathrm{NNLO,VP}}(\mathrm{had})$ is the next-to-next-to-leading order vacuum-polarization correction (Kurz *et al.*, 2014b)

$$a_e^{\mathrm{NNLO,VP}}(\mathrm{had}) = 0.0280(10) \times 10^{-12}, \quad (104)$$

and where $a_e^{\mathrm{LL}}(\mathrm{had})$ is the hadronic light-by-light scattering term given by Prades, de Rafael, and Vainshtein (2010)

$$a_e^{\mathrm{LL}}(\mathrm{had}) = 0.035(10) \times 10^{-12}. \quad (105)$$

The total hadronic contribution is

$$a_e(\mathrm{had}) = 1.734(15) \times 10^{-12} = 14.95(13) \times 10^{-10} a_e. \quad (106)$$

RIGHTSLINK

The theoretical value is the sum of all the terms:

$$a_e(\text{th}) = a_e(\text{QED}) + a_e(\text{weak}) + a_e(\text{had}), \quad (107)$$

and has the standard uncertainty

$$u[a_e(\text{th})] = 0.037 \times 10^{-12} = 0.32 \times 10^{-10} a_e, \quad (108)$$

where the largest contributions to the uncertainty are from the 8th- and 10th-order QED terms. This uncertainty is taken into account in the least-squares adjustment by writing

$$a_e(\text{th}) = a_e(\alpha) + \delta_e, \quad (109)$$

where $0.000(37) \times 10^{-12}$ is the input datum for δ_e. It is noteworthy that the uncertainty of $a_e(\text{th})$ is significantly smaller than the uncertainty of the most accurate experimental value (see following section), which is $2.4 \times 10^{-10} a_e$.

2. Measurements of a_e

Two experimental values of a_e obtained using a Penning trap were initially included in CODATA-10. The first is the classic 1987 result from the University of Washington discussed in CODATA-98 with a relative standard uncertainty $u_r = 3.7 \times 10^{-9}$ and which assumes that *CPT* invariance holds for the electron-positron system (Van Dyck, Schwinberg, and Dehmelt, 1987). The second is the much more accurate 2008 result from Harvard University discussed in CODATA-10 with $u_r = 2.4 \times 10^{-10}$ (Hanneke, Fogwell, and Gabrielse, 2008). These results are items *B*22.1 and *B*22.2 in Table XVIII, Sec. XIII, with identifications UWash-87 and HarvU-08; the values of α that can be inferred from them based on the theory of a_e discussed in the previous section are given in Table XX, Sec. XIII.A. The University of Washington result was not included in the final adjustment on which the CODATA 2010 recommended values are based because of its comparatively low weight and is also omitted from the 2014 final adjustment. It is only considered to help provide an overall picture of the data available for the determination of the 2014 recommended value of α.

B. Muon magnetic-moment anomaly a_μ

Only the measured value of the muon magnetic-moment anomaly was included in the 2010 adjustment of the constants due to concerns about some aspects of the theory. The concerns still remain, thus the Task Group decided not to employ the theoretical expression for a_μ in the 2014 adjustment. The theory and measurement of a_μ and the reasons for the Task Group decision are presented in the following sections.

1. Theory of a_μ

The relevant mass-dependent terms are

$$A_2^{(4)}(m_\mu/m_e) = 1.094\,258\,3092(72) \to 5.06 \times 10^{-3} a_\mu, \quad (110)$$

$$A_2^{(4)}(m_\mu/m_\tau) = 0.000\,078\,079(14) \to 3.61 \times 10^{-7} a_\mu, \quad (111)$$

$$A_2^{(6)}(m_\mu/m_e) = 22.868\,379\,98(17) \to 2.46 \times 10^{-4} a_\mu, \quad (112)$$

$$A_2^{(6)}(m_\mu/m_\tau) = 0.000\,360\,63(11) \to 3.88 \times 10^{-9} a_\mu, \quad (113)$$

$$A_2^{(8)}(m_\mu/m_e) = 132.6852(60) \to 3.31 \times 10^{-6} a_\mu, \quad (114)$$

$$A_2^{(8)}(m_\mu/m_\tau) = 0.042\,4941(53) \to 1.06 \times 10^{-9} a_\mu, \quad (115)$$

$$A_2^{(10)}(m_\mu/m_e) = 742.18(87) \to 4.30 \times 10^{-8} a_\mu, \quad (116)$$

$$A_2^{(10)}(m_\mu/m_\tau) = -0.068(5) \to -3.94 \times 10^{-12} a_\mu, \quad (117)$$

$$A_3^{(6)}(m_\mu/m_e, m_\mu/m_\tau) = 0.000\,527\,762(94) \to 5.67 \times 10^{-9} a_\mu, \quad (118)$$

$$A_3^{(8)}(m_\mu/m_e, m_\mu/m_\tau) = 0.062\,72(4) \to 1.57 \times 10^{-9} a_\mu. \quad (119)$$

$$A_3^{(10)}(m_\mu/m_e, m_\mu/m_\tau) = 2.011(10) \to 1.17 \times 10^{-10} a_\mu. \quad (120)$$

New mass-dependent contributions reported since CODATA-10 are Eqs. (114), (116), (117), (119), and (120) from Aoyama *et al.* (2012a) and Eq. (115) from Kurz *et al.* (2014a).

The total for $a_\mu(\text{QED})$ is

$$a_\mu(\text{QED}) = \sum_{n=1}^{\infty} C_e^{(2n)} \left(\frac{\alpha}{\pi}\right)^n, \quad (121)$$

with

$$\begin{aligned} C_\mu^{(2)} &= 0.5, \\ C_\mu^{(4)} &= 0.765\,857\,423(16), \\ C_\mu^{(6)} &= 24.050\,509\,82(27), \\ C_\mu^{(8)} &= 130.8774(61), \\ C_\mu^{(10)} &= 751.92(93). \end{aligned} \quad (122)$$

Based on the 2014 recommended value of α, this yields

$$a_\mu(\text{QED}) = 0.001\,165\,847\,188\,58(87) \quad [7.4 \times 10^{-10}], \quad (123)$$

where an uncertainty of 0.8×10^{-12} is included to account for uncalculated 12th-order terms (Aoyama *et al.*, 2012a).

As for the electron, there are additional contributions:

$$a_\mu(\text{th}) = a_\mu(\text{QED}) + a_\mu(\text{weak}) + a_\mu(\text{had}). \quad (124)$$

The primarily electroweak contribution is (Czarnecki, Marciano, and Vainshtein, 2003; Gnendiger, Stöckinger, and Stöckinger-Kim, 2013)

$$a_\mu(\text{weak}) = 154(1) \times 10^{-11}. \quad (125)$$

Separate contributions (lowest-order vacuum polarization, next-to-lowest-order, and light-by-light) to the hadronic term are

$$a_\mu(\text{had}) = a_\mu^{\text{LO,VP}}(\text{had}) + a_\mu^{\text{NLO,VP}}(\text{had}) + a_\mu^{\text{LL}}(\text{had}) + \cdots, \quad (126)$$

RIGHTSLINK

where (Hagiwara *et al.*, 2011)

$$a_\mu^{\mathrm{LO,VP}}(\mathrm{had}) = 6949(43)\times 10^{-11}, \tag{127}$$

$$a_\mu^{\mathrm{NLO,VP}}(\mathrm{had}) = -98.40(72)\times 10^{-11}, \tag{128}$$

and (Jegerlehner and Nyffeler, 2009)

$$a_\mu^{\mathrm{LL}}(\mathrm{had}) = 116(40)\times 10^{-11}. \tag{129}$$

The total hadronic contribution is then

$$a_\mu(\mathrm{had}) = 6967(59)\times 10^{-11}. \tag{130}$$

In analogy with the electron we have finally

$$a_\mu(\mathrm{th}) = a_\mu(\mathrm{QED}) + 7121(59)\times 10^{-11}, \tag{131}$$

with the standard uncertainty

$$u[a_\mu(\mathrm{th})] = 59\times 10^{-11} = 51\times 10^{-11} a_\mu. \tag{132}$$

The largest contributions to the uncertainty are from $a_\mu^{\mathrm{LO,VP}}(\mathrm{had})$ and $a_\mu^{\mathrm{LL}}(\mathrm{had})$; their respective uncertainties of 43×10^{-11} and 40×10^{-11} are nearly the same. By comparison, the 0.087×10^{-11} uncertainty of $a_\mu(\mathrm{QED})$ is negligible. However, the 63×10^{-11} uncertainty of the experimental value of a_μ, which is discussed in the following section, and $u[a_\mu(\mathrm{th})]$ are nearly the same. Based on the 2014 recommended value of α, Eq. (131) yields

$$a_\mu(\mathrm{th}) = 1.165\,918\,39(59)\times 10^{-3} \tag{133}$$

for the theoretically predicted value of a_μ.

2. Measurement of a_μ: Brookhaven

The experimental determination of a_μ at Brookhaven National Laboratory (BNL), Upton, New York, USA, has been discussed in the past four CODATA reports. The quantity measured is the anomaly difference frequency $f_a = f_s - f_c$, where $f_s = |g_\mu|(e\hbar/2m_\mu)B/h$ is the muon spin-flip (or precession) frequency in the applied magnetic flux density B and $f_c = eB/2\pi m_\mu$ is the corresponding muon cyclotron frequency. The flux density is eliminated from these expressions by determining its value using proton nuclear magnetic resonance (NMR) measurements. This means that the muon anomaly is calculated from

$$a_\mu(\mathrm{exp}) = \frac{\overline{R}}{|\mu_\mu/\mu_\mathrm{p}| - \overline{R}} \tag{134}$$

where $\overline{R} = f_a/\overline{f}_\mathrm{p}$ and $\overline{f}_\mathrm{p}$ is the free proton NMR frequency corresponding to the average flux density B seen by the muons in their orbits in the muon storage ring.

The final value of $\overline{R}$ obtained in the experiment is, from Table XV of Bennett *et al.* (2006),

$$\overline{R} = 0.003\,707\,2063(20), \tag{135}$$

which is used as an input datum in the 2014 adjustment and is the same as used in the 2010 adjustment. It is datum *B*24 in Table XVIII with identification BNL-06. Based on this value of $\overline{R}$, Eq. (134), and the 2014 recommended value of μ_μ/μ_p, whose uncertainty is negligible in this context, the experimental value of the muon anomaly is

$$a_\mu(\mathrm{exp}) = 1.165\,920\,89(63)\times 10^{-3}. \tag{136}$$

Further, with the aid of Eq. (225), the equation for $\overline{R}$ can be written as

$$\overline{R} = -\frac{a_\mu}{1+a_\mathrm{e}}\frac{m_\mathrm{e}}{m_\mu}\frac{\mu_\mathrm{e}}{\mu_\mathrm{p}}, \tag{137}$$

where use has been made of the relations $g_\mathrm{e} = -2(1+a_\mathrm{e})$, $g_\mu = -2(1+a_\mu)$, and a_e is replaced by the theoretical expression given in Eq. (109) for the observational equation. If the theory of a_μ were not problematic and used in adjustment calculations, then a_μ in Eq. (137) would be its theoretical expression, which mainly depends on α. If the theory is omitted, then a_μ in that equation is simply taken to be an adjusted constant. The following section discusses why the Task Group decided to do the latter.

3. Comparison of theory and experiment for a_μ

The difference between the experimental value of a_μ in Eq. (136) and the theoretical value in Eq. (133) is $250(86)\times 10^{-11}$, which is 2.9 times the standard uncertainty of the difference or 2.9σ. The terms $a_\mu^{\mathrm{LO,VP}}(\mathrm{had})$ and $a_\mu^{\mathrm{LL}}(\mathrm{had})$ are the dominant contributors to the uncertainty of $a_\mu(\mathrm{th})$, and a smaller value of either will increase the disagreement while a larger value will decrease it.

The value for $a_\mu^{\mathrm{LO,VP}}(\mathrm{had})$ used to obtain $a_\mu(\mathrm{th})$ is $6949(43)\times 10^{-11}$, but an equally credible value, $6923(42)\times 10^{-11}$, is also available (Davier *et al.*, 2011). If it is used instead, the discrepancy is $276(86)\times 10^{-11}$ or 3.2σ. Both values are based on very thorough analyses using theory and experimental data from the production of hadrons in e^+e^- collisions. Davier *et al.* (2011) also obtain the value $7015(47)\times 10^{-11}$ using both e^+e^- annihilation data and data from the decay of the τ into hadrons. For this value the discrepancy is reduced to 2.1σ. A result due to Jegerlehner and Szafron (2011) also obtained using e^+e^- annihilation data and τ decay data but which is only in marginal agreement with this value is $6910(47)\times 10^{-11}$. However, it agrees with the first two values, which are based solely on e^+e^- data. For this value the discrepancy is 3.3σ. In a lengthy paper Benayoun *et al.* (2013) used the hidden local symmetry model or HLS to obtain values of $a_\mu^{\mathrm{LO,VP}}(\mathrm{had})$ that are significantly smaller than others and that lead to a discrepancy of between 4σ and 5σ. However, Davier and Malaescu (2013) give a number of reasons why these values may not be reliable.

The value for $a_\mu^{\mathrm{LL}}(\mathrm{had})$ used to obtain $a_\mu(\mathrm{th})$ is $116(40)\times 10^{-11}$, but there are other credible values in the

RIGHTSLINK

literature. For example, Prades, de Rafael, and Vainshtein (2010) give $105(26)\times10^{-11}$ while Melnikov and Vainshtein (2004) find $136(25)\times10^{-11}$. A more recent value, due to Narukawa *et al.* (2014), is $118(20)\times10^{-11}$, and the largest is $188(4)\times10^{-11}$ reported by Goecke, Fischer, and Williams (2013). Others range from $80(40)\times10^{-11}$ to $107(17)\times10^{-11}$. Recent brief overviews of $a_\mu^{\rm LL}(\rm had)$ may be found in Dorokhov, Radzhabov, and Zhevlakov (2014a, 2014b), Nyffeler (2014), and Adikaram *et al.* (2015), which describe the many obstacles to obtaining a reliable estimate of its value. The conclusion that emerges from these papers is that $a_\mu^{\rm LL}(\rm had)$ is quite model dependent and the reliability of the estimates is questionable. Note that in calculating the value $116(40)\times10^{-11}$ used to obtain Eq. (133), Nyffeler (2009) adds the uncertainty components linearly and rounds the result up from 39×10^{-11} to 40×10^{-11}. This result is also thoroughly discussed in the detailed review by Jegerlehner and Nyffeler (2009) (see especially Table 13).

Although much work has been done over the past 4 years to improve the theory of a_μ, the discrepancy between experiment and theory remains at about the 3σ level. Further, there is a significant spread in the values of $a_\mu^{\rm LO,VP}(\rm had)$ and $a_\mu^{\rm LL}(\rm had)$, the two most problematic contributions to $a_\mu(\rm th)$; it is not obvious which are the best values. Expanding the uncertainty of $a_\mu(\rm th)$ to reflect this spread would reduce its contribution to the determination of the 2014 CODATA recommended value of a_μ significantly. Expanding the uncertainties of both $a_\mu(\rm th)$ and $a_\mu(\rm exp)$ to reduce the discrepancy to an acceptable level and including both would mean that the recommended value would cease to be a useful reference value for future comparisons of theory and experiment; it might tend to cover up an important physics problem rather than emphasizing it. For all these reasons, the Task Group chose not to include $a_\mu(\rm th)$ in the 2014 adjustment and to base the 2014 recommended value on experiment only as was the case in 2010.

C. Proton magnetic moment in nuclear magnetons μ_p/μ_N

The 2010 recommended value of the magnetic moment of the proton μ_p in units of the nuclear magneton $\mu_N = e\hbar/2m_p$ has a relative standard uncertainty $u_r = 8.2\times10^{-9}$. It was not measured directly but calculated from the relation $\mu_p/\mu_N = (\mu_p/\mu_B)[A_r(\rm p)/A_r(\rm e)]$, where $A_r(\rm e)$ and $A_r(\rm p)$ are adjusted constants and $\mu_B = e\hbar/2m_e$ is the Bohr magneton. The proton magnetic moment in units of μ_B is calculated from $\mu_p/\mu_B = (\mu_e/\mu_B)/(\mu_e/\mu_p)$, where $|\mu_e/\mu_B| = 1 + a_e$ is extremely well known and μ_e/μ_p is an adjusted constant determined mainly by the experimentally measured value of the bound-state magnetic-moment ratio in hydrogen $\mu_e(\rm H)/\mu_p(\rm H)$ taken as an input datum.

Now, however, a directly determined value of μ_p/μ_N with $u_r = 3.3\times10^{-9}$ obtained from measurements on a single proton in a double Penning trap at the Institut für Physik, Johannes Gutenberg Universität Mainz (or simply the University of Mainz), Mainz, Germany, is available for inclusion in the 2014 adjustment. The spin-flip transition frequency in a magnetic flux density B is

$$\omega_s = \frac{\Delta E}{\hbar} = \frac{2\mu_p B}{\hbar}, \tag{138}$$

and the cyclotron frequency for the proton is

$$\omega_c = \frac{eB}{m_p}. \tag{139}$$

The ratio for the same magnetic flux density B is just

$$\frac{\omega_s}{\omega_c} = \frac{\mu_p}{\mu_N}. \tag{140}$$

The value employed as an input datum in the 2014 adjustment is

$$\frac{\mu_p}{\mu_N} = 2.792\,847\,3498(93) \quad [3.3\times10^{-9}], \tag{141}$$

which is the result reported by Mooser *et al.* (2014) but with an additional digit for both the value and uncertainty provided to the Task Group by coauthor Blaum (2014). This value, which we identify as UMZ-14, is the culmination of an extensive research program carried out over many years. Descriptions of the key advances made in the development of the double Penning trap used in the experiment are given in a number of publications (Ulmer, Blaum *et al.*, 2011; Ulmer, Rodegheri *et al.*, 2011; Mooser *et al.*, 2013; Mooser, Kracke *et al.*, 2013; Ulmar *et al.*, 2013).

The double Penning trap consists of a precision trap of inner diameter 7 mm and an analysis trap of inner diameter 3.6 mm connected by transport electrodes, all mounted in the horizontal bore of a superconducting magnet with $B \approx 1.89$ T. Storage times for a single proton of no less than 1 year are achieved by enclosing the entire apparatus in a sealed vacuum chamber cooled to 4 K where pressures below 10^{-14} Pa are reached. The measurement sequence is straightforward but its implementation is complex; the cited papers should be consulted for details. Sputtered atoms created by electrons from a field emission gun hitting a polyethylene target are ionized in the center of the precision trap. A single proton is obtained from the resulting ion cloud, its cyclotron frequency of approximately 29 MHz is determined, and an electromagnetic signal near the proton's precession frequency of approximately 81 MHz is applied to it. The proton is then transported to the analysis trap where the spin state of the proton is determined and the proton returned to the precision trap. By varying the frequency of the spin-flip signal and repeating the process many times, a resonance curve of the probability $P(\omega_s/\omega_c)$ as a function of ω_s is obtained. Its maximum is located at $\omega_s/\omega_c = \mu_p/\mu_N$. The statistical relative standard uncertainty of the value given in Eq. (141) is 2.6×10^{-9}, and the net fractional correction for systematic effects is $-0.64(2.04)\times10^{-9}$. The largest contributor by far to the uncertainty of the net correction is the 2×10^{-9} relative uncertainty assigned by Mooser *et al.* (2014) for the possible effect of nonlinear drifts of the magnetic field.

The relationships given at the beginning of this section show how the 2010 recommended value of μ_p/μ_N is based on the relation

RIGHTSLINK

$$\frac{\mu_p}{\mu_N} = -(1 + a_e)\frac{A_r(p)}{A_r(e)}\frac{\mu_p}{\mu_e}, \tag{142}$$

which is the source of the observational equation $B29$ in Table XXIV.

For completeness, we note that a value of μ_p/μ_N with $u_r = 8.9 \times 10^{-6}$ from the double Penning trap in an earlier stage of development has been published by the Mainz group (Rodegheri *et al.*, 2012), as has a value with $u_r = 2.5 \times 10^{-6}$ obtained by a direct measurement at Harvard University with a different type of Penning trap (Lees *et al.*, 2012). Also noteworthy is the use of a similar double Penning trap at CERN to test *CPT* invariance by comparing the antiproton-to-proton charge-to-mass ratio, demonstrating that they agree within an uncertainty of 69 parts in 10^{12} (DiSciacca *et al.*, 2013).

D. Atomic *g*-factors in hydrogenic ^{12}C and ^{28}Si and A_r(e)

The most accurate values of the relative atomic mass of the electron $A_r(e)$ are obtained from measurements of the electron g-factor in hydrogenic ions, silicon and carbon in particular, and theoretical expressions for the g-factors. In fact, the uncertainties of the values so obtained are now so small that none of the data previously used to determine $A_r(e)$ remain of interest.

For a hydrogenic ion X with a spinless nucleus and atomic number Z, the energy-level shift in an applied magnetic flux density $\boldsymbol{B}$ in the z direction is given by

$$E = -\boldsymbol{\mu}\cdot\boldsymbol{B} = -g(X)\frac{e}{2m_e}J_z B, \tag{143}$$

where J_z is the electron angular-momentum projection in the z direction and $g(X)$ is the atomic g-factor. In the ground $1S_{1/2}$ state, $J_z = \pm\hbar/2$, so the splitting between the two levels is

$$\Delta E = |g(X)|\frac{e\hbar}{2m_e}B, \tag{144}$$

and the spin-flip transition frequency is

$$\omega_s = \frac{\Delta E}{\hbar} = |g(X)|\frac{eB}{2m_e}. \tag{145}$$

In the same flux density, the ion's cyclotron frequency is

$$\omega_c = \frac{q_X B}{m_X}, \tag{146}$$

where $q_X = (Z-1)e$ is the net charge of the ion and m_X is its mass. Thus the frequency ratio is

$$\frac{\omega_s}{\omega_c} = \frac{|g(X)|}{2(Z-1)}\frac{m_X}{m_e} = \frac{|g(X)|}{2(Z-1)}\frac{A_r(X)}{A_r(e)}, \tag{147}$$

where $A_r(X)$ is the relative atomic mass of the ion.

1. Theory of the bound-electron *g*-factor

The bound-electron g-factor is given by

$$g(X) = g_D + \Delta g_{rad} + \Delta g_{rec} + \Delta g_{ns} + \cdots, \tag{148}$$

where the individual terms on the right-hand side are the Dirac value, radiative corrections, recoil corrections, nuclear-size corrections, and the dots represent possible additional corrections not already included. Tables XI and XII give the numerical values of the various contributions.

The Dirac value is (Breit, 1928)

$$\begin{aligned} g_D &= -\frac{2}{3}\left[1 + 2\sqrt{1-(Z\alpha)^2}\right] \\ &= -2\left[1 - \frac{1}{3}(Z\alpha)^2 - \frac{1}{12}(Z\alpha)^4 - \frac{1}{24}(Z\alpha)^6 + \cdots\right], \end{aligned} \tag{149}$$

where the only uncertainty is due to the uncertainty in α.

Radiative corrections are given by

$$\Delta g_{rad} = -2\sum_{n=1}^{\infty} C_e^{(2n)}(Z\alpha)\left(\frac{\alpha}{\pi}\right)^n, \tag{150}$$

where the limits

$$\lim_{Z\alpha\to 0} C_e^{(2n)}(Z\alpha) = C_e^{(2n)} \tag{151}$$

are given in Eq. (99).

The first term is (Faustov, 1970; Grotch, 1970; Close and Osborn, 1971; Pachucki, Jentschura, and Yerokhin, 2004; Pachucki *et al.*, 2005)

TABLE XI. Theoretical contributions and total value for the g-factor of hydrogenic carbon 12 based on the 2014 recommended values of the constants

Contribution	Value	Source
Dirac g_D	−1.998 721 354 392 1(6)	Eq. (149)
$\Delta g_{SE}^{(2)}$	−0.002 323 672 435(4)	Eq. (157)
$\Delta g_{VP}^{(2)}$	0.000 000 008 511	Eq. (160)
$\Delta g^{(4)}$	0.000 003 545 677(25)	Eq. (164)
$\Delta g^{(6)}$	−0.000 000 029 618	Eq. (166)
$\Delta g^{(8)}$	0.000 000 000 111	Eq. (167)
$\Delta g^{(10)}$	−0.000 000 000 001	Eq. (168)
Δg_{rec}	−0.000 000 087 629	Eqs. (169), (170)
Δg_{ns}	−0.000 000 000 408(1)	Eq. (172)
$g(^{12}C^{5+})$	−2.001 041 590 183(26)	Eq. (173)

TABLE XII. Theoretical contributions and total value for the g-factor of hydrogenic silicon 28 based on the 2014 recommended values of the constants

Contribution	Value	Source
Dirac g_D	−1.993 023 571 557(3)	Eq. (149)
$\Delta g_{SE}^{(2)}$	−0.002 328 917 47(5)	Eq. (157)
$\Delta g_{VP}^{(2)}$	0.000 000 234 81(1)	Eq. (160)
$\Delta g^{(4)}$	0.000 003 5521(17)	Eq. (164)
$\Delta g^{(6)}$	−0.000 000 029 66	Eq. (166)
$\Delta g^{(8)}$	0.000 000 000 11	Eq. (167)
$\Delta g^{(10)}$	−0.000 000 000 00	Eq. (168)
Δg_{rec}	−0.000 000 205 88	Eqs. (169), (170)
Δg_{ns}	−0.000 000 020 53(3)	Eq. (172)
$g(^{28}Si^{13+})$	−1.995 348 9581(17)	Eq. (173)

RIGHTSLINK

$$C^{(2)}_{e,SE}(Z\alpha) = \frac{1}{2}\left\{1 + \frac{(Z\alpha)^2}{6} + (Z\alpha)^4\left[\frac{32}{9}\ln(Z\alpha)^{-2} + \frac{247}{216} - \frac{8}{9}\ln k_0 - \frac{8}{3}\ln k_3\right] + (Z\alpha)^5 R_{SE}(Z\alpha)\right\}, \quad (152)$$

where

$$\ln k_0 = 2.984\,128\,556, \quad (153)$$

$$\ln k_3 = 3.272\,806\,545, \quad (154)$$

$$R_{SE}(6\alpha) = 22.160(10), \quad (155)$$

$$R_{SE}(14\alpha) = 20.999(2). \quad (156)$$

Values for the remainder function $R_{SE}(Z\alpha)$ are based on extrapolations from numerical calculations at higher Z (Yerokhin, Indelicato, and Shabaev, 2002, 2004; Pachucki, Jentschura, and Yerokhin, 2004); see also Yerokhin and Jentschura (2008, 2010). In CODATA-10, the values for carbon and oxygen were taken directly from Pachucki, Jentschura, and Yerokhin (2004). The value for silicon in Eq. (156) is obtained here by extrapolation of the data in Yerokhin, Indelicato, and Shabaev (2004) with a fitting function of the form $a + (Z\alpha)[b + c\ln(Z\alpha)^{-2} + d\ln^2(Z\alpha)^{-2}]$. We thus have

$$C^{(2)}_{e,SE}(6\alpha) = 0.500\,183\,606\,65(80), \quad C^{(2)}_{e,SE}(14\alpha) = 0.501\,312\,630(11). \quad (157)$$

The lowest-order vacuum-polarization correction consists of a wave-function correction and a potential correction, each of which can be separated into a lowest-order Uehling potential contribution and a Wichmann-Kroll higher-order contribution. The wave-function correction is (Beier, 2000; Beier *et al.*, 2000; Karshenboim, 2000; Karshenboim, Ivanov, and Shabaev, 2001a, 2001b)

$$C^{(2)}_{e,VPwf}(6\alpha) = -0.000\,001\,840\,3431(43), \quad C^{(2)}_{e,VPwf}(14\alpha) = -0.000\,051\,091\,98(22). \quad (158)$$

For the potential correction, the Uehling contribution vanishes (Beier *et al.*, 2000), and for the Wichmann-Kroll part, we take the value of Lee *et al.* (2005), which has a negligible uncertainty from omitted binding corrections for the present level of accuracy. This gives

$$C^{(2)}_{e,VPp}(6\alpha) = 0.000\,000\,008\,201(11), \quad C^{(2)}_{e,VPp}(14\alpha) = 0.000\,000\,5467(11). \quad (159)$$

The total vacuum polarization is the sum of Eqs. (158) and (159):

$$C^{(2)}_{e,VP}(6\alpha) = C^{(2)}_{e,VPwf}(6\alpha) + C^{(2)}_{e,VPp}(6\alpha) = -0.000\,001\,832\,142(12),$$
$$C^{(2)}_{e,VP}(14\alpha) = C^{(2)}_{e,VPwf}(14\alpha) + C^{(2)}_{e,VPp}(14\alpha) = -0.000\,050\,5452(11). \quad (160)$$

One-photon corrections are the sum of Eqs. (157) and (160):

$$C^{(2)}_{e}(6\alpha) = C^{(2)}_{e,SE}(6\alpha) + C^{(2)}_{e,VP}(6\alpha) = 0.500\,181\,774\,51(80),$$
$$C^{(2)}_{e}(14\alpha) = C^{(2)}_{e,SE}(14\alpha) + C^{(2)}_{e,VP}(14\alpha) = 0.501\,262\,085(11), \quad (161)$$

which yields

$$\Delta g^{(2)}_{rad} = -2C^{(2)}_{e}(Z\alpha)\left(\frac{\alpha}{\pi}\right) = -0.002\,323\,663\,924(4) \quad \text{for } Z = 6$$
$$= -0.002\,328\,682\,65(5) \quad \text{for } Z = 14. \quad (162)$$

The leading binding correction is known to all orders in α/π (Eides and Grotch, 1997; Czarnecki, Melnikov, and Yelkhovsky, 2001):

$$C^{(2n)}_{e}(Z\alpha) = C^{(2n)}_{e}\left(1 + \frac{(Z\alpha)^2}{6} + \cdots\right). \quad (163)$$

To order $(Z\alpha)^4$, the two-photon correction for the ground S state is (Pachucki *et al.*, 2005; Jentschura *et al.*, 2006)

$$C^{(4)}_{e}(Z\alpha) = C^{(4)}_{e}\left(1 + \frac{(Z\alpha)^2}{6}\right) + (Z\alpha)^4\left[\frac{14}{9}\ln(Z\alpha)^{-2} + \frac{991\,343}{155\,520} - \frac{2}{9}\ln k_0 - \frac{4}{3}\ln k_3 + \frac{679\pi^2}{12\,960} - \frac{1441\pi^2}{720}\ln 2 + \frac{1441}{480}\zeta(3)\right] + \mathcal{O}(Z\alpha)^5$$
$$= -0.328\,5778(23) \quad \text{for } Z = 6$$
$$= -0.329\,17(15) \quad \text{for } Z = 14, \quad (164)$$

where $C^{(4)}_{e} = -0.328\,478\,444\,00\ldots$, and where $\ln k_0$ and $\ln k_3$ are given in Eqs. (153) and (154). Pachucki *et al.* (2005) have estimated the uncertainty due to uncalculated higher-order contributions to be

$$u[C^{(4)}_{e}(Z\alpha)] = 2|(Z\alpha)^5 C^{(4)}_{e} R_{SE}(Z\alpha)|, \quad (165)$$

which we use as the uncertainty. Since the remainder functions differ only by about 1% for carbon and silicon, the main Z dependence of the uncertainty is given by the factor $(Z\alpha)^5$. We shall assume that the uncertainty of the two-photon correction is completely correlated for the two charged ions. As a consequence, information from the silicon measured value will effectively be included in the theoretical prediction for the carbon value through the least-squares adjustment formalism.

Jentschura (2009) and Yerokhin and Harman (2013) have calculated two-loop vacuum-polarization diagrams of the same order as the uncertainty in Eq. (164).

Equation (163) gives the leading two terms of the higher-loop contributions. The corrections are

RIGHTSLINK

$$C_e^{(6)}(Z\alpha) = C_e^{(6)}\left(1 + \frac{(Z\alpha)^2}{6} + \cdots\right)$$
$$= 1.181\,611\ldots \quad \text{for } Z = 6$$
$$= 1.183\,289\ldots \quad \text{for } Z = 14, \tag{166}$$

where $C_e^{(6)} = 1.181\,234\,017\ldots$,

$$C_e^{(8)}(Z\alpha) = C_e^{(8)}\left(1 + \frac{(Z\alpha)^2}{6} + \cdots\right)$$
$$= -1.912\,67(84)\ldots \quad \text{for } Z = 6$$
$$= -1.915\,38(84)\ldots \quad \text{for } Z = 14, \tag{167}$$

where $C_e^{(8)} = -1.912\,06(84)$, and

$$C_e^{(10)}(Z\alpha) = C_e^{(10)}\left(1 + \frac{(Z\alpha)^2}{6} + \cdots\right)$$
$$= 7.79(34)\ldots \quad \text{for } Z = 6$$
$$= 7.80(34)\ldots \quad \text{for } Z = 14, \tag{168}$$

where $C_e^{(10)} = 7.79(34)$.

Recoil of the nucleus gives a correction proportional to the electron-nucleus mass ratio. It can be written as $\Delta g_{\rm rec} = \Delta g_{\rm rec}^{(0)} + \Delta g_{\rm rec}^{(2)} + \cdots$, where the two terms are zero and first order in α/π, respectively. The first term is (Eides and Grotch, 1997; Shabaev and Yerokhin, 2002)

$$\Delta g_{\rm rec}^{(0)} = \left\{ -(Z\alpha)^2 + \frac{(Z\alpha)^4}{3\left[1 + \sqrt{1-(Z\alpha)^2}\right]^2} - (Z\alpha)^5 P(Z\alpha) \right\} \frac{m_e}{m_N}$$
$$+ (1+Z)(Z\alpha)^2 \left(\frac{m_e}{m_N}\right)^2$$
$$= -0.000\,000\,087\,70\ldots \quad \text{for } Z = 6$$
$$= -0.000\,000\,206\,04\ldots \quad \text{for } Z = 14, \tag{169}$$

where m_N is the mass of the nucleus. Mass ratios, based on the current adjustment values of the constants, are $m_e/m(^{12}C^{6+}) = 0.000\,045\,727\,5\ldots$ and $m_e/m(^{28}Si^{14+}) = 0.000\,019\,613\,6\ldots$ [see Eqs. (10) and (3)]. For silicon, we use the interpolated value $P(14\alpha) = 7.162\,23(1)$.

For $\Delta g_{\rm rec}^{(2)}$, we have

$$\Delta g_{\rm rec}^{(2)} = \frac{\alpha}{\pi}\frac{(Z\alpha)^2}{3}\frac{m_e}{m_N} + \cdots$$
$$= 0.000\,000\,000\,06\ldots \quad \text{for } Z = 6$$
$$= 0.000\,000\,000\,15\ldots \quad \text{for } Z = 14. \tag{170}$$

The uncertainty in $\Delta g_{\rm rec}^{(2)}$ is negligible compared to that of $\Delta g_{\rm rad}^{(2)}$.

The nuclear-size correction is given to lowest order in $(Z\alpha)^2$ by (Karshenboim, 2000)

$$\Delta g_{\rm ns} = -\frac{8}{3}(Z\alpha)^4 \left(\frac{R_N}{\lambda\!\!\!^{-}_C}\right)^2, \tag{171}$$

where R_N is the bound-state nuclear rms charge radius and $\lambda\!\!\!^{-}_C$ is the Compton wavelength of the electron divided by 2π. Glazov and Shabaev (2002) have calculated additional corrections within perturbation theory. Scaling their results with the squares of updated values for the nuclear radii $R_N = 2.4703(22)$ fm and $R_N = 3.1223(24)$ fm from the compilation of Angeli (2004) for ^{12}C and ^{28}Si respectively yields

$$\Delta g_{\rm ns} = -0.000\,000\,000\,408(1) \quad \text{for } ^{12}C,$$
$$\Delta g_{\rm ns} = -0.000\,000\,020\,53(3) \quad \text{for } ^{16}Si. \tag{172}$$

Tables XI and XII list the contributions discussed above and totals given by

$$g(^{12}C^{5+}) = -2.001\,041\,590\,183(26),$$
$$g(^{28}Si^{13+}) = -1.995\,348\,9581(17). \tag{173}$$

For the purpose of the least-squares adjustment, we write the theoretical expressions for the g-factors as

$$g(^{12}C^{5+}) = g_C(\alpha) + \delta_C,$$
$$g(^{28}Si^{13+}) = g_{Si}(\alpha) + \delta_{Si}, \tag{174}$$

where the first term on the right-hand side of each expression gives the calculated value along with its functional dependence on α. The second term contains the theoretical uncertainty in the calculated value, except for the component due to uncertainty in α, which is taken into account by the least-squares algorithm through the first term. We thus have

$$\delta_C = 0.0(2.6) \times 10^{-11}, \tag{175}$$
$$\delta_{Si} = 0.0(1.7) \times 10^{-9}. \tag{176}$$

In each case, the uncertainty is dominated by uncalculated two-loop higher-order terms, which are expected to be mainly proportional to $(Z\alpha)^5$. For the one-loop self energy, approximately 85% of the remainder scales as $(Z\alpha)^5$ between C and Si [see Eqs. (155) and (156)]. As a conservative estimate, we shall assume that 80% of the uncertainty scales as $(Z\alpha)^5$ in the case of the two-loop uncertainty. As a result, information from measurement of the Si g-factor will provide information about the two-loop uncertainty in C and vice versa through the covariance of the deltas in the least-squares adjustment. The covariance of δ_C and δ_{Si} is

$$u(\delta_C, \delta_{Si}) = 3.4 \times 10^{-20}, \tag{177}$$

which corresponds to a correlation coefficient of $r(\delta_C, \delta_{Si}) = 0.79$.

2. Measurements of $g(^{12}C^{5+})$ and $g(^{28}Si^{13+})$

As discussed at the start of Sec. V.D, recent measurements of the electron g-factor in hydrogenic carbon and silicon together with theory provide a value of $A_r(e)$ with an uncertainty so small that the data used in the CODATA 2010 adjustment to determine $A_r(e)$ are no longer competitive and need not be considered. As indicated at the end of that section, the experimental quantities actually determined are the ratios of the electron spin precession (or spin-flip) frequency in

RIGHTSLINK

hydrogenic carbon and silicon ions to the cyclotron frequency of the ions, both in the same magnetic flux density. The result used in the 2014 adjustment for hydrogenic silicon is

$$\frac{\omega_s(^{28}Si^{13+})}{\omega_c(^{28}Si^{13+})} = 3912.866\,064\,84(19) \quad [4.8\times10^{-11}]. \quad (178)$$

This value, determined by the group at the Max-Planck-Institut für Kernphysik (MPIK), Heidelberg, Germany, is based on additional information including a detailed uncertainty budget provided to the Task Group by the experimenters (Sturm, 2015). The information was needed to calculate the covariance between the silicon result and the MPIK carbon result discussed below. The value in Eq. (178) differs slightly from that published by the MPIK group (Sturm *et al.*, 2013) as a consequence of the group's reassessment of several small corrections for systematic effects (Sturm, 2015). The net fractional correction applied to the uncorrected ratio to obtain the final ratio given by Sturm *et al.* (2013) is -638.9×10^{-12} while the net fractional correction applied to obtain Eq. (178) is -678.5×10^{-12}. The largest of these corrections by far, $-659(33)\times10^{-12}$, is due to image charge and the next largest, $-20(10)\times10^{-12}$, is due to frequency pulling. The statistical relative uncertainty of eight individual measurements is 33×10^{-12}. We identify the result in Eq. (178) as MPIK-15.

Both the silicon and carbon ratios were obtained using the MPIK triple cylindrical Penning trap operating at $B = 3.8$ T and in thermal contact with a liquid helium bath. This trap is similar in design and operation to the double Penning trap used to directly measure μ_p/μ_N as discussed in Sec. V.C. The first stage of the experiment occurs in the creation trap in which ions are created; the second stage is carried out in the analysis trap where the spin state of a single ion is determined; the third stage occurs in the precision trap where the cyclotron frequency is measured and a spin flip is attempted by applying a 105 GHz microwave signal. The ion is transferred back to the analysis trap where the spin state of the ion is again determined, thereby determining if the spin-flip attempt in the precision trap was successful. The process is then repeated. The development of the trap and associated measurement techniques over a number of years that has allowed uncertainties below 5 parts in 10^{11} to be achieved are discussed in several papers (Blaum *et al.*, 2009; Sturm *et al.*, 2010; Sturm, Wagner, Schabinger, and Blaum, 2011; Ulmer, Blaum *et al.*, 2011) and results using $^{28}Si^{13+}$ that reflect experimental improvements have been reported (Sturm, Wagner, Schabinger, Zatorski *et al.*, 2011; Schabinger *et al.*, 2012; Sturm *et al.*, 2013).

For hydrogenic carbon we use

$$\frac{\omega_s(^{12}C^{5+})}{\omega_c(^{12}C^{5+})} = 4376.210\,500\,87(12) \quad [2.8\times10^{-11}], \quad (179)$$

which is also based on additional information supplied to the Task Group (Sturm *et al.*, 2015) at the same time as that for silicon and similar in nature. The high-accuracy carbon result was first published in a letter to Nature (Sturm *et al.*, 2014) and differs slightly from Eq. (179) but the value subsequently published in the detailed report on the experiment is the same (Köhler *et al.*, 2015). The net fractional correction applied to the uncorrected ratio is -283.3×10^{-12}, with the largest components being for image charge and frequency pulling at $-282.4.\times10^{-12}$ and 2.20×10^{-12}, respectively. The statistical relative uncertainty of the individual measurements is 23×10^{-12}. The detailed report gives a comprehensive discussion of the MPIK trap including many possible systematic effects and their uncertainties. We identify the result in Eq. (179) as MPIK-15.

The carbon and silicon frequency ratios in Eqs. (178) and (179) are correlated. Based on the detailed uncertainty budgets for the two experiments supplied to the Task Group (Sturm, 2015) the correlation coefficient is

$$r\left[\frac{\omega_s(^{12}C^{5+})}{\omega_c(^{12}C^{5+})}, \frac{\omega_s(^{28}Si^{13+})}{\omega_c(^{28}Si^{13+})}\right] = 0.347, \quad (180)$$

which is mostly due to the image charge correction.

The frequency ratios are related to the ion and electron masses by

$$\frac{\omega_s(^{12}C^{5+})}{\omega_c(^{12}C^{5+})} = -\frac{g(^{12}C^{5+})}{10A_r(e)}\left[12 - 5A_r(e) + \frac{\Delta E_B(^{12}C^{5+})}{m_u c^2}\right], \quad (181)$$

and

$$\frac{\omega_s(^{28}Si^{13+})}{\omega_c(^{28}Si^{13+})} = -\frac{g_e(^{28}Si^{13+})}{14A_r(e)}A_r(^{28}Si^{13+}), \quad (182)$$

where $A_r(^{28}Si^{13+})$ is taken to be an adjusted constant and is related to the input datum $A_r(^{28}Si)$ by [see Eq. (3)]

$$A_r(^{28}Si^{13+}) = A_r(^{28}Si) - 13A_r(e) + \frac{\Delta E_B(^{28}Si^{13+})}{m_u c^2}. \quad (183)$$

With the aid of Eq. (4) this becomes the observational equation for $A_r(^{28}Si^{13+})$, which is $B19$ in Table XXIV. Because $A_r(^{12}C) = 12$ exactly, such an additional observational equation is unnecessary for carbon; Eq. (181) becomes the observational equation for $\omega_s(^{12}C^{5+})/\omega_c(^{12}C^{5+})$ simply by using Eq. (4) to modify its last term (see $B15$ in Table XXIV).

The silicon frequency ratio yields for the relative atomic mass of the electron

$$A_r(e) = 0.000\,548\,579\,909\,19(46) \quad [8.3\times10^{-10}], \quad (184)$$

and the carbon frequency ratio gives

$$A_r(e) = 0.000\,548\,579\,909\,070(17) \quad [3.1\times10^{-11}]. \quad (185)$$

If both data are used, we obtain

$$A_r(e) = 0.000\,548\,579\,909\,069(16) \quad [2.9\times10^{-11}]. \quad (186)$$

The slight shift in value and reduction in uncertainty in Eq. (186) as compared to Eq. (185) is due to the information about the higher-order terms in the theory resulting from the silicon measurement. If the covariance in the theory given by Eq. (177) is taken to be zero, the result from using both

RIGHTSLINK

measurements is the same as the result based only on the carbon datum, within the uncertainty displayed in the equations.

We note that in the 2010 adjustment, the uncertainty of $A_r(p)$ was much lower than that of $A_r(e)$. As a result, the ratio $A_r(e)/A_r(p)$ from the analysis of antiprotonic helium transition frequencies together with the value for $A_r(p)$ provided a competitive value for $A_r(e)$. Now that $A_r(e)$ is more accurately known, the value of $A_r(e)$ combined with the ratio $A_r(e)/A_r(p)$ provides a new value for $A_r(p)$. However, despite improvement in the theory of antiprotonic helium (Korobov, Hilico, and Karr, 2014), the uncertainty of the derived value of $A_r(p)$ is much too large for it to be used in the 2014 adjustment.

VI. Magnetic-Moment Ratios and the Muon-Electron Mass Ratio

Free-particle magnetic-moment ratios can be obtained from experiments that measure moment ratios in bound states by applying theoretical corrections relating the free moment ratios to the bound moment ratios.

The magnetic moment of a nucleus with spin $\boldsymbol{I}$ is

$$\boldsymbol{\mu} = g\frac{e}{2m_p}\boldsymbol{I}, \tag{187}$$

where g is the g-factor of the nucleus, e is the elementary charge, and m_p is the proton mass. The magnitude of the magnetic moment is defined to be

$$\mu = g\mu_N i, \tag{188}$$

where $\mu_N = e\hbar/2m_p$ is the nuclear magneton, and i is the maximum spin projection I_z, defined by $\boldsymbol{I}^2 = i(i+1)\hbar^2$.

In the Pauli approximation, the Hamiltonian for a hydrogen atom in the ground state in an applied magnetic flux density $\boldsymbol{B}$ is

$$\mathcal{H} = \frac{\Delta\omega_H}{\hbar}\boldsymbol{s}\cdot\boldsymbol{I} - g_e(H)\frac{\mu_B}{\hbar}\boldsymbol{s}\cdot\boldsymbol{B} - g_p(H)\frac{\mu_N}{\hbar}\boldsymbol{I}\cdot\boldsymbol{B}, \tag{189}$$

where $\Delta\omega_H$ is the ground-state hyperfine frequency, $\boldsymbol{s}$ is the electron spin as given in Eq. (79), and μ_B is given by Eq. (81). The coefficients $g_e(H)$ and $g_p(H)$ are bound-state g-factors and are related to the corresponding free g-factors g_e and g_p by the theoretical corrections given below. The analogous corrections for deuterium, muonium and helium-3 are also given.

A. Theoretical ratios of atomic bound-particle to free-particle g-factors

Theoretical binding corrections to g-factors are as follows. References for the calculations are given in previous detailed CODATA reports.

Hydrogen:

$$\frac{g_e(H)}{g_e} = 1 - \frac{1}{3}(Z\alpha)^2 - \frac{1}{12}(Z\alpha)^4 + \frac{1}{4}(Z\alpha)^2\left(\frac{\alpha}{\pi}\right) + \frac{1}{2}(Z\alpha)^2\frac{m_e}{m_p} + \frac{1}{2}\left(A_1^{(4)} - \frac{1}{4}\right)(Z\alpha)^2\left(\frac{\alpha}{\pi}\right)^2 - \frac{5}{12}(Z\alpha)^2\left(\frac{\alpha}{\pi}\right)\frac{m_e}{m_p} + \ldots, \tag{190}$$

$$\frac{g_p(H)}{g_p} = 1 - \frac{1}{3}\alpha(Z\alpha) - \frac{97}{108}\alpha(Z\alpha)^3 + \frac{1}{6}\alpha(Z\alpha)\frac{m_e}{m_p}\frac{3+4a_p}{1+a_p} + \ldots, \tag{191}$$

where $A_1^{(4)}$ is given in Eq. (87), and the proton magnetic-moment anomaly is $a_p = \mu_p/(e\hbar/2m_p) - 1 \approx 1.793$.

Deuterium:

$$\frac{g_e(D)}{g_e} = 1 - \frac{1}{3}(Z\alpha)^2 - \frac{1}{12}(Z\alpha)^4 + \frac{1}{4}(Z\alpha)^2\left(\frac{\alpha}{\pi}\right) + \frac{1}{2}(Z\alpha)^2\frac{m_e}{m_d} + \frac{1}{2}\left(A_1^{(4)} - \frac{1}{4}\right)(Z\alpha)^2\left(\frac{\alpha}{\pi}\right)^2 - \frac{5}{12}(Z\alpha)^2\left(\frac{\alpha}{\pi}\right)\frac{m_e}{m_d} + \ldots, \tag{192}$$

$$\frac{g_d(D)}{g_d} = 1 - \frac{1}{3}\alpha(Z\alpha) - \frac{97}{108}\alpha(Z\alpha)^3 + \frac{1}{6}\alpha(Z\alpha)\frac{m_e}{m_d}\frac{3+4a_d}{1+a_d} + \ldots, \tag{193}$$

where the deuteron magnetic-moment anomaly is $a_d = \mu_d/(e\hbar/m_d) - 1 \approx -0.143$.

Muonium (see Sec. VI.B):

$$\frac{g_e(Mu)}{g_e} = 1 - \frac{1}{3}(Z\alpha)^2 - \frac{1}{12}(Z\alpha)^4 + \frac{1}{4}(Z\alpha)^2\left(\frac{\alpha}{\pi}\right) + \frac{1}{2}(Z\alpha)^2\frac{m_e}{m_\mu} + \frac{1}{2}\left(A_1^{(4)} - \frac{1}{4}\right)(Z\alpha)^2\left(\frac{\alpha}{\pi}\right)^2 - \frac{5}{12}(Z\alpha)^2\left(\frac{\alpha}{\pi}\right)\frac{m_e}{m_\mu} - \frac{1}{2}(1+Z)(Z\alpha)^2\left(\frac{m_e}{m_\mu}\right)^2 + \ldots, \tag{194}$$

$$\frac{g_\mu(Mu)}{g_\mu} = 1 - \frac{1}{3}\alpha(Z\alpha) - \frac{97}{108}\alpha(Z\alpha)^3 + \frac{1}{2}\alpha(Z\alpha)\frac{m_e}{m_\mu} + \frac{1}{12}\alpha(Z\alpha)\left(\frac{\alpha}{\pi}\right)\frac{m_e}{m_\mu} - \frac{1}{2}(1+Z)\alpha(Z\alpha)\left(\frac{m_e}{m_\mu}\right)^2 + \ldots. \tag{195}$$

Helium-3:

$$\frac{\mu_h(^3He)}{\mu_h} = 1 - 59.967\,43(10)\times 10^{-6}, \tag{196}$$

which has been calculated by Rudziński, Puchalski, and Pachucki (2009). However, this ratio is not used as an input datum because it is not coupled to any other data, but allows the Task Group to provide a recommended value for the unshielded helion magnetic moment along with other related quantities.

Numerical values for the corrections in Eqs. (190) to (195) are listed in Table XIII; uncertainties are negligible. See

RIGHTSLINK

TABLE XIII. Theoretical values for various bound-particle to free-particle g-factor ratios relevant to the 2014 adjustment based on the 2014 recommended values of the constants

Ratio	Value
$g_e(H)/g_e$	$1 - 17.7054 \times 10^{-6}$
$g_p(H)/g_p$	$1 - 17.7354 \times 10^{-6}$
$g_e(D)/g_e$	$1 - 17.7126 \times 10^{-6}$
$g_d(D)/g_d$	$1 - 17.7461 \times 10^{-6}$
$g_e(Mu)/g_e$	$1 - 17.5926 \times 10^{-6}$
$g_\mu(Mu)/g_\mu$	$1 - 17.6254 \times 10^{-6}$

Ivanov, Karshenboim, and Lee (2009) for a negligible additional term.

1. Ratio measurements

The experimental magnetic-moment and bound-state magnetic-moment ratios and magnetic-moment shielding corrections that were used as input data in the 2010 adjustment are used again in the 2014 adjustment; they are *B*30–B35.1, *B*37, and *B*38 in Table XVIII, Sec. XIII. A concise cataloging of these data is given in CODATA-10 and each measurement has been discussed fully in at least one of the previous detailed CODATA reports. The observational equations for these data are given in Table XXIV and the adjusted constants in those equations are identified in Table XXVI, both in Sec. XIII. Any relevant correlation coefficients for these data may be found in Table XIX, also in Sec. XIII. The theoretical bound-particle to free-particle g-factor ratios in the observational equations, which are taken to be exact because their uncertainties are negligible, are given in Table XIII. The symbol μ'_p denotes the magnetic moment of a proton in a spherical sample of pure H_2O at 25 °C surrounded by vacuum; and the symbol μ'_h denotes the magnetic moment of a helion bound in a ^{3}He atom. Although the exact shape and temperature of the gaseous ^{3}He sample is unimportant, we assume that it is spherical, at 25 °C, and surrounded by vacuum.

In general, the bound magnetic moment of a particle, for example, that of p, d, t, or h, is related to its free value by $\mu(\text{bound}) = (1-\sigma)\mu(\text{free})$, where σ is the nuclear magnetic shielding correction or parameter. For the hydrogen-deuterium molecule HD, $\sigma_p(HD)$ and $\sigma_d(HD)$ are the shielding corrections for the proton and deuteron in HD, respectively. Since σ is small, one may define $\sigma_{dp} = \sigma_d(HD) - \sigma_p(HD)$ and write $\mu_p(HD)/\mu_d(HD) = [1 + \sigma_{dp} + \mathcal{O}(\sigma^2)]\mu_p/\mu_d$. This also applies to the hydrogen-tritium or HT molecule: $\sigma_{tp} = \sigma_t(HT) - \sigma_p(HT)$ and $\mu_p(HT)/\mu_t(HT) = [1 + \sigma_{tp} + \mathcal{O}(\sigma^2)]\mu_p/\mu_t$.

Two new relevant data have become available since the closing date of the 2010 adjustment. Garbacz *et al.* (2012) at the University of Warsaw, Warsaw, Poland determined the ratio $\mu_p(HD)/\mu_d(HD)$ by separately measuring, in the same magnetic flux density B, the nuclear magnet resonance (NMR) frequencies $\omega_p(HD)$ and $\omega_d(HD)$ of the proton and deuteron in HD. Their result is

$$\frac{\mu_p(HD)}{\mu_d(HD)} = \frac{1}{2}\frac{\omega_p(HD)}{\omega_d(HD)} = 3.257\,199\,514(21) \quad [6.6 \times 10^{-9}]. \tag{197}$$

The factor 1/2 arises because the spin quantum number for the proton is 1/2 while for the deuteron it is 1. We identify this result, which is taken as an input datum in the 2014 adjustment, as UWars-12; it is item *B*35.2 in Table XVIII and is the second value of this ratio now available with an uncertainty less than 1 part in 10^8. Its observational equation, *B*35 in Table XXIV, is the same as for the other value, identified as StPtrsb-03.

The UWars result was obtained using a technique developed at the university and described by Jackowski, Jaszuński, and Wilczek (2010). The NMR measurements of the frequencies $\omega_p(HD)$ and $\omega_d(HD)$ were carried using a variable gaseous sample that contained HD of a sufficiently low density that the HD-HD molecular interactions were inconsequential and neon of density between 11 mol/L and 2 mol/L so that the observed frequencies could be extrapolated to zero neon density with an uncertainty of 0.5 Hz. The neon was used to increase the pressure of the sample thereby facilitating the NMR measurements. There were no uncertainties of significance from systematic effects (Jackowski, 2015).

The NMR measurements on the HT molecule carried out in St. Petersburg, Russia that led to a value for $\mu_t(HT)/\mu_p(HT)$ with $u_r = 9.4 \times 10^{-9}$ and which was used as an input datum in the 2010 adjustment have continued (Aleksandrov and Neronov, 2011). The new value reported by Neronov and Aleksandrov (2011), which is in agreement with the earlier value, is

$$\frac{\mu_t(HT)}{\mu_p(HT)} = 1.066\,639\,8933(21) \quad [2.0 \times 10^{-9}]. \tag{198}$$

This result, input datum *B*36 in Table XVIII and identified as StPtrsb-11, replaces the earlier result because of its significantly smaller uncertainty. Its observational equation is *B*36 in Table XXIV.

The reduced uncertainty was achieved by decreasing the magnetic field inhomogeneity across the sample and by measuring the difference $\omega_p(HD) - \omega_p(HT)$ using a commercial NMR spectrometer operating at 9.4 T and using the result to determine $\omega_t(HT)/\omega_p(HT)$ from the measured value of $\omega_t(HT)/\omega_p(HD)$. The latter frequency ratio was obtained with a specially designed, laboratory-made spectrometer operating at 2.1 T. Use of HD as a buffer gas in the NMR sample was necessary to reduce the diffusion displacement of the HT molecules. The value given in Eq. (198) is the mean of 10 individual values and its assigned uncertainty is the simple standard deviation of these values rather than that of their mean as initially assigned by Neronov and Aleksandrov (2011). This uncertainty, chosen by the Task Group to better reflect possible systematic effects, was discussed with and accepted by Neronov (2015).

For completeness, we briefly mention new and potentially relevant data that were not considered for inclusion in the

RIGHTSLINK

2014 adjustment. More accurate theoretical values for σ_{dp} and σ_{tp} were reported by Puchalski, Komasa, and Pachucki (2015) but did not become available until well after the 31 December 2014 closing date of the adjustment. They are $\sigma_{dp} = 20.20(2) \times 10^{-9}$ and $\sigma_{tp} = 24.14(2) \times 10^{-9}$ compared with $\sigma_{dp} = 15(2) \times 10^{-9}$ and $\sigma_{tp} = 20(3) \times 10^{-9}$ used in the adjustment (input data *B*37 and *B*38 in Table XVIII).

Also, the St. Petersburg NMR researchers reported a value for $\omega_h(^3\text{He})/\omega_p(\text{H}_2)$ (Neronov and Seregin, 2012), the NMR frequency ratio of the helion in ^{3}He to that of a proton in H_2, and also for $\sigma_p(\text{H}_2) - \sigma_p(\text{H}_2\text{O})$ (Neronov and Seregin, 2014), the difference in the magnetic screening constants for the proton in H_2 and H_2O. However, the unavailability of detailed uncertainty budgets for these two results precluded their consideration for possible inclusion in the adjustment.

B. Muonium transition frequencies, the muon-proton magnetic-moment ratio μ_μ/μ_p, and muon-electron mass ratio m_μ/m_e

Muonium (Mu) is an atom consisting of a positive muon and an electron in a bound state. Measurements of muonium ground-state hyperfine transitions in a magnetic field provide information on the muon-proton magnetic-moment ratio as well as the muon-electron mass ratio. This information is obtained by an analysis of the Zeeman transition resonances in an applied magnetic flux density.

The theoretical expression for the hyperfine splitting may be factorized into a part that exhibits the main dependence on various fundamental constants and a function $\mathcal{F}$ that depends only weakly on them. We write

$$\Delta\nu_{\text{Mu}}(\text{th}) = \Delta\nu_{\text{F}}\mathcal{F}(\alpha, m_e/m_\mu), \tag{199}$$

where

$$\Delta\nu_{\text{F}} = \frac{16}{3} cR_\infty Z^3\alpha^2 \frac{m_e}{m_\mu}\left(1 + \frac{m_e}{m_\mu}\right)^{-3} \tag{200}$$

is the Fermi formula. In order to identify the source of the terms, some of the theoretical expressions are for a muon with charge Ze rather than e.

1. Theory of the muonium ground-state hyperfine splitting

Presented here is a brief summary of the present theory of $\Delta\nu_{\text{Mu}}$. Complete results of the relevant calculations are given along with references to new work; references to the original literature included in earlier detailed CODATA reports are not repeated.

The general expression for the hyperfine splitting is

$$\Delta\nu_{\text{Mu}}(\text{th}) = \Delta\nu_{\text{D}} + \Delta\nu_{\text{rad}} + \Delta\nu_{\text{rec}} + \Delta\nu_{\text{r-r}} + \Delta\nu_{\text{weak}} + \Delta\nu_{\text{had}}, \tag{201}$$

where the terms labeled D, rad, rec, r-r, weak, and had account for the Dirac, radiative, recoil, radiative-recoil, electroweak, and hadronic contributions to the hyperfine splitting, respectively.

The Dirac equation yields

$$\Delta\nu_{\text{D}} = \Delta\nu_{\text{F}}(1 + a_\mu)\left[1 + \frac{3}{2}(Z\alpha)^2 + \frac{17}{8}(Z\alpha)^4 + \cdots\right], \tag{202}$$

where a_μ is the muon magnetic-moment anomaly.

The radiative corrections are

$$\Delta\nu_{\text{rad}} = \Delta\nu_{\text{F}}(1 + a_\mu)\left[D^{(2)}(Z\alpha)\left(\frac{\alpha}{\pi}\right) + D^{(4)}(Z\alpha)\left(\frac{\alpha}{\pi}\right)^2 + D^{(6)}(Z\alpha)\left(\frac{\alpha}{\pi}\right)^3 + \cdots\right], \tag{203}$$

where the functions $D^{(2n)}(Z\alpha)$ are contributions from n virtual photons. The leading term is

$$D^{(2)}(Z\alpha) = A_1^{(2)} + \left(\ln 2 - \frac{5}{2}\right)\pi Z\alpha + \left[-\frac{2}{3}\ln^2(Z\alpha)^{-2} + \left(\frac{281}{360} - \frac{8}{3}\ln 2\right)\ln(Z\alpha)^{-2} + 16.9037\ldots\right](Z\alpha)^2 + \left[\left(\frac{5}{2}\ln 2 - \frac{547}{96}\right)\ln(Z\alpha)^{-2}\right]\pi(Z\alpha)^3 + G(Z\alpha)(Z\alpha)^3, \tag{204}$$

where $A_1^{(2)} = \frac{1}{2}$, as in Eq. (86). The function $G(Z\alpha)$ accounts for all higher-order contributions in powers of $Z\alpha$; it can be divided into self-energy and vacuum-polarization contributions, $G(Z\alpha) = G_{\text{SE}}(Z\alpha) + G_{\text{VP}}(Z\alpha)$. Yerokhin and Jentschura (2008, 2010) have calculated the one-loop self energy for the muonium hyperfine splitting with the result

$$G_{\text{SE}}(\alpha) = -13.8308(43), \tag{205}$$

which agrees with the value $G_{\text{SE}}(\alpha) = -13.8(3)$ from an earlier calculation by Yerokhin *et al.* (2005), as well as with other previous estimates. The vacuum-polarization part is (Karshenboim, Ivanov, and Shabaev, 1999, 2000)

$$G_{\text{VP}}(\alpha) = 7.227(9) + \cdots, \tag{206}$$

where the dots denote uncalculated Wichmann-Kroll contributions.

For $D^{(4)}(Z\alpha)$, we have

$$D^{(4)}(Z\alpha) = A_1^{(4)} + 0.770\,99(2)\pi Z\alpha + \left[-\frac{1}{3}\ln^2(Z\alpha)^{-2} - 0.6390\ldots \times \ln(Z\alpha)^{-2} + 10(2.5)\right](Z\alpha)^2 + \cdots, \tag{207}$$

where $A_1^{(4)}$ is given in Eq. (87), and the coefficient of $\pi Z\alpha$ has been calculated by Mondéjar, Piclum, and Czarnecki (2010).

The next term is

$$D^{(6)}(Z\alpha) = A_1^{(6)} + \cdots, \tag{208}$$

where the leading contribution $A_1^{(6)}$ is given in Eq. (88), but only partial results of relative order $Z\alpha$ have been calculated (Eides and Shelyuto, 2007). Higher-order functions $D^{(2n)}(Z\alpha)$ with $n > 3$ are expected to be negligible.

RIGHTSLINK

The recoil contribution is

$$\Delta\nu_{\rm rec} = \Delta\nu_{\rm F}\frac{m_{\rm e}}{m_\mu}\left(-\frac{3}{1-(m_{\rm e}/m_\mu)^2}\ln\left(\frac{m_\mu}{m_{\rm e}}\right)\frac{Z\alpha}{\pi}+\frac{1}{(1+m_{\rm e}/m_\mu)^2}\left\{\ln(Z\alpha)^{-2}-8\ln 2+\frac{65}{18}\right.\right.$$
$$\left.+\left[\frac{9}{2\pi^2}\ln^2\left(\frac{m_\mu}{m_{\rm e}}\right)+\left(\frac{27}{2\pi^2}-1\right)\ln\left(\frac{m_\mu}{m_{\rm e}}\right)+\frac{93}{4\pi^2}+\frac{33\zeta(3)}{\pi^2}-\frac{13}{12}-12\ln 2\right]\frac{m_{\rm e}}{m_\mu}\right\}(Z\alpha)^2$$
$$\left.+\left\{-\frac{3}{2}\ln\left(\frac{m_\mu}{m_{\rm e}}\right)\ln(Z\alpha)^{-2}-\frac{1}{6}\ln^2(Z\alpha)^{-2}+\left(\frac{101}{18}-10\ln 2\right)\ln(Z\alpha)^{-2}+40(10)\right\}\frac{(Z\alpha)^3}{\pi}\right)+\cdots, \quad (209)$$

as discussed in CODATA-02.

The radiative-recoil contribution is

$$\Delta\nu_{\rm r\text{-}r} = \Delta\nu_{\rm F}\left(\frac{\alpha}{\pi}\right)^2\frac{m_{\rm e}}{m_\mu}\left\{\left[-2\ln^2\left(\frac{m_\mu}{m_{\rm e}}\right)+\frac{13}{12}\ln\left(\frac{m_\mu}{m_{\rm e}}\right)\right.\right.$$
$$+\frac{21}{2}\zeta(3)+\frac{\pi^2}{6}+\frac{35}{9}\Big]+\Big[\frac{4}{3}\ln^2\alpha^{-2}$$
$$\left.+\left(\frac{16}{3}\ln 2-\frac{341}{180}\right)\ln\alpha^{-2}-40(10)\right]\pi\alpha$$
$$\left.+\left[-\frac{4}{3}\ln^3\left(\frac{m_\mu}{m_{\rm e}}\right)+\frac{4}{3}\ln^2\left(\frac{m_\mu}{m_{\rm e}}\right)\right]\frac{\alpha}{\pi}\right\}$$
$$-\Delta\nu_{\rm F}\alpha^2\left(\frac{m_{\rm e}}{m_\mu}\right)^2\left(6\ln 2+\frac{13}{6}\right)+\cdots, \quad (210)$$

where, for simplicity, the explicit dependence on Z is not shown.

New radiative-recoil contributions arising from all single-logarithmic and nonlogarithmic three-loop corrections are due to Eides and Shelyuto (2014):

$$\Delta\nu_{\rm F}\left(\frac{\alpha}{\pi}\right)^3\frac{m_{\rm e}}{m_\mu}\left\{\left[-6\pi^2\ln 2+\frac{\pi^2}{3}+\frac{27}{8}\right]\ln\frac{m_\mu}{m_{\rm e}}+68.507(2)\right\}$$
$$=-30.99\ \text{Hz}. \quad (211)$$

Additional radiative-recoil corrections have been calculated, but are negligibly small, less than 0.5 Hz. Uncalculated remaining terms of the same order as those included in Eq. (211) are estimated by Eides and Shelyuto (2014) to be about 10 Hz to 15 Hz.

The electroweak contribution due to the exchange of a Z^0 boson is (Eides, 1996)

$$\Delta\nu_{\rm weak} = -65\ \text{Hz}, \quad (212)$$

while for the hadronic vacuum-polarization contribution we have (Nomura and Teubner, 2013)

$$\Delta\nu_{\rm had} = 232.7(1.4)\ \text{Hz}. \quad (213)$$

A negligible contribution (≈0.0065 Hz) from the hadronic light-by-light correction has been given by Karshenboim, Shelyuto, and Vainshtein (2008).

The approach used to evaluate the uncertainty of the theoretical expression for $\Delta\nu_{\rm Mu}$ is described in detail in CODATA-02. The only change for CODATA-14 is that the probable error estimates of uncertainties that were subsequently multiplied by 1.48 to convert them to standard uncertainties (that is, 1 standard deviation estimates) are now assumed to have been standard uncertainty estimates in the first place and are not multiplied by 1.48. This change was motivated by conversations with Eides (2015).

Four sources of uncertainty in $\Delta\nu_{\rm Mu}(\text{th})$ are $\Delta\nu_{\rm rad}$, $\Delta\nu_{\rm rec}$, $\Delta\nu_{\rm r-r}$, and $\Delta\nu_{\rm had}$ in Eq. (201), although the uncertainty in the latter is now so small that it is of only marginal interest. The total uncertainty in $\Delta\nu_{\rm rad}$ is 5 Hz and consists of two components: 4 Hz from an uncertainty of 1 in $G_{\rm VP}(\alpha)$ due to the uncalculated Wichmann-Kroll contribution of order $\alpha(Z\alpha)^3$, and 3 Hz from the uncertainty 2.5 of the number 10 in the function $D^{(4)}(Z\alpha)$.

For $\Delta\nu_{\rm rec}$, the total uncertainty is 64 Hz and is due to three components: 53 Hz from 2 times the uncertainty 10 of the number 40 in Eq. (209) as discussed in CODATA-02; 34 Hz due to a possible recoil correction of order $\Delta\nu_{\rm F}(m_{\rm e}/m_\mu)\times(Z\alpha)^3\ln(m_{\rm e}/m_\mu)$; and 6 Hz to reflect a possible recoil term of order $\Delta\nu_{\rm F}(m_{\rm e}/m_\mu)\times(Z\alpha)^4\ln^2(Z\alpha)^{-2}$.

The total uncertainty in $\Delta\nu_{\rm r-r}$ is 55 Hz, with 53 Hz from 2 times the uncertainty 10 of the number −40 in Eq. (210) as above, and 15 Hz as discussed in connection with the newly included radiative-recoil contribution, Eq. (211). The uncertainty of $\Delta\nu_{\rm had}$ is 1.4 Hz from Eq. (213). The final uncertainty in $\Delta\nu_{\rm Mu}(\text{th})$ is thus

$$u[\Delta\nu_{\rm Mu}(\text{th})] = 85\ \text{Hz}. \quad (214)$$

For the least-squares calculations, we use as the theoretical expression for the hyperfine splitting

$$\Delta\nu_{\rm Mu}(\text{th}) = \Delta\nu_{\rm Mu}\left(R_\infty, \alpha, \frac{m_{\rm e}}{m_\mu}, a_\mu\right)+\delta_{\rm Mu}, \quad (215)$$

where the input datum for the additive correction $\delta_{\rm Mu} = 0(85)$ Hz, which accounts for the uncertainty of the theoretical expression, is data item *B*28 in Table XVIII.

The above theory yields

$$\Delta\nu_{\rm Mu} = 4\,463\,302\,868(271)\ \text{Hz}\quad[6.1\times10^{-8}] \quad (216)$$

using values of the constants obtained from the 2014 adjustment without the two measured values of $\Delta\nu_{\rm Mu}$ discussed in the following section. The main source of uncertainty in this value is the mass ratio $m_{\rm e}/m_\mu$.

RIGHTSLINK

2. Measurements of muonium transition frequencies and values of μ_μ/μ_p and m_μ/m_e

The two most precise determinations of muonium Zeeman transition frequencies were carried out at the Clinton P. Anderson Meson Physics Facility at Los Alamos (LAMPF), New Mexico, USA, and were reviewed in detail in CODATA-98. The results are as follows.

Data reported in 1982 by Mariam (1981) and Mariam *et al.* (1982) are

$$\Delta\nu_{Mu} = 4\,463\,302.88(16)\ \text{kHz} \quad [3.6\times10^{-8}], \tag{217}$$

$$\nu(f_p) = 627\,994.77(14)\ \text{kHz} \quad [2.2\times10^{-7}], \tag{218}$$

$$r[\Delta\nu_{Mu}, \nu(f_p)] = 0.227, \tag{219}$$

where f_p is 57.972 993 MHz, corresponding to the magnetic flux density of about 1.3616 T used in the experiment, and $r[\Delta\nu_{Mu}, \nu(f_p)]$ is the correlation coefficient of $\Delta\nu_{Mu}$ and $\nu(f_p)$. The data reported in 1999 by Liu *et al.* (1999) are

$$\Delta\nu_{Mu} = 4\,463\,302\,765(53)\ \text{Hz} \quad [1.2\times10^{-8}], \tag{220}$$

$$\nu(f_p) = 668\,223\,166(57)\ \text{Hz} \quad [8.6\times10^{-8}], \tag{221}$$

$$r[\Delta\nu_{Mu}, \nu(f_p)] = 0.195, \tag{222}$$

where f_p is 72.320 000 MHz, corresponding to the flux density of approximately 1.7 T used in the experiment, and $r[\Delta\nu_{Mu}, \nu(f_p)]$ is the correlation coefficient of $\Delta\nu_{Mu}$ and $\nu(f_p)$. The data in Eqs. (217), (218), (220), and (221) are data items *B*27.1, *B*25, *B*27.2, and *B*26, respectively, in Table XVIII.

The expression for the magnetic-moment ratio is

$$\frac{\mu_{\mu^+}}{\mu_p} = \frac{\Delta\nu_{Mu}^2 - \nu^2(f_p) + 2s_e f_p \nu(f_p)}{4s_e f_p^2 - 2f_p\nu(f_p)} \left(\frac{g_\mu(\text{Mu})}{g_\mu}\right)^{-1}, \tag{223}$$

where $\Delta\nu_{Mu}$ and $\nu(f_p)$ are the sum and difference of two measured transition frequencies, f_p is the free proton NMR reference frequency corresponding to the flux density used in the experiment, $g_\mu(\text{Mu})/g_\mu$ is the bound-state correction for the muon in muonium given in Table XIII, and

$$s_e = \frac{\mu_e}{\mu_p}\frac{g_e(\text{Mu})}{g_e}, \tag{224}$$

where $g_e(\text{Mu})/g_e$ is the bound-state correction for the electron in muonium given in the same table.

The muon to electron mass ratio m_μ/m_e and the muon to proton magnetic-moment ratio μ_μ/μ_p are related by

$$\frac{m_\mu}{m_e} = \left(\frac{\mu_e}{\mu_p}\right)\left(\frac{\mu_\mu}{\mu_p}\right)^{-1}\left(\frac{g_\mu}{g_e}\right). \tag{225}$$

A least-squares adjustment using the LAMPF data, the 2014 recommended values of R_∞, μ_e/μ_p, g_e, and g_μ, together with Eqs. (199), (200) and Eqs. (223) to (225), yields

$$\frac{\mu_{\mu^+}}{\mu_p} = 3.183\,345\,24(37) \quad [1.2\times10^{-7}], \tag{226}$$

$$\frac{m_\mu}{m_e} = 206.768\,276(24) \quad [1.2\times10^{-7}], \tag{227}$$

$$\alpha^{-1} = 137.036\,0013(79) \quad [5.8\times10^{-8}]. \tag{228}$$

The muonium value of α in Eq. (228) is compared to other values in Table XX.

The uncertainty of m_μ/m_e in Eq. (227) is nearly 5 times as large as the uncertainty of the 2014 recommended value and follows from Eqs. (223) to (225). It has the same relative uncertainty as the moment ratio in Eq. (226). However, taken together the experimental value of and theoretical expression for the hyperfine splitting essentially determine the value of the product $\alpha^2 m_e/m_\mu$, as is evident from Eqs. (199) and (200), with an uncertainty dominated by the 1.9×10^{-8} relative uncertainty in the theory.

On the other hand, in the full least-squares adjustment the value of α is determined by other data which in turn determines the value of m_μ/m_e with a significantly smaller uncertainty than that of Eq. (227).

VII. Quotient of Planck Constant and Particle Mass $h/m(X)$ and α

A value of the fine-structure constant α can be obtained from a measurement of $h/m(X)$ through the expression

$$\alpha = \left[\frac{2R_\infty}{c}\frac{A_r(X)}{A_r(e)}\frac{h}{m(X)}\right]^{1/2}, \tag{229}$$

which follows from the definition of the Rydberg constant $R_\infty = \alpha^2 m_e c/2h$, and where $A_r(X)$ is the relative atomic mass of particle X with mass $m(X)$. The relative standard uncertainties of R_∞ and $A_r(e)$ are about 6×10^{-12} and 3×10^{-11}, respectively, and the relative uncertainty of the relative atomic mass of a number of atoms is a few times 10^{-10} or less. Hence, a measurement of $h/m(X)$ with u_r of 1×10^{-9} can provide a value of α with the highly competitive relative uncertainty of 5×10^{-10}.

Two values of $h/m(X)$ obtained using atom interferometry techniques were initially included as input data in CODATA-10 and the same values are initially included in CODATA-14. The first value is the result for $h/m(^{133}\text{Cs})$ obtained at Stanford University, Stanford, California, USA, reported by Wicht *et al.* (2002) with $u_r = 1.5\times10^{-8}$. This experiment is discussed in CODATA-06 and the result is input datum *B*46 in Table XVIII, Sec. XIII, and is labeled StanfU-02. The value of α inferred from it with $u_r = 7.7\times10^{-9}$ is given in Table XX.

The Stanford result for $h/m(^{133}\text{Cs})$ was not included as an input datum in the final adjustment on which the 2010 recommended values are based because of its low weight, and is omitted from the 2014 final adjustment for the same reason. However, it is discussed in order to provide a complete picture of the available data relevant to α.

The second value of $h/m(X)$, which is included in the final 2014 adjustment, is the result for $h/m(^{87}\text{Rb})$ determined at LKB in Paris with $u_r = 1.2\times10^{-9}$ and reported by Bouchendira

RIGHTSLINK

et al. (2011). The experiment is discussed in CODATA-10 and the result, labeled LKB-11, is datum *B*48 in Table XVIII; the value of α inferred from it with $u_r = 6.2 \times 10^{-10}$ is given in Table XX. Although it has the second smallest uncertainty of the 14 values of α in that table, its uncertainty is still about 2.6 times that of the value with the smallest uncertainty, that from the Harvard University measurement of a_e. Nevertheless, the comparison of the values of α from the two experiments provides a useful test of the QED theory of a_e. Such a comparison is discussed in Sec. XV.B of the Summary and Conclusions portion of this report.

We conclude this section by noting that a value of $h/m(^{133}\mathrm{Cs})$ with $u_r = 4.0 \times 10^{-9}$ can in principle be obtained from the measurement by Lan *et al.* (2013) of the Compton frequency of the mass of the cesium-133 atom $\nu_C(^{133}\mathrm{Cs})$ using atom interferometry since $h/m(^{133}\mathrm{Cs}) = c^2/\nu_C(^{133}\mathrm{Cs})$. However, Müller (2015) informed the Task Group that small corrections have recently been identified that were not included in the reported result and consequently it should not be considered. A new result with a highly competitive uncertainty is anticipated.

VIII. Electrical Measurements

The principal focus of this portion of the paper is the several moving-coil watt-balance (or simply watt-balance) measurements of $K_J^2 R_K = 4/h$ that have become available in the past 4 years, where $K_J = 2e/h$ is the Josephson constant and $R_K = h/e^2 = \mu_0 c/2\alpha$ is the von Klitzing constant. Nevertheless, the 13 legacy electrical input data that were initially included in the 2010 adjustment in order to investigate data robustness and the exactness of the relations $K_J = 2e/h$ and $R_K = h/e^2$ but were omitted from the final adjustment on which the 2010 recommended values are based because of their low weight are again initially included in the 2014 adjustment for the same purpose. These input data are items *B*39.1 through *B*43.5 and *B*45 in Table XVIII, Sec. XIII. They are five measurements of the gyromagnetic ratio of the proton and helion by the low and high field methods, five measurements of R_K using a calculable capacitor, one measurement of K_J using a mercury electrometer and another using a capacitor voltage balance, and one measurement of the Faraday constant using a silver dissolution electrometer. A brief explanation of these different kinds of measurements and a more detailed cataloging of the 13 data are given in CODATA-10 and each measurement has been discussed fully in at least one of the previous four detailed CODATA reports. The observational equations for these 13 data are *B*39 – *B*43 and *B*45 in Table XXIV and the adjusted constants in those equations are in Table XXVI, both in Sec. XIII. Any relevant correlation coefficients for these data are listed in Table XIX, also in Sec. XIII. Table XX or XXI in Sec. XIII.A compares the data among themselves and with other data through the values of either α or h that they infer. Three comments are in order before beginning the discussion of individual watt-balance experiments.

First, some watt-balance researchers find it useful to define the exact, conventional value of the Planck constant $h_{90} = 4/K_{J-90}^2 R_{K-90} = 6.626\,068\,854\ldots \times 10^{-34}$ J s to express the results of their watt-balance determinations of $K_J^2 R_K$ and hence h (see Table I, Sec. II).

Second, it was discovered that the unit of mass disseminated by the International Bureau of Weights and Measures (BIPM), Sèvres, France, starting about 2000 and extending into 2014 gradually became offset from the SI unit of mass. The latter is defined by assigning to the mass of the international prototype of the kilogram (IPK), which is maintained at the BIPM, the value 1 kg exactly (Stock *et al.*, 2015). The discovery was made during the Extraordinary Calibration Campaign undertaken at the BIPM to ensure that watt-balance measurements of h and the x-ray-crystal-density (XRCD) determinations of N_A (see Sec. IX.B) are closely tied to the IPK in preparation for the adoption of the new SI by the 26th CGPM in 2018. The BIPM working standards used to calibrate client standards had lost mass and in 2014 were offset from the mass of the IPK by 35 μg. As a consequence, some watt-balance values of h had to be decreased by 35 parts in 10^9 and the XRCD values of N_A had to be increased by a similar amount.

Our third comment has to do with the measurement of g, the local acceleration due to gravity. The basic watt-balance equation is $UI = m_s g v$, where U is the voltage induced between the terminals of a coil moving in a magnetic flux density B with velocity v; and I is the current in the coil in the same flux density B when the force on the coil due to I and B just balances the weight $m_s g$ of a standard of mass m_s. Although commercial absolute free-fall gravimeters that use optical interferometry to measure the position of a falling reflector are capable of determining g with a relative uncertainty of a few parts in 10^9, recently there has been concern about the correction due to the finite speed of the propagation of light, or so-called "speed of light correction." This correction for a 20 cm drop is usually about 1 part in 10^8. In particular, Rothleitner, Niebauer, and Francis (2014) claim that the correction normally applied for this effect is too large by a third. However, Baumann *et al.* (2015) have recently carried out a very extensive theoretical and experimental investigation of the problem and have convincingly shown that this is not the case.

The resulting values of $K_J^2 R_K$ from the seven watt-balance experiments we consider are items *B*44.1–B44.7 in Table XVIII, Sec. XIII. This quantity is the actual input datum employed in least-squares calculations using as its observational equation $K_J^2 R_K \doteq 4/h$. The resulting values of h are compared with each other and with inferred values of h from other experiments in Table XXI, Sec. XIII.A.

A. NPL watt balance

There are two watt-balance results from the National Physical Laboratory (NPL), Teddington, UK, both with relative standard uncertainties $u_r = 2.0 \times 10^{-7}$. NPL-90, item *B*44.1 in Table XVIII, is discussed in CODATA-98 and is from the first truly high-accuracy watt-balance experiment carried out (Kibble, Robinson, and Belliss, 1990). The design of the NPL Mark I apparatus was unique in that the moving coil consisted of two flat rectangular coils above one another in a vertical plane and hung between the poles of a conventional electromagnet.

RIGHTSLINK

Item *B*44.5, NPL-12, is discussed in CODATA-10 and was obtained using the NPL Mark II watt balance. This apparatus has cylindrical symmetry about a vertical axis and employs a horizontal circular coil hung in the gap between two concentric annular permanent magnets (Robinson, 2012); some details of the balance are given in CODATA-98. Just prior to the transfer of the apparatus to the National Research Council (NRC), Ottawa, Canada, in the summer of 2009, Robinson (2012) identified two possible systematic effects in the weighing mode of the experiment. Lack of time necessitated taking them into account by including a comparatively large additional uncertainty component in the experiment's uncertainty budget, which in turn led to the final comparatively large uncertainty of the final result. Although this value has not been corrected for the BIPM mass-standard problem discussed above, it is of little consequence because of the small size of the correction compared with the final uncertainty. The correlation coefficient of the NPL-90 and NPL-12 results is 0.0025 and thus they are only slightly correlated (Robinson, 2012).

B. METAS watt balance

Reported by Eichenberger *et al.* (2011), the result from the Federal Institute for Metrology (METAS), Bern-Wabern, Switzerland, item *B*44.3 with identification METAS-11, is discussed in CODATA-10. Its relative uncertainty of 2.9×10^{-7} was too large for it to be included in the 2010 final adjustment but is initially included in the 2014 adjustment for tests of data robustness and the exactness of the Josephson and quantum-Hall-effect relations $K_J = 2e/h$ and $R_K = h/e^2$. No correction for the mass-standard problem has been made to this result; because of the comparatively large uncertainty of METAS-11, it is of no consequence.

C. LNE watt balance

The Laboratoire National de Métrologie et d'Essais (LNE), Trappes, France, initiated its watt-balance project in 2001. The various elements of the LNE balance were developed with continued characterization and improvements of each. The first result became available in a preprint in December 2014 and is

$$h = 6.626\,0688(17)\times10^{-34}\ \text{J s}\quad[2.6\times10^{-7}], \tag{230}$$

which is equivalent to

$$K_J^2R_K = 6.036\,7619(15)\times10^{33}\ \text{J}^{-1}\,\text{s}^{-1}\quad[2.6\times10^{-7}]. \tag{231}$$

The result was subsequently published by Thomas *et al.* (2015), but although the value of h remained the same as in the preprint, the relative uncertainty was increased to 3.1×10^{-7} with a corresponding increase in the absolute uncertainty. The preprint uncertainty is used in all calculations, but with no significant consequence because of its comparatively large size. Indeed, because of its low weight, the LNE result as given in Eq. (231), which is item *B*44.7 with identification LNE-15 in Table XVIII, is omitted from the 2014 final adjustment. It should also be noted that Thomas *et al.* (2015) have not corrected the LNE result for the BIPM mass-standard shift, which in the LNE case is only −3.7 parts in 10^9.

The LNE watt balance uses a cylindrical geometry and a permanent magnet as does the NPL Mark II balance. One of its unique features is that during the moving-coil mode, the balance beam and its suspension used in the weighing mode is moved as a single element, which avoids using the balance beam to move the coil. Details of the balance, which was operated in air to obtain its first result but has the capability to operate in vacuum, are given in the paper by Thomas *et al.* (2015) and the references cited therein. The two largest uncertainty components, in parts in 10^7, are 2.4 for the voltage measurements and 1.2 for the velocity measurement, which includes the correction for the refractive index of air and the verticality of the laser beams.

D. NIST watt balance

There are two watt-balance results from NIST to be considered. NIST-98, item *B*44.2 with $u_r = 8.7\times10^{-8}$, is discussed in CODATA-98 and was obtained using the second generation NIST watt balance called NIST-2 (Williams *et al.*, 1998). In this apparatus an axially symmetric radial magnetic flux density is generated by a specially designed, 1.5 m high magnet consisting of upper and lower superconducting solenoids and smaller compensating windings mounted in a Dewar; the moving coil is circular, mounted horizontally in air, and encircles the Dewar.

After the publication of this result the NIST researchers not only renovated the facility in which the apparatus was used but completely reconstructed it with little remaining of the earlier NIST-2 watt balance, the major exception being the superconducting magnet. In the new watt balance, called NIST-3 and discussed in CODATA-06, the entire balance mechanism and coil are in vacuum. The new apparatus was subsequently used to obtain a result for $K_J^2R_K$ that turned out to be identical to the 1998 result but with $u_r = 3.6\times10^{-8}$ (Steiner *et al.*, 2007). This result, with identification NIST-07 and discussed in CODATA-06, was included in both the 2006 and 2010 final adjustments. However, in the 2006 final adjustment, because of the inconsistencies among several data that contributed to the determination of h, including NIST-98 and NIST-07 and the measurement of the molar volume of natural silicon by the International Avogadro Coordination (IAC), their uncertainties were increased by the expansion factor 1.5 to reduce the relevant residuals to less than 2. Similar inconsistencies were present in 2010, especially between NIST-07 and the newly reported XRCD result for N_A by the IAC denoted IAC-11. As a consequence, the expansion factor used in the 2010 final adjustment was increased to 2.

NIST researchers were well aware of this problem and of the disagreement of NIST-07 with the NRC watt-balance result NRC-12 reported in early 2012 by Steele *et al.* (2012). They were also aware of the fact that NIST-3 had produced stable values of h from October 2004 to March 2010 when the value suddenly changed for no apparent reason. To address these issues, NIST experimenters carried out six series of new measurements lasting between 3 days and 3 weeks starting in

RIGHTSLINK

December 2012 and ending in November 2013 with the aim of producing an independent value. To this end, the measurements were conducted blindly and NIST-3 was first closely inspected and a number of significant changes made to it in order to improve its performance, as described by Schlamminger *et al.* (2014). The result of this effort as reported in the latter paper and denoted NIST-14 is in reasonable agreement with NRC-12 and IAC-11, and its uncertainty $u_r = 4.5 \times 10^{-8}$ is less than 5 parts in 10^8.

To answer the question "What is the best value of $K_J^2 R_K$, and hence h, that can be deduced from 10 years of NIST-3 data?" Schlamminger *et al.* (2015) thoroughly reviewed all such data after correcting the new 2012 to 2013 data downward by the fractional amount 35×10^{-9} to account for the BIPM mass-standard shift. They divide the data into three epochs, 2004 to 2009, 2010 to 2011, and 2012 to 2013, calculate the result for each epoch, and take as the best value the average of the three. For the uncertainty they take the relative uncertainty 4.5×10^{-8} of NIST-14 and combine it in quadrature with an additional component of 3.5×10^{-8}, which is one-half the approximate 7×10^{-8} fractional difference between NIST-07 and the average of the three individual values. This additional component is to account for the lack of understanding of the cause of the 7 parts in 10^8 difference. Thus following Schlamminger *et al.* (2015), we employ for the NIST-3 result

$$h = h_{90}[1 + 77(57) \times 10^{-9}], \tag{232}$$

which is equivalent to

$$h = 6.626\,069\,36(38) \times 10^{-34}\ \text{J s} \quad [5.7 \times 10^{-8}], \tag{233}$$

$$K_J^2 R_K = 6.036\,761\,43(34) \times 10^{33}\ \text{J}^{-1}\,\text{s}^{-1} \quad [5.7 \times 10^{-8}], \tag{234}$$

where this last value is item *B*44.4 in Table XVIII with identification NIST-15. The NIST-98 and NIST-15 values of $K_J^2 R_K$ are correlated and Schlamminger *et al.* (2015) estimate their correlation coefficient to be 0.09. This coefficient is included in Table XIX and is used in all relevant calculations.

E. NRC watt balance

The entire NPL Mark II apparatus was dismantled and shipped to NRC in the summer of 2009 where in due course it was reassembled and recommissioned in a newly constructed laboratory. A first result with $u_r = 6.5 \times 10^{-8}$ was obtained and reported by Steele *et al.* (2012). This result includes experimentally measured corrections for the effect of the stretching of the beryllium copper flexures that support the moving coil under load, and for the effect of the tilting of the support base of the balance when the mass lift is loaded and unloaded. These are the effects that Robinson (2012) had identified but because of a lack of time could only take into account through a comparatively large additional uncertainty component. The corrections could not be retroactively applied to the NPL-12 result, because a new set of flexures were installed after the balance arrived at NRC as a result of an accident that damaged the original flexures. Subsequently, as described by Sanchez *et al.* (2013), modifications were made to the balance that reduced these effects to a negligible level.

NRC experimenters continued to make important improvements to the NRC watt balance and subsequently carried out four measurement campaigns between September and December 2013 using four different mass standards (Sanchez *et al.*, 2014). They are a 1 kg gold-plated copper cylinder, a 500 g diamond turned silicon cylinder, a 500 g gold-plated piece of copper, and a 250 g piece of silicon. The data set for each consists of 142, 111, 107, and 148 data points, obtained over 14, 11, 15 and 15, days, respectively. The Type A (statistical) uncertainty for the four values of h/h_{90} obtained from each of the four mass standards is taken to be the standard deviation of the mean of each day's result from that standard. The Type B uncertainty (from systematic effects) for each value of h/h_{90} is based on an uncertainty budget containing 51 components distributed over seven major categories. For the result from the Au-Cu 1 kg mass standard, the four largest in parts in 10^9 are 9.0 for the mass of the standard, 6.9 for resistance, 5.9 for alignment, and 5.7 for gravimetry. The latter two topics are discussed in detail by Liard *et al.* (2014) and Sanchez and Wood (2014). The total relative uncertainty for h/h_{90} obtained from the 14 individual values determined using this mass standard is 14.4×10^{-9}. The 35 parts in 10^9 reduction of the NRC value of h/h_{90} initially reported by Sanchez *et al.* (2014) due to the BIPM mass-standard shift is documented by Sanchez *et al.* (2015) and it is the value given therein that we take as the final result of the NRC experiment:

$$h = h_{90}[1 + 189(18) \times 10^{-9}], \tag{235}$$

which is equivalent to

$$h = 6.626\,070\,11(12) \times 10^{-34}\ \text{J s} \quad [1.8 \times 10^{-8}], \tag{236}$$

$$K_J^2 R_K = 6.036\,760\,76(11) \times 10^{33}\ \text{J}^{-1}\,\text{s}^{-1} \quad [1.8 \times 10^{-8}], \tag{237}$$

where this last value is input datum *B*44.6 in Table XVIII with identification NRC-15. Although the value for h/h_{90} and its uncertainty given by Sanchez *et al.* (2014) were obtained from the four individual values by a somewhat unusual method, an alternate analysis based on the calculation of a weighted mean of correlated values yields essentially the same value and uncertainty (Wood, 2013). As can be seen from Table XXI, the NRC result has the smallest uncertainty of any single determination of h.

For completeness, we note that Xu *et al.* (2016) at the National Institute of Metrology (NIM), Beijing, PRC, recently published a value for h with $u_r = 2.6 \times 10^{-6}$ in agreement with other values but obtained using the generalized joule balance method. This approach, under development at NIM since 2007, is a variant of the watt-balance approach; the reported value is a consequence of the ongoing NIM investigation of the

RIGHTSLINK

feasibility of using a joule balance to achieve a competitive uncertainty.

IX. Measurements Involving Silicon Crystals

The three naturally occurring isotopes of silicon are ^{28}Si, ^{29}Si, and ^{30}Si, and for natural silicon the amount-of-substance fractions $x(^{A}\mathrm{Si})$ of these isotopes are approximately 0.92, 0.05, and 0.03, respectively. Here we discuss experimental results involving nearly perfect natural silicon single crystals as well as nearly perfect highly enriched silicon single crystals for which $x(^{28}\mathrm{Si}) \approx 0.999\,96$.

A. Measurements with natural silicon

The natural silicon results employed in the 2010 adjustment are used in the 2014 adjustment without change. Natural silicon experimental data have been discussed in previous CODATA reports including CODATA-10. The measured quantities of interest are the {220} crystal lattice spacing $d_{220}(X)$ of a number of different crystals X determined in meters using a combined x ray and optical interferometer or XROI; and the fractional differences $[d_{220}(X) - d_{220}(\mathrm{ref})]/d_{220}(\mathrm{ref})$, where ref is a reference crystal, determined using a lattice comparator based on x-ray double crystal nondispersive diffractometry. The eight natural crystals of interest are denoted WASO 4.2a, WASO 04, WASO 17, NRLM3, NRLM4, MO*, ILL, and N, and $d_{220}(X)$ of each is taken to be an adjusted constant (variable) in our least-squares calculations. For simplicity, the simplified forms W4.2a, W04, W17, NR3, and NR4 are used in quantity symbols for the first five crystals.

The CODATA-14 input data for the {220} lattice spacings of MO*, WASO 04, and WASO 4.2a are listed in Table XVIII and are data items *B*60, *B*61, *B*62.1, and *B*62.2, respectively; their identifications are either INRIM-08, INRIM-09, or PTB-81. The input data for the fractional differences of the various crystals of interest are items *B*50–B59 in the same table and are labeled NIST-99, NIST-97, NIST-06, PTB-98, or PTB-03. The correlation coefficients of these data are given in Table XIX and their observational equations may be found in Table XXIV. Item *B*58, the fractional difference between the {220} lattice spacing of an ideal natural silicon crystal d_{220} and $d_{220}(\mathrm{W04})$, is discussed in CODATA-06 following Eq. (312). The laboratories for which INRIM, NIST, and PTB, as well as for FSUJ and NMIJ in subsequent paragraphs, are identifiers may be found in the list of symbols and abbreviations near the end of this paper.

The copper $\mathrm{K}\alpha_1$ x unit, symbol $\mathrm{xu}(\mathrm{CuK}\alpha_1)$, the molybdenum $\mathrm{K}\alpha_1$ x unit, symbol $\mathrm{xu}(\mathrm{MoK}\alpha_1)$, and the ångström star, symbol Å* are historic x-ray units used in the past but still of current interest. They are defined by assigning an exact, conventional value to the wavelength of the $\mathrm{CuK}\alpha_1$, $\mathrm{MoK}\alpha_1$, and $\mathrm{WK}\alpha_1$ x-ray lines when each is expressed in its corresponding unit. These assigned wavelengths for $\lambda(\mathrm{CuK}\alpha_1)$, $\lambda(\mathrm{MoK}\alpha_1)$, and $\lambda(\mathrm{WK}\alpha_1)$ are 1537.400 $\mathrm{xu}(\mathrm{CuK}\alpha_1)$, 707.400 $\mathrm{xu}(\mathrm{MoK}\alpha_1)$, and 0.209 010 0 Å*, respectively. The four experimental input data relevant to these units, which are the measured ratios of $\mathrm{CuK}\alpha_1$, $\mathrm{MoK}\alpha_1$, and $\mathrm{WK}\alpha_1$ wavelengths to the {220} lattice spacings of WASO 4.2a and N, are items *B*68–B71 in Table XVIII; they are labeled either FSUJ/PTB-91, NIST-73, or NIST-79. To obtain recommended values in meters for the units $\mathrm{xu}(\mathrm{CuK}\alpha_1)$, $\mathrm{xu}(\mathrm{MoK}\alpha_1)$, and Å*, they are taken as adjusted constants; the input data are then expressed in terms of these constants and the appropriate {220} lattice spacing of the silicon crystal used to obtain them. The resulting observational equations for these input data are given in Table XXIV.

B. Determination of N_A with enriched silicon

The IAC project to determine N_A using the x-ray-crystal-density (XRCD) method was initiated in 2004 and is being carried out by a group of researchers from a number of different institutions, mostly national metrology institutes.

The first enriched silicon result for N_A from the IAC project, formally published in 2011, was included as an input datum in the 2010 final adjustment and is discussed in CODATA-10. In the IAC work the silicon samples are highly polished, highly pure, and nearly crystographically perfect spheres of nominal mass 1 kg initially designated AVO28-S5 and AVO28-S8. The basic equation for the XRCD determination of N_A using a perfect silicon crystal is

$$N_A = \frac{A_r(\mathrm{Si}) M_u}{\sqrt{8}\, d_{220}^3\, \rho(\mathrm{Si})}. \tag{238}$$

In the IAC experiment, the macroscopic silicon mass density $\rho(\mathrm{Si})$ is obtained from the relation $\rho(\mathrm{Si}) = m_s/V_s$, where m_s is the mass of the sphere and is determined by weighing, and $V_s = (\pi d_s^3/6)$ is the volume of the sphere and is obtained from d_s, the sphere's mean diameter, which is determined by optical interferometry. The lattice spacing d_{220} of the silicon boule from which the sphere was fabricated is measured with an XROI using representative silicon samples from the boule. The mean relative atomic mass of the silicon atoms $A_r(\mathrm{Si})$ is determined from representative samples by measuring the amount-of-substance ratios $R_{29/28} = n(^{29}\mathrm{Si})/n(^{28}\mathrm{Si})$ and $R_{30/28} = n(^{30}\mathrm{Si})/n(^{28}\mathrm{Si})$ using isotope dilution mass spectrometry and calculating $A_r(\mathrm{Si})$ from the well-known values of $A_r(^{A}\mathrm{Si})$.

Two other aspects of the experiment are equally important. Equation (238) applies only to a pure silicon sphere. In practice, the surface of a sphere is contaminated with a physisorbed water layer, a chemisorbed water layer, a carbonaceous layer, and an SiO_2 layer. Thus it is necessary to determine the mass and thickness of these layers so that the measured value of the mass of the sphere m_s and the measured value of the mean diameter of the sphere d_s can be corrected for the surface layers and thereby apply to the silicon core. It is also necessary to characterize the material properties of the silicon, for example, its impurities such as interstial oxygen and substitutional carbon, nonimpurity point defects, dislocations, vacancies, and microscopic voids, and to apply

RIGHTSLINK

corrections to the measured mass of the sphere, {220} lattice spacing, and mean diameter as appropriate.

The IAC researchers continued their work after the publication of their first result and instituted a number of improvements after carefully examining all significant aspects of the experiment. This effort is described in detail by Azuma *et al.* (2015) and in the references cited therein. It is beyond the scope of this review to discuss the many advances made, but two are especially noteworthy. Metallic contaminants in the form of Cu, Ni, and Zn silicide compounds were discovered during the course of the work that led to the 2011 result, most likely arising from the polishing process, and had to be taken into account. This led to an increased uncertainty for the required surface-layer correction. To overcome this problem the spheres were reetched and carefully repolished.

The second improvement involves the determination of the amount-of-substance ratios, and thus the value of $A_r(\mathrm{Si})$. In the new work the ratios were measured independently at PTB, NMIJ, and NIST using a multicollector inductively coupled plasma mass spectrometer and isotope dilution. The solvent and diluent used in the three institutes was tetramethylammonium hydroxide (TMAH), which significantly reduced the baseline level of the ion currents to be measured compared with the levels usually seen with the normally used NaOH. For this and other reasons discussed in detail by Azuma *et al.* (2015), the ratios obtained by Yang *et al.* (2012) using NaOH were not employed in the calculation of the new IAC value of N_A. See Kuramoto *et al.* (2015), Mana *et al.* (2015), Massa *et al.* (2015), Mizushima *et al.* (2015), Pramann *et al.* (2015), Waseda *et al.* (2015), and Zhang *et al.* (2015).

The two new values of N_A reported by Azuma *et al.* (2015) and which are used as input data in the 2014 adjustment are

$$N_A = 6.022\,140\,99(18) \times 10^{23}\ \mathrm{mol}^{-1} \quad [3.0 \times 10^{-8}], \quad (239)$$

$$N_A = 6.022\,140\,76(12) \times 10^{23}\ \mathrm{mol}^{-1} \quad [2.0 \times 10^{-8}]. \quad (240)$$

The first result is the 2011 value used in CODATA-10 increased by 3 parts in 10^8 by Azuma *et al.* (2015) to reflect the recalibration of the mass standards used in its determination as a consequence of the extraordinary calibration campaign against the international prototype of the kilogram discussed in Sec. VIII. The second result is the value reported by Azuma *et al.* (2015) as a consequence of the extensive IAC efforts of the past 4 years and is the weighted mean of the results obtained from spheres AVO28-S5c and AVO28-S8c. (The additional letter c has been added by the researchers to distinguish the reetched and repolished spheres used in the new work from the spheres used in the earlier work.) The uncertainty assigned to the value for N_A obtained from sphere AVO28-S5c is 21 parts in 10^9, and for the value obtained from sphere AVO28-S8c is 23 parts in 10^9. The two largest uncertainty components for AVO28-S5c are 10 parts in 10^9 for surface characterization and 16 parts in 10^9 for sphere volume as calculated from the mean diameter. It should be noted that the two values of N_A are correlated; the IAC researchers report the correlation coefficient to be 0.17 (Mana *et al.*, 2015).

The two values of N_A in Eqs. (239) and (240) are items $B63.1$ and $B63.2$ in Table XVIII with identifiers IAC-11 and IAC-15, the values of h that can be inferred from them are given in Table XXI, and their observational equation, which also shows how h can be derived from N_A, may be found in Table XXIV. How these results compare with other data and their role in the 2014 adjustment are discussed in Sec. XIII.

X. Thermal Physical Quantities

Table XIV summarizes the 11 results for the thermal physical quantities R, k/h, and A_ϵ/R, the molar gas constant, the quotient of the Boltzmann and Planck constants, and the quotient of the molar polarizability of a gas and the molar gas constant, respectively, that are taken as input data in the 2014 adjustment. They are data items $B64.1 - B66$ in Table XVIII with correlation coefficients as given in Table XIX and observational equations as given in Table XXVII. Values of the Boltzmann constant k that can be inferred from these data are given in Table XXII and are graphically compared in Fig. 5.

There are five new input data that contribute to the 2014 determination of the Boltzmann constant, three from acoustic gas thermometry (NPL-13, NIM-13, and LNE-15), one from Johnson noise thermometry (NIM/NIST-15), and one from dielectric-constant gas thermometry (PTB-15). Not every value in Table XIV appears in the cited references. For some, additional digits have been provided to the Task Group to reduce rounding errors; for others, the actual measured value of R is recovered from the reported value of k and the Avogadro constant N_A used by the researchers to calculate k. Finally, some of the input data incorporate changes based upon newly available information, as discussed in Sec. X.A.2.

Since there is no serious discrepant input data for the inferred value of the Boltzmann constant for either the 2010 or 2014 adjustment, the result for k from refractive index gas thermometry (Schmidt *et al.*, 2007) and for k/h from Johnson noise thermometry (Benz *et al.*, 2011) that were initially considered but not included in the final 2010 adjustment due to their large uncertainties are not considered for the 2014 adjustment.

A. Molar gas constant *R*, acoustic gas thermometry

The measurement of R by the method of acoustic gas thermometry (AGT) is based on the following expressions for the square of the speed of sound in a real gas of atoms or molecules in thermal equilibrium at thermodynamic temperature T and pressure p and occupying a volume V:

$$c_a^2(T,p) = A_0(T) + A_1(T)p + A_2(T)p^2 + A_3(T)p^3 + \cdots. \quad (241)$$

Here $A_1(T)$, $A_2(T)$, etc. are related to the density virial coefficients and their temperature derivatives. In the limit $p \to 0$, this becomes

RIGHTSLINK

TABLE XIV. Summary of thermal physical measurements relevant to the 2014 adjustment (see text for details). AGT: acoustic gas thermometry; JNT: Johnson noise thermometry; cylindrical, spherical, quasispherical: shape of resonator used; JE and QHE: Josephson effect voltage and quantum-Hall-effect resistance standards; DCGT: dielectric-constant gas thermometry

Source	Ident.[a]	Quant.	Method	Value	Rel. stand. uncert u_r
Colclough, Quinn, and Chandler (1979)	NPL-79	R	AGT, cylindrical, argon	8.314 504(70) J mol^{-1} K^{-1}	8.4×10^{-6}
Moldover *et al.* (1988)	NIST-88	R	AGT, spherical, argon	8.314 470(15) J mol^{-1} K^{-1}	1.8×10^{-6}
Pitre *et al.* (2009)	LNE-09	R	AGT, quasispherical, helium	8.314 467(23) J mol^{-1} K^{-1}	2.7×10^{-6}
Sutton *et al.* (2010)	NPL-10	R	AGT, quasispherical, argon	8.314 468(26) J mol^{-1} K^{-1}	3.2×10^{-6}
Gavioso *et al.* (2010)	INRIM-10	R	AGT, spherical, helium	8.314 412(63) J mol^{-1} K^{-1}	7.5×10^{-6}
Pitre *et al.* (2011)	LNE-11	R	AGT, quasispherical, argon	8.314 455(12) J mol^{-1} K^{-1}	1.4×10^{-6}
Lin *et al.* (2013)	NIM-13	R	AGT, cylindrical, argon	8.314 455(31) J mol^{-1} K^{-1}	3.7×10^{-6}
de Podesta *et al.* (2013)	NPL-13	R	AGT, quasispherical, argon	8.314 4544(75) J mol^{-1} K^{-1}	9.0×10^{-7}
Pitre *et al.* (2015)	LNE-15	R	AGT, quasispherical, helium	8.314 4615(84) J mol^{-1} K^{-1}	1.0×10^{-6}
Qu *et al.* (2015)	NIM/NIST-15	k/h	JNT, JE and QHE	$2.083\,6658(80)\times10^{10}$ Hz K^{-1}	3.9×10^{-6}
Gaiser, Zandt, and Fellmuth (2015)	PTB-15	A_ϵ/R	DCGT, helium	$6.221\,128(25)\times10^{-8}$ m^3 K J^{-1}	4.0×10^{-6}

[a]NPL: National Physical Laboratory, Teddington, UK; NIST: National Institute of Standards and Technology, Gaithersburg, Maryland, and Boulder, Colorado, USA; LNE: Laboritoire Commun de Métrologie (LCM), Saint-Denis, France, of the Laboratoire National de Métrologie et d'Essais (LNE); INRIM: Instituto Nazionale di Ricerca Metrologica, Torino, Italy; NIM: National Institute of Metrology, Beijing, PRC; PTB: Physikalisch-Technische Bundesanstalt, Braunschweig and Berlin, Germany.

$$c_a^2(T,0) = A_0(T) = \frac{\gamma_0 RT}{A_r(X)M_u}, \tag{242}$$

where $\gamma_0 = c_p/c_V$ is the ratio of the specific heat capacity of the gas at constant pressure to that at constant volume and is 5/3 for an ideal monotonic gas. The basic experimental approach to determining the speed of sound of a gas, usually argon or helium, is to measure the acoustic resonant frequencies of a cavity at or near the triple point of water, $T_{TPW} = 273.16$ K, at various pressures and extrapolating to $p = 0$. The cavities are either cylindrical of fixed or variable length, or spherical, but most commonly quasispherical in the form of a triaxial ellipsoid. This shape removes the degeneracy of the microwave resonances used to measure the volume of the resonator in order to calculate $c_a^2(T, p)$ from the measured acoustic frequencies and the corresponding acoustic resonator eigenvalues known from theory. The cavities are formed by carefully joining hemispherical cavities.

In practice, the determination of R by AGT with a relative standard uncertainty of order 1 part in 10^6 is complex; the application of numerous corrections is required as well as the investigation of many possible sources of error. For a review of the advances made in AGT in the past 25 years, see Moldover *et al.* (2014).

1. New values

a. NIM 2013. Lin *et al.* (2013) report a result for the Boltzmann constant from an improved version of an earlier experiment (Zhang *et al.*, 2011) using argon in a single 80 mm long fixed cylindrical cavity measured by two-color optical interferometry. The shape of the cavity has been made more cylindrical and the thermometry improved. Two different grades of argon with measured relative isotopic abundances were used with two different methods of supporting the cavity. Analysis of the acoustic data was improved by accounting for second-order perturbations to the frequencies from the thermoviscous boundary layer.

The reported calculated value of the Boltzmann constant uses the CODATA-10 value of N_A, implying the measured value

$$R = 8.314\,455(31)\ \text{J mol}^{-1}\ \text{K}^{-1} \quad [3.7\times10^{-6}]. \tag{243}$$

The largest uncertainty component, 2.9 parts in 10^6, is due to inconsistent values determined from the various acoustic modes.

b. NPL 2013. de Podesta *et al.* (2013) used a quasispherical copper triaxial ellipsoid cavity with a nominal radius of 62 mm filled with argon to determine R. The cavity was suspended from the top of a copper container designed to create a nearly isothermal environment. The initial value reported is

$$R = 8.314\,4787(59)\ \text{J mol}^{-1}\ \text{K}^{-1} \quad [7.1\times10^{-7}]. \tag{244}$$

The low uncertainty is attributed to the near-perfect shape and surface condition of the cavity achieved by precise diamond turning techniques during fabrication. The largest uncertainty component, 3.5 parts in 10^7, is from the determination of the molar mass of the argon used in the experiment.

c. LNE 2015. Pitre *et al.* (2015) used a quasispherical copper triaxial ellipsoid cavity with a nominal radius of 50 mm filled with helium. The experiment was performed in quasi-adiabatic thermal conditions, instead of standard, constant heat-flux conditions. The reported calculated value of the Boltzmann constant uses the CODATA-10 value of N_A, implying the measured value

$$R = 8.314\,4615(84)\ \text{J mol}^{-1}\ \text{K}^{-1} \quad [1.0\times10^{-6}]. \tag{245}$$

The dominant source of uncertainty, 6.2 parts in 10^7, arises from the acoustic frequency measurements.

RIGHTSLINK

2. Updated values

The following updates and corrections for the AGT input data are summarized in Moldover, Gavioso, and Newell (2015), along with a detailed description of the correlation coefficients given in Table XIX. The AGT values and uncertainties in Table XIV incorporate all the corrections listed below.

a. Molar mass of argon. During the period from October to December 2014, three important studies on the molar mass of argon $M(\mathrm{Ar})$ were performed to investigate the difference of 2.74 parts in 10^6 between the results from LNE-11 and NPL-13 (Yang *et al.*, 2015). The LNE-11 value is based on $M(\mathrm{Ar})$ determinations from the Institute for Reference Materials and Measurements (IRMM), Geel, Belgium (Valkiers *et al.*, 2010). The NPL-13 estimate of $M(\mathrm{Ar})$ is based on a comparison at the Scottish Universities Environmental Research Centre (SUERC), University of Glasgow, Glasgow, Scotland, of the isotopic composition of the experimental gas with the isotopic composition of argon from atmospheric air (de Podesta *et al.*, 2013), assuming the atmospheric air had the same argon isotopic abundance as the analysis performed by Lee *et al.* (2006) at the Korea Research Institute of Standards and Science (KRISS), Taedoc Science Town, Republic of Korea. The results of these studies were discussed at the meeting of the CIPM Consultative Committee for Thermometry Task Group for the SI (CCT TG-SI) in Eltville, Germany, on 6 February 2015 in conjunction with the 2015 Fundamental Constants Meeting co-organized by the Task Group (Karshenboim, Mohr, and Newell, 2015).

In the first study, the isotopic composition of samples of argon gas previously measured at the IRMM were remeasured. The analysis showed disagreements in values of $M(\mathrm{Ar})$ of up to 3.5 parts in 10^6. In the second study, the isotopic composition of a sample of argon gas used for isotherm 5 of NPL-13 was remeasured. The estimate of $M(\mathrm{Ar})$ was 2.73 parts in 10^6 lower than the corresponding SUERC estimate. In the third study, mass spectrometry measurements were made on a series of argon samples from NIM, INRIM, NPL, NMIJ and LNE on which corresponding speed-of-sound measurements had been made at LNE. The results showed the expected correlation between the two sets of measurements. From this study an inference of the required correction to the SUERC estimate of the NPL-13 isotherm 5 molar mass of −3.6 parts in 10^6 was apparent. However, KRISS considered their direct measurement of this sample to have a lower uncertainty. The inference of the required correction to the LNE-11 $M(\mathrm{Ar})$ was not strong enough to suggest a meaningful change in its value.

Although the estimated relative statistical uncertainty for the KRISS $M(\mathrm{Ar})$ measurements was 0.61×10^{-6}, KRISS considered it likely that the isotope ratio $R(^{38}\mathrm{Ar}/^{36}\mathrm{Ar})$ may be in error because it disagrees distinctly with measurements from Lee *et al.* (2006). For this reason an additional relative uncertainty of 0.35×10^{-6} was added in quadrature to yield an overall relative uncertainty for the KRISS $M(\mathrm{Ar})$ measurements of 0.7×10^{-6}.

Based on the studies at KRISS it was agreed upon by all participants of the CCT TG-SI meeting that for the 2014 CODATA adjustment, the NPL-13 determination of the molar gas constant will rely on the KRISS value and uncertainty of $M(\mathrm{Ar})$, resulting in a fractional correction of -2.73×10^{-6} and a total relative uncertainty of 0.9×10^{-6} (de Podesta *et al.*, 2015). It was also agreed that while the LNE-11 value of the molar gas constant will continue to use the determination of $M(\mathrm{Ar})$ from IRMM, the relative uncertainty will be that of KRISS, namely 0.7×10^{-6}. Similarly since the previous NPL-10 result used the $M(\mathrm{Ar})$ value from IRMM, the relative uncertainty component for $M(\mathrm{Ar})$ for NPL-10 was increased to 0.7×10^{-6}.

b. Molar mass of helium. Based upon the measured $^3\mathrm{He}/^4\mathrm{He}$ abundance ratios spanning 0.05×10^{-6} to 0.5×10^{-6} from samples taken from 12 natural gas wells in the USA (Aldrich and Nier, 1948), the expected reduction in $M(^4\mathrm{He})$ due to naturally occurring $^3\mathrm{He}$ is fractionally from 0.012×10^{-6} to 0.12×10^{-6}. The two gas analyses given in the paper by Gavioso *et al.* (2015) are consistent with this expectation (see Sec. X.D). In contrast, the ratio of speed-of-sound measurements using two different, commercially produced, highly purified helium samples given in the paper reporting LNE-15 differed by the surprisingly large value of 0.44 parts in 10^6. This observation was taken into account by including an additional uncertainty component of 0.5 parts in 10^6. Based upon the possibility that the concentration of $^3\mathrm{He}$ may be higher than expected, an additional relative uncertainty component of 0.5×10^{-6} was incorporated in the LNE-09 result. It should finally be noted that certain natural gases in Taiwan have $^3\mathrm{He}/^4\mathrm{He}$ abundance ratios as large as 3.8×10^{-6} (Sano, Wakita, and Huang, 1986). Clearly, future helium-based low-uncertainty AGT determinations of R must measure the $^3\mathrm{He}$ concentration in the gas samples used.

c. Thermal conductivity of argon. An improved estimate for the thermal conductivity of argon became available for the 2014 CODATA adjustment [see supplementary data in Moldover *et al.* (2014)]. A change in thermal conductivity affects the estimate for the thermal boundary layer thickness close to the wall of the cavity, resulting in a correction for all resonant frequencies at all pressures. For the 2014 CODATA adjustment, these corrections are applied to the lowest uncertainty results for AGT using argon. In parts in 10^6, the corrections to NIST-88 (Moldover, 2015), LNE-11 (Pitre, 2015), and NPL-13 (de Podesta *et al.*, 2015) are −0.16, −0.16, and −0.192, respectively, with inconsequential decreases in the uncertainties.

B. Quotient *k*/*h*, Johnson noise thermometry

The Nyquist theorem predicts that, with a fractional error of less than 1 part in 10^6 at frequencies less than 10 MHz and temperatures greater than 250 K,

$$\langle U^2\rangle = 4kTR_s\Delta f\,. \tag{246}$$

Here $\langle U^2\rangle$ is the mean-square voltage, or Johnson noise voltage, in a measurement bandwidth of frequency Δf across the terminals of a resistor of resistance R_s in thermal equilibrium at thermodynamic temperature T. If $\langle U^2\rangle$ is measured in

RIGHTSLINK

terms of the Josephson constant $K_J = 2e/h$ and R_s in terms of the von Klitzing constant $R_K = h/e^2$, then the measurement yields a value of k/h.

Continuing the pioneering work of Benz *et al.* (2011), Qu *et al.* (2015) report an improved determination of the Boltzmann constant using such a method. The reported value is

$$k_{90} = 1.380\,6513(53) \times 10^{-23}\ \text{J K}^{-1} \quad [3.9 \times 10^{-6}], \qquad (247)$$

where k_{90} in the SI unit J/K is the result of a Johnson noise experiment when the voltage and resistance are measured in conventional electrical units defined by K_{J-90} and R_{K-90}. Following the analysis given in CODATA-98 [see Eqs. (29d) and (317)], it can be shown that $k_{90}/h_{90} = k/h$. Using the value of h_{90} (see the introduction to Sec. VIII), the measured value of k/h is

$$k/h = 2.083\,6658(80) \times 10^{10}\ \text{Hz K}^{-1} \quad [3.9 \times 10^{-6}], \qquad (248)$$

as given in Table XIV.

In the Qu *et al.* (2015) experiment, digitally synthesized pseudonoise voltages V_Q are generated by means of a pulse-biased Josephson junction array. These known voltages are compared to the unknown thermal-noise voltages V_R generated by a specially designed 200 Ω resistor in a well regulated thermal cell at or near T_{TPW}. Since the spectral density of the noise voltage of a 200 Ω resistor at 273.16 K is only 1.74 $\text{nV}\sqrt{\text{Hz}}$, it is measured using a low-noise, two-channel, cross-correlation technique that enables the resistor signal to be extracted from uncorrelated amplifier noise of comparable amplitude and spectral density. The final result is based on measurements integrated over a bandwidth of 575 kHz and a total integration time of about 33 d.

The dominant uncertainty contributions of 3.2 parts in 10^6 and 1.8 parts in 10^6 are from the statistical uncertainty of the $\langle V_R^2/V_Q^2\rangle$ ratio measurement and the ambiguity associated with the spectral mismatch model, respectively.

C. Quotient A_ϵ/R, dielectric-constant gas thermometry

The virial expansion of the equation of state for a real gas of amount of substance n in a volume V is

$$p = \rho RT[1 + \rho B(T) + \rho^2 C(T) + \rho^3 D(T) + \cdots], \qquad (249)$$

where $\rho = n/V$ is the amount-of-substance density of the gas at thermodynamic temperature T, and $B(T)$, $C(T)$, etc. are the virial coefficients. The Clausius-Mossotti equation is

$$\frac{\epsilon_r - 1}{\epsilon_r + 2} = \rho A_\epsilon[1 + \rho B_\epsilon(T) + \rho^2 C_\epsilon(T) + \rho^3 D_\epsilon(T) + \cdots], \qquad (250)$$

where $\epsilon_r = \epsilon/\epsilon_0$ is the relative dielectric constant (relative permittivity) of the gas, ϵ is its dielectric constant, ϵ_0 is the exactly known electric constant, A_ϵ is the molar polarizability of the atoms, and $B_\epsilon(T)$, $C_\epsilon(T)$, etc., are the dielectric virial coefficients. By appropriately combining Eqs. (249) and (250), an expression is obtained from which A_ϵ/R can be experimentally determined by measuring ϵ_r at a known constant temperature such as T_{TPW} and at different pressures and extrapolating to zero pressure.

In practice, dielectric-constant gas thermometry measures the fractional change in capacitance of a specially constructed capacitor, first without helium gas and then with helium gas at a known pressure. The static electric polarizability of a gas atom α_0, A_ϵ, R, and k are related by $A_\epsilon/R = \alpha_0/3\epsilon_0 k$, which shows that if α_0 is known sufficiently well from theory, then a competitive value of k can be obtained if the quotient A_ϵ/R can be measured with a sufficiently small uncertainty.

Piszczatowski *et al.* (2015) have calculated the static electric polarizability of ^{4}He in atomic units to be

$$\alpha_0^*(^4\text{He}) = 1.383\,760\,77(14)\ \text{a. u.} \quad [1.0 \times 10^{-7}], \qquad (251)$$

from which the static electric polarizability of ^{4}He in SI units is

$$\alpha_0(^4\text{He}) = 4\pi\epsilon_0 a_0^3 \alpha_0^*(^4\text{He}), \qquad (252)$$

where a_0 and ϵ_0 are the Bohr radius and electric constant, respectively.

Superseding previous preliminary results (Fellmuth *et al.*, 2011; Gaiser and Fellmuth, 2012), Gaiser *et al.* (2013) report a final value of A_ϵ/R from dielectric-constant gas thermometry with an updated uncertainty given by Gaiser, Zandt, and Fellmuth (2015):

$$A_\epsilon/R = 6.221\,128(25) \times 10^{-8}\ \text{m}^3\,\text{K J}^{-1} \quad [4.0 \times 10^{-6}]. \qquad (253)$$

The dominant uncertainty components are the fitted coefficient from the 10 isotherms (statistical) and the effective compressibility of the capacitor assembly at 2.6 parts in 10^6 and 2.4 parts in 10^6, respectively.

D. Other data

For completeness we note the following result that became available only after the 31 December 2014 closing date of the 2014 adjustment. Gavioso *et al.* (2015) obtained the very competitive value $R = 8.314\,4743(88)\ \text{J mol}^{-1}\,\text{K}^{-1}\,[1.06 \times 10^{-6}]$ using acoustic gas thermometry with a misaligned spherical cavity with a nominal radius of 90 mm filled with helium. This value is 1.47 parts in 10^6 larger than the 2014 CODATA value.

E. Stefan-Boltzmann constant σ

The Stefan-Boltzmann constant is related to c, h, and k by $\sigma = 2\pi^5 k^4/15h^3c^2$, which, with the aid of the relations $k = R/N_A$ and $N_A h = cA_r(e)M_u\alpha^2/2R_\infty$, can be expressed in terms of the molar gas constant and other adjusted constants as

$$\sigma = \frac{32\pi^5 h}{15c^6}\left(\frac{R_\infty R}{A_r(e)M_u\alpha^2}\right)^4. \qquad (254)$$

RIGHTSLINK

TABLE XV. Summary of the results of measurements of the Newtonian constant of gravitation relevant to the 2014 adjustment

Source	Identification[a]	Method	$10^{11}\ G$(m^3 kg^{-1} s^{-2})	Rel. stand. uncert. u_r
Luther and Towler (1982)	NIST-82	Fiber torsion balance, dynamic mode	6.672 48(43)	6.4×10^{-5}
Karagioz and Izmailov (1996)	TR&D-96	Fiber torsion balance, dynamic mode	6.672 9(5)	7.5×10^{-5}
Bagley and Luther (1997)	LANL-97	Fiber torsion balance, dynamic mode	6.673 98(70)	1.0×10^{-4}
Gundlach and Merkowitz (2000, 2002)	UWash-00	Fiber torsion balance, dynamic compensation	6.674 255(92)	1.4×10^{-5}
Quinn *et al.* (2001)	BIPM-01	Strip torsion balance, compensation mode, static deflection	6.675 59(27)	4.0×10^{-5}
Kleinevoß (2002) and Kleinvoß *et al.* (2002)	UWup-02	Suspended body, displacement	6.674 22(98)	1.5×10^{-4}
Armstrong and Fitzgerald (2003)	MSL-03	Strip torsion balance, compensation mode	6.673 87(27)	4.0×10^{-5}
Hu, Guo, and Luo (2005)	HUST-05	Fiber torsion balance, dynamic mode	6.672 22(87)	1.3×10^{-4}
Schlamminger *et al.* (2006)	UZur-06	Stationary body, weight change	6.674 25(12)	1.9×10^{-5}
Luo *et al.* (2009) and Tu *et al.* (2010)	HUST-09	Fiber torsion balance, dynamic mode	6.673 49(18)	2.7×10^{-5}
Parks and Faller (2010)	JILA-10	Suspended body, displacement	6.672 34(14)	2.1×10^{-5}
Quinn *et al.* (2013, 2014)	BIPM-14	Strip torsion balance, compensation mode, static deflection	6.675 54(16)	2.4×10^{-5}
Prevedelli *et al.* (2014) and Rosi *et al.* (2014)	LENS-14	Double atom interferometer gravity gradiometer	6.671 91(99)	1.5×10^{-4}
Newman *et al.* (2014)	UCI-14	Cryogenic torsion balance, dynamic mode	6.674 35(13)	1.9×10^{-5}

[a]NIST: National Institute of Standards and Technology, Gaithersburg, Maryland, and Boulder, Colorado, USA; TR&D: Tribotech Research and Development Company, Moscow, Russian Federation; LANL: Los Alamos National Laboratory, Los Alamos, New Mexico, USA; UWash: University of Washington, Seattle, Washington, USA; BIPM: International Bureau of Weights and Measures, Sèvres, France; UWup: University of Wuppertal, Wuppertal, Germany; MSL: Measurement Standards Laboratory, Lower Hutt, New Zealand; HUST: Huazhong University of Science and Technology, Wuhan, PRC; UZur: University of Zurich, Zurich, Switzerland; JILA: JILA, University of Colorado and National Institute of Standards and Technology, Boulder, Colorado, USA; LENS: European Laboratory for Non-Linear Spectroscopy, University of Florence, Florence, Italy; UCI: University of California, Irvine, Irvine, California, USA.

Since no competitive directly measured value of σ is available for the 2014 adjustment, the 2014 recommended value is obtained from this equation.

XI. Newtonian Constant of Gravitation *G*

Table XV summarizes the 14 measured values of the Newtonian constant of gravitation G of interest in the 2014 adjustment. Because the values are independent of the other data relevant to the current adjustment, and because there is no known quantitative theoretical relationship between G and other adjusted constants, they contribute only to the determination of the 2014 recommended value of G. The calculation of this value is discussed in Sec. XIII.B.1.

While three new values for G have become available for the 2014 CODATA adjustment, the data remain discrepant. The first is a competitive result from the International Bureau of Weights and Measures (BIPM) (Quinn *et al.*, 2013, 2014) obtained using a similar but completely rebuilt apparatus as was used to obtain the BIPM 2001 result. The second, based on a unique technique involving atom interferometry, is from the European Laboratory for Non-linear Spectroscopy (LENS) (Prevedelli *et al.*, 2014; Rosi *et al.*, 2014). Although not competitive, the conceptually different approach could help identify errors that have proved elusive in other experiments. The third is from the University of California, Irvine (Newman *et al.*, 2014) and is a highly competitive result from data collected over a 7-year span using a cryogenic torsion balance.

The previously reported measurements of G as discussed in past Task Group reports remain unchanged with one exception. It was discovered that the reported correlation coefficient between the 2005 and 2009 result from the Huazhong University of Science and Technology, HUST-05 and HUST-09, was unphysical. As described below, a reexamination of the uncertainty analysis has led to slight reductions in the HUST-05 value and in the correlation coefficient of the two results.

For simplicity, in the following text, we write G as a numerical factor multiplying G_0, where

$$G_0 = 10^{-11}\ \text{kg}^{-1}\,\text{m}^3\,\text{s}^{-2}. \tag{255}$$

A. Updated values

1. Huazhong University of Science and Technology

The initially assigned covariance of the HUST-05 and HUST-09 values of G exceeded the variance of the HUST-09 value which had the smaller uncertainty of the two. As a result the weighted mean of the two values was outside the interval between them, which is unphysical (Cox *et al.*, 2006; Bich, 2013).

In collaboration with the HUST researchers, the uncertainty budgets and corrections of both the HUST-05 and HUST-09 measurements were reviewed. Upon further examination, the 2010 correlation coefficient between HUST-05 and HUST-09 of 0.234 contained a misassigned contribution due to fiber anelasticity of 0.098. While the suspension fibers in both experiments were 25 μm diameter tungsten wire, the individual wires used were different. Moreover the HUST-05

RIGHTSLINK

anelasticity correction was estimated from the pendulum quality factor Q as predicted by Kuroda (1995), whereas for HUST-09 it was directly measured (Luo *et al.*, 2009). After careful reevaluation of all correlations and removing the anelasticity correction, the correlation coefficient between HUST-05 and HUST-09 was reduced to 0.134.

Since the Q for the HUST-05 torsion pendulum was approximately 3.6×10^4, the positive bias due to fiber anelasticity was originally neglected. For the 2014 adjustment, the HUST-05 value has been reduced by 8.8 parts in 10^6 based on the Kuroda correction with the result that the HUST-05 input datum is now

$$G = 6.672\,22(87)G_0 \quad [1.3 \times 10^{-4}]. \tag{256}$$

B. New values

1. International Bureau of Weights and Measures

A new result from the BIPM, labeled BIPM-14, has been reported by Quinn *et al.* (2013, 2014) using the same principles of a flexure strip torsion balance operating in either of two different modes as in the previous BIPM experiment: compensation mode (cm) and deflection mode (dm) (Quinn *et al.*, 2001). However, almost all of the apparatus was rebuilt or replaced. Extensive tests were performed and improvements made on key parameters, including test and source mass coordinates, calibration of angle measurements, calibration of ac voltage and capacitance electrical instruments, timing measurements for period of oscillation, and precision of torque measurements. With all identified errors taken into account, the results for the two modes are

$$G_{\rm cm} = 6.675\,15(41)G_0 \quad [6.1 \times 10^{-5}], \tag{257}$$

$$G_{\rm dm} = 6.675\,86(36)G_0 \quad [5.4 \times 10^{-5}]. \tag{258}$$

The largest uncertainty component for each mode is 47 parts in 10^6 from angle measurements, but the angle measurements are anticorrelated between the two modes. Taking into consideration all correlations, the reported weighted mean and uncertainty from the two modes is

$$G = 6.675\,54(16)G_0 \quad [2.4 \times 10^{-5}], \tag{259}$$

which agrees well with the 2001 BIPM result. This agreement is noteworthy, because only the source masses and their carousel in the original apparatus were not replaced; the source masses were reduced in height and remeasured, and the experiment was also rebuilt in a different BIPM laboratory. Quinn *et al.* (2014) conclude that the 2014 and 2001 BIPM values of G are not correlated.

2. European Laboratory for Non-Linear Spectroscopy, University of Florence

A novel measurement technique to measure G using atom interferometry instead of a precision mechanical balance has recently been completed by the European Laboratory for Non-Linear Spectroscopy at the University of Florence (Prevedelli *et al.*, 2014; Rosi *et al.*, 2014). Labeled LENS-14, the experiment combines two vertically separated atomic clouds forming a double atom-interferometer-gravity gradiometer that measures the change in the gravity gradient when a well-characterized source mass is displaced.

The experimental design uses a double differential configuration that greatly reduces the sensitivity to common-mode spurious signals. Two atomic rubidium clouds are launched in the vertical direction with a vertical separation of approximately 30 cm in a juggling sequence. The two clouds are simultaneously interrogated by the same Raman three-pulse interferometric sequence. The difference in the phase shifts between the upper and lower interferometers measures the gravity gradient. The gravity gradient is then modulated by the symmetric placement of the 516 kg tungsten source mass in two different vertical positions around the double atom interferometer. To further cancel common-mode spurious effects the two-photon recoil used to split and recombine the wave packets in the interferometers is reversed.

The value of G is extracted by calculating the source mass gravitational potential and the phase shift for single-atom trajectories, carrying out Monte Carlo simulations of the atomic cloud, and estimating other corrections not taken into account by the Monte Carlo simulation. The final result is

$$G = 6.671\,91(99)G_0 \quad [1.5 \times 10^{-4}]. \tag{260}$$

The leading uncertainty components arise from the determination of the atomic cloud size, center, and launch direction, and the tungsten source mass position, and in parts in 10^6 are 61, 38, 36, and 38, respectively. Although the final uncertainty is not presently competitive, determinations of G using atom interferometry could be more competitive in the future.

3. University of California, Irvine

A highly competitive result from data collected over a 7 year span using a cryogenic torsion balance operating below 4 K in a dynamic mode with two orientations for the source mass has recently been reported by researchers from the University of California, Irvine (Newman *et al.*, 2014), labeled UCI-14. The advantages of cryogenic operation are a much higher torsion pendulum Q, which greatly reduces the systematic bias predicted by Kuroda (1995), much lower thermal noise acting on the balance, greatly reduced fiber-property dependence on temperature variation, excellent temperature control, easy to maintain high vacuum, and ease of including effective magnetic shielding with superconducting material. The source mass is a pair of copper rings that produces an extremely uniform gravity gradient over a large region centered on the torsion balance test mass. However, by necessity it is located 40 cm from the test mass (i.e. outside the vacuum dewar), thus greatly reducing the period-change signal of the torsion balance. The torsion balance test mass is a thin fused silica

RIGHTSLINK

plate as pioneered by Gundlach and Merkowitz (2000) that, when combined with the ring source masses, minimizes the sensitivity to test mass shape, mass distribution, and placement.

Over the 7 year span three fibers were used. Fiber 1 was an as-drawn CuBe fiber, fiber 2 a heat-treated CuBe fiber, and fiber 3 an as-drawn 5056 aluminium-alloy fiber. It was observed that the Birge ratio for the data within each run was much larger than expected. A total of 27 variants of data analysis methods were used for each fiber to test the robustness of the data, with the resulting 27 values of G varying over a range of 14, 24, and 20 parts in 10^6 for fibers 1, 2, and 3, respectively. The final analysis uses an unweighted average for each run, a weighted average over runs for each fiber with a Birge ratio uncertainty expansion, and an outlier identification protocol. An additional uncertainty component equal to half of the range of G values determined during a robustness test is included in the final values of G from the three fibers, which are

$$G_1 = 6.674\,350(97)G_0 \quad [1.5\times10^{-5}], \tag{261}$$

$$G_2 = 6.674\,08(15)G_0 \quad [2.2\times10^{-5}], \tag{262}$$

$$G_3 = 6.674\,55(13)G_0 \quad [2.0\times10^{-5}]. \tag{263}$$

Instead of an averaged value of G from the three fibers as published by Newman *et al.* (2014), the Task Group decided to use a weighted mean of the three values with a correlated relative uncertainty of 8.6 parts in 10^6 between each pair of fibers due to uncertainties associated with the source and test masses. The final UCI-14 input datum is

$$G = 6.674\,35(13)G_0 \quad [1.9\times10^{-5}], \tag{264}$$

where the uncertainty is taken to be the average of the three uncertainties as assigned by the researchers rather than that of the weighted mean since it better reflects the researchers view of the reliability of their measurements.

XII. Electroweak Quantities

There are a few cases in the 2014 adjustment, as in previous adjustments, where an inexact constant that is used in the analysis of input data is not treated as an adjusted quantity, because the adjustment has a negligible effect on its value. Three such constants, used in the calculation of the theoretical expression for the electron magnetic-moment anomaly a_e, are the mass of the tau lepton m_τ, the Fermi coupling constant G_F, and sine squared of the weak mixing angle $\sin^2\theta_W$; they are obtained from the most recent report of the Particle Data Group (Olive *et al.*, 2014):

$$m_\tau c^2 = 1776.82(16)\ \text{MeV} \quad [9.0\times10^{-5}], \tag{265}$$

$$\frac{G_F}{(\hbar c)^3} = 1.166\,3787(6)\times10^{-5}\ \text{GeV}^{-2} \quad [5.1\times10^{-7}], \tag{266}$$

$$\sin^2\theta_W = 0.2223(21) \quad [9.5\times10^{-3}]. \tag{267}$$

We use the definition $\sin^2\theta_W = 1-(m_W/m_Z)^2$, where m_W and m_Z are, respectively, the masses of the $W^\pm$ and Z^0 bosons, because it is employed in the calculation of the electroweak contributions to a_e (Czarnecki, Krause, and Marciano, 1996). The Particle Data Group's recommended value for the mass ratio of these bosons is $m_W/m_Z = 0.8819(12)$, which leads to the value of $\sin^2\theta_W$ given above.

The values of these constants are the same as used in CODATA-10, which were taken from the 2010 Particle Data Group report (Nakamura *et al.*, 2010), except that for $G_F/(\hbar c)^3$. The 2014 value exceeds the 2010 value by the fractional amount 1.3×10^{-5} and its uncertainty is about one eighth that of the 2010 value. The value for $G_F/(\hbar c)^3$ is taken from p. 139 of Olive *et al.* (2014).

XIII. Analysis of Data

The input data discussed in the previous sections are analyzed in this section, and based on that analysis the data used to determine the 2014 CODATA recommended values of the constants are selected. We closely follow the approach used in CODATA-10. The input data are given in Tables XVI, XVII, XVIII, and XIX. For ease of presentation the relevant covariances among the data are given in the form of correlation coefficients, but the actual covariances are used in all calculations. There are 15 types of input data with two or more values and the data of the same type generally agree among themselves; that is, there are no differences between like data that exceed $2u_{\text{diff}}$, the standard uncertainty of the difference. The major exception is the values of the Newtonian constant of gravitation G. These are listed in Table XXVII and because the G data are independent of all other data, they are treated separately in Sec. XIII.B.1. A minor exception is the difference between items $B44.2$ and $B44.6$, the NIST-98 and NRC-15 watt-balance values of $K_J^2R_K$; for these $u_{\text{diff}} = 2.04$.

A. Comparison of data through inferred values of α, h, and k

The extent to which the data agree is shown in this section by directly comparing values of α, h, and k that can be inferred from different experiments. However, the inferred value is for comparison purposes only; the datum from which it is obtained, not the inferred value, is used in the least-squares calculations.

Table XX and Figs. 1 and 2 compare values of α calculated from the indicated input data. They are obtained using the appropriate observational equation for the corresponding input datum as given in Table XXIV and the 2014 recommended values of the constants other than α that enter that equation. The table and figures show that a large majority of the values of α agree, and thus the data from which they are obtained agree; of the 91 differences between the 14 values of α, there are only eight that exceed $2u_{\text{diff}}$ and these are in the range 2.02 to 2.60. Six are between α from item $B39.1$, the NIST-89 result for $\Gamma'_{p-90}(\text{lo})$, and α from $B22.1$, $B22.2$, $B43.1$, $B43.3$, $B46$, and $B48$. The other two are between α from item

RIGHTSLINK

TABLE XVI. Summary of principal input data for the determination of the 2014 recommended value of the Rydberg constant R_∞

Item number	Input datum	Value	Relative standard uncertainty [a] u_r	Identification	Sec.
*A*1	$\delta_H(1S_{1/2})$	0.0(2.5) kHz	$[7.5\times10^{-13}]$	Theory	IV.A.1.l
*A*2	$\delta_H(2S_{1/2})$	0.00(31) kHz	$[3.8\times10^{-13}]$	Theory	IV.A.1.l
*A*3	$\delta_H(3S_{1/2})$	0.000(91) kHz	$[2.5\times10^{-13}]$	Theory	IV.A.1.l
*A*4	$\delta_H(4S_{1/2})$	0.000(39) kHz	$[1.9\times10^{-13}]$	Theory	IV.A.1.l
*A*5	$\delta_H(6S_{1/2})$	0.000(15) kHz	$[1.6\times10^{-13}]$	Theory	IV.A.1.l
*A*6	$\delta_H(8S_{1/2})$	0.0000(63) kHz	$[1.2\times10^{-13}]$	Theory	IV.A.1.l
*A*7	$\delta_H(2P_{1/2})$	0.000(28) kHz	$[3.5\times10^{-14}]$	Theory	IV.A.1.l
*A*8	$\delta_H(4P_{1/2})$	0.0000(38) kHz	$[1.9\times10^{-14}]$	Theory	IV.A.1.l
*A*9	$\delta_H(2P_{3/2})$	0.000(28) kHz	$[3.5\times10^{-14}]$	Theory	IV.A.1.l
*A*10	$\delta_H(4P_{3/2})$	0.0000(38) kHz	$[1.9\times10^{-14}]$	Theory	IV.A.1.l
*A*11	$\delta_H(8D_{3/2})$	0.000 00(44) kHz	$[8.5\times10^{-15}]$	Theory	IV.A.1.l
*A*12	$\delta_H(12D_{3/2})$	0.000 00(13) kHz	$[5.7\times10^{-15}]$	Theory	IV.A.1.l
*A*13	$\delta_H(4D_{5/2})$	0.0000(35) kHz	$[1.7\times10^{-14}]$	Theory	IV.A.1.l
*A*14	$\delta_H(6D_{5/2})$	0.0000(10) kHz	$[1.1\times10^{-14}]$	Theory	IV.A.1.l
*A*15	$\delta_H(8D_{5/2})$	0.000 00(44) kHz	$[8.5\times10^{-15}]$	Theory	IV.A.1.l
*A*16	$\delta_H(12D_{5/2})$	0.000 00(13) kHz	$[5.7\times10^{-15}]$	Theory	IV.A.1.l
*A*17	$\delta_D(1S_{1/2})$	0.0(2.3) kHz	$[6.9\times10^{-13}]$	Theory	IV.A.1.l
*A*18	$\delta_D(2S_{1/2})$	0.00(29) kHz	$[3.5\times10^{-13}]$	Theory	IV.A.1.l
*A*19	$\delta_D(4S_{1/2})$	0.000(36) kHz	$[1.7\times10^{-13}]$	Theory	IV.A.1.l
*A*20	$\delta_D(8S_{1/2})$	0.0000(60) kHz	$[1.2\times10^{-13}]$	Theory	IV.A.1.l
*A*21	$\delta_D(8D_{3/2})$	0.000 00(44) kHz	$[8.5\times10^{-15}]$	Theory	IV.A.1.l
*A*22	$\delta_D(12D_{3/2})$	0.000 00(13) kHz	$[5.6\times10^{-15}]$	Theory	IV.A.1.l
*A*23	$\delta_D(4D_{5/2})$	0.0000(35) kHz	$[1.7\times10^{-14}]$	Theory	IV.A.1.l
*A*24	$\delta_D(8D_{5/2})$	0.000 00(44) kHz	$[8.5\times10^{-15}]$	Theory	IV.A.1.l
*A*25	$\delta_D(12D_{5/2})$	0.000 00(13) kHz	$[5.7\times10^{-15}]$	Theory	IV.A.1.l
*A*26.1	$\nu_H(1S_{1/2}-2S_{1/2})$	2 466 061 413 187.035(10) kHz	4.2×10^{-15}	MPQ-11	IV.A.2
*A*26.2	$\nu_H(1S_{1/2}-2S_{1/2})$	2 466 061 413 187.018(11) kHz	4.4×10^{-15}	MPQ-13	IV.A.2
*A*27	$\nu_H(1S_{1/2}-3S_{1/2})$	2 922 743 278 678(13) kHz	4.4×10^{-12}	LKB-10	IV.A.2
*A*28	$\nu_H(2S_{1/2}-8S_{1/2})$	770 649 350 012.0(8.6) kHz	1.1×10^{-11}	LK/SY-97	IV.A.2
*A*29	$\nu_H(2S_{1/2}-8D_{3/2})$	770 649 504 450.0(8.3) kHz	1.1×10^{-11}	LK/SY-97	IV.A.2
*A*30	$\nu_H(2S_{1/2}-8D_{5/2})$	770 649 561 584.2(6.4) kHz	8.3×10^{-12}	LK/SY-97	IV.A.2
*A*31	$\nu_H(2S_{1/2}-12D_{3/2})$	799 191 710 472.7(9.4) kHz	1.2×10^{-11}	LK/SY-98	IV.A.2
*A*32	$\nu_H(2S_{1/2}-12D_{5/2})$	799 191 727 403.7(7.0) kHz	8.7×10^{-12}	LK/SY-98	IV.A.2
*A*33	$\nu_H(2S_{1/2}-4S_{1/2})-\frac{1}{4}\nu_H(1S_{1/2}-2S_{1/2})$	4 797 338(10) kHz	2.1×10^{-6}	MPQ-95	IV.A.2
*A*34	$\nu_H(2S_{1/2}-4D_{5/2})-\frac{1}{4}\nu_H(1S_{1/2}-2S_{1/2})$	6 490 144(24) kHz	3.7×10^{-6}	MPQ-95	IV.A.2
*A*35	$\nu_H(2S_{1/2}-6S_{1/2})-\frac{1}{4}\nu_H(1S_{1/2}-3S_{1/2})$	4 197 604(21) kHz	4.9×10^{-6}	LKB-96	IV.A.2
*A*36	$\nu_H(2S_{1/2}-6D_{5/2})-\frac{1}{4}\nu_H(1S_{1/2}-3S_{1/2})$	4 699 099(10) kHz	2.2×10^{-6}	LKB-96	IV.A.2
*A*37	$\nu_H(2S_{1/2}-4P_{1/2})-\frac{1}{4}\nu_H(1S_{1/2}-2S_{1/2})$	4 664 269(15) kHz	3.2×10^{-6}	YaleU-95	IV.A.2
*A*38	$\nu_H(2S_{1/2}-4P_{3/2})-\frac{1}{4}\nu_H(1S_{1/2}-2S_{1/2})$	6 035 373(10) kHz	1.7×10^{-6}	YaleU-95	IV.A.2
*A*39	$\nu_H(2S_{1/2}-2P_{3/2})$	9 911 200(12) kHz	1.2×10^{-6}	HarvU-94	IV.A.2
*A*40.1	$\nu_H(2P_{1/2}-2S_{1/2})$	1 057 845.0(9.0) kHz	8.5×10^{-6}	HarvU-86	IV.A.2
*A*40.2	$\nu_H(2P_{1/2}-2S_{1/2})$	1 057 862(20) kHz	1.9×10^{-5}	USus-79	IV.A.2
*A*41	$\nu_D(2S_{1/2}-8S_{1/2})$	770 859 041 245.7(6.9) kHz	8.9×10^{-12}	LK/SY-97	IV.A.2
*A*42	$\nu_D(2S_{1/2}-8D_{3/2})$	770 859 195 701.8(6.3) kHz	8.2×10^{-12}	LK/SY-97	IV.A.2
*A*43	$\nu_D(2S_{1/2}-8D_{5/2})$	770 859 252 849.5(5.9) kHz	7.7×10^{-12}	LK/SY-97	IV.A.2
*A*44	$\nu_D(2S_{1/2}-12D_{3/2})$	799 409 168 038.0(8.6) kHz	1.1×10^{-11}	LK/SY-98	IV.A.2
*A*45	$\nu_D(2S_{1/2}-12D_{5/2})$	799 409 184 966.8(6.8) kHz	8.5×10^{-12}	LK/SY-98	IV.A.2
*A*46	$\nu_D(2S_{1/2}-4S_{1/2})-\frac{1}{4}\nu_D(1S_{1/2}-2S_{1/2})$	4 801 693(20) kHz	4.2×10^{-6}	MPQ-95	IV.A.2
*A*47	$\nu_D(2S_{1/2}-4D_{5/2})-\frac{1}{4}\nu_D(1S_{1/2}-2S_{1/2})$	6 494 841(41) kHz	6.3×10^{-6}	MPQ-95	IV.A.2
*A*48	$\nu_D(1S_{1/2}-2S_{1/2})-\nu_H(1S_{1/2}-2S_{1/2})$	670 994 334.606(15) kHz	2.2×10^{-11}	MPQ-10	IV.A.2
*A*49	r_p	0.879(11) fm	1.3×10^{-2}	rp-14	IV.A.3
*A*50	r_d	2.130(10) fm	4.7×10^{-3}	rd-98	IV.A.3

[a]The values in brackets are relative to the frequency equivalent of the binding energy of the indicated level.

RIGHTSLINK

$B40$, the KR/VN-98 result for $\Gamma'_{h-90}(lo)$, and α from items $B43.1$ and $B43.3$.

The inconsistency of these two gyromagnetic ratios has been discussed in previous CODATA reports and is not a serious issue because their self-sensitivity coefficients S_c (a measure of their weights in an adjustment, see Sec. XIII.B) are less than 0.01. Therefore the two ratios are omitted from the final adjustment on which the 2014 CODATA recommended values are based. This was also the case in the 2006 and 2010 adjustments. They are initially considered again, as are other data, to test data robustness and the exactness of the relations $K_J = 2e/h$ and $R_K = h/e^2$ (see Sec. XIII.B.3).

Because of the large uncertainties of most of the values of α compared with the uncertainties of those from $B22.2$, the HarvU-08 result for a_e, and $B48$, the LKB-11 result for $h/m(^{87}Rb)$, the 2014 recommended value of α is essentially determined by these two input data. Figure 2 compares them through their inferred values of α and shows how their consistency has changed since 2010, but not because the measured values of a_e and $h/m(^{87}Rb)$ have changed. Rather, it is because the a_e QED theoretical expression and the value of $A_r(e)$ required to determine α from $h/m(^{87}Rb)$ have changed. The UWash-87 result for a_e, the $h/m(^{133}Cs)$ result, the three $\Gamma'_{x-90}(lo)$ results, and the five R_K results are omitted from the 2010 final adjustment because of their low weights and are omitted from the 2014 final adjustment for the same reason.

Table XXI and Figs. 3 and 4 compare values of h obtained from the indicated input data. They show that the vast majority of the values of h agree, and thus the data from which they are obtained agree; of the 91 differences between h values, only one exceeds $2u_{diff}$. The two values are from input datum $B44.2$ and $B44.6$, the NIST-98 and NRC-15 watt-balance results for $K_J^2 R_K$, but the difference is only $2.04u_{diff}$. The first five values of h in the table, each with relative standard uncertainty

TABLE XVII. Correlation coefficients $r(x_i, x_j) \geq 0.0001$ of the input data related to R_∞ in Table XVI. For simplicity, the two items of data to which a particular correlation coefficient corresponds are identified by their item numbers in Table XVI

$r(A1, A2) = 0.9905$	$r(A6, A19) = 0.7404$	$r(A26.1, A26.2) = 0.7069$	$r(A31, A44) = 0.0901$
$r(A1, A3) = 0.9900$	$r(A6, A20) = 0.9851$	$r(A28, A29) = 0.3478$	$r(A31, A45) = 0.1136$
$r(A1, A4) = 0.9873$	$r(A7, A8) = 0.0237$	$r(A28, A30) = 0.4532$	$r(A32, A35) = 0.0278$
$r(A1, A5) = 0.7640$	$r(A9, A10) = 0.0237$	$r(A28, A31) = 0.0899$	$r(A32, A36) = 0.0553$
$r(A1, A6) = 0.7627$	$r(A11, A12) = 0.0006$	$r(A28, A32) = 0.1206$	$r(A32, A41) = 0.1512$
$r(A1, A17) = 0.9754$	$r(A11, A21) = 0.9999$	$r(A28, A35) = 0.0225$	$r(A32, A42) = 0.1647$
$r(A1, A18) = 0.9656$	$r(A11, A22) = 0.0003$	$r(A28, A36) = 0.0448$	$r(A32, A43) = 0.1750$
$r(A1, A19) = 0.9619$	$r(A12, A21) = 0.0003$	$r(A28, A41) = 0.1225$	$r(A32, A44) = 0.1209$
$r(A1, A20) = 0.7189$	$r(A12, A22) = 0.9999$	$r(A28, A42) = 0.1335$	$r(A32, A45) = 0.1524$
$r(A2, A3) = 0.9897$	$r(A13, A14) = 0.0006$	$r(A28, A43) = 0.1419$	$r(A33, A34) = 0.1049$
$r(A2, A4) = 0.9870$	$r(A13, A15) = 0.0006$	$r(A28, A44) = 0.0980$	$r(A33, A46) = 0.2095$
$r(A2, A5) = 0.7638$	$r(A13, A16) = 0.0006$	$r(A28, A45) = 0.1235$	$r(A33, A47) = 0.0404$
$r(A2, A6) = 0.7625$	$r(A13, A23) = 0.9999$	$r(A29, A30) = 0.4696$	$r(A34, A46) = 0.0271$
$r(A2, A17) = 0.9656$	$r(A13, A24) = 0.0003$	$r(A29, A31) = 0.0934$	$r(A34, A47) = 0.0467$
$r(A2, A18) = 0.9754$	$r(A13, A25) = 0.0003$	$r(A29, A32) = 0.1253$	$r(A35, A36) = 0.1412$
$r(A2, A19) = 0.9616$	$r(A14, A15) = 0.0006$	$r(A29, A35) = 0.0234$	$r(A35, A41) = 0.0282$
$r(A2, A20) = 0.7187$	$r(A14, A16) = 0.0006$	$r(A29, A36) = 0.0466$	$r(A35, A42) = 0.0307$
$r(A3, A4) = 0.9864$	$r(A14, A23) = 0.0003$	$r(A29, A41) = 0.1273$	$r(A35, A43) = 0.0327$
$r(A3, A5) = 0.7633$	$r(A14, A24) = 0.0003$	$r(A29, A42) = 0.1387$	$r(A35, A44) = 0.0226$
$r(A3, A6) = 0.7620$	$r(A14, A25) = 0.0003$	$r(A29, A43) = 0.1475$	$r(A35, A45) = 0.0284$
$r(A3, A17) = 0.9651$	$r(A15, A16) = 0.0006$	$r(A29, A44) = 0.1019$	$r(A36, A41) = 0.0561$
$r(A3, A18) = 0.9648$	$r(A15, A23) = 0.0003$	$r(A29, A45) = 0.1284$	$r(A36, A42) = 0.0612$
$r(A3, A19) = 0.9611$	$r(A15, A24) = 0.9999$	$r(A30, A31) = 0.1209$	$r(A36, A43) = 0.0650$
$r(A3, A20) = 0.7183$	$r(A15, A25) = 0.0003$	$r(A30, A32) = 0.1622$	$r(A36, A44) = 0.0449$
$r(A4, A5) = 0.7613$	$r(A16, A23) = 0.0003$	$r(A30, A35) = 0.0303$	$r(A36, A45) = 0.0566$
$r(A4, A6) = 0.7600$	$r(A16, A24) = 0.0003$	$r(A30, A36) = 0.0602$	$r(A37, A38) = 0.0834$
$r(A4, A17) = 0.9625$	$r(A16, A25) = 0.9999$	$r(A30, A41) = 0.1648$	$r(A41, A42) = 0.5699$
$r(A4, A18) = 0.9622$	$r(A17, A18) = 0.9897$	$r(A30, A42) = 0.1795$	$r(A41, A43) = 0.6117$
$r(A4, A19) = 0.9755$	$r(A17, A19) = 0.9859$	$r(A30, A43) = 0.1908$	$r(A41, A44) = 0.1229$
$r(A4, A20) = 0.7163$	$r(A17, A20) = 0.7368$	$r(A30, A44) = 0.1319$	$r(A41, A45) = 0.1548$
$r(A5, A6) = 0.5881$	$r(A18, A19) = 0.9856$	$r(A30, A45) = 0.1662$	$r(A42, A43) = 0.6667$
$r(A5, A17) = 0.7448$	$r(A18, A20) = 0.7366$	$r(A31, A32) = 0.4750$	$r(A42, A44) = 0.1339$
$r(A5, A18) = 0.7445$	$r(A19, A20) = 0.7338$	$r(A31, A35) = 0.0207$	$r(A42, A45) = 0.1687$
$r(A5, A19) = 0.7417$	$r(A21, A22) = 0.0002$	$r(A31, A36) = 0.0412$	$r(A43, A44) = 0.1423$
$r(A5, A20) = 0.5543$	$r(A23, A24) = 0.0001$	$r(A31, A41) = 0.1127$	$r(A43, A45) = 0.1793$
$r(A6, A17) = 0.7435$	$r(A23, A25) = 0.0001$	$r(A31, A42) = 0.1228$	$r(A44, A45) = 0.5224$
$r(A6, A18) = 0.7433$	$r(A24, A25) = 0.0002$	$r(A31, A43) = 0.1305$	$r(A46, A47) = 0.0110$

RIGHTSLINK

TABLE XVIII. Summary of principal input data for the determination of the 2014 recommended values of the fundamental constants (R_∞ and G excepted)

Item number	Input datum	Value	Relative standard uncertainty [a] u_r	Identification	Sec. and Eq.
$B1$	$A_r(n)$	1.008 664 915 85(49)	4.9×10^{-10}	AME-12	III.A
$B2$	$A_r(^1H)$	1.007 825 032 231(93)	9.3×10^{-11}	AME-12	III.A
$B3$	$\Delta E_B(^1H^+)/hc$	$1.096\,787\,717\,4307(10)\times10^7$ m^{-1}	9.1×10^{-13}	ASD-14	III.B
$B4$ [b]	$A_r(^3H)$	3.016 049 2779(24)	7.9×10^{-10}	AME-12	III.A
$B5$ [b]	$\Delta E_B(^3H^+)/hc$	$1.097\,185\,4390(13)\times10^7$ m^{-1}	1.2×10^{-9}	ASD-14	III.B
$B6$	$A_r(^4He)$	4.002 603 254 130(63)	1.6×10^{-11}	AME-12	III.A
$B7$	$\Delta E_B(^4He^{2+})/hc$	$6.372\,195\,4487(28)\times10^7$ m^{-1}	4.4×10^{-10}	ASD-14	III.B
$B8$	$\omega_c(d)/\omega_c(^{12}C^{6+})$	0.992 996 654 743(20)	2.0×10^{-11}	UWash-15	III.C (5)
$B9$ [c]	$\omega_c(h)/\omega_c(^{12}C^{6+})$	1.326 365 862 193(19)	1.4×10^{-11}	UWash-15	III.C (6)
$B10$	$\Delta E_B(^{12}C^{6+})/hc$	$83.083\,962(72)\times10^7$ m^{-1}	8.7×10^{-7}	ASD-14	III.B
$B11$ [c]	$\omega_c(HD^+)/\omega_c(^3He^+)$	0.998 048 085 153(48)	4.8×10^{-11}	FSU-15	III.C (11)
$B12$	$\omega_c(HD^+)/\omega_c(t)$	0.998 054 687 288(48)	4.8×10^{-11}	FSU-15	III.C (12)
$B13$	$\Delta E_I(^3He^+)/hc$	43 888 919.36(3) m^{-1}	6.8×10^{-10}	ASD-14	III.C (17)
$B14$	$\Delta E_I(HD^+)/hc$	13 122 468.415(6) m^{-1}	4.6×10^{-10}	Literature	III.C (19)
$B15$	$\omega_s(^{12}C^{5+})/\omega_c(^{12}C^{5+})$	4376.210 500 87(12)	2.8×10^{-11}	MPIK-15	V.D.2 (179)
$B16$	$\Delta E_B(^{12}C^{5+})/hc$	$43.563\,345(72)\times10^7$ m^{-1}	1.7×10^{-6}	ASD-14	III.B
$B17$	δ_C	$0.0(2.6)\times10^{-11}$	$[1.3\times10^{-11}]$	Theory	V.D.1 (175)
$B18$	$\omega_s(^{28}Si^{13+})/\omega_c(^{28}Si^{13+})$	3912.866 064 84(19)	4.8×10^{-11}	MPIK-15	V.D.2 (178)
$B19$	$A_r(^{28}Si)$	27.976 926 534 65(44)	1.6×10^{-11}	AME-12	III.A
$B20$	$\Delta E_B(^{28}Si^{13+})/hc$	$420.608(19)\times10^7$ m^{-1}	4.4×10^{-5}	ASD-14	III.B
$B21$	δ_{Si}	$0.0(1.7)\times10^{-9}$	$[8.3\times10^{-10}]$	Theory	V.D.1 (176)
$B22.1$ [b]	a_e	$1.159\,652\,1883(42)\times10^{-3}$	3.7×10^{-9}	UWash-87	V.A.2
$B22.2$	a_e	$1.159\,652\,180\,73(28)\times10^{-3}$	2.4×10^{-10}	HarvU-08	V.A.2
$B23$	δ_e	$0.000(37)\times10^{-12}$	$[0.32\times10^{-10}]$	Theory	V.A.1 (109)
$B24$	$\overline{R}$	0.003 707 2063(20)	5.4×10^{-7}	BNL-06	V.B.2 (135)
$B25$	ν(58 MHz)	627 994.77(14) kHz	2.2×10^{-7}	LAMPF-82	VI.B.2 (218)
$B26$	ν(72 MHz)	668 223 166(57) Hz	8.6×10^{-8}	LAMPF-99	VI.B.2 (221)
$B27.1$	$\Delta\nu_{Mu}$	4 463 302.88(16) kHz	3.6×10^{-8}	LAMPF-82	VI.B.2 (217)
$B27.2$	$\Delta\nu_{Mu}$	4 463 302 765(53) Hz	1.2×10^{-8}	LAMPF-99	VI.B.2 (220)
$B28$	δ_{Mu}	0(85) Hz	$[1.9\times10^{-8}]$	Theory	VI.B.1 (215)
$B29$	μ_p/μ_N	2.792 847 3498(93)	3.3×10^{-9}	UMZ-14	V.C (141)
$B30$	$\mu_e(H)/\mu_p(H)$	−658.210 7058(66)	1.0×10^{-8}	MIT-72	VI.A.1
$B31$	$\mu_d(D)/\mu_e(D)$	$-4.664\,345\,392(50)\times10^{-4}$	1.1×10^{-8}	MIT-84	VI.A.1
$B32$	$\mu_e(H)/\mu'_p$	−658.215 9430(72)	1.1×10^{-8}	MIT-77	VI.A.1
$B33$	μ'_h/μ'_p	−0.761 786 1313(33)	4.3×10^{-9}	NPL-93	VI.A.1
$B34$	μ_n/μ'_p	−0.684 996 94(16)	2.4×10^{-7}	ILL-79	VI.A.1
$B35.1$	$\mu_p(HD)/\mu_d(HD)$	3.257 199 531(29)	8.9×10^{-9}	StPtrsb-03	VI.A.1
$B35.2$	$\mu_p(HD)/\mu_d(HD)$	3.257 199 514(21)	6.6×10^{-9}	WarsU-12	VI.A.1 (197)
$B36$	$\mu_t(HT)/\mu_p(HT)$	1.066 639 8933(21)	2.0×10^{-9}	StPtrsb-11	VI.A.1 (198)
$B37$	σ_{dp}	$15(2)\times10^{-9}$		StPtrsb-03	VI.A.1
$B38$	σ_{tp}	$20(3)\times10^{-9}$		StPtrsb-03	VI.A.1
$B39.1$ [b]	$\Gamma'_{p-90}(lo)$	$2.675\,154\,05(30)\times10^8$ s^{-1} T^{-1}	1.1×10^{-7}	NIST-89	VIII
$B39.2$ [b]	$\Gamma'_{p-90}(lo)$	$2.675\,1530(18)\times10^8$ s^{-1} T^{-1}	6.6×10^{-7}	NIM-95	VIII
$B40$ [b]	$\Gamma'_{h-90}(lo)$	$2.037\,895\,37(37)\times10^8$ s^{-1} T^{-1}	1.8×10^{-7}	KR/VN-98	VIII
$B41.1$ [b]	$\Gamma'_{p-90}(hi)$	$2.675\,1525(43)\times10^8$ s^{-1} T^{-1}	1.6×10^{-6}	NIM-95	VIII
$B41.2$ [b]	$\Gamma'_{p-90}(hi)$	$2.675\,1518(27)\times10^8$ s^{-1} T^{-1}	1.0×10^{-6}	NPL-79	VIII
$B42.1$ [b]	K_J	483 597.91(13) GHz V^{-1}	2.7×10^{-7}	NMI-89	VIII
$B42.2$ [b]	K_J	483 597.96(15) GHz V^{-1}	3.1×10^{-7}	PTB-91	VIII
$B43.1$ [b]	R_K	25 812.808 31(62) Ω	2.4×10^{-8}	NIST-97	VIII
$B43.2$ [b]	R_K	25 812.8071(11) Ω	4.4×10^{-8}	NMI-97	VIII
$B43.3$ [b]	R_K	25 812.8092(14) Ω	5.4×10^{-8}	NPL-88	VIII
$B43.4$ [b]	R_K	25 812.8084(34) Ω	1.3×10^{-7}	NIM-95	VIII
$B43.5$ [b]	R_K	25 812.8081(14) Ω	5.3×10^{-8}	LNE-01	VIII

RIGHTSLINK

TABLE XVIII. Summary of principal input data for the determination of the 2014 recommended values of the fundamental constants (R_∞ and G excepted)—Continued

Item number	Input datum	Value	Relative standard uncertainty [a] u_r	Identification	Sec. and Eq.
$B44.1$ [b]	$K_J^2 R_K$	$6.036\,7625(12) \times 10^{33}$ J^{-1} s^{-1}	2.0×10^{-7}	NPL-90	VIII.A
$B44.2$	$K_J^2 R_K$	$6.036\,761\,85(53) \times 10^{33}$ J^{-1} s^{-1}	8.7×10^{-8}	NIST-98	VIII.D
$B44.3$ [b]	$K_J^2 R_K$	$6.036\,7617(18) \times 10^{33}$ J^{-1} s^{-1}	2.9×10^{-7}	METAS-11	VIII.B
$B44.4$	$K_J^2 R_K$	$6.036\,761\,43(34) \times 10^{33}$ J^{-1} s^{-1}	5.7×10^{-8}	NIST-15	VIII.D (234)
$B44.5$ [b]	$K_J^2 R_K$	$6.036\,7597(12) \times 10^{33}$ J^{-1} s^{-1}	2.0×10^{-7}	NPL-12	VIII.A
$B44.6$	$K_J^2 R_K$	$6.036\,760\,76(11) \times 10^{33}$ J^{-1} s^{-1}	1.8×10^{-8}	NRC-15	VIII.E (237)
$B44.7$ [b]	$K_J^2 R_K$	$6.036\,7619(15) \times 10^{33}$ J^{-1} s^{-1}	2.6×10^{-7}	LNE-15	VIII.C (231)
$B45$ [b]	$\mathcal{F}_{90}$	96 485.39(13) C mol^{-1}	1.3×10^{-6}	NIST-80	VIII
$B46$ [b]	$h/m(^{133}\mathrm{Cs})$	$3.002\,369\,432(46) \times 10^{-9}$ m^2 s^{-1}	1.5×10^{-8}	StanfU-02	VII
$B47$ [b]	$A_r(^{133}\mathrm{Cs})$	132.905 451 9615(86)	6.5×10^{-11}	AME-12	III.A
$B48$	$h/m(^{87}\mathrm{Rb})$	$4.591\,359\,2729(57) \times 10^{-9}$ m^2 s^{-1}	1.2×10^{-9}	LKB-11	VII
$B49$	$A_r(^{87}\mathrm{Rb})$	86.909 180 5319(65)	7.5×10^{-11}	AME-12	III.A
$B50$	$1 - d_{220}(\mathrm{W17})/d_{220}(\mathrm{ILL})$	$-8(22) \times 10^{-9}$		NIST-99	IX.A
$B51$	$1 - d_{220}(\mathrm{MO}^*)/d_{220}(\mathrm{ILL})$	$86(27) \times 10^{-9}$		NIST-99	IX.A
$B52$	$1 - d_{220}(\mathrm{NR3})/d_{220}(\mathrm{ILL})$	$33(22) \times 10^{-9}$		NIST-99	IX.A
$B53$	$1 - d_{220}(\mathrm{N})/d_{220}(\mathrm{W17})$	$7(22) \times 10^{-9}$		NIST-97	IX.A
$B54$	$d_{220}(\mathrm{W4.2a})/d_{220}(\mathrm{W04}) - 1$	$-1(21) \times 10^{-9}$		PTB-98	IX.A
$B55.1$	$d_{220}(\mathrm{W17})/d_{220}(\mathrm{W04}) - 1$	$22(22) \times 10^{-9}$		PTB-98	IX.A
$B55.2$	$d_{220}(\mathrm{W17})/d_{220}(\mathrm{W04}) - 1$	$11(21) \times 10^{-9}$		NIST-06	IX.A
$B56$	$d_{220}(\mathrm{MO}^*)/d_{220}(\mathrm{W04}) - 1$	$-103(28) \times 10^{-9}$		PTB-98	IX.A
$B57.1$	$d_{220}(\mathrm{NR3})/d_{220}(\mathrm{W04}) - 1$	$-23(21) \times 10^{-9}$		PTB-98	IX.A
$B57.2$	$d_{220}(\mathrm{NR3})/d_{220}(\mathrm{W04}) - 1$	$-11(21) \times 10^{-9}$		NIST-06	IX.A
$B58$	$d_{220}/d_{220}(\mathrm{W04}) - 1$	$10(11) \times 10^{-9}$		PTB-03	IX.A
$B59$	$d_{220}(\mathrm{NR4})/d_{220}(\mathrm{W04}) - 1$	$25(21) \times 10^{-9}$		NIST-06	IX.A
$B60$	$d_{220}(\mathrm{MO}^*)$	192 015.5508(42) fm	2.2×10^{-8}	INRIM-08	IX.A
$B61$	$d_{220}(\mathrm{W04})$	192 015.5702(29) fm	1.5×10^{-8}	INRIM-09	IX.A
$B62.1$	$d_{220}(\mathrm{W4.2a})$	192 015.5691(29) fm	1.5×10^{-8}	INRIM-09	IX.A
$B62.2$	$d_{220}(\mathrm{W4.2a})$	192 015.563(12) fm	6.2×10^{-8}	PTB-81	IX.A
$B63.1$	N_A	$6.022\,140\,99(18) \times 10^{23}$ m^3 mol^{-1}	3.0×10^{-8}	IAC-11	IX.B (239)
$B63.2$	N_A	$6.022\,140\,76(12) \times 10^{23}$ m^3 mol^{-1}	2.0×10^{-8}	IAC-15	IX.B (240)
$B64.1$ [b]	R	8.314 504(70) J mol^{-1} K^{-1}	8.4×10^{-6}	NPL-79	X.A
$B64.2$	R	8.314 470(15) J mol^{-1} K^{-1}	1.8×10^{-6}	NIST-88	X.A
$B64.3$	R	8.314 467(23) J mol^{-1} K^{-1}	2.7×10^{-6}	LNE-09	X.A
$B64.4$	R	8.314 468(26) J mol^{-1} K^{-1}	3.2×10^{-6}	NPL-10	X.A
$B64.5$ [b]	R	8.314 412(63) J mol^{-1} K^{-1}	7.5×10^{-6}	INRIM-10	X.A
$B64.6$	R	8.314 455(12) J mol^{-1} K^{-1}	1.4×10^{-6}	LNE-11	X.A
$B64.7$	R	8.314 455(31) J mol^{-1} K^{-1}	3.7×10^{-6}	NIM-13	X.A (243)
$B64.8$	R	8.314 4544(75) J mol^{-1} K^{-1}	9.0×10^{-7}	NPL-13	X.A
$B64.9$	R	8.314 4615(84) J mol^{-1} K^{-1}	1.0×10^{-6}	LNE-15	X.A (245)
$B65$	k/h	$2.083\,6658(80) \times 10^{10}$ Hz K^{-1}	3.9×10^{-6}	NIM/NIST-15	X.B (248)
$B66$	A_ϵ/R	$6.221\,128(25) \times 10^{-8}$ m^3 K J^{-1}	4.0×10^{-6}	PTB-15	X.C (253)
$B67$	$\alpha_0(^4\mathrm{He})/4\pi\epsilon_0 a_0^3$	1.383 760 77(14)	1.0×10^{-7}	Theory	X.C (251)
$B68$	$\lambda(\mathrm{CuK}\alpha_1)/d_{220}(\mathrm{W4.2a})$	0.802 327 11(24)	3.0×10^{-7}	FSUJ/PTB-91	IX.A
$B69$	$\lambda(\mathrm{CuK}\alpha_1)/d_{220}(\mathrm{N})$	0.802 328 04(77)	9.6×10^{-7}	NIST-73	IX.A
$B70$	$\lambda(\mathrm{WK}\alpha_1)/d_{220}(\mathrm{N})$	0.108 852 175(98)	9.0×10^{-7}	NIST-79	IX.A
$B71$	$\lambda(\mathrm{MoK}\alpha_1)/d_{220}(\mathrm{N})$	0.369 406 04(19)	5.3×10^{-7}	NIST-73	IX.A

[a]The values in brackets are relative to the quantities $g(^{12}\mathrm{C}^{5+})$, $g(^{28}\mathrm{Si}^{13+})$, a_e, or $\Delta\nu_{\mathrm{Mu}}$ as appropriate.
[b]Datum not included in the final least-squares adjustment that provides the recommended values of the constants.
[c]Datum included in the final least-squares adjustment with an expanded uncertainty.

$u_r < 10^{-7}$, are compared in Fig. 4. The five input data from which these values are obtained are included in the final adjustment and determine the 2014 recommended value of h. The input data from which the next nine values of h with u_r from 2.0×10^{-7} to 1.6×10^{-6} are omitted from the final adjustment because of their low weight.

Table XXII and Fig. 5 compare values of k obtained from the indicated input data. Although most of the source data are

RIGHTSLINK

TABLE XIX. Correlation coefficients $r(x_i, x_j) \geq 0.001$ of the input data in Table XVIII. For simplicity, the two items of data to which a particular correlation coefficient corresponds are identified by their item numbers in Table XVIII

$r(B1, B2) = -0.133$	$r(B42.1, B64.2) = 0.068$	$r(B52, B57.2) = -0.367$	$r(B64.2, B64.7) = 0.001$
$r(B1, B19) = -0.015$	$r(B44.1, B44.5) = 0.003$	$r(B52, B59) = 0.065$	$r(B64.2, B64.8) = 0.003$
$r(B1, B47) = -0.007$	$r(B44.2, B44.4) = 0.090$	$r(B53, B55.2) = 0.504$	$r(B64.3, B64.4) = 0.002$
$r(B1, B49) = -0.007$	$r(B47, B49) = 0.102$	$r(B53, B57.2) = 0.066$	$r(B64.3, B64.5) = 0.001$
$r(B2, B19) = 0.165$	$r(B50, B51) = 0.421$	$r(B53, B59) = 0.066$	$r(B64.3, B64.6) = 0.011$
$r(B2, B47) = 0.058$	$r(B50, B52) = 0.516$	$r(B54, B55.1) = 0.469$	$r(B64.3, B64.8) = 0.006$
$r(B2, B49) = 0.063$	$r(B50, B53) = -0.288$	$r(B54, B56) = 0.372$	$r(B64.3, B64.9) = 0.018$
$r(B8, B9) = 0.306$	$r(B50, B55.2) = -0.367$	$r(B54, B57.1) = 0.502$	$r(B64.4, B64.6) = 0.113$
$r(B10, B16) = 1.000$	$r(B50, B57.2) = 0.065$	$r(B55.1, B56) = 0.347$	$r(B64.4, B64.8) = 0.007$
$r(B11, B12) = 0.875$	$r(B50, B59) = 0.065$	$r(B55.1, B57.1) = 0.469$	$r(B64.4, B64.9) = 0.005$
$r(B15, B18) = 0.347$	$r(B51, B52) = 0.421$	$r(B55.2, B57.2) = 0.509$	$r(B64.5, B64.9) = 0.002$
$r(B17, B21) = 0.791$	$r(B51, B53) = 0.096$	$r(B55.2, B59) = 0.509$	$r(B64.6, B64.7) = 0.001$
$r(B19, B47) = 0.033$	$r(B51, B55.2) = 0.053$	$r(B56, B57.1) = 0.372$	$r(B64.6, B64.8) = 0.016$
$r(B19, B49) = 0.041$	$r(B51, B57.2) = 0.053$	$r(B57.2, B59) = 0.509$	$r(B64.6, B64.9) = 0.254$
$r(B25, B27.1) = 0.227$	$r(B51, B59) = 0.053$	$r(B63.1, B63.2) = 0.170$	$r(B64.7, B64.8) = 0.084$
$r(B26, B27.2) = 0.195$	$r(B52, B53) = 0.117$	$r(B64.2, B64.4) = 0.001$	$r(B64.8, B64.9) = 0.016$
$r(B39.2, B41.1) = -0.014$	$r(B52, B55.2) = 0.065$	$r(B64.2, B64.6) = 0.002$	

TABLE XX. Inferred values of the fine-structure constant α in order of increasing standard uncertainty obtained from the indicated experimental data in Table XVIII

Primary source	Item number	Identification	Sec. and Eq.	α^{-1}	Relative standard uncertainty u_r
a_e	B22.2	HarvU-08	V.A.2	137.035 999 160(33)	2.4×10^{-10}
$h/m(^{87}\mathrm{Rb})$	B48	LKB-11	VII	137.035 998 996(85)	6.2×10^{-10}
a_e	B22.1	UWash-87	V.A.2	137.035 998 27(50)	3.7×10^{-9}
$h/m(^{133}\mathrm{Cs})$	B46	StanfU-02	VII	137.036 0000(11)	7.7×10^{-9}
R_K	B43.1	NIST-97	VIII	137.036 0037(33)	2.4×10^{-8}
$\Gamma'_{p-90}(lo)$	B39.1	NIST-89	VIII	137.035 9879(51)	3.7×10^{-8}
R_K	B43.2	NMI-97	VIII	137.035 9973(61)	4.4×10^{-8}
R_K	B43.5	LNE-01	VIII	137.036 0023(73)	5.3×10^{-8}
R_K	B43.3	NPL-88	VIII	137.036 0083(73)	5.4×10^{-8}
$\Delta\nu_{Mu}$	B27.1, B27.2	LAMPF	VI.B.2 (228)	137.036 0013(79)	5.8×10^{-8}
$\Gamma'_{h-90}(lo)$	B40	KR/VN-98	VIII	137.035 9852(82)	6.0×10^{-8}
R_K	B43.4	NIM-95	VIII	137.036 004(18)	1.3×10^{-7}
$\Gamma'_{p-90}(lo)$	B39.2	NIM-95	VIII	137.036 006(30)	2.2×10^{-7}
ν_H, ν_D			IV.A.1.m (71)	137.035 992(55)	4.0×10^{-7}

acoustic gas thermometry measurements of R, values of $k = R/N_A$ are compared, because k is one of the defining constants of the new SI (see Sec. I.B.1) and $u_r(N_A) \ll u_r(R)$. The table and figure show that all the values of k are in excellent agreement, and thus so are the data from which they are obtained; of the 55 differences between k values, none exceed $2u_{diff}$ and the largest is only 0.96. Moreover, it turns out that only the NPL-79 and INRIM-10 results for R have insufficient weight to be included in the 2014 final adjustment, although they had sufficient weight to be included in the 2010 final adjustment.

B. Multivariate analysis of data

Our multivariate analysis of the data employs a well-known least-squares method that allows correlations among the input data to be properly taken into account. Used in the four previous adjustments, it is described in Appendix E of CODATA-98 and the references cited therein. It is recalled from that appendix that a least-squares adjustment is characterized by the number of input data N, number of variables or adjusted constants M, degrees of freedom $\nu = N - M$, statistic χ^2, probability $p(\chi^2|\nu)$ of obtaining an observed value of χ^2 that large or larger for the given value of ν, Birge ratio $R_B = \sqrt{\chi^2/\nu}$ (χ^2/ν is often called the reduced χ^2), and the normalized residual of the ith input datum $r_i = (x_i - \langle x_i \rangle)/u_i$, where x_i is the input datum, $\langle x_i \rangle$ its adjusted value, and u_i its standard uncertainty.

The observational equations for the input data are given in Tables XXIII and XXIV. These equations are written in terms of a particular independent subset of constants (broadly interpreted) called adjusted constants. These are the variables (or unknowns) of the adjustment. The least-squares calculation yields values of the adjusted constants that predict values of the

RIGHTSLINK

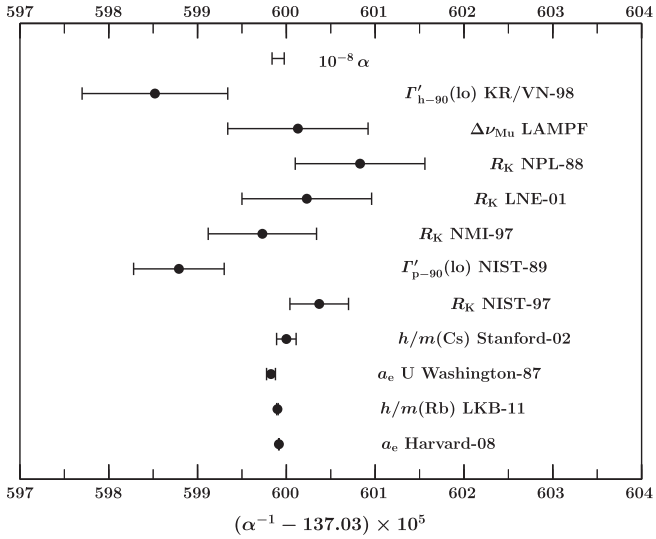

FIG. 1. Values of the fine-structure constant α with $u_{\rm r} < 10^{-7}$ inferred from the input data in Table XVIII in order of decreasing uncertainty from top to bottom (see Table XX).

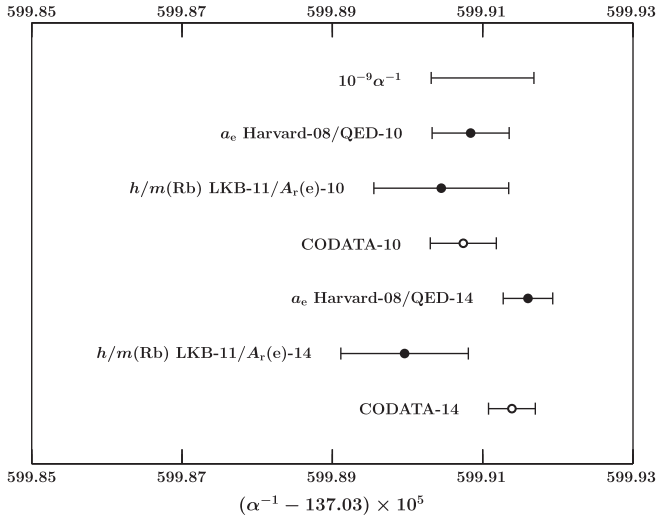

FIG. 2. Comparison of input data $B22.2$ (HarvU-08) and $B48$ (LKB-11) through their inferred values of α. QED-10 and QED-14 mean the QED theoretical expression for $a_{\rm e}$ at the time of the 2010 and 2014 CODATA constants adjustments, and $A_{\rm r}$(e)-10 and $A_{\rm r}$(e)-14 have the same meaning for $A_{\rm r}$(e). Both $B22.2$ and $B48$ have the same value in the 2010 and 2014 adjustments and are essentially the sole determinants of the recommended value of α in each.

input data through their observational equations that best agree with the data themselves in the least-squares sense. The adjusted constants used in the 2014 calculations are given in Tables XXV and XXVI.

The symbol $\doteq$ in an observational equation indicates that an input datum of the type on the left-hand side is ideally given by the expression on the right-hand side containing adjusted constants. But because the equation is one of an overdetermined set that relates a datum to adjusted constants, the two sides are not necessarily equal. The best estimate of the value of an input datum is its observational equation evaluated with the least-squares adjusted values of the adjusted constants on which its observational equation depends. For some input data such as $\delta_{\rm e}$ and R, the observational equation is simply $\delta_{\rm e} \doteq \delta_{\rm e}$ and $R \doteq R$.

The bound-state g-factor ratios in the observational equations of Table XXIV are treated as fixed quantities with negligible uncertainties (see Table XIII, Sec. VI.A). The frequency $f_{\rm p}$ is not an adjusted constant but is included in the equation for data items $B25$ and $B26$ to indicate that they are functions of $f_{\rm p}$. Finally, the observational equations for items and $B25$ and $B26$, which are based on Eqs. (223)–(225) of Sec. VI.B.2, include the theoretical expressions for $a_{\rm e}$ and $\Delta\nu_{\rm Mu}$ which are given as observational equations $B22$ and $B27$ in Table XXIV.

Also recalled from Appendix E of CODATA-98 is the self-sensitivity coefficient $S_{\rm c}$ for an input datum, which is a measure of the influence of that datum on the adjusted value of the

TABLE XXI. Inferred values of the Planck constant h in order of increasing standard uncertainty obtained from the indicated experimental data in Table XVIII

Primary source	Item number	Identification	Sec. and Eq.	$h/(\mathrm{J\,s})$	Relative standard uncertainty $u_{\rm r}$
$K_{\rm J}^2 R_{\rm K}$	$B44.6$	NRC-15	VIII.E (237)	$6.626\,070\,11(12) \times 10^{-34}$	1.8×10^{-8}
$N_{\rm A}(^{28}{\rm Si})$	$B63.2$	IAC-15	IX.B (240)	$6.626\,070\,15(13) \times 10^{-34}$	2.0×10^{-8}
$N_{\rm A}(^{28}{\rm Si})$	$B63.1$	IAC-11	IX.B (239)	$6.626\,069\,89(20) \times 10^{-34}$	3.0×10^{-8}
$K_{\rm J}^2 R_{\rm K}$	$B44.4$	NIST-15	VIII.D (234)	$6.626\,069\,36(38) \times 10^{-34}$	5.7×10^{-8}
$K_{\rm J}^2 R_{\rm K}$	$B44.2$	NIST-98	VIII.D	$6.626\,068\,91(58) \times 10^{-34}$	8.7×10^{-8}
$K_{\rm J}^2 R_{\rm K}$	$B44.5$	NPL-12	VIII.A	$6.626\,0712(13) \times 10^{-34}$	2.0×10^{-7}
$K_{\rm J}^2 R_{\rm K}$	$B44.1$	NPL-90	VIII.A	$6.626\,0682(13) \times 10^{-34}$	2.0×10^{-7}
$K_{\rm J}^2 R_{\rm K}$	$B44.7$	LNE-15	VIII.C (231)	$6.626\,0688(17) \times 10^{-34}$	2.6×10^{-7}
$K_{\rm J}^2 R_{\rm K}$	$B44.3$	METAS-11	VIII.B	$6.626\,0691(20) \times 10^{-34}$	2.9×10^{-7}
$K_{\rm J}$	$B42.1$	NMI-89	VIII	$6.626\,0684(36) \times 10^{-34}$	5.4×10^{-7}
$K_{\rm J}$	$B42.2$	PTB-91	VIII	$6.626\,0670(42) \times 10^{-34}$	6.3×10^{-7}
$\Gamma'_{\rm p-90}$(hi)	$B41.2$	NPL-79	VIII	$6.626\,0730(67) \times 10^{-34}$	1.0×10^{-6}
$\mathcal{F}_{90}$	$B45$	NIST-80	VIII	$6.626\,0658(88) \times 10^{-34}$	1.3×10^{-6}
$\Gamma'_{\rm p-90}$(hi)	$B41.1$	NIM-95	VIII	$6.626\,071(11) \times 10^{-34}$	1.6×10^{-6}

RIGHTSLINK

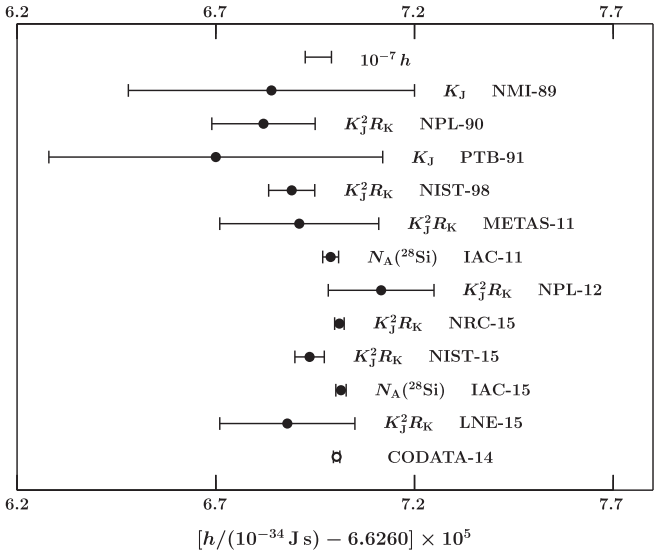

FIG. 3. Values of the Planck constant h with $u_r < 10^{-6}$ inferred from the input data in Table XVIII and the 2014 CODATA recommended value in chronological order from top to bottom (see Table XXI).

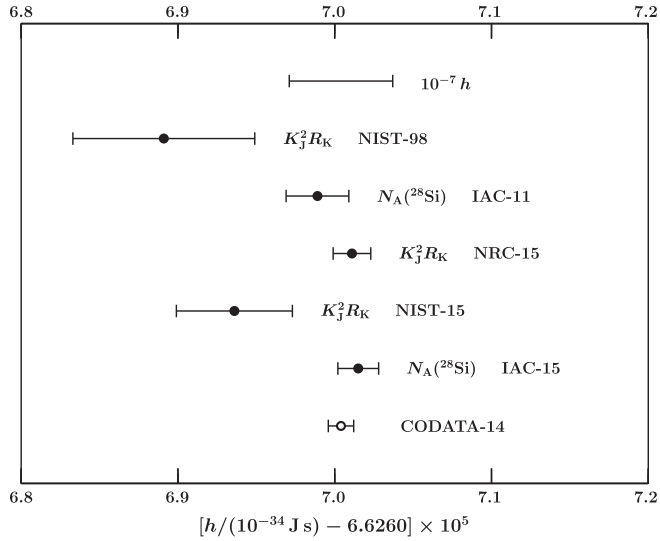

FIG. 4. Values of the Planck constant h with $u_r < 10^{-7}$ inferred from the input data in Table XVIII and the 2014 CODATA recommended value in chronological order from top to bottom (see Table XXI). The input data from which these values are inferred are included in the final adjustment on which the 2014 recommended values are based.

quantity of which the datum is an example. As in previous adjustments, in general, for an input datum to be included in the final adjustment on which the 2014 recommended values are based, its value of S_c must be greater than 0.01, or 1%, which means that its uncertainty must be no more than about a factor of 10 larger than the uncertainty of the adjusted value of that quantity; see Sec. I.D of CODATA-98 for the justification of this 1% cutoff. However, the exclusion of a datum is not followed if, for example, a datum with $S_c < 0.01$ is part of a group of data obtained in a given experiment where most of the other data have self-sensitivity coefficients > 0.01. It is also not followed for G, but in this case it is because of the significant disagreement of the available data and hence lack of motivation for anything beyond a simple weighted mean. Indeed, because the G data are independent of all other data and can be treated separately, and because they determine only one variable, in this case the multivariate analysis becomes simply the calculation of their weighted mean.

1. Data related to the Newtonian constant of gravitation G

The 14 values of G to be considered are summarized in Table XV of Sec. XI and are discussed in the text accompanying it. For easy reference they are listed in Table XXVII of this section and are graphically compared in Fig. 6. The last three results in the table and figure, BIPM-14, LENS-14, and UCI-14, have become available since 2010. Although the BIPM-14 and UCI-14 results have the comparatively small relative standard uncertainties $u_r = 24 \times 10^{-6}$ and $u_r = 19 \times 10^{-6}$, respectively, they have not reduced the quite large inconsistencies among the G data that have plagued them for some 20 years and which are evident in the table and figure.

Indeed, of the 91 differences among the 14 results, 45 are larger than $2u_{\mathrm{diff}}$ and 22 are larger than $4u_{\mathrm{diff}}$. The five largest, $15.1u_{\mathrm{diff}}$, $11.4u_{\mathrm{diff}}$, $10.7u_{\mathrm{diff}}$, $10.5u_{\mathrm{diff}}$, and $10.4u_{\mathrm{diff}}$, are

TABLE XXII. Inferred values of the Boltzmann constant k in order of increasing standard uncertainty obtained from the indicated experimental data in Table XVIII

Primary source	Item number	Identification	Section	$k/(\mathrm{J\,K^{-1}})$	Relative standard uncertainty u_r
R	$B64.8$	NPL-13	X.A	$1.380\,6476(12) \times 10^{-23}$	9.0×10^{-7}
R	$B64.9$	LNE-15	X.A	$1.380\,6487(14) \times 10^{-23}$	1.0×10^{-6}
R	$B64.6$	LNE-11	X.A	$1.380\,6477(19) \times 10^{-23}$	1.4×10^{-6}
R	$B64.2$	NIST-88	X.A	$1.380\,6501(25) \times 10^{-23}$	1.8×10^{-6}
R	$B64.3$	LNE-09	X.A	$1.380\,6497(38) \times 10^{-23}$	2.7×10^{-6}
R	$B64.4$	NPL-10	X.A	$1.380\,6498(44) \times 10^{-23}$	3.2×10^{-6}
R	$B64.7$	NIM-13	X.A	$1.380\,6477(51) \times 10^{-23}$	3.7×10^{-6}
k/h	$B65$	NIM/NIST-15	X.B	$1.380\,6513(53) \times 10^{-23}$	3.9×10^{-6}
A_ϵ/R	$B66$	PTB-15	X.C	$1.380\,6509(55) \times 10^{-23}$	4.0×10^{-6}
R	$B64.5$	INRIM-10	X.A	$1.380\,641(10) \times 10^{-23}$	7.5×10^{-6}
R	$B64.1$	NPL-79	X.A	$1.380\,656(12) \times 10^{-23}$	8.4×10^{-6}

RIGHTSLINK

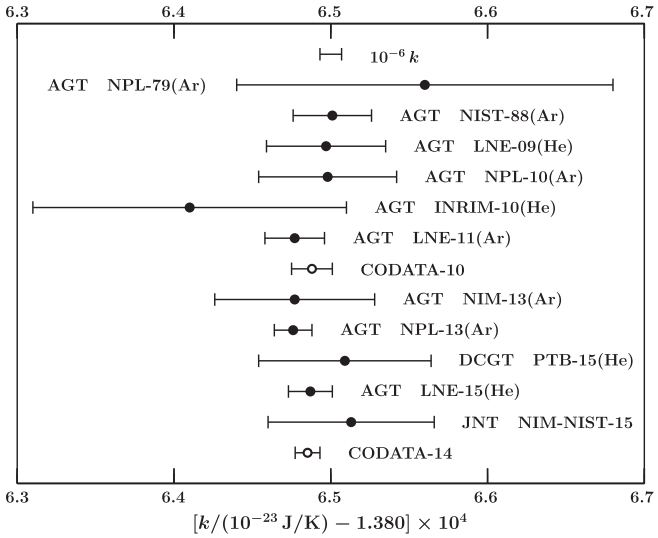

FIG. 5. Values of the Boltzmann constant k inferred from the input data in Table XVIII and the 2010 and 2014 CODATA recommended values in chronological order from top to bottom (see Table XXII). AGT: acoustic gas thermometry; DCGT: dielectric-constant gas thermometry; JNT: Johnson noise thermometry.

between JILA-10 and BIPM-14, UWash-00, BIPM-01, UCI-14, and UZur-06, respectively. The weighted mean of the 14 results is $6.674\,083(50)G_0$ $[7.5\times10^{-6}]$, where $G_0 = 10^{-11}\ \mathrm{kg^{-1}\,m^3\,s^{-2}}$. For this calculation $\chi^2 = 319.3$, $p(319.3|13) \approx 0$, and $R_B = 4.96$. Nine data have normalized residuals $|r_i| > 2$: JILA-10, BIPM-14, BIPM-01, NIST-82, HUST-09, TR&D-96, LENS-14, HUST-05, and UCI-14; their respective values are −12.5, 9.1, 5.6, −3.7, 3.3, 2.4, 2.2, 2.1, and 2.1.

Because of their comparatively small uncertainties, there is little impact if this calculation is repeated with just the six G results with $u_r < 30\times10^{-6}$. These are, in order of increasing uncertainty, UWash-00, UZur-06, UCI-14, JILA-10, BIPM-14, and HUST-09. Their weighted mean is $6.674\,077(52)G_0$ $[7.8\times10^{-6}]$, with $\chi^2 = 258.6$, $p(258.6|13) \approx 0$, and $R_B = 7.19$; their respective normalized residuals r_i are 1.9, 1.4, 2.2, −12.4, 9.1, and −3.3. The significant disagreement of the JILA-10 and BIPM-14 results with the four other low-uncertainty results is apparent. Additional calculations have been carried out, for example, one in which the JILA-10, BIPM-01, and BIPM-14 results are omitted. The weighted mean of the remaining 11 data is $6.674\,121(57)G_0$ $[8.6\times10^{-6}]$, with $\chi^2 = 49.8$, $p(49.8|13) = 2.9\times10^{-6}$, and $R_B = 2.2$. The value of G is not significantly different from the two other weighted-mean values and deleting the three data increases the χ^2 probability by 10 orders of magnitude. Nevertheless, for all practical purposes it is still very small.

In 2010 the Task Group decided to take as the recommended value of G the weighted mean and its uncertainty of the 11 values then available (essentially the first 11 values in Tables XV and XXVII), but after multiplying the initially assigned uncertainty of each value by the factor 14, called the expansion factor. The number 14 was chosen so that the smallest and largest of the 11 values differed from the recommended value

TABLE XXIII. Observational equations that express the input data related to R_∞ in Table XVI as functions of the adjusted constants in Table XXV. The numbers in the first column correspond to the numbers in the first column of Table XVI. Energy levels of hydrogenic atoms are discussed in Sec. IV.A. Note that $E_X(nL_j)/h$ is proportional to cR_∞ and independent of h, hence h is not an adjusted constant in these equations. See Sec. XIII.B for an explanation of the symbol ≐

Type of input datum	Observational equation
A1–A16	$\delta_H(nL_j) \doteq \delta_H(nL_j)$
A17–A25	$\delta_D(nL_j) \doteq \delta_D(nL_j)$
A26–A32, A39, A40	$\nu_H(n_1L_{1j_1} - n_2L_{2j_2}) \doteq [E_H(n_2L_{2j_2}; R_\infty, \alpha, A_r(e), A_r(p), r_p, \delta_H(n_2L_{2j_2})) - E_H(n_1L_{1j_1}; R_\infty, \alpha, A_r(e), A_r(p), r_p, \delta_H(n_1L_{1j_1}))]/h$
A33–A38	$\nu_H(n_1L_{1j_1} - n_2L_{2j_2}) - \frac{1}{4}\nu_H(n_3L_{3j_3} - n_4L_{4j_4}) \doteq \{E_H(n_2L_{2j_2}; R_\infty, \alpha, A_r(e), A_r(p), r_p, \delta_H(n_2L_{2j_2})) - E_H(n_1L_{1j_1}; R_\infty, \alpha, A_r(e), A_r(p), r_p, \delta_H(n_1L_{1j_1})) - \frac{1}{4}[E_H(n_4L_{4j_4}; R_\infty, \alpha, A_r(e), A_r(p), r_p, \delta_H(n_4L_{4j_4})) - E_H(n_3L_{3j_3}; R_\infty, \alpha, A_r(e), A_r(p), r_p, \delta_H(n_3L_{3j_3}))]\}/h$
A41–A45	$\nu_D(n_1L_{1j_1} - n_2L_{2j_2}) \doteq [E_D(n_2L_{2j_2}; R_\infty, \alpha, A_r(e), A_r(d), r_d, \delta_D(n_2L_{2j_2})) - E_D(n_1L_{1j_1}; R_\infty, \alpha, A_r(e), A_r(d), r_d, \delta_D(n_1L_{1j_1}))]/h$
A46–A47	$\nu_D(n_1L_{1j_1} - n_2L_{2j_2}) - \frac{1}{4}\nu_D(n_3L_{3j_3} - n_4L_{4j_4}) \doteq \{E_D(n_2L_{2j_2}; R_\infty, \alpha, A_r(e), A_r(d), r_d, \delta_D(n_2L_{2j_2})) - E_D(n_1L_{1j_1}; R_\infty, \alpha, A_r(e), A_r(d), r_d, \delta_D(n_1L_{1j_1})) - \frac{1}{4}[E_D(n_4L_{4j_4}; R_\infty, \alpha, A_r(e), A_r(d), r_d, \delta_D(n_4L_{4j_4})) - E_D(n_3L_{3j_3}; R_\infty, \alpha, A_r(e), A_r(d), r_d, \delta_D(n_3L_{3j_3}))]\}/h$
A48	$\nu_D(1S_{1/2} - 2S_{1/2}) - \nu_H(1S_{1/2} - 2S_{1/2}) \doteq \{E_D(2S_{1/2}; R_\infty, \alpha, A_r(e), A_r(d), r_d, \delta_D(2S_{1/2})) - E_D(1S_{1/2}; R_\infty, \alpha, A_r(e), A_r(d), r_d, \delta_D(1S_{1/2})) - [E_H(2S_{1/2}; R_\infty, \alpha, A_r(e), A_r(p), r_p, \delta_H(2S_{1/2})) - E_H(1S_{1/2}; R_\infty, \alpha, A_r(e), A_r(p), r_p, \delta_H(1S_{1/2}))]\}/h$
A49	$r_p \doteq r_p$
A50	$r_d \doteq r_d$

RIGHTSLINK

TABLE XXIV. Observational equations that express the input data in Table XVIII as functions of the adjusted constants in Table XXVI. The numbers in the first column correspond to the numbers in the first column of Table XVIII. For simplicity, the lengthier functions are not explicitly given. See Sec. XIII.B for an explanation of the symbol $\doteq$

Type of input datum	Observational equation	Sec.
*B*1	$A_r(n) \doteq A_r(n)$	III.A
*B*2	$A_r(^1H) \doteq A_r(p) + A_r(e) - \Delta E_B(^1H^+)\alpha^2 A_r(e)/2R_\infty hc$	III.B
*B*3	$\Delta E_B(^1H^+)/hc \doteq \Delta E_B(^1H^+)/hc$	III.B
*B*4	$A_r(^3H) \doteq A_r(t) + A_r(e) - \Delta E_B(^3H^+)\alpha^2 A_r(e)/2R_\infty hc$	III.B
*B*5	$\Delta E_B(^3H^+)/hc \doteq \Delta E_B(^3H^+)/hc$	III.B
*B*6	$A_r(^4He) \doteq A_r(\alpha) + 2A_r(e) - \Delta E_B(^4He^{2+})\alpha^2 A_r(e)/2R_\infty hc$	III.B
*B*7	$\Delta E_B(^4He^{2+})/hc \doteq \Delta E_B(^4He^{2+})/hc$	III.B
*B*8	$\dfrac{\omega_c(d)}{\omega_c(^{12}C^{6+})} \doteq \dfrac{12 - 6A_r(e) + \Delta E_B(^{12}C^{6+})\alpha^2 A_r(e)/2R_\infty hc}{6A_r(d)}$	III.C
*B*9	$\dfrac{\omega_c(h)}{\omega_c(^{12}C^{6+})} \doteq \dfrac{12 - 6A_r(e) + \Delta E_B(^{12}C^{6+})\alpha^2 A_r(e)/2R_\infty hc}{3A_r(h)}$	III.C
*B*10	$\Delta E_B(^{12}C^{6+})/hc \doteq \Delta E_B(^{12}C^{6+})/hc$	III.B
*B*11	$\dfrac{\omega_c(HD^+)}{\omega_c(^3He^+)} \doteq \dfrac{A_r(h) + A_r(e) - E_I(^3He^+)\alpha^2 A_r(e)/2R_\infty hc}{A_r(p) + A_r(d) + A_r(e) - E_I(HD^+)\alpha^2 A_r(e)/2R_\infty hc}$	III.C
*B*12	$\dfrac{\omega_c(HD^+)}{\omega_c(t)} \doteq \dfrac{A_r(t)}{A_r(p) + A_r(d) + A_r(e) - E_I(HD^+)\alpha^2 A_r(e)/2R_\infty hc}$	III.C
*B*13	$E_I(^3He^+)/hc \doteq E_I(^3He^+)/hc$	III.B
*B*14	$E_I(HD^+)/hc \doteq E_I(HD^+)/hc$	III.B
*B*15	$\dfrac{\omega_s(^{12}C^{5+})}{\omega_c(^{12}C^{5+})} \doteq -\dfrac{g_C(\alpha) + \delta_C}{10A_r(e)}[12 - 5A_r(e) + \Delta E_B(^{12}C^{5+})\alpha^2 A_r(e)/2R_\infty hc]$	V.D.2
*B*16	$\Delta E_B(^{12}C^{5+})/hc \doteq \Delta E_B(^{12}C^{5+})/hc$	III.B
*B*17	$\delta_C \doteq \delta_C$	V.D.1
*B*18	$\dfrac{\omega_s(^{28}Si^{13+})}{\omega_c(^{28}Si^{13+})} \doteq -\dfrac{g_{Si}(\alpha) + \delta_{Si}}{26A_r(e)}A_r(^{28}Si^{13+})$	V.D.2
*B*19	$A_r(^{28}Si) \doteq A_r(^{28}Si^{13+}) + 13A_r(e) - \Delta E_B(^{28}Si^{13+})\alpha^2 A_r(e)/2R_\infty hc$	III.B
*B*20	$\Delta E_B(^{28}Si^{13+})/hc \doteq \Delta E_B(^{28}Si^{13+})/hc$	III.B
*B*21	$\delta_{Si} \doteq \delta_{Si}$	V.D.1
*B*22	$a_e \doteq a_e(\alpha) + \delta_e$	V.A.1
*B*23	$\delta_e \doteq \delta_e$	V.A.1
*B*24	$\overline{R} \doteq -\dfrac{a_\mu}{1 + a_e(\alpha) + \delta_e}\dfrac{m_e}{m_\mu}\dfrac{\mu_e}{\mu_p}$	V.B.2
*B*25, *B*26	$\nu(f_p) \doteq \nu\left(f_p; R_\infty, \alpha, \dfrac{m_e}{m_\mu}, a_\mu, \dfrac{\mu_e}{\mu_p}, \delta_e, \delta_{Mu}\right)$	VI.B.2
*B*27	$\Delta\nu_{Mu} \doteq \Delta\nu_{Mu}\left(R_\infty, \alpha, \dfrac{m_e}{m_\mu}, a_\mu\right) + \delta_{Mu}$	VI.B.1
*B*28	$\delta_{Mu} \doteq \delta_{Mu}$	VI.B.1
*B*29	$\dfrac{\mu_p}{\mu_N} \doteq -(1 + a_e(\alpha) + \delta_e)\dfrac{A_r(p)}{A_r(e)}\dfrac{\mu_p}{\mu_e}$	V.C
*B*30	$\dfrac{\mu_e(H)}{\mu_p(H)} \doteq \dfrac{g_e(H)}{g_e}\left(\dfrac{g_p(H)}{g_p}\right)^{-1}\dfrac{\mu_e}{\mu_p}$	VI.A.1
*B*31	$\dfrac{\mu_d(D)}{\mu_e(D)} \doteq \dfrac{g_d(D)}{g_d}\left(\dfrac{g_e(D)}{g_e}\right)^{-1}\dfrac{\mu_d}{\mu_e}$	VI.A.1
*B*32	$\dfrac{\mu_e(H)}{\mu'_p} \doteq \dfrac{g_e(H)}{g_e}\dfrac{\mu_e}{\mu'_p}$	VI.A.1
*B*33	$\dfrac{\mu'_h}{\mu'_p} \doteq \dfrac{\mu'_h}{\mu'_p}$	VI.A.1
*B*34	$\dfrac{\mu_n}{\mu'_p} \doteq \dfrac{\mu_n}{\mu'_p}$	VI.A.1
*B*35	$\dfrac{\mu_p(HD)}{\mu_d(HD)} \doteq [1 + \sigma_{dp}]\dfrac{\mu_p}{\mu_e}\dfrac{\mu_e}{\mu_d}$	VI.A.1
*B*36	$\dfrac{\mu_t(HT)}{\mu_p(HT)} \doteq [1 - \sigma_{tp}]\dfrac{\mu_t}{\mu_p}$	VI.A.1
*B*37	$\sigma_{dp} \doteq \sigma_{dp}$	VI.A.1

RIGHTSLINK

TABLE XXIV. Observational equations that express the input data in Table XVIII as functions of the adjusted constants in Table XXVI. The numbers in the first column correspond to the numbers in the first column of Table XVIII. For simplicity, the lengthier functions are not explicitly given. See Sec. XIII.B for an explanation of the symbol $\doteq$ —Continued

Type of input datum	Observational equation	Sec.
*B*38	$\sigma_{tp} \doteq \sigma_{tp}$	VI.A.1
*B*39	$\Gamma'_{p-90}(\text{lo}) \doteq -\dfrac{K_{J-90}R_{K-90}[1+a_e(\alpha)+\delta_e]\alpha^3}{2\mu_0 R_\infty}\left(\dfrac{\mu_e}{\mu'_p}\right)^{-1}$	VIII
*B*40	$\Gamma'_{h-90}(\text{lo}) \doteq \dfrac{K_{J-90}R_{K-90}[1+a_e(\alpha)+\delta_e]\alpha^3}{2\mu_0 R_\infty}\left(\dfrac{\mu_e}{\mu'_p}\right)^{-1}\dfrac{\mu'_h}{\mu'_p}$	VIII
*B*41	$\Gamma'_{p-90}(\text{hi}) \doteq -\dfrac{c[1+a_e(\alpha)+\delta_e]\alpha^2}{K_{J-90}R_{K-90}R_\infty h}\left(\dfrac{\mu_e}{\mu'_p}\right)^{-1}$	VIII
*B*42	$K_J \doteq \left(\dfrac{8\alpha}{\mu_0 ch}\right)^{1/2}$	VIII
*B*43	$R_K \doteq \dfrac{\mu_0 c}{2\alpha}$	VIII
*B*44	$K_J^2 R_K \doteq \dfrac{4}{h}$	VIII
*B*45	$\mathcal{F}_{90} \doteq \dfrac{cM_u A_r(e)\alpha^2}{K_{J-90}R_{K-90}R_\infty h}$	VIII
*B*46, *B*48	$\dfrac{h}{m(X)} \doteq \dfrac{A_r(e)}{A_r(X)}\dfrac{c\alpha^2}{2R_\infty}$	VII
*B*47, *B*49	$A_r(X) \doteq A_r(X)$	III.A
*B*50–B59	$\dfrac{d_{220}(X)}{d_{220}(Y)} - 1 \doteq \dfrac{d_{220}(X)}{d_{220}(Y)} - 1$	IX.A
*B*60–B62	$d_{220}(X) \doteq d_{220}(X)$	IX.A
*B*63	$N_A \doteq \dfrac{cM_u A_r(e)\alpha^2}{2R_\infty h}$	IX.B
*B*64	$R \doteq R$	X.A
*B*65	$\dfrac{k}{h} \doteq \dfrac{2R_\infty R}{cM_u A_r(e)\alpha^2}$	X.B
*B*66	$\dfrac{A_\epsilon}{R} \doteq \dfrac{\alpha_0(^4\text{He})}{4\pi\epsilon_0 a_0^3}\dfrac{cM_u A_r(e)\alpha^5}{96\pi^2 Rh R_\infty^4}$	X.C
*B*67	$\dfrac{\alpha_0(^4\text{He})}{4\pi\epsilon_0 a_0^3} \doteq \dfrac{\alpha_0(^4\text{He})}{4\pi\epsilon_0 a_0^3}$	X.C
*B*68, *B*69	$\dfrac{\lambda(\text{CuK}\alpha_1)}{d_{220}(X)} \doteq \dfrac{1537.400\text{xu}(\text{CuK}\alpha_1)}{d_{220}(X)}$	IX.A
*B*70	$\dfrac{\lambda(\text{WK}\alpha_1)}{d_{220}(\text{N})} \doteq \dfrac{0.209\,010\,0\ \text{Å}^*}{d_{220}(\text{N})}$	IX.A
*B*71	$\dfrac{\lambda(\text{MoK}\alpha_1)}{d_{220}(\text{N})} \doteq \dfrac{707.831\text{xu}(\text{MoK}\alpha_1)}{d_{220}(\text{N})}$	IX.A

by about twice its uncertainty. This reduced each $|r_i|$ to less than 1. To achieve this level of consistency for the 14 values now available would require an expansion factor of about 16. After due consideration the Task Group decided that it would be more appropriate to follow its usual approach of treating inconsistent data, namely, to choose an expansion factor that reduces each $|r_i|$ to less than 2. It concluded that the resulting uncertainty would better reflect the current situation in light of the new low-uncertainty UCI-14 result with $u_r = 19 \times 10^{-6}$, which agrees well with the low-uncertainty UWash-00 and UZur-06 results with $u_r = 14 \times 10^{-6}$ and $u_r = 19 \times 10^{-6}$, respectively. Thus based on an expansion factor of 6.3, the 2014 CODATA recommended value is

$$G = 6.674\,08(31) \times 10^{-11}\ \text{kg}^{-1}\,\text{m}^3\,\text{s}^{-2} \quad [47 \times 10^{-6}]. \quad (268)$$

(Note that when the same expansion factor is applied to both members of a correlated pair, its square is also applied to their covariance so their correlation coefficient is unchanged. When the expansion factor is applied to one member of a correlated pair, just the expansion factor is applied to the covariance.) For this calculation $\chi^2 = 8.1$, $p(8.1|13) = 0.84$, and $R_B = 0.79$. As might be expected, JILA-10 and BIPM-14 still have the largest values of r_i: 1.98 and 1.45, respectively. The other 12 values of $|r_i|$ are less than 0.01.

In this calculation S_c is less than 0.01 for five of the 14 input data. If they are omitted, the value for G in Eq. (268) increases by 2 in the last place, but its two-digit uncertainty is unchanged. Although excluding such data is the Task Group's usual practice, it is not implemented in this case, because of the significant disagreements among the data and the desirability of having the recommended value reflect all the data.

RIGHTSLINK

TABLE XXV. The 28 adjusted constants (variables) used in the least-squares multivariate analysis of the Rydberg-constant data given in Table XVI. These adjusted constants appear as arguments of the functions on the right-hand side of the observational equations of Table XXIII

Adjusted constant	Symbol
Rydberg constant	R_∞
Bound-state proton rms charge radius	r_p
Bound-state deuteron rms charge radius	r_d
Additive correction to $E_H(1S_{1/2})/h$	$\delta_H(1S_{1/2})$
Additive correction to $E_H(2S_{1/2})/h$	$\delta_H(2S_{1/2})$
Additive correction to $E_H(3S_{1/2})/h$	$\delta_H(3S_{1/2})$
Additive correction to $E_H(4S_{1/2})/h$	$\delta_H(4S_{1/2})$
Additive correction to $E_H(6S_{1/2})/h$	$\delta_H(6S_{1/2})$
Additive correction to $E_H(8S_{1/2})/h$	$\delta_H(8S_{1/2})$
Additive correction to $E_H(2P_{1/2})/h$	$\delta_H(2P_{1/2})$
Additive correction to $E_H(4P_{1/2})/h$	$\delta_H(4P_{1/2})$
Additive correction to $E_H(2P_{3/2})/h$	$\delta_H(2P_{3/2})$
Additive correction to $E_H(4P_{3/2})/h$	$\delta_H(4P_{3/2})$
Additive correction to $E_H(8D_{3/2})/h$	$\delta_H(8D_{3/2})$
Additive correction to $E_H(12D_{3/2})/h$	$\delta_H(12D_{3/2})$
Additive correction to $E_H(4D_{5/2})/h$	$\delta_H(4D_{5/2})$
Additive correction to $E_H(6D_{5/2})/h$	$\delta_H(6D_{5/2})$
Additive correction to $E_H(8D_{5/2})/h$	$\delta_H(8D_{5/2})$
Additive correction to $E_H(12D_{5/2})/h$	$\delta_H(12D_{5/2})$
Additive correction to $E_D(1S_{1/2})/h$	$\delta_D(1S_{1/2})$
Additive correction to $E_D(2S_{1/2})/h$	$\delta_D(2S_{1/2})$
Additive correction to $E_D(4S_{1/2})/h$	$\delta_D(4S_{1/2})$
Additive correction to $E_D(8S_{1/2})/h$	$\delta_D(8S_{1/2})$
Additive correction to $E_D(8D_{3/2})/h$	$\delta_D(8D_{3/2})$
Additive correction to $E_D(12D_{3/2})/h$	$\delta_D(12D_{3/2})$
Additive correction to $E_D(4D_{5/2})/h$	$\delta_D(4D_{5/2})$
Additive correction to $E_D(8D_{5/2})/h$	$\delta_D(8D_{5/2})$
Additive correction to $E_D(12D_{5/2})/h$	$\delta_D(12D_{5/2})$

TABLE XXVI. Variables used in the least-squares adjustment of the constants. They are arguments of the functions on the right-hand side of the observational equations in Table XXIV

Adjusted constant	Symbol
Neutron relative atomic mass	$A_r(n)$
Electron relative atomic mass	$A_r(e)$
Proton relative atomic mass	$A_r(p)$
$^1H^+$ electron removal energy	$\Delta E_B(^1H^+)$
Triton relative atomic mass	$A_r(t)$
$^3H^+$ electron removal energy	$\Delta E_B(^3H^+)$
Alpha particle relative atomic mass	$A_r(\alpha)$
$^4He^{2+}$ electron removal energy	$\Delta E_B(^4He^{2+})$
Deuteron relative atomic mass	$A_r(d)$
Helion relative atomic mass	$A_r(h)$
$^{12}C^{6+}$ electron removal energy	$\Delta E_B(^{12}C^{6+})$
$^3He^+$ electron ionization energy	$\Delta E_I(^3He^+)$
HD^+ electron ionization energy	$\Delta E_I(HD^+)$
$^{12}C^{5+}$ electron removal energy	$\Delta E_B(^{12}C^{5+})$
Additive correction to $g_C(\alpha)$	δ_C
$^{28}Si^{13+}$ relative atomic mass	$A_r(^{28}Si^{13+})$
$^{28}Si^{13+}$ electron removal energy	$\Delta E_B(^{28}Si^{13+})$
Additive correction to $g_{Si}(\alpha)$	δ_{Si}
Fine-structure constant	α
Additive correction to a_e(th)	δ_e
Muon magnetic-moment anomaly	a_μ
Electron-muon mass ratio	m_e/m_μ
Electron-proton magnetic-moment ratio	μ_e/μ_p
Additive correction to $\Delta\nu_{Mu}$(th)	δ_{Mu}
Deuteron-electron magnetic-moment ratio	μ_d/μ_e
Shielded helion to shielded proton magnetic-moment ratio	μ'_h/μ'_p
Neutron to shielded proton magnetic-moment ratio	μ_n/μ'_p
Shielding difference of d and p in HD	σ_{dp}
Triton-proton magnetic-moment ratio	μ_t/μ_p
Shielding difference of t and p in HT	σ_{tp}
Electron to shielded proton magnetic-moment ratio	μ_e/μ'_p
Planck constant	h
^{133}Cs relative atomic mass	$A_r(^{133}Cs)$
^{87}Rb relative atomic mass	$A_r(^{87}Rb)$
d_{220} of Si crystal WASO 17	d_{220}(W17)
d_{220} of Si crystal ILL	d_{220}(ILL)
d_{220} of Si crystal MO*	d_{220}(MO*)
d_{220} of Si crystal NR3	d_{220}(NR3)
d_{220} of Si crystal N	d_{220}(N)
d_{220} of Si crystal WASO 4.2a	d_{220}(W4.2a)
d_{220} of Si crystal WASO 04	d_{220}(W04)
d_{220} of an ideal Si crystal	d_{220}
d_{220} of Si crystal NR4	d_{220}(NR4)
Molar gas constant	R
Static electric dipole polarizability of ^{4}He in atomic units	$\alpha_0^*(^4He)$
Copper $K\alpha_1$ x unit	xu(CuKα_1)
Ångstrom star	Å*
Molybdenum $K\alpha_1$ x unit	xu(MoKα_1)

2. Data related to all other constants

Tables XXVIII and XXIX summarize 12 least-squares analyses of the input data in Tables XVI and XVIII, including their correlation coefficients in Tables XVII and XIX; they are discussed in the following paragraphs. Because the adjusted value of R_∞ is essentially the same for all five adjustments summarized in Table XXVIII and equal to that of adjustment 3 of Table XXIX, the values are not listed in Table XXVIII. (Note that adjustment 3 in Tables XXVIII and XXIX is the same adjustment.)

Adjustment 1. The initial adjustment includes all of the input data, four of which have values of $|r_i|$ that are problematically larger than 2. They are $B2$, the AME-12 result for $A_r(^1H)$, $B11$ and $B12$, the FSU-15 results for $\omega_c(HD^+)/\omega_c(^3He^+)$ and $\omega_c(HD^+)/\omega_c(t)$, and $B39.1$, the NIST-89 result for $\Gamma'_{p-90}(lo)$. Their respective values of r_i are 2.61, 4.06, 3.57, and 2.20. The NIST-89 datum was discussed above in connection with inferred values of α and because it is of no real concern it is not discussed further. The other three residuals are due to the inconsistency of $B9$, the UWash-15 result for $\omega_c(h)/\omega_c(^{12}C^{6+})$, and $B11$. Although u_r is 1.4×10^{-11} and 4.8×10^{-11} for $B9$ and $B11$, respectively, which are quite small, their inconsistency becomes apparent by comparing the values of $A_r(^3He)$ that they infer; the result is that the value from $B11$ exceeds that from $B9$ by $3.9u_{diff}$ (Myers *et al.*, 2015; Zafonte and Van Dyck, 2015). Because the reason for this discrepancy is unknown and both frequency ratios are credible,

RIGHTSLINK

TABLE XXVII. Summary of values of G used to determine the 2014 recommended value (see also Table XV, Sec. XI)

Item number	Value[a] (10^{-11} m^3 kg^{-1} s^{-2})	Relative standard uncertainty u_r	Identification
$G1$	6.672 48(43)	6.4×10^{-5}	NIST-82
$G2$	6.672 9(5)	7.5×10^{-5}	TR&D-96
$G3$	6.673 98(70)	1.0×10^{-4}	LANL-97
$G4$	6.674 255(92)	1.4×10^{-5}	UWash-00
$G5$	6.675 59(27)	4.0×10^{-5}	BIPM-01
$G6$	6.674 22(98)	1.5×10^{-4}	UWup-02
$G7$	6.673 87(27)	4.0×10^{-5}	MSL-03
$G8$	6.672 22(87)	1.3×10^{-4}	HUST-05
$G9$	6.674 25(12)	1.9×10^{-5}	UZur-06
$G10$	6.673 49(18)	2.7×10^{-5}	HUST-09
$G11$	6.672 34(14)	2.1×10^{-5}	JILA-10
$G12$	6.675 54(16)	2.4×10^{-5}	BIPM-14
$G13$	6.671 91(99)	1.5×10^{-4}	LENS-14
$G14$	6.674 35(13)	1.9×10^{-5}	UCI-14

[a]Correlation coefficients: $r(G1, G3) = 0.351$; $r(G8, G10) = 0.134$.

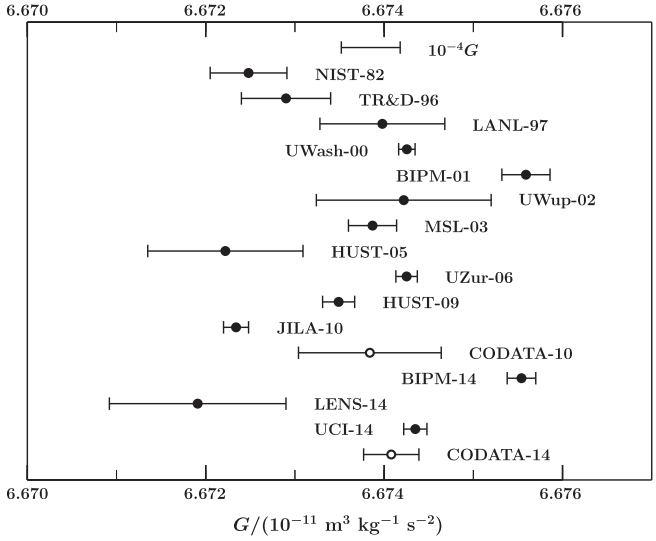

FIG. 6. Values of the Newtonian constant of gravitation G in Table XXVII and the 2010 and 2014 CODATA recommended values in chronological order from top to bottom.

the Task Group decided to include both in the final adjustment with a sufficiently large expansion factor so that $r_i < 2$ for both. It was also decided to include the companion ratios $\omega_c(\mathrm{d})/\omega_c(^{12}\mathrm{C}^{6+})$ ($B8$) and $\omega_c(\mathrm{HD}^+)/\omega_c(t)$ ($B12$) with $u_r = 2.0\times10^{-11}$ and 4.8×10^{-11}, respectively, without an expansion factor.

Adjustment 2. This adjustment uses all the data with an expansion factor of 2.8 applied to the uncertainties of data $B9$ and $B11$, resulting in $r_i = 1.95$ for $B11$ and $r_i = 1.73$ for $B12$. This also results in the reduction of r_i of $B2$ from 2.61 to 0.49. The complex relationships, apparent from their observational equations, between input data $B2$, $B8$ and $B9$, and $B11$ and $B12$, and the adjusted constants $A_r(\mathrm{p})$, $A_r(\mathrm{d})$, and $A_r(\mathrm{h})$, are responsible for the somewhat surprising effect of the expansion factor on r_i (see Table XXIV). The expansion factor has no effect on the values of α and h, as can be seen from Table XXVIII.

Adjustment 3. Adjustment 3 is the adjustment on which the 2014 CODATA recommended values are based and as such is called the "final adjustment." It differs from adjustment 2 in that, following the prescription described above, 22 of the initial input data, all from Table XVIII, with values of $S_c < 0.01$ in adjustment 2 are omitted. These are $B4$, $B22.1$, $B39.1$ to $B44.1$, $B44.3$, $B44.5$, $B44.7$ to $B46$, $B64.1$, and $B64.5$. (The range in values of S_c for the deleted data is 0.0000 to 0.0096, and no datum with a value of $S_c > 1$ was "converted" to a value with $S_c < 1$ due to the expansion factor.) Further, because $A_r(^3\mathrm{H})$, item $B4$, is deleted as an input datum due to its low weight, the value of $\Delta E_B(^3\mathrm{H}^+)/hc$, item $B5$, which is not relevant to any other input datum, is also deleted and omitted as an adjusted constant. The situation is exactly the same for $h/m(^{133}\mathrm{Cs})$, item $B46$, and $A_r(^{133}\mathrm{Cs})$, item $B47$. This brings the total number of omitted data to 24. Table XXVIII shows that deleting them has inconsequential impact on the values of α and h. The data for the final adjustment are quite consistent, as demonstrated by the value of χ^2: $p(42.4|54) = 0.87$.

Adjustments 4 and 5. The purpose of these adjustments is to test the robustness of the 2014 recommended values of α and h by omitting the most accurate data that determine these constants. Adjustment 4 differs from adjustment 2 in that the four data that provide values of α with the smallest uncertainties are deleted, namely, items $B22.2$, $B48$, $B22.1$, and $B46$, which are the two values of a_e and the $h/m(X)$ values for ^{133}Cs and ^{87}Rb; see the first four entries of Table XX. [For the same reason as in adjustment 3, in adjustment 4 the value of $A_r(^{133}\mathrm{Cs})$ is also deleted as an input datum and $A_r(^{133}\mathrm{Cs})$ as an adjusted constant; the same applies to $A_r(^{87}\mathrm{Rb})$.] Adjustment 5 differs from adjustment 2 in that the five data that provide values of h with the smallest uncertainties are deleted, namely, items $B44.6$, $B63.2$, $B63.1$, $B44.4$, and $B44.2$, which are three

RIGHTSLINK

TABLE XXVIII. Summary of the results of some of the least-squares adjustments used to analyze the input data given in Tables XVI, XVII, XVIII, and XIX. The values of α and h are those obtained in the adjustment, N is the number of input data, M is the number of adjusted constants, $\nu = N - M$ is the degrees of freedom, and $R_B = \sqrt{\chi^2/\nu}$ is the Birge ratio. See the text for an explanation and discussion of each adjustment, but in brief, adjustment 1 is all the data; 2 is the same as 1 except with the uncertainties of the two cyclotron frequency ratios related to the helion multiplied by 2.8; 3 is 2 with the low-weight input data deleted and is the adjustment on which the 2014 recommended values are based; 4 is 2 with the input data that provide the most accurate values of α deleted; and 5 is 1 with the input data that provide the most accurate values of h deleted as well as the low-weight data for α

Adj.	N	M	ν	χ^2	R_B	α^{-1}	$u_r(\alpha^{-1})$	h/(J s)	$u_r(h)$
1	151	75	76	85.6	1.06	137.035 999 136(31)	2.3×10^{-10}	$6.626\,070\,031(81) \times 10^{-34}$	1.2×10^{-8}
2	151	75	76	65.5	0.93	137.035 999 136(31)	2.3×10^{-10}	$6.626\,070\,031(81) \times 10^{-34}$	1.2×10^{-8}
3	127	73	54	42.4	0.89	137.035 999 139(31)	2.3×10^{-10}	$6.626\,070\,040(81) \times 10^{-34}$	1.2×10^{-8}
4	145	73	71	58.4	0.90	137.035 9997(13)	9.5×10^{-9}	$6.626\,070\,00(10) \times 10^{-34}$	1.5×10^{-8}
5	135	74	61	41.0	0.82	137.035 999 138(31)	2.3×10^{-10}	$6.626\,069\,39(72) \times 10^{-34}$	1.1×10^{-7}

TABLE XXIX. Summary of the results of some of the least-squares adjustments used to analyze the input data related to R_∞. The values of R_∞, r_p, and r_d are those obtained in the indicated adjustment, N is the number of input data, M is the number of adjusted constants, $\nu = N - M$ is the degrees of freedom, and $R_B = \sqrt{\chi^2/\nu}$ is the Birge ratio. See the text for an explanation and discussion of each adjustment, but in brief, adjustment 6 is 3, but the scattering data for the nuclear radii are omitted; 7 is 3, but with only the hydrogen data included (but not the isotope shift); 8 is 7 with the r_p datum deleted; 9 and 10 are similar to 7 and 8, but for the deuterium data; 11 is 3 with the muonic Lamb-shift value of r_p included; and 12 is 11, but without the scattering values of r_p and r_d

Adj.	N	M	ν	χ^2	R_B	R_∞/m^{-1}	$u_r(R_\infty)$	r_p/fm	r_d/fm
3	127	73	54	42.4	0.89	10 973 731.568 508(65)	5.9×10^{-12}	0.8751(61)	2.1413(25)
6	125	73	52	41.0	0.89	10 973 731.568 517(82)	7.4×10^{-12}	0.8759(77)	2.1416(31)
7	109	63	46	38.0	0.91	10 973 731.568 533(74)	6.7×10^{-12}	0.8774(69)	
8	108	63	45	38.0	0.92	10 973 731.568 523(94)	8.6×10^{-12}	0.8764(89)	
9	92	56	36	28.0	0.88	10 973 731.568 36(13)	1.1×10^{-11}		2.1287(93)
10	91	56	35	28.0	0.89	10 973 731.568 27(30)	2.7×10^{-11}		2.121(25)
11	128	73	55	72.8	1.15	10 973 731.568 157(10)	9.4×10^{-13}	0.841 00(39)	2.127 65(18)
12	126	73	53	60.8	1.07	10 973 731.568 157(10)	9.4×10^{-13}	0.840 95(39)	2.127 63(18)

watt-balance values of $K_J^2 R_K$ and two XRCD-enriched silicon values of N_A; see the first five entries of Table XXI. The results of these two adjustments are reasonable: Table XXVIII shows that the value of α from the less accurate α-related data used in adjustment 4, and the value of h from the less accurate h-related data used in adjustment 5, agree with the corresponding recommended values from adjustment 3.

Adjustments 6 to 12. The purpose of the seven adjustments summarized in Table XXIX is to investigate the data that determine the recommended values of R_∞, r_p, and r_d. Results from adjustment 3, the final adjustment, are included in the table for reference purposes. We begin with a discussion of adjustments 6 to 10, which are derived from adjustment 3 by deleting selected input data. We then discuss adjustments 11 and 12, which examine the impact of the value of the proton rms charge radius derived from the measurement of the Lamb shift in muonic hydrogen discussed in Sec. IV.A.3.c and given in Eq. (78). Note that the value of R_∞ depends only weakly on the data in Table XVIII.

In adjustment 6, the electron scattering values of r_p and r_d, data items *A*49 and *A*50 in Table XVI, are deleted from adjustment 3. Thus, the values of these two quantities from adjustment 6 are based solely on H and D spectroscopic data and are called the spectroscopic values of r_p and r_d:

$$r_p = 0.8759(77)\ \text{fm}, \tag{269}$$

$$r_d = 2.1416(31)\ \text{fm}. \tag{270}$$

It is evident from a comparison of the results of this adjustment and adjustment 3 that the scattering values of the radii play a comparatively small role in determining the 2014 recommended values of R_∞, r_p and r_d.

Adjustment 7 is based on only hydrogen data, including the scattering values of r_p but not the difference between the $1S_{1/2} - 2S_{1/2}$ transition frequencies in H and D, item *A*48 in Table XVI, known as the isotope shift. Adjustment 8 differs from adjustment 7 in that the scattering value of r_p is deleted. Adjustments 9 and 10 are similar to 7 and 8 but are based on only deuterium data; that is, adjustment 9 includes the scattering value of r_d but not the isotope shift, while for adjustment 10 the scattering value is deleted. The results of these four adjustments show the dominant role of the hydrogen data and the importance of the isotope shift in determining the recommended value of r_d. Further, the four values of R_∞ from these adjustments agree with the 2014 recommended value, and the two values of r_p and of r_d also agree with their respective recommended values: the largest difference from the recommended value for the eight results is $1.4u_{\text{diff}}$.

RIGHTSLINK

Adjustment 11 differs from adjustment 3 in that it includes the muonic hydrogen value $r_p = 0.840\,87(39)$ fm, and adjustment 12 differs from adjustment 11 in that the two scattering values of the nuclear radii are deleted. Because the muonic hydrogen value is significantly smaller and has a significantly smaller uncertainty than the purely spectroscopic value of adjustment 6 as well as the scattering value, it has a major impact on the results of adjustments 11 and 12, as can be seen from Table XXIX: for both adjustments the value of R_∞ shifts down by over 5 standard deviations and its uncertainty is reduced by a factor grater than 6. Moreover, and not surprisingly, the values of r_p and of r_d from both adjustments are significantly smaller than the recommended values and have significantly smaller uncertainties. The inconsistency between the muonic hydrogen result for r_p and the spectroscopic and scattering results is further demonstrated by the comparatively low probability of χ^2 for adjustment 11: $p(72.8|55) = 0.0054$. The 2014 recommended value of r_p and the purely spectroscopic value, which is that from adjustment 6, exceed the muonic hydrogen value by $5.6u_{\text{diff}}$ and $4.5u_{\text{diff}}$, respectively.

The impact of the muonic hydrogen value of r_p can also be seen by examining for adjustments 3, 11, and 12 the normalized residuals and self-sensitivity coefficients of the principal experimental data that determine R_∞, namely, items $A26.1$ to $A50$ in Table XVI. In brief, $|r_i|$ for these data in the final adjustment range from near 0 to 1.13 for item $A50$, the r_d scattering result, with the vast majority being less than 1. For the three greater than 1, $|r_i|$ is 1.03, 1.02, and 1.02. The value of S_c is 1.00 for items $A26.1$ and $A26.2$ together, which are the two hydrogen $1S_{1/2} - 2S_{1/2}$ transition frequencies; it is also 1.00 for $A48$, the H-D isotope shift. For item $A49$, the scattering value of r_p, it is 0.31. Most others are a few percent, although some values of S_c are near 0.

The situation is markedly different for adjustment 12. First, $|r_i|$ for item $A30$, the hydrogen transition frequency involving the $8D_{5/2}$ state, is 3.12 compared to 1.03 in adjustment 3; and items $A41$, $A42$, and $A43$, deuterium transitions involving the $8S_{1/2}$, $8D_{3/2}$, and $8D_{5/2}$ states, are now 2.54, 2.47, and 3.12, respectively, compared to 0.56, 0.34, and 0.86. Further, ten other transitions have residuals in the range 1.04 to 1.80. As a result, with this proton radius, the predictions of the theory for hydrogen and deuterium transition frequencies are not generally consistent with the experiments. Equally noteworthy is the fact that, although S_c for items $A26.1$ and $A26.2$ together and $A48$ remain equal to 1.00, for all other transition frequencies S_c is less than 0.01, which means that they play an inconsequential role in determining R_∞. The results for adjustment 11, which includes the scattering values of the nuclear radii as well as the muonic hydrogen value, are similar.

Because of the impact of the latter value on the internal consistency of the R_∞ data and its continued disagreement with the spectroscopic and scattering values, the Task Group decided, as it did for the 2010 adjustment, that it was premature to include it as an input datum in the 2014 final adjustment; it was deemed more prudent to continue to wait and see if further research can resolve what has come to be called the "proton radius puzzle"; see Sec. IV.A.3.c for additional discussion.

3. Test of the Josephson and quantum-Hall-effect relations

As in the three previous CODATA adjustments, the exactness of the relations $K_J = 2e/h$ and $R_K = h/e^2$ is investigated by writing

$$K_J = \frac{2e}{h}(1+\epsilon_J) = \left(\frac{8\alpha}{\mu_0 ch}\right)^{1/2}(1+\epsilon_J), \tag{271}$$

$$R_K = \frac{h}{e^2}(1+\epsilon_K) = \frac{\mu_0 c}{2\alpha}(1+\epsilon_K), \tag{272}$$

where ϵ_J and ϵ_K are unknown correction factors taken to be additional adjusted constants. Replacing the relations $K_J = 2e/h$ and $R_K = h/e^2$ in the analysis leading to the observational equations in Table XXIV with the generalizations in Eqs. (271) and (272) leads to the modified observational equations given in Table XXX.

Although the NIM/NIST-15 result for k/h, item $B65$, was obtained using the Josephson and quantum-Hall effects, it is not included in the tests of the relations $K_J = 2e/h$ and $R_K = h/e^2$, because of its comparatively large uncertainty.

The results of six different adjustments are summarized in Table XXXI. An entry of 0 in the ϵ_K column means that it is assumed $R_K = h/e^2$ in the corresponding adjustment; similarly, an entry of 0 in the ϵ_J column means that it is assumed $K_J = 2e/h$ in the corresponding adjustment. The following remarks apply to the six adjustments.

Adjustment (i) differs from adjustment 2 summarized in Table XXVIII only in that the assumption $K_J = 2e/h$ and $R_K = h/e^2$ is relaxed. For this adjustment, $N = 153$, $M = 77$, $\nu = N - M = 76$, $\chi^2 = 64.1$, $p(64.1|76) = 0.83$, and $R_B = 0.92$. Examination of the table shows that ϵ_K is consistent with

TABLE XXX. Generalized observational equations that express input data $B32 - B38$ in Table XVIII as functions of the adjusted constants in Tables XXV and XXVI with the additional adjusted constants ϵ_J and ϵ_K as given in Eqs. (271) and (272). The numbers in the first column correspond to the numbers in the first column of Table XVIII. For simplicity, the lengthier functions are not explicitly given. See Sec. XIII.B for an explanation of the symbol $\doteq$

Type of input datum	Generalized observational equation
$B39^*$	$\Gamma'_{p-90}(\text{lo}) \doteq -\dfrac{K_{J-90}R_{K-90}[1+a_e(\alpha,\delta_e)]\alpha^3}{2\mu_0 R_\infty(1+\epsilon_J)(1+\epsilon_K)}\left(\dfrac{\mu_{e^-}}{\mu'_p}\right)^{-1}$
$B40^*$	$\Gamma'_{h-90}(\text{lo}) \doteq \dfrac{K_{J-90}R_{K-90}[1+a_e(\alpha,\delta_e)]\alpha^3}{2\mu_0 R_\infty(1+\epsilon_J)(1+\epsilon_K)}\left(\dfrac{\mu_{e^-}}{\mu'_p}\right)^{-1}\dfrac{\mu'_h}{\mu'_p}$
$B41^*$	$\Gamma'_{p-90}(\text{hi}) \doteq -\dfrac{c[1+a_e(\alpha,\delta_e)]\alpha^2}{K_{J-90}R_{K-90}R_\infty h}(1+\epsilon_J)(1+\epsilon_K)\left(\dfrac{\mu_{e^-}}{\mu'_p}\right)^{-1}$
$B43^*$	$R_K \doteq \dfrac{\mu_0 c}{2\alpha}(1+\epsilon_K)$
$B42^*$	$K_J \doteq \left(\dfrac{8\alpha}{\mu_0 ch}\right)^{1/2}(1+\epsilon_J)$
$B44^*$	$K_J^2 R_K \doteq \dfrac{4}{h}(1+\epsilon_J)^2(1+\epsilon_K)$
$B45^*$	$\mathcal{F}_{90} \doteq \dfrac{cM_u A_r(e)\alpha^2}{K_{J-90}R_{K-90}R_\infty h}(1+\epsilon_J)(1+\epsilon_K)$

RIGHTSLINK

TABLE XXXI. Summary of the results of several least-squares adjustments to investigate the relations $K_J = (2e/h)(1+\epsilon_J)$ and $R_K = (h/e^2)(1+\epsilon_K)$. See the text for an explanation and discussion of each adjustment, but in brief, adjustment (i) uses all the data, (ii) assumes $K_J = 2e/h$ (that is, $\epsilon_J = 0$) and obtains ϵ_K from the five measured values of R_K, (iii) is based on the same assumption and obtains ϵ_K from the two values of the proton gyromagnetic ratio and one value of the helion gyromagnetic ratio, (iv) is (iii) but assumes $R_K = h/e^2$ (that is, $\epsilon_K = 0$) and obtains ϵ_J in place of ϵ_K, (v) and (vi) are based on the same assumption and obtain ϵ_J from all the measured values given in Table XVIII for the quantities indicated

Adj.	Data included	$10^8\epsilon_K$	$10^8\epsilon_J$
(i)	All	2.2(1.8)	−0.9(1.5)
(ii)	R_K	2.8(1.8)	0
(iii)	$\Gamma'_{p,h-90}$(lo)	−25.5(9.3)	0
(iv)	$\Gamma'_{p,h-90}$(lo)	0	−25.5(9.3)
(v)	Γ'_{p-90}(hi), K_J, $K_J^2R_K$, $\mathcal{F}_{90}$	0	8.2(71.9)
(vi)	Γ'_{p-90}(hi), K_J, $K_J^2R_K$, $\mathcal{F}_{90}$, N_A	0	0.7(1.2)

0 within 1.2 times its uncertainty of 1.8×10^{-8}, while ϵ_J is consistent with 0 within its uncertainty of 1.5×10^{-8}.

Adjustments (ii) and (iii) focus on ϵ_K; ϵ_J is set equal to 0 and values of ϵ_K are calculated from data whose observational equations are independent of h. Adjustment (ii) uses the five results for R_K, items *B*43.1 to *B*43.5, and (iii) uses the three low-field gyromagnetic ratio results, items *B*39.1, *B*39.2, and *B*40 [the three together are denoted by $\Gamma'_{p,h-90}$(lo)]. We see from Table XXXI that the values of ϵ_K resulting from the two adjustments not only have opposite signs but disagree significantly: their difference is $3.0u_{diff}$. Their disagreement reflects the fact that while the five inferred values of α from R_K are consistent among themselves and with the highly accurate value from a_e, the inferred value from the NIST-89 result for Γ'_{p-90}(lo) (item *B*39.1), which has the smallest uncertainty of the three low-field gyromagnetic ratios, is not (see Table XX, Sec. XIII.A)

Adjustments (iv) to (vi) focus on ϵ_J; ϵ_K is set equal to 0 and values of ϵ_J are calculated from data whose observational equations, with the exception of adjustment (iv), are dependent on h. Because ϵ_J and ϵ_K enter the observational equations for the gyromagnetic ratios in the symmetric form $(1+\epsilon_J)(1+\epsilon_K)$, the numerical result from adjustments (iii) and (iv) are identical. Although ϵ_J from adjustment (iv) has the opposite sign of ϵ_J from adjustments (v) and (vi), it agrees with ϵ_J from adjustment (v) because of that result's extremely large uncertainty. However, it does disagree with the adjustment (vi) result: their difference is $2.8u_{diff}$.

In summary, we recall that rather limited conclusions could be drawn from the similar analysis presented in CODATA-10, because of the disagreement between the NIST-07 watt-balance measurement of h and the IAC-11 XRCD enriched silicon measurement of N_A. With the resolution of the disagreement by the replacement of the earlier NIST result with NIST-15 and the agreement of its inferred value of h with other values (see Table XXI, Sec. XIII.A), the only remaining issue is the values of ϵ_K and ϵ_J from $\Gamma'_{p,h-90}$(lo). However, these three data are dominated by the NIST-89 Γ'_{p-90}(lo) result and as discussed in Sec. XIII.A, the inconsistency of this datum has been of concern in past adjustments and because of its low weight is not included in the 2006 and 2010 final adjustments, or in the 2014 final adjustment. It can thus be concluded that the current data show the Josephson and quantum-Hall-effect relations to be exact within 2 parts in 10^8.

One way to test the universality of the Josephson and quantum-Hall-effect relations is to investigate their material dependence. Recently, Ribeiro-Palau *et al.* (2015) obtained agreement between the quantized Hall resistance in a graphene (two-dimensional graphite) device and a GaAs/AlGaAs heterostructure device well within the 8.2 parts in 10^{11} uncertainty of their measurement. This is slightly better than the previous best graphene-GaAs/AlGaAs comparison, which obtained agreement within the 8.7 parts in 10^{11} uncertainty of the experiment (Janssen *et al.*, 2012). Another way is to "close the metrology triangle" by using a single electron tunneling (SET) device that generates a quantized current $I = ef$ when an alternating voltage of frequency f is applied to it. The current I is then compared to a current obtained from Josephson and quantum-Hall-effect devices. The status of such efforts was briefly discussed in the same section of CODATA-10 and little has changed since. Two relevant papers not referenced in CODATA-10 are by Devoille *et al.* (2012) and Scherer and Camarota (2012).

XIV. The 2014 CODATA Recommended Values

A. Calculational details

The 151 input data and their many correlation coefficients initially considered for inclusion in the 2014 CODATA adjustment of the values of the constants are given in Tables XVI, XVII, XVIII, and XIX. The 2014 recommended values are based on adjustment 3, the final adjustment, summarized in Table XXVIII and discussed in the associated text. Adjustment 3 omits 22 of the 151 initially considered input data, namely, items *B*4, *B*22.1, *B*39.1 to *B*44.1, *B*44.3, *B*44.5, *B*44.7 to *B*46, *B*64.1, and *B*64.5, because of their low weight (self-sensitivity coefficient S_c less than 0.01). However, because the observational equation for $A_r(^3\mathrm{H})$, item *B*4, depends on $\Delta E_B(^3\mathrm{H}^+)/hc$ and item *B*4 is deleted due to its low weight, the value of $\Delta E_B(^3\mathrm{H}^+)/hc$, item *B*5, is also deleted as an adjusted constant. The same statement applies to $h/m(^{133}\mathrm{Cs})$, item *B*46, and $A_r(^{133}\mathrm{Cs})$, item *B*47. Further, the initial uncertainties of two input data, items *B*11 and *B*12, are multiplied by the expansion factor 2.8. As a consequence, the normalized residual r_i of each as well as that of item *B*2 is reduced to below 2.

Each input datum in this final adjustment has a self-sensitivity coefficient S_c greater than 0.01, or is a subset of the data of an experiment or series of experiments that provide an input datum or input data with $S_c > 0.01$. Not counting such input data with $S_c < 0.01$, the five data with $|r_i| > 1.2$ are *B*11, *B*12, *B*44.2, *B*44.4, and *B*48; their values of r_i are 1.95, 1.71, 1.96, 1.84, and 1.68, respectively.

The 2014 recommended values are calculated from the set of best estimated values, in the least-squares sense, of 75 adjusted constants, including G, and their variances and covariances,

RIGHTSLINK

TABLE XXXII. An abbreviated list of the CODATA recommended values of the fundamental constants of physics and chemistry based on the 2014 adjustment

Quantity	Symbol	Numerical value	Unit	Relative std. uncert. u_r
Speed of light in vacuum	c, c_0	299 792 458	m s^{-1}	Exact
Magnetic constant	μ_0	$4\pi \times 10^{-7}$	N A^{-2}	
		$= 12.566\,370\,614\ldots \times 10^{-7}$	N A^{-2}	Exact
Electric constant $1/\mu_0 c^2$	ϵ_0	$8.854\,187\,817\ldots \times 10^{-12}$	F m^{-1}	Exact
Newtonian constant of gravitation	G	$6.674\,08(31) \times 10^{-11}$	m^3 kg^{-1} s^{-2}	4.7×10^{-5}
Planck constant	h	$6.626\,070\,040(81) \times 10^{-34}$	J s	1.2×10^{-8}
$h/2\pi$	$\hbar$	$1.054\,571\,800(13) \times 10^{-34}$	J s	1.2×10^{-8}
Elementary charge	e	$1.602\,176\,6208(98) \times 10^{-19}$	C	6.1×10^{-9}
Magnetic flux quantum $h/2e$	Φ_0	$2.067\,833\,831(13) \times 10^{-15}$	Wb	6.1×10^{-9}
Conductance quantum $2e^2/h$	G_0	$7.748\,091\,7310(18) \times 10^{-5}$	S	2.3×10^{-10}
Electron mass	m_e	$9.109\,383\,56(11) \times 10^{-31}$	kg	1.2×10^{-8}
Proton mass	m_p	$1.672\,621\,898(21) \times 10^{-27}$	kg	1.2×10^{-8}
Proton-electron mass ratio	m_p/m_e	1836.152 673 89(17)		9.5×10^{-11}
Fine-structure constant $e^2/4\pi\epsilon_0\hbar c$	α	$7.297\,352\,5664(17) \times 10^{-3}$		2.3×10^{-10}
inverse fine-structure constant	α^{-1}	137.035 999 139(31)		2.3×10^{-10}
Rydberg constant $\alpha^2 m_e c/2h$	R_∞	10 973 731.568 508(65)	m^{-1}	5.9×10^{-12}
Avogadro constant	N_A, L	$6.022\,140\,857(74) \times 10^{23}$	mol^{-1}	1.2×10^{-8}
Faraday constant $N_A e$	F	96 485.332 89(59)	C mol^{-1}	6.2×10^{-9}
Molar gas constant	R	8.314 4598(48)	J mol^{-1} K^{-1}	5.7×10^{-7}
Boltzmann constant R/N_A	k	$1.380\,648\,52(79) \times 10^{-23}$	J K^{-1}	5.7×10^{-7}
Stefan-Boltzmann constant $(\pi^2/60)k^4/\hbar^3 c^2$	σ	$5.670\,367(13) \times 10^{-8}$	W m^{-2} K^{-4}	2.3×10^{-6}
		Non-SI units accepted for use with the SI		
Electron volt (e/C) J	eV	$1.602\,176\,6208(98) \times 10^{-19}$	J	6.1×10^{-9}
(Unified) atomic mass unit $\frac{1}{12}m(^{12}\mathrm{C})$	u	$1.660\,539\,040(20) \times 10^{-27}$	kg	1.2×10^{-8}

together with (i) those constants that have exact values such as μ_0 and c; and (ii) the values of m_τ, G_F, and $\sin^2\theta_W$ given in Sec. XII of this report. See Sec. V.B of CODATA-98 for details.

B. Tables of values

Tables XXXII, XXXIII, XXXIV, XXXV, XXXVI, XXXVII, XXXVIII, and XXXIX give the 2014 CODATA recommended values of the basic constants and conversion factors of physics and chemistry and related quantities. They are identical in form and content to their 2010 counterparts in that no constants are added or deleted.

It should be noted that the values of the four helion-related constants are calculated from the adjusted constant μ'_h/μ'_p and the theoretically predicted shielding correction $\sigma_h = 59.967\,43(10) \times 10^{-6}$ due to Rudziński, Puchalski, and Pachucki (2009) using the relation $\mu'_h = \mu_h(1 - \sigma_h)$; see Sec. VI.A.

Table XXXII is a highly abbreviated list of the values of the constants and conversion factors most commonly used. Table XXXIII is a much more extensive list of values categorized as follows: UNIVERSAL; ELECTROMAGNETIC; ATOMIC AND NUCLEAR; and PHYSICOCHEMICAL. The ATOMIC AND NUCLEAR category is subdivided into 11 subcategories: General; Electroweak; Electron, e; Muon, μ; Tau, τ; Proton, p; Neutron, n; Deuteron, d; Triton, t; Helion, h; and Alpha particle, α. Table XXXIV gives the variances, covariances, and correlation coefficients of a selected group of constants. (Use of the covariance matrix is discussed in Appendix E of CODATA-98.) Table XXXV gives the internationally adopted values of various quantities; Table XXXVI lists the values of a number of x-ray-related quantities; Table XXXVII lists the values of various non-SI units; and Tables XXXVIII and XXXIX give the values of various energy equivalents.

All of the values given in these tables are available on the website of the Fundamental Constants Data Center of the NIST Physical Measurement Laboratory at http://physics.nist.gov/constants. In fact, this electronic version of the 2014 CODATA recommended values of the constants enables users to obtain the correlation coefficient of any two constants listed in the tables. It also allows users to automatically convert the value of an energy-related quantity expressed in one unit to the corresponding value expressed in another unit (in essence, an automated version of Tables XXXVIII and XXXIX).

XV. Summary and Conclusion

Here we (i) compare the 2014 to the 2010 recommended values of the constants and identify those new results that have contributed most to the changes in the 2010 values; (ii) present several conclusions that can be drawn from the 2014 recommended values and the input data from which they are obtained; and (iii) identify new experimental and theoretical work that can advance our knowledge of the values of the constants.

Topic (iii) is relevant to the plan of the 26th General Conference on Weights and Measures (CGPM) to adopt at its

RIGHTSLINK

TABLE XXXIII. The CODATA recommended values of the fundamental constants of physics and chemistry based on the 2014 adjustment

Quantity	Symbol	Numerical value	Unit	Relative std. uncert. u_r
		UNIVERSAL		
Speed of light in vacuum	c, c_0	299 792 458	$m\,s^{-1}$	Exact
Magnetic constant	μ_0	$4\pi \times 10^{-7}$	$N\,A^{-2}$	
		$= 12.566\,370\,614\ldots \times 10^{-7}$	$N\,A^{-2}$	Exact
Electric constant $1/\mu_0 c^2$	ϵ_0	$8.854\,187\,817\ldots \times 10^{-12}$	$F\,m^{-1}$	Exact
Characteristic impedance of vacuum $\mu_0 c$	Z_0	376.730 313 461 ...	Ω	Exact
Newtonian constant of gravitation	G	$6.674\,08(31) \times 10^{-11}$	$m^3\,kg^{-1}\,s^{-2}$	4.7×10^{-5}
	$G/\hbar c$	$6.708\,61(31) \times 10^{-39}$	$(GeV/c^2)^{-2}$	4.7×10^{-5}
Planck constant	h	$6.626\,070\,040(81) \times 10^{-34}$	J s	1.2×10^{-8}
		$4.135\,667\,662(25) \times 10^{-15}$	eV s	6.1×10^{-9}
$h/2\pi$	$\hbar$	$1.054\,571\,800(13) \times 10^{-34}$	J s	1.2×10^{-8}
		$6.582\,119\,514(40) \times 10^{-16}$	eV s	6.1×10^{-9}
	$\hbar c$	197.326 9788(12)	MeV fm	6.1×10^{-9}
Planck mass $(\hbar c/G)^{1/2}$	m_P	$2.176\,470(51) \times 10^{-8}$	kg	2.3×10^{-5}
energy equivalent	$m_P c^2$	$1.220\,910(29) \times 10^{19}$	GeV	2.3×10^{-5}
Planck temperature $(\hbar c^5/G)^{1/2}/k$	T_P	$1.416\,808(33) \times 10^{32}$	K	2.3×10^{-5}
Planck length $\hbar/m_P c = (\hbar G/c^3)^{1/2}$	l_P	$1.616\,229(38) \times 10^{-35}$	m	2.3×10^{-5}
Planck time $l_P/c = (\hbar G/c^5)^{1/2}$	t_P	$5.391\,16(13) \times 10^{-44}$	s	2.3×10^{-5}
		ELECTROMAGNETIC		
Elementary charge	e	$1.602\,176\,6208(98) \times 10^{-19}$	C	6.1×10^{-9}
	e/h	$2.417\,989\,262(15) \times 10^{14}$	$A\,J^{-1}$	6.1×10^{-9}
Magnetic flux quantum $h/2e$	Φ_0	$2.067\,833\,831(13) \times 10^{-15}$	Wb	6.1×10^{-9}
Conductance quantum $2e^2/h$	G_0	$7.748\,091\,7310(18) \times 10^{-5}$	S	2.3×10^{-10}
inverse of conductance quantum	G_0^{-1}	12 906.403 7278(29)	Ω	2.3×10^{-10}
Josephson constant[a] $2e/h$	K_J	$483\,597.8525(30) \times 10^9$	$Hz\,V^{-1}$	6.1×10^{-9}
von Klitzing constant[b] $h/e^2 = \mu_0 c/2\alpha$	R_K	25 812.807 4555(59)	Ω	2.3×10^{-10}
Bohr magneton $e\hbar/2m_e$	μ_B	$927.400\,9994(57) \times 10^{-26}$	$J\,T^{-1}$	6.2×10^{-9}
		$5.788\,381\,8012(26) \times 10^{-5}$	$eV\,T^{-1}$	4.5×10^{-10}
	μ_B/h	$13.996\,245\,042(86) \times 10^9$	$Hz\,T^{-1}$	6.2×10^{-9}
	μ_B/hc	46.686 448 14(29)	$m^{-1}\,T^{-1}$	6.2×10^{-9}
	μ_B/k	0.671 714 05(39)	$K\,T^{-1}$	5.7×10^{-7}
Nuclear magneton $e\hbar/2m_p$	μ_N	$5.050\,783\,699(31) \times 10^{-27}$	$J\,T^{-1}$	6.2×10^{-9}
		$3.152\,451\,2550(15) \times 10^{-8}$	$eV\,T^{-1}$	4.6×10^{-10}
	μ_N/h	7.622 593 285(47)	$MHz\,T^{-1}$	6.2×10^{-9}
	μ_N/hc	$2.542\,623\,432(16) \times 10^{-2}$	$m^{-1}\,T^{-1}$	6.2×10^{-9}
	μ_N/k	$3.658\,2690(21) \times 10^{-4}$	$K\,T^{-1}$	5.7×10^{-7}
		ATOMIC AND NUCLEAR		
		General		
Fine-structure constant $e^2/4\pi\epsilon_0\hbar c$	α	$7.297\,352\,5664(17) \times 10^{-3}$		2.3×10^{-10}
inverse fine-structure constant	α^{-1}	137.035 999 139(31)		2.3×10^{-10}
Rydberg constant $\alpha^2 m_e c/2h$	R_∞	10 973 731.568 508(65)	m^{-1}	5.9×10^{-12}
	$R_\infty c$	$3.289\,841\,960\,355(19) \times 10^{15}$	Hz	5.9×10^{-12}
	$R_\infty hc$	$2.179\,872\,325(27) \times 10^{-18}$	J	1.2×10^{-8}
		13.605 693 009(84)	eV	6.1×10^{-9}
Bohr radius $\alpha/4\pi R_\infty = 4\pi\epsilon_0\hbar^2/m_e e^2$	a_0	$0.529\,177\,210\,67(12) \times 10^{-10}$	m	2.3×10^{-10}
Hartree energy $e^2/4\pi\epsilon_0 a_0 = 2R_\infty hc = \alpha^2 m_e c^2$	E_h	$4.359\,744\,650(54) \times 10^{-18}$	J	1.2×10^{-8}
		27.211 386 02(17)	eV	6.1×10^{-9}
Quantum of circulation	$h/2m_e$	$3.636\,947\,5486(17) \times 10^{-4}$	$m^2\,s^{-1}$	4.5×10^{-10}
	h/m_e	$7.273\,895\,0972(33) \times 10^{-4}$	$m^2\,s^{-1}$	4.5×10^{-10}
		Electroweak		
Fermi coupling constant[c]	$G_F/(\hbar c)^3$	$1.166\,3787(6) \times 10^{-5}$	GeV^{-2}	5.1×10^{-7}
Weak mixing angle[d] θ_W (on-shell scheme)				
$\sin^2\theta_W = s_W^2 \equiv 1 - (m_W/m_Z)^2$	$\sin^2\theta_W$	0.2223(21)		9.5×10^{-3}
		Electron, e^-		
Electron mass	m_e	$9.109\,383\,56(11) \times 10^{-31}$	kg	1.2×10^{-8}
		$5.485\,799\,090\,70(16) \times 10^{-4}$	u	2.9×10^{-11}

RIGHTSLINK

TABLE XXXIII. The CODATA recommended values of the fundamental constants of physics and chemistry based on the 2014 adjustment—Continued

Quantity	Symbol	Numerical value	Unit	Relative std. uncert. u_r
energy equivalent	$m_e c^2$	$8.187\,105\,65(10) \times 10^{-14}$	J	1.2×10^{-8}
		0.510 998 9461(31)	MeV	6.2×10^{-9}
Electron-muon mass ratio	m_e/m_μ	$4.836\,331\,70(11) \times 10^{-3}$		2.2×10^{-8}
Electron-tau mass ratio	m_e/m_τ	$2.875\,92(26) \times 10^{-4}$		9.0×10^{-5}
Electron-proton mass ratio	m_e/m_p	$5.446\,170\,213\,52(52) \times 10^{-4}$		9.5×10^{-11}
Electron-neutron mass ratio	m_e/m_n	$5.438\,673\,4428(27) \times 10^{-4}$		4.9×10^{-10}
Electron-deuteron mass ratio	m_e/m_d	$2.724\,437\,107\,484(96) \times 10^{-4}$		3.5×10^{-11}
Electron-triton mass ratio	m_e/m_t	$1.819\,200\,062\,203(84) \times 10^{-4}$		4.6×10^{-11}
Electron-helion mass ratio	m_e/m_h	$1.819\,543\,074\,854(88) \times 10^{-4}$		4.9×10^{-11}
Electron to alpha particle mass ratio	m_e/m_α	$1.370\,933\,554\,798(45) \times 10^{-4}$		3.3×10^{-11}
Electron charge to mass quotient	$-e/m_e$	$-1.758\,820\,024(11) \times 10^{11}$	C kg^{-1}	6.2×10^{-9}
Electron molar mass $N_A m_e$	$M(e)$, M_e	$5.485\,799\,090\,70(16) \times 10^{-7}$	kg mol^{-1}	2.9×10^{-11}
Compton wavelength $h/m_e c$	λ_C	$2.426\,310\,2367(11) \times 10^{-12}$	m	4.5×10^{-10}
$\lambda_C/2\pi = \alpha a_0 = \alpha^2/4\pi R_\infty$	$\lambda\!\!\!^{-}{}_C$	$386.159\,267\,64(18) \times 10^{-15}$	m	4.5×10^{-10}
Classical electron radius $\alpha^2 a_0$	r_e	$2.817\,940\,3227(19) \times 10^{-15}$	m	6.8×10^{-10}
Thomson cross section $(8\pi/3)r_e^2$	σ_e	$0.665\,245\,871\,58(91) \times 10^{-28}$	m^2	1.4×10^{-9}
Electron magnetic moment	μ_e	$-928.476\,4620(57) \times 10^{-26}$	J T^{-1}	6.2×10^{-9}
to Bohr magneton ratio	μ_e/μ_B	$-1.001\,159\,652\,180\,91(26)$		2.6×10^{-13}
to nuclear magneton ratio	μ_e/μ_N	$-1838.281\,972\,34(17)$		9.5×10^{-11}
Electron magnetic-moment anomaly $\lvert\mu_e\rvert/\mu_B - 1$	a_e	$1.159\,652\,180\,91(26) \times 10^{-3}$		2.3×10^{-10}
Electron g-factor $-2(1 + a_e)$	g_e	$-2.002\,319\,304\,361\,82(52)$		2.6×10^{-13}
Electron-muon magnetic-moment ratio	μ_e/μ_μ	206.766 9880(46)		2.2×10^{-8}
Electron-proton magnetic-moment ratio	μ_e/μ_p	$-658.210\,6866(20)$		3.0×10^{-9}
Electron to shielded proton magnetic-moment ratio (H_2O, sphere, 25 °C)	μ_e/μ'_p	$-658.227\,5971(72)$		1.1×10^{-8}
Electron-neutron magnetic-moment ratio	μ_e/μ_n	960.920 50(23)		2.4×10^{-7}
Electron-deuteron magnetic-moment ratio	μ_e/μ_d	$-2143.923\,499(12)$		5.5×10^{-9}
Electron to shielded helion magnetic-moment ratio (gas, sphere, 25 °C)	μ_e/μ'_h	864.058 257(10)		1.2×10^{-8}
Electron gyromagnetic ratio $2\lvert\mu_e\rvert/\hbar$	γ_e	$1.760\,859\,644(11) \times 10^{11}$	s^{-1} T^{-1}	6.2×10^{-9}
	$\gamma_e/2\pi$	28 024.951 64(17)	MHz T^{-1}	6.2×10^{-9}
		Muon, μ^-		
Muon mass	m_μ	$1.883\,531\,594(48) \times 10^{-28}$	kg	2.5×10^{-8}
		0.113 428 9257(25)	u	2.2×10^{-8}
energy equivalent	$m_\mu c^2$	$1.692\,833\,774(43) \times 10^{-11}$	J	2.5×10^{-8}
		105.658 3745(24)	MeV	2.3×10^{-8}
Muon-electron mass ratio	m_μ/m_e	206.768 2826(46)		2.2×10^{-8}
Muon-tau mass ratio	m_μ/m_τ	$5.946\,49(54) \times 10^{-2}$		9.0×10^{-5}
Muon-proton mass ratio	m_μ/m_p	0.112 609 5262(25)		2.2×10^{-8}
Muon-neutron mass ratio	m_μ/m_n	0.112 454 5167(25)		2.2×10^{-8}
Muon molar mass $N_A m_\mu$	$M(\mu)$, M_μ	$0.113\,428\,9257(25) \times 10^{-3}$	kg mol^{-1}	2.2×10^{-8}
Muon Compton wavelength $h/m_\mu c$	$\lambda_{C,\mu}$	$11.734\,441\,11(26) \times 10^{-15}$	m	2.2×10^{-8}
$\lambda_{C,\mu}/2\pi$	$\lambda\!\!\!^{-}{}_{C,\mu}$	$1.867\,594\,308(42) \times 10^{-15}$	m	2.2×10^{-8}
Muon magnetic moment	μ_μ	$-4.490\,448\,26(10) \times 10^{-26}$	J T^{-1}	2.3×10^{-8}
to Bohr magneton ratio	μ_μ/μ_B	$-4.841\,970\,48(11) \times 10^{-3}$		2.2×10^{-8}
to nuclear magneton ratio	μ_μ/μ_N	$-8.890\,597\,05(20)$		2.2×10^{-8}
Muon magnetic-moment anomaly $\lvert\mu_\mu\rvert/(e\hbar/2m_\mu) - 1$	a_μ	$1.165\,920\,89(63) \times 10^{-3}$		5.4×10^{-7}
Muon g-factor $-2(1 + a_\mu)$	g_μ	$-2.002\,331\,8418(13)$		6.3×10^{-10}
Muon-proton magnetic-moment ratio	μ_μ/μ_p	$-3.183\,345\,142(71)$		2.2×10^{-8}
		Tau, τ^-		
Tau mass[e]	m_τ	$3.167\,47(29) \times 10^{-27}$	kg	9.0×10^{-5}
		1.907 49(17)	u	9.0×10^{-5}
energy equivalent	$m_\tau c^2$	$2.846\,78(26) \times 10^{-10}$	J	9.0×10^{-5}
		1776.82(16)	MeV	9.0×10^{-5}

RIGHTSLINK

TABLE XXXIII. The CODATA recommended values of the fundamental constants of physics and chemistry based on the 2014 adjustment—Continued

Quantity	Symbol	Numerical value	Unit	Relative std. uncert. u_r
Tau-electron mass ratio	m_τ/m_e	3477.15(31)		9.0×10^{-5}
Tau-muon mass ratio	m_τ/m_μ	16.8167(15)		9.0×10^{-5}
Tau-proton mass ratio	m_τ/m_p	1.893 72(17)		9.0×10^{-5}
Tau-neutron mass ratio	m_τ/m_n	1.891 11(17)		9.0×10^{-5}
Tau molar mass $N_A m_\tau$	$M(\tau)$, M_τ	$1.907\,49(17)\times10^{-3}$	kg mol^{-1}	9.0×10^{-5}
Tau Compton wavelength $h/m_\tau c$	$\lambda_{C,\tau}$	$0.697\,787(63)\times10^{-15}$	m	9.0×10^{-5}
$\lambda_{C,\tau}/2\pi$	$\lambda\!\!\!^{-}_{C,\tau}$	$0.111\,056(10)\times10^{-15}$	m	9.0×10^{-5}
		Proton, p		
Proton mass	m_p	$1.672\,621\,898(21)\times10^{-27}$	kg	1.2×10^{-8}
		1.007 276 466 879(91)	u	9.0×10^{-11}
energy equivalent	$m_p c^2$	$1.503\,277\,593(18)\times10^{-10}$	J	1.2×10^{-8}
		938.272 0813(58)	MeV	6.2×10^{-9}
Proton-electron mass ratio	m_p/m_e	1836.152 673 89(17)		9.5×10^{-11}
Proton-muon mass ratio	m_p/m_μ	8.880 243 38(20)		2.2×10^{-8}
Proton-tau mass ratio	m_p/m_τ	0.528 063(48)		9.0×10^{-5}
Proton-neutron mass ratio	m_p/m_n	0.998 623 478 44(51)		5.1×10^{-10}
Proton charge-to-mass quotient	e/m_p	$9.578\,833\,226(59)\times10^{7}$	C kg^{-1}	6.2×10^{-9}
Proton molar mass $N_A m_p$	$M(p)$, M_p	$1.007\,276\,466\,879(91)\times10^{-3}$	kg mol^{-1}	9.0×10^{-11}
Proton Compton wavelength $h/m_p c$	$\lambda_{C,p}$	$1.321\,409\,853\,96(61)\times10^{-15}$	m	4.6×10^{-10}
$\lambda_{C,p}/2\pi$	$\lambda\!\!\!^{-}_{C,p}$	$0.210\,308\,910\,109(97)\times10^{-15}$	m	4.6×10^{-10}
Proton rms charge radius	r_p	$0.8751(61)\times10^{-15}$	m	7.0×10^{-3}
Proton magnetic moment	μ_p	$1.410\,606\,7873(97)\times10^{-26}$	J T^{-1}	6.9×10^{-9}
to Bohr magneton ratio	μ_p/μ_B	$1.521\,032\,2053(46)\times10^{-3}$		3.0×10^{-9}
to nuclear magneton ratio	μ_p/μ_N	2.792 847 3508(85)		3.0×10^{-9}
Proton g-factor $2\mu_p/\mu_N$	g_p	5.585 694 702(17)		3.0×10^{-9}
Proton-neutron magnetic-moment ratio	μ_p/μ_n	−1.459 898 05(34)		2.4×10^{-7}
Shielded proton magnetic moment				
(H_2O, sphere, 25 °C)	μ'_p	$1.410\,570\,547(18)\times10^{-26}$	J T^{-1}	1.3×10^{-8}
to Bohr magneton ratio	μ'_p/μ_B	$1.520\,993\,128(17)\times10^{-3}$		1.1×10^{-8}
to nuclear magneton ratio	μ'_p/μ_N	2.792 775 600(30)		1.1×10^{-8}
Proton magnetic shielding correction				
$1-\mu'_p/\mu_p$ (H_2O, sphere, 25 °C)	σ'_p	$25.691(11)\times10^{-6}$		4.4×10^{-4}
Proton gyromagnetic ratio $2\mu_p/\hbar$	γ_p	$2.675\,221\,900(18)\times10^{8}$	s^{-1} T^{-1}	6.9×10^{-9}
	$\gamma_p/2\pi$	42.577 478 92(29)	MHz T^{-1}	6.9×10^{-9}
Shielded proton gyromagnetic ratio				
$2\mu'_p/\hbar$ (H_2O, sphere, 25 °C)	γ'_p	$2.675\,153\,171(33)\times10^{8}$	s^{-1} T^{-1}	1.3×10^{-8}
	$\gamma'_p/2\pi$	42.576 385 07(53)	MHz T^{-1}	1.3×10^{-8}
		Neutron, n		
Neutron mass	m_n	$1.674\,927\,471(21)\times10^{-27}$	kg	1.2×10^{-8}
		1.008 664 915 88(49)	u	4.9×10^{-10}
energy equivalent	$m_n c^2$	$1.505\,349\,739(19)\times10^{-10}$	J	1.2×10^{-8}
		939.565 4133(58)	MeV	6.2×10^{-9}
Neutron-electron mass ratio	m_n/m_e	1838.683 661 58(90)		4.9×10^{-10}
Neutron-muon mass ratio	m_n/m_μ	8.892 484 08(20)		2.2×10^{-8}
Neutron-tau mass ratio	m_n/m_τ	0.528 790(48)		9.0×10^{-5}
Neutron-proton mass ratio	m_n/m_p	1.001 378 418 98(51)		5.1×10^{-10}
Neutron-proton mass difference	m_n-m_p	$2.305\,573\,77(85)\times10^{-30}$	kg	3.7×10^{-7}
		0.001 388 449 00(51)	u	3.7×10^{-7}
energy equivalent	$(m_n-m_p)c^2$	$2.072\,146\,37(76)\times10^{-13}$	J	3.7×10^{-7}
		1.293 332 05(48)	MeV	3.7×10^{-7}
Neutron molar mass $N_A m_n$	$M(n)$, M_n	$1.008\,664\,915\,88(49)\times10^{-3}$	kg mol^{-1}	4.9×10^{-10}
Neutron Compton wavelength $h/m_n c$	$\lambda_{C,n}$	$1.319\,590\,904\,81(88)\times10^{-15}$	m	6.7×10^{-10}
$\lambda_{C,n}/2\pi$	$\lambda\!\!\!^{-}_{C,n}$	$0.210\,019\,415\,36(14)\times10^{-15}$	m	6.7×10^{-10}
Neutron magnetic moment	μ_n	$-0.966\,236\,50(23)\times10^{-26}$	J T^{-1}	2.4×10^{-7}
to Bohr magneton ratio	μ_n/μ_B	$-1.041\,875\,63(25)\times10^{-3}$		2.4×10^{-7}
to nuclear magneton ratio	μ_n/μ_N	−1.913 042 73(45)		2.4×10^{-7}

RIGHTSLINK

TABLE XXXIII. The CODATA recommended values of the fundamental constants of physics and chemistry based on the 2014 adjustment—Continued

Quantity	Symbol	Numerical value	Unit	Relative std. uncert. u_r
Neutron g-factor $2\mu_n/\mu_N$	g_n	−3.826 085 45(90)		2.4×10^{-7}
Neutron-electron magnetic-moment ratio	μ_n/μ_e	$1.040\,668\,82(25)\times10^{-3}$		2.4×10^{-7}
Neutron-proton magnetic-moment ratio	μ_n/μ_p	−0.684 979 34(16)		2.4×10^{-7}
Neutron to shielded proton magnetic-moment ratio (H_2O, sphere, 25 °C)	μ_n/μ'_p	−0.684 996 94(16)		2.4×10^{-7}
Neutron gyromagnetic ratio $2\lvert\mu_n\rvert/\hbar$	γ_n	$1.832\,471\,72(43)\times10^{8}$	$s^{-1}\,T^{-1}$	2.4×10^{-7}
	$\gamma_n/2\pi$	29.164 6933(69)	$MHz\,T^{-1}$	2.4×10^{-7}
		Deuteron, d		
Deuteron mass	m_d	$3.343\,583\,719(41)\times10^{-27}$	kg	1.2×10^{-8}
		2.013 553 212 745(40)	u	2.0×10^{-11}
energy equivalent	m_dc^2	$3.005\,063\,183(37)\times10^{-10}$	J	1.2×10^{-8}
		1875.612 928(12)	MeV	6.2×10^{-9}
Deuteron-electron mass ratio	m_d/m_e	3670.482 967 85(13)		3.5×10^{-11}
Deuteron-proton mass ratio	m_d/m_p	1.999 007 500 87(19)		9.3×10^{-11}
Deuteron molar mass N_Am_d	$M(d)$, M_d	$2.013\,553\,212\,745(40)\times10^{-3}$	$kg\,mol^{-1}$	2.0×10^{-11}
Deuteron rms charge radius	r_d	$2.1413(25)\times10^{-15}$	m	1.2×10^{-3}
Deuteron magnetic moment	μ_d	$0.433\,073\,5040(36)\times10^{-26}$	$J\,T^{-1}$	8.3×10^{-9}
to Bohr magneton ratio	μ_d/μ_B	$0.466\,975\,4554(26)\times10^{-3}$		5.5×10^{-9}
to nuclear magneton ratio	μ_d/μ_N	0.857 438 2311(48)		5.5×10^{-9}
Deuteron g-factor μ_d/μ_N	g_d	0.857 438 2311(48)		5.5×10^{-9}
Deuteron-electron magnetic-moment ratio	μ_d/μ_e	$-4.664\,345\,535(26)\times10^{-4}$		5.5×10^{-9}
Deuteron-proton magnetic-moment ratio	μ_d/μ_p	0.307 012 2077(15)		5.0×10^{-9}
Deuteron-neutron magnetic-moment ratio	μ_d/μ_n	−0.448 206 52(11)		2.4×10^{-7}
		Triton, t		
Triton mass	m_t	$5.007\,356\,665(62)\times10^{-27}$	kg	1.2×10^{-8}
		3.015 500 716 32(11)	u	3.6×10^{-11}
energy equivalent	m_tc^2	$4.500\,387\,735(55)\times10^{-10}$	J	1.2×10^{-8}
		2808.921 112(17)	MeV	6.2×10^{-9}
Triton-electron mass ratio	m_t/m_e	5496.921 535 88(26)		4.6×10^{-11}
Triton-proton mass ratio	m_t/m_p	2.993 717 033 48(22)		7.5×10^{-11}
Triton molar mass N_Am_t	$M(t)$, M_t	$3.015\,500\,716\,32(11)\times10^{-3}$	$kg\,mol^{-1}$	3.6×10^{-11}
Triton magnetic moment	μ_t	$1.504\,609\,503(12)\times10^{-26}$	$J\,T^{-1}$	7.8×10^{-9}
to Bohr magneton ratio	μ_t/μ_B	$1.622\,393\,6616(76)\times10^{-3}$		4.7×10^{-9}
to nuclear magneton ratio	μ_t/μ_N	2.978 962 460(14)		4.7×10^{-9}
Triton g-factor $2\mu_t/\mu_N$	g_t	5.957 924 920(28)		4.7×10^{-9}
		Helion, h		
Helion mass	m_h	$5.006\,412\,700(62)\times10^{-27}$	kg	1.2×10^{-8}
		3.014 932 246 73(12)	u	3.9×10^{-11}
energy equivalent	m_hc^2	$4.499\,539\,341(55)\times10^{-10}$	J	1.2×10^{-8}
		2808.391 586(17)	MeV	6.2×10^{-9}
Helion-electron mass ratio	m_h/m_e	5495.885 279 22(27)		4.9×10^{-11}
Helion-proton mass ratio	m_h/m_p	2.993 152 670 46(29)		9.6×10^{-11}
Helion molar mass N_Am_h	$M(h)$, M_h	$3.014\,932\,246\,73(12)\times10^{-3}$	$kg\,mol^{-1}$	3.9×10^{-11}
Helion magnetic moment	μ_h	$-1.074\,617\,522(14)\times10^{-26}$	$J\,T^{-1}$	1.3×10^{-8}
to Bohr magneton ratio	μ_h/μ_B	$-1.158\,740\,958(14)\times10^{-3}$		1.2×10^{-8}
to nuclear magneton ratio	μ_h/μ_N	−2.127 625 308(25)		1.2×10^{-8}
Helion g-factor $2\mu_h/\mu_N$	g_h	−4.255 250 616(50)		1.2×10^{-8}
Shielded helion magnetic moment (gas, sphere, 25 °C)	μ'_h	$-1.074\,553\,080(14)\times10^{-26}$	$J\,T^{-1}$	1.3×10^{-8}
to Bohr magneton ratio	μ'_h/μ_B	$-1.158\,671\,471(14)\times10^{-3}$		1.2×10^{-8}
to nuclear magneton ratio	μ'_h/μ_N	−2.127 497 720(25)		1.2×10^{-8}
Shielded helion to proton magnetic-moment ratio (gas, sphere, 25 °C)	μ'_h/μ_p	−0.761 766 5603(92)		1.2×10^{-8}
Shielded helion to shielded proton magnetic-moment ratio (gas/H_2O, spheres, 25 °C)	μ'_h/μ'_p	−0.761 786 1313(33)		4.3×10^{-9}

RIGHTSLINK

TABLE XXXIII. The CODATA recommended values of the fundamental constants of physics and chemistry based on the 2014 adjustment—Continued

Quantity	Symbol	Numerical value	Unit	Relative std. uncert. u_r
Shielded helion gyromagnetic ratio				
$2\lvert\mu'_h\rvert/\hbar$ (gas, sphere, 25 °C)	γ'_h	$2.037\,894\,585(27)\times10^{8}$	$s^{-1}\,T^{-1}$	1.3×10^{-8}
	$\gamma'_h/2\pi$	32.434 099 66(43)	$MHz\,T^{-1}$	1.3×10^{-8}
		Alpha particle, α		
Alpha particle mass	m_α	$6.644\,657\,230(82)\times10^{-27}$	kg	1.2×10^{-8}
		4.001 506 179 127(63)	u	1.6×10^{-11}
energy equivalent	$m_\alpha c^2$	$5.971\,920\,097(73)\times10^{-10}$	J	1.2×10^{-8}
		3727.379 378(23)	MeV	6.2×10^{-9}
Alpha particle to electron mass ratio	m_α/m_e	7294.299 541 36(24)		3.3×10^{-11}
Alpha particle to proton mass ratio	m_α/m_p	3.972 599 689 07(36)		9.2×10^{-11}
Alpha particle molar mass $N_A m_\alpha$	$M(\alpha)$, M_α	$4.001\,506\,179\,127(63)\times10^{-3}$	$kg\,mol^{-1}$	1.6×10^{-11}
		PHYSICOCHEMICAL		
Avogadro constant	N_A, L	$6.022\,140\,857(74)\times10^{23}$	mol^{-1}	1.2×10^{-8}
Atomic mass constant				
$m_u = \frac{1}{12}m(^{12}C) = 1$ u	m_u	$1.660\,539\,040(20)\times10^{-27}$	kg	1.2×10^{-8}
energy equivalent	$m_u c^2$	$1.492\,418\,062(18)\times10^{-10}$	J	1.2×10^{-8}
		931.494 0954(57)	MeV	6.2×10^{-9}
Faraday constant[f] $N_A e$	F	96 485.332 89(59)	$C\,mol^{-1}$	6.2×10^{-9}
Molar Planck constant	$N_A h$	$3.990\,312\,7110(18)\times10^{-10}$	$J\,s\,mol^{-1}$	4.5×10^{-10}
	$N_A hc$	0.119 626 565 582(54)	$J\,m\,mol^{-1}$	4.5×10^{-10}
Molar gas constant	R	8.314 4598(48)	$J\,mol^{-1}\,K^{-1}$	5.7×10^{-7}
Boltzmann constant R/N_A	k	$1.380\,648\,52(79)\times10^{-23}$	$J\,K^{-1}$	5.7×10^{-7}
		$8.617\,3303(50)\times10^{-5}$	$eV\,K^{-1}$	5.7×10^{-7}
	k/h	$2.083\,6612(12)\times10^{10}$	$Hz\,K^{-1}$	5.7×10^{-7}
	k/hc	69.503 457(40)	$m^{-1}\,K^{-1}$	5.7×10^{-7}
Molar volume of ideal gas RT/p				
$T = 273.15$ K, $p = 100$ kPa	V_m	$22.710\,947(13)\times10^{-3}$	$m^3\,mol^{-1}$	5.7×10^{-7}
Loschmidt constant N_A/V_m	n_0	$2.651\,6467(15)\times10^{25}$	m^{-3}	5.7×10^{-7}
Molar volume of ideal gas RT/p				
$T = 273.15$ K, $p = 101.325$ kPa	V_m	$22.413\,962(13)\times10^{-3}$	$m^3\,mol^{-1}$	5.7×10^{-7}
Loschmidt constant N_A/V_m	n_0	$2.686\,7811(15)\times10^{25}$	m^{-3}	5.7×10^{-7}
Sackur-Tetrode (absolute entropy) constant[g]				
$\frac{5}{2} + \ln[(2\pi m_u kT_1/h^2)^{3/2}kT_1/p_0]$				
$T_1 = 1$ K, $p_0 = 100$ kPa	S_0/R	−1.151 7084(14)		1.2×10^{-6}
$T_1 = 1$ K, $p_0 = 101.325$ kPa		−1.164 8714(14)		1.2×10^{-6}
Stefan-Boltzmann constant $(\pi^2/60)k^4/\hbar^3c^2$	σ	$5.670\,367(13)\times10^{-8}$	$W\,m^{-2}\,K^{-4}$	2.3×10^{-6}
First radiation constant $2\pi hc^2$	c_1	$3.741\,771\,790(46)\times10^{-16}$	$W\,m^2$	1.2×10^{-8}
First radiation constant for spectral radiance $2hc^2$	c_{1L}	$1.191\,042\,953(15)\times10^{-16}$	$W\,m^2\,sr^{-1}$	1.2×10^{-8}
Second radiation constant hc/k	c_2	$1.438\,777\,36(83)\times10^{-2}$	m K	5.7×10^{-7}
Wien displacement law constants				
$b = \lambda_{max}T = c_2/4.965\,114\,231\ldots$	b	$2.897\,7729(17)\times10^{-3}$	m K	5.7×10^{-7}
$b' = \nu_{max}/T = 2.821\,439\,372\ldots c/c_2$	b'	$5.878\,9238(34)\times10^{10}$	$Hz\,K^{-1}$	5.7×10^{-7}

[a]See Table XXXV for the conventional value adopted internationally for realizing representations of the volt using the Josephson effect.
[b]See Table XXXV for the conventional value adopted internationally for realizing representations of the ohm using the quantum-Hall effect.
[c]Value recommended by the Particle Data Group (Olive *et al.*, 2014).
[d]Based on the ratio of the masses of the W and Z bosons m_W/m_Z recommended by the Particle Data Group (Olive *et al.*, 2014). The value for $\sin^2\theta_W$ they recommend, which is based on a particular variant of the modified minimal subtraction ($\overline{MS}$) scheme, is $\sin^2\hat{\theta}_W(M_Z) = 0.231\,26(5)$.
[e]This and all other values involving m_τ are based on the value of $m_\tau c^2$ in MeV recommended by the Particle Data Group (Olive *et al.*, 2014).
[f]The numerical value of F to be used in coulometric chemical measurements is 96 485.3251(12) [1.2×10^{-8}] when the relevant current is measured in terms of representations of the volt and ohm based on the Josephson and quantum-Hall effects and the internationally adopted conventional values of the Josephson and von Klitzing constants K_{J-90} and R_{K-90} given in Table XXXV.
[g]The entropy of an ideal monoatomic gas of relative atomic mass A_r is given by $S = S_0 + \frac{3}{2}R\ln A_r - R\ln(p/p_0) + \frac{5}{2}R\ln(T/K)$.

RIGHTSLINK

TABLE XXXIV. The variances, covariances, and correlation coefficients of the values of a selected group of constants based on the 2014 CODATA adjustment. The numbers in bold above the main diagonal are 10^{16} times the numerical values of the relative covariances; the numbers in bold on the main diagonal are 10^{16} times the numerical values of the relative variances; and the numbers in italics below the main diagonal are the correlation coefficients.[a]

	α	h	e	m_e	N_A	m_e/m_μ	F
α	**0.0005**	**0.0005**	**0.0005**	**−0.0005**	**0.0005**	**−0.0010**	**0.0010**
h	*0.0176*	**1.5096**	**0.7550**	**1.5086**	**−1.5086**	**−0.0010**	**−0.7536**
e	*0.0361*	*0.9998*	**0.3778**	**0.7540**	**−0.7540**	**−0.0010**	**−0.3763**
m_e	*−0.0193*	*0.9993*	*0.9985*	**1.5097**	**−1.5097**	**0.0011**	**−0.7556**
N_A	*0.0193*	*−0.9993*	*−0.9985*	*−1.0000*	**1.5097**	**−0.0011**	**0.7557**
m_e/m_μ	*−0.0202*	*−0.0004*	*−0.0007*	*0.0004*	*−0.0004*	**4.9471**	**−0.0021**
F	*0.0745*	*−0.9957*	*−0.9939*	*−0.9985*	*0.9985*	*−0.0015*	**0.3794**

[a]The relative covariance is $u_r(x_i, x_j) = u(x_i, x_j)/(x_i x_j)$, where $u(x_i, x_j)$ is the covariance of x_i and x_j; the relative variance is $u_r^2(x_i) = u_r(x_i, x_i)$: and the correlation coefficient is $r(x_i, x_j) = u(x_i, x_j)/[u(x_i)u(x_j)]$.

TABLE XXXV. Internationally adopted values of various quantities

Quantity	Symbol	Numerical value	Unit	Relative std. uncert. u_r
Relative atomic mass[a] of ^{12}C	$A_r(^{12}C)$	12		Exact
Molar mass constant	M_u	1×10^{-3}	kg mol^{-1}	Exact
Molar mass of ^{12}C	$M(^{12}C)$	12×10^{-3}	kg mol^{-1}	Exact
Conventional value of Josephson constant[b]	K_{J-90}	483 597.9	GHz V^{-1}	Exact
Conventional value of von Klitzing constant[c]	R_{K-90}	25 812.807	Ω	Exact
Standard-state pressure		100	kPa	Exact
Standard atmosphere		101.325	kPa	Exact

[a]The relative atomic mass $A_r(X)$ of particle X with mass $m(X)$ is defined by $A_r(X) = m(X)/m_u$, where $m_u = m(^{12}C)/12 = M_u/N_A = 1$ u is the atomic mass constant, M_u is the molar mass constant, N_A is the Avogadro constant, and u is the unified atomic mass unit. Thus the mass of particle X is $m(X) = A_r(X)$ u and the molar mass of X is $M(X) = A_r(X)M_u$.
[b]This is the value adopted internationally for realizing representations of the volt using the Josephson effect.
[c]This is the value adopted internationally for realizing representations of the ohm using the quantum-Hall effect.

TABLE XXXVI. Values of some x-ray-related quantities based on the 2014 CODATA adjustment of the values of the constants

Quantity	Symbol	Numerical value	Unit	Relative std. uncert. u_r
Cu x unit: $\lambda(CuK\alpha_1)/1\,537.400$	$xu(CuK\alpha_1)$	$1.002\,076\,97(28) \times 10^{-13}$	m	2.8×10^{-7}
Mo x unit: $\lambda(MoK\alpha_1)/707.831$	$xu(MoK\alpha_1)$	$1.002\,099\,52(53) \times 10^{-13}$	m	5.3×10^{-7}
Ångström star: $\lambda(WK\alpha_1)/0.209\,010\,0$	Å*	$1.000\,014\,95(90) \times 10^{-10}$	m	9.0×10^{-7}
Lattice parameter[a] of Si (in vacuum, 22.5 °C)	a	$543.102\,0504(89) \times 10^{-12}$	m	1.6×10^{-8}
{220} lattice spacing of Si $a/\sqrt{8}$ (in vacuum, 22.5 °C)	d_{220}	$192.015\,5714(32) \times 10^{-12}$	m	1.6×10^{-8}
Molar volume of Si $M(Si)/\rho(Si) = N_A a^3/8$ (in vacuum, 22.5 °C)	$V_m(Si)$	$12.058\,832\,14(61) \times 10^{-6}$	m^3 mol^{-1}	5.1×10^{-8}

[a]This is the lattice parameter (unit cell edge length) of an ideal single crystal of naturally occurring Si free of impurities and imperfections and is deduced from measurements on extremely pure and nearly perfect single crystals of Si by correcting for the effects of impurities.

meeting in Paris in the fall of 2018 a resolution that will revise the SI. In the "new SI," as it has come to be called to distinguish it from the present SI, the definitions of the kilogram, ampere, kelvin, and mole are linked to exact values of the Planck constant h, elementary charge e, Boltzmann constant k, and Avogadro constant N_A, in much the same way as the present definition of the meter is linked to an exact value of the speed of light in vacuum c. CODATA, through its Task Group on Fundamental Constants, is to provide the values of h, e, k, and N_A for the new definitions by carrying out a special least-squares adjustment during the summer of 2017. Details of the proposed new-SI may be found on the BIPM website at bipm.org/en/measurement-units/new-si/ [see also Milton, Davis, and Fletcher (2014)].

A. Comparison of 2014 and 2010 CODATA recommended values

Table XL compares the 2014 and 2010 recommended values of a representative group of constants. The regularities observed

RIGHTSLINK

TABLE XXXVII. The values in SI units of some non-SI units based on the 2014 CODATA adjustment of the values of the constants

Quantity	Symbol	Numerical value	Unit	Relative std. uncert. u_r
		Non-SI units accepted for use with the SI		
Electron volt: (e/C) J	eV	$1.602\,176\,6208(98)\times10^{-19}$	J	6.1×10^{-9}
(Unified) atomic mass unit: $\frac{1}{12}m(^{12}\mathrm{C})$	u	$1.660\,539\,040(20)\times10^{-27}$	kg	1.2×10^{-8}
		Natural units (n.u.)		
n.u. of velocity	c, c_0	299 792 458	m s^{-1}	Exact
n.u. of action: $h/2\pi$	$\hbar$	$1.054\,571\,800(13)\times10^{-34}$	J s	1.2×10^{-8}
		$6.582\,119\,514(40)\times10^{-16}$	eV s	6.1×10^{-9}
	$\hbar c$	197.326 9788(12)	MeV fm	6.1×10^{-9}
n.u. of mass	m_e	$9.109\,383\,56(11)\times10^{-31}$	kg	1.2×10^{-8}
n.u. of energy	$m_e c^2$	$8.187\,105\,65(10)\times10^{-14}$	J	1.2×10^{-8}
		0.510 998 9461(31)	MeV	6.2×10^{-9}
n.u. of momentum	$m_e c$	$2.730\,924\,488(34)\times10^{-22}$	kg m s^{-1}	1.2×10^{-8}
		0.510 998 9461(31)	MeV/c	6.2×10^{-9}
n.u. of length: $\hbar/m_e c$	$\lambda\!\!\!^{-}_C$	$386.159\,267\,64(18)\times10^{-15}$	m	4.5×10^{-10}
n.u. of time	$\hbar/m_e c^2$	$1.288\,088\,667\,12(58)\times10^{-21}$	s	4.5×10^{-10}
		Atomic units (a.u.)		
a.u. of charge	e	$1.602\,176\,6208(98)\times10^{-19}$	C	6.1×10^{-9}
a.u. of mass	m_e	$9.109\,383\,56(11)\times10^{-31}$	kg	1.2×10^{-8}
a.u. of action: $h/2\pi$	$\hbar$	$1.054\,571\,800(13)\times10^{-34}$	J s	1.2×10^{-8}
a.u. of length: Bohr radius (bohr) $\alpha/4\pi R_\infty$	a_0	$0.529\,177\,210\,67(12)\times10^{-10}$	m	2.3×10^{-10}
a.u. of energy: Hartree energy (hartree) $e^2/4\pi\epsilon_0 a_0 = 2R_\infty hc = \alpha^2 m_e c^2$	E_h	$4.359\,744\,650(54)\times10^{-18}$	J	1.2×10^{-8}
a.u. of time	$\hbar/E_h$	$2.418\,884\,326\,509(14)\times10^{-17}$	s	5.9×10^{-12}
a.u. of force	E_h/a_0	$8.238\,723\,36(10)\times10^{-8}$	N	1.2×10^{-8}
a.u. of velocity: αc	$a_0 E_h/\hbar$	$2.187\,691\,262\,77(50)\times10^{6}$	m s^{-1}	2.3×10^{-10}
a.u. of momentum	$\hbar/a_0$	$1.992\,851\,882(24)\times10^{-24}$	kg m s^{-1}	1.2×10^{-8}
a.u. of current	$eE_h/\hbar$	$6.623\,618\,183(41)\times10^{-3}$	A	6.1×10^{-9}
a.u. of charge density	e/a_0^3	$1.081\,202\,3770(67)\times10^{12}$	C m^{-3}	6.2×10^{-9}
a.u. of electric potential	E_h/e	27.211 386 02(17)	V	6.1×10^{-9}
a.u. of electric field	E_h/ea_0	$5.142\,206\,707(32)\times10^{11}$	V m^{-1}	6.1×10^{-9}
a.u. of electric field gradient	E_h/ea_0^2	$9.717\,362\,356(60)\times10^{21}$	V m^{-2}	6.2×10^{-9}
a.u. of electric dipole moment	ea_0	$8.478\,353\,552(52)\times10^{-30}$	C m	6.2×10^{-9}
a.u. of electric quadrupole moment	ea_0^2	$4.486\,551\,484(28)\times10^{-40}$	C m^2	6.2×10^{-9}
a.u. of electric polarizability	$e^2a_0^2/E_h$	$1.648\,777\,2731(11)\times10^{-41}$	C^2 m^2 J^{-1}	6.8×10^{-10}
a.u. of 1st hyperpolarizability	$e^3a_0^3/E_h^2$	$3.206\,361\,329(20)\times10^{-53}$	C^3 m^3 J^{-2}	6.2×10^{-9}
a.u. of 2nd hyperpolarizability	$e^4a_0^4/E_h^3$	$6.235\,380\,085(77)\times10^{-65}$	C^4 m^4 J^{-3}	1.2×10^{-8}
a.u. of magnetic flux density	$\hbar/ea_0^2$	$2.350\,517\,550(14)\times10^{5}$	T	6.2×10^{-9}
a.u. of magnetic dipole moment: $2\mu_B$	$\hbar e/m_e$	$1.854\,801\,999(11)\times10^{-23}$	J T^{-1}	6.2×10^{-9}
a.u. of magnetizability	$e^2a_0^2/m_e$	$7.891\,036\,5886(90)\times10^{-29}$	J T^{-2}	1.1×10^{-9}
a.u. of permittivity: $10^7/c^2$	e^2/a_0E_h	$1.112\,650\,056\ldots\times10^{-10}$	F m^{-1}	Exact

in the numbers in columns 2 to 4 arise because the values of many constants are obtained from expressions proportional to the fine-structure constant α, Planck constant h, or molar gas constant R raised to various powers. For example, the first six quantities are obtained from expressions proportional to α^a, where $|a| = 1$, 2, 3, or 6. The next 15 quantities, from h to the magnetic moment of the proton μ_p, are calculated from expressions containing the factor h^a, where $|a| = 1$ or $1/2$. And the five quantities from R to the Stefan-Boltzmann constant σ are proportional to R^a, where $|a| = 1$ or 4.

Additional comments on some of the entries in Table XL are as follows.

(i) The shift and uncertainty reduction of the 2014 recommended value of α is mainly due to the availability for the first time of a numerically calculated result for the tenth-order coefficient $A_1^{(10)}$ (12 672 Feynman diagrams) in the theoretical expression for a_e; see Sec. V.A.1. The value used in 2010, based on a procedure described in CODATA-98, is 0.0(4.6) compared with the newly available value 7.79(34) used in 2014.

(ii) In the 2010 adjustment inconsistencies among watt-balance measurements of h and the value inferred from an x-ray-crystal-density (XRCD) measurement of N_A using highly enriched silicon led the Task Group to expand the uncertainties assigned to these data by a multiplicative factor, or expansion factor, of 2. These inconsistencies have since been resolved and further,

RIGHTSLINK

RIGHTSLINK

TABLE XXXVIII. The values of some energy equivalents derived from the relations $E = mc^2 = hc/\lambda = h\nu = kT$, and based on the 2014 CODATA adjustment of the values of the constants; 1 eV = (e/C) J, 1 u = $m_u = \frac{1}{12}m(^{12}\mathrm{C}) = 10^{-3}$ kg mol$^{-1}/N_A$, and $E_h = 2R_\infty hc = \alpha^2 m_e c^2$ is the Hartree energy (hartree)

	Relevant unit			
	J	kg	m^{-1}	Hz
1 J	$(1\ \mathrm{J}) = 1\ \mathrm{J}$	$(1\ \mathrm{J})/c^2 = 1.112\,650\,056\ldots \times 10^{-17}$ kg	$(1\ \mathrm{J})/hc = 5.034\,116\,651(62) \times 10^{24}\ \mathrm{m}^{-1}$	$(1\ \mathrm{J})/h = 1.509\,190\,205(19) \times 10^{33}$ Hz
1 kg	$(1\ \mathrm{kg})c^2 = 8.987\,551\,787\ldots \times 10^{16}$ J	$(1\ \mathrm{kg}) = 1$ kg	$(1\ \mathrm{kg})c/h = 4.524\,438\,411(56) \times 10^{41}\ \mathrm{m}^{-1}$	$(1\ \mathrm{kg})c^2/h = 1.356\,392\,512(17) \times 10^{50}$ Hz
1 m^{-1}	$(1\ \mathrm{m}^{-1})hc = 1.986\,445\,824(24) \times 10^{-25}$ J	$(1\ \mathrm{m}^{-1})h/c = 2.210\,219\,057(27) \times 10^{-42}$ kg	$(1\ \mathrm{m}^{-1}) = 1\ \mathrm{m}^{-1}$	$(1\ \mathrm{m}^{-1})c = 299\,792\,458$ Hz
1 Hz	$(1\ \mathrm{Hz})h = 6.626\,070\,040(81) \times 10^{-34}$ J	$(1\ \mathrm{Hz})h/c^2 = 7.372\,497\,201(91) \times 10^{-51}$ kg	$(1\ \mathrm{Hz})\ c = 3.335\,640\,951\ldots \times 10^{-9}\ \mathrm{m}^{-1}$	$(1\ \mathrm{Hz}) = 1$ Hz
1 K	$(1\ \mathrm{K})k = 1.380\,648\,52(79) \times 10^{-23}$ J	$(1\ \mathrm{K})k/c^2 = 1.536\,178\,65(88) \times 10^{-40}$ kg	$(1\ \mathrm{K})k/hc = 69.503\,457(40)\ \mathrm{m}^{-1}$	$(1\ \mathrm{K})k/h = 2.083\,6612(12) \times 10^{10}$ Hz
1 eV	$(1\ \mathrm{eV}) = 1.602\,176\,6208(98) \times 10^{-19}$ J	$(1\ \mathrm{eV})/c^2 = 1.782\,661\,907(11) \times 10^{-36}$ kg	$(1\ \mathrm{eV})/hc = 8.065\,544\,005(50) \times 10^{5}\ \mathrm{m}^{-1}$	$(1\ \mathrm{eV})/h = 2.417\,989\,262(15) \times 10^{14}$ Hz
1 u	$(1\ \mathrm{u})c^2 = 1.492\,418\,062(18) \times 10^{-10}$ J	$(1\ \mathrm{u}) = 1.660\,539\,040(20) \times 10^{-27}$ kg	$(1\ \mathrm{u})c/h = 7.513\,006\,6166(34) \times 10^{14}\ \mathrm{m}^{-1}$	$(1\ \mathrm{u})c^2/h = 2.252\,342\,7206(10) \times 10^{23}$ Hz
1 E_h	$(1\ E_h) = 4.359\,744\,650(54) \times 10^{-18}$ J	$(1\ E_h)/c^2 = 4.850\,870\,129(60) \times 10^{-35}$ kg	$(1\ E_h)/hc = 2.194\,746\,313\,702(13) \times 10^{7}\ \mathrm{m}^{-1}$	$(1\ E_h)/h = 6.579\,683\,920\,711(39) \times 10^{15}$ Hz

TABLE XXXIX. The values of some energy equivalents derived from the relations $E = mc^2 = hc/\lambda = h\nu = kT$ and based on the 2014 CODATA adjustment of the values of the constants; 1 eV = (e/C) J, 1 u = $m_u = \frac{1}{12}m(^{12}\mathrm{C}) = 10^{-3}$ kg mol$^{-1}/N_A$, and $E_h = 2R_\infty hc = \alpha^2 m_e c^2$ is the Hartree energy (hartree)

	Relevant unit			
	K	eV	u	E_h
1 J	$(1\ \mathrm{J})/k = 7.242\,9731(42) \times 10^{22}$ K	$(1\ \mathrm{J}) = 6.241\,509\,126(38) \times 10^{18}$ eV	$(1\ \mathrm{J})/c^2 = 6.700\,535\,363(82) \times 10^{9}$ u	$(1\ \mathrm{J}) = 2.293\,712\,317(28) \times 10^{17}\ E_h$
1 kg	$(1\ \mathrm{kg})c^2/k = 6.509\,6595(37) \times 10^{39}$ K	$(1\ \mathrm{kg})c^2 = 5.609\,588\,650(34) \times 10^{35}$ eV	$(1\ \mathrm{kg}) = 6.022\,140\,857(74) \times 10^{26}$ u	$(1\ \mathrm{kg})c^2 = 2.061\,485\,823(25) \times 10^{34}\ E_h$
1 m^{-1}	$(1\ \mathrm{m}^{-1})hc/k = 1.438\,777\,36(83) \times 10^{-2}$ K	$(1\ \mathrm{m}^{-1})hc = 1.239\,841\,9739(76) \times 10^{-6}$ eV	$(1\ \mathrm{m}^{-1})h/c = 1.331\,025\,049\,00(61) \times 10^{-15}$ u	$(1\ \mathrm{m}^{-1})hc = 4.556\,335\,252\,767(27) \times 10^{-8}\ E_h$
1 Hz	$(1\ \mathrm{Hz})h/k = 4.799\,2447(28) \times 10^{-11}$ K	$(1\ \mathrm{Hz})h = 4.135\,667\,662(25) \times 10^{-15}$ eV	$(1\ \mathrm{Hz})h/c^2 = 4.439\,821\,6616(20) \times 10^{-24}$ u	$(1\ \mathrm{Hz})h = 1.519\,829\,846\,0088(90) \times 10^{-16}\ E_h$
1 K	$(1\ \mathrm{K}) = 1$ K	$(1\ \mathrm{K})k = 8.617\,3303(50) \times 10^{-5}$ eV	$(1\ \mathrm{K})k/c^2 = 9.251\,0842(53) \times 10^{-14}$ u	$(1\ \mathrm{K})k = 3.166\,8105(18) \times 10^{-6}\ E_h$
1 eV	$(1\ \mathrm{eV})/k = 1.160\,452\,21(67) \times 10^{4}$ K	$(1\ \mathrm{eV}) = 1$ eV	$(1\ \mathrm{eV})/c^2 = 1.073\,544\,1105(66) \times 10^{-9}$ u	$(1\ \mathrm{eV}) = 3.674\,932\,248(23) \times 10^{-2}\ E_h$
1 u	$(1\ \mathrm{u})c^2/k = 1.080\,954\,38(62) \times 10^{13}$ K	$(1\ \mathrm{u})c^2 = 931.494\,0954(57) \times 10^{6}$ eV	$(1\ \mathrm{u}) = 1$ u	$(1\ \mathrm{u})c^2 = 3.423\,177\,6902(16) \times 10^{7}\ E_h$
1 E_h	$(1\ E_h)/k = 3.157\,7513(18) \times 10^{5}$ K	$(1\ E_h) = 27.211\,386\,02(17)$ eV	$(1\ E_h)/c^2 = 2.921\,262\,3197(13) \times 10^{-8}$ u	$(1\ E_h) = 1\ E_h$

TABLE XL. Comparison of the 2014 and 2010 CODATA recommended values of a representative group of constants. Here D_r is the 2014 value minus the 2010 value divided by the standard uncertainty u of the 2010 value

Quantity	2014 rel. std. uncert. u_r	Ratio 2010 u_r to 2014 u_r	D_r
α	2.3×10^{-10}	1.4	−1.4
R_K	2.3×10^{-10}	1.4	1.4
a_0	2.3×10^{-10}	1.4	−1.4
λ_C	4.5×10^{-10}	1.4	−1.4
r_e	6.8×10^{-10}	1.4	−1.4
σ_e	1.4×10^{-9}	1.4	−1.4
h	1.2×10^{-8}	3.6	1.6
m_e	1.2×10^{-8}	3.6	1.6
m_h	1.2×10^{-8}	3.6	1.6
m_α	1.2×10^{-8}	3.6	1.6
N_A	1.2×10^{-8}	3.6	−1.6
E_h	1.2×10^{-8}	3.6	1.6
c_1	1.2×10^{-8}	3.6	1.6
e	6.1×10^{-9}	3.6	1.6
K_J	6.1×10^{-9}	3.6	−1.6
F	6.2×10^{-9}	3.6	−1.7
γ'_p	1.3×10^{-8}	2.0	−1.5
μ_B	6.2×10^{-9}	3.6	1.5
μ_N	6.2×10^{-9}	3.6	1.5
μ_e	6.2×10^{-9}	3.6	−1.5
μ_p	6.9×10^{-9}	3.4	1.3
R	5.7×10^{-7}	1.6	−0.3
k	5.7×10^{-7}	1.6	−0.2
V_m	5.7×10^{-7}	1.6	−0.3
c_2	5.7×10^{-7}	1.6	0.3
σ	2.3×10^{-6}	1.6	−0.3
G	4.7×10^{-5}	2.6	0.3
R_∞	5.9×10^{-12}	0.8	−0.6
m_e/m_p	9.5×10^{-11}	4.3	−1.9
m_e/m_μ	2.2×10^{-8}	1.1	0.3
$A_r(e)$	2.9×10^{-11}	13.8	−1.8
$A_r(p)$	9.0×10^{-11}	1.0	0.7
$A_r(n)$	4.9×10^{-10}	0.9	−0.3
$A_r(d)$	2.0×10^{-11}	1.9	0.4
$A_r(t)$	3.6×10^{-11}	22.8	1.2
$A_r(h)$	3.9×10^{-11}	21.3	−0.0
$A_r(\alpha)$	1.6×10^{-11}	1.0	0.0
d_{220}	1.6×10^{-8}	1.0	0.0
g_e	2.6×10^{-13}	1.0	−0.5
g_μ	6.3×10^{-10}	1.0	0.0
μ_p/μ_B	3.0×10^{-9}	2.7	−0.3
μ_p/μ_N	3.0×10^{-9}	2.7	−0.2
μ_n/μ_N	2.4×10^{-7}	1.0	−0.0
μ_d/μ_N	5.5×10^{-9}	1.5	0.0
μ_e/μ_p	3.0×10^{-9}	2.7	−0.3
μ_n/μ_p	2.4×10^{-7}	1.0	−0.0
μ_d/μ_p	5.0×10^{-9}	1.5	0.3

an improved watt-balance result for h with a relative uncertainty of 1.8×10^{-8} and an improved XRCD-Avogadro constant inferred value of h with a relative uncertainty of 2.0×10^{-8} have become available for the 2014 adjustment. Because the data are now sufficiently consistent that it is no longer necessary to increase uncertainties as in 2010, the relative uncertainty of the 2014 recommended value of h is 1.2×10^{-8} compared to 4.4×10^{-8} for the 2010 value.

(iii) The 2010 recommended value of R is based on six acoustic-gas-thermometry (AGT) results with relative uncertainties in the range 1.2×10^{-6} to 8.4×10^{-6} while the 2014 recommended value is based mainly on seven AGT results with relative uncertainties in the range 0.90×10^{-6} to 3.7×10^{-6}. Of these seven, three are new results, two of which have uncertainties of 0.90×10^{-6} and 1.0×10^{-6}, respectively. Also contributing to the determination of the 2014 recommended value of R is a Johnson noise thermometry measurement of k/h and a dielectric-constant gas thermometry measurement of A_ϵ/R with relative uncertainties of 3.9×10^{-6} and 4.0×10^{-6}, respectively. It is the significant advances made in AGT in the past four years that have led to the reduction of the uncertainty of the recommended value of R by nearly 40%. The consistency of the new and previous AGT results have led to the comparatively small shift of the 2014 value from that of 2010.

(iv) Other constants in Table XL whose changes are worth noting are G, m_e/m_p, $A_r(e)$, $A_r(t)$, $A_r(h)$, μ_p/μ_B, μ_p/μ_N, and μ_e/μ_p. The 2010 recommended value of G with relative uncertainty 12×10^{-5} is the weighted mean of 11 results whose *a priori* uncertainties were increased by an expansion factor of 14 so that the smallest and largest result differed from the recommended value by about twice the latter's uncertainty. For the 2014 adjustment the Task Group decided to follow its usual practice and to choose an expansion factor that reduces the normalized residual of each datum to less than 2. Thus in 2014 the expansion factor is 6.3 and the weighted mean of the 14 available values, which is the 2014 recommended value, has a relative uncertainty of 4.7×10^{-5}. The shift of the 2014 value from the 2010 value is due to the three new results that became available for the 2014 adjustment.

The reduction in uncertainty of m_e/m_p is a consequence of the large reduction in uncertainty of $A_r(e)$, which resulted from measurement of the ratio of the electron spin-flip frequency of the $^{12}C^{5+}$ ion to the cyclotron frequency of the ion in the same magnetic flux density, and the same ratio for $^{28}Si^{13+}$, with the extraordinarily small relative uncertainties of 2.8×10^{-11} and 4.8×10^{-11}, respectively. The significant reduction in uncertainty of $A_r(t)$ and $A_r(h)$ is the result of the measurement of two pairs of cyclotron frequency ratios carried out in two different laboratories, the first being that of d and h to $^{12}C^{6+}$ with relative uncertainties of 2.0×10^{-11} and 1.4×10^{-11}; and the second is that of HD^+ to $^3He^+$ and to t with relative uncertainties for each of 4.8×10^{-11}. However, because of the significant inconsistency of the values of $A_r(^3He)$ implied by the second ratio of the first pair and the first ratio of the second pair, the Task Group applied a multiplicative factor of 2.8 to the uncertainties of these two ratios in order to reduce the residual of each to less than 2 in the final adjustment on which

RIGHTSLINK

the 2014 recommended values are based. Finally, the reduction in the uncertainties of μ_p/μ_B, μ_p/μ_N, and μ_e/μ_p are a consequence of a new, directly measured value of μ_p/μ_N with a relative uncertainty of 3.3×10^{-9}.

B. Some implications of the 2014 CODATA recommended values and adjustment for metrology and physics

1. Conventional electrical units

The conventional values $K_{J-90}=483\,597.9$ GHz/V and $R_{K-90}=25\,812.807\ \Omega$ adopted in 1990 for the Josephson and von Klitzing constants established conventional units of voltage and resistance, V_{90} and Ω_{90}, given by $V_{90}=(K_{J-90}/K_J)$ V and $\Omega_{90}=(R_K/R_{K-90})\ \Omega$. Other conventional electric units follow from V_{90} and Ω_{90}, for example, $A_{90}=V_{90}/\Omega_{90}$, $C_{90}=A_{90}$ s, $W_{90}=A_{90}V_{90}$, $F_{90}=C_{90}/V_{90}$, and $H_{90}=\Omega_{90}$ s, which are the conventional units of current, charge, power, capacitance, and inductance, respectively, (Taylor and Mohr, 2001). The 2014 adjustment gives for the relations between K_J and K_{J-90}, and for R_K and R_{K-90},

$$K_J=K_{J-90}[1-9.83(61)\times10^{-8}], \tag{273}$$

$$R_K=R_{K-90}[1+1.765(23)\times10^{-8}], \tag{274}$$

which lead to

$$V_{90}=[1+9.83(61)\times10^{-8}]\ \text{V}, \tag{275}$$

$$\Omega_{90}=[1+1.765(23)\times10^{-8}]\ \Omega, \tag{276}$$

$$A_{90}=[1+8.06(61)\times10^{-8}]\ \text{A}, \tag{277}$$

$$C_{90}=[1+8.06(61)\times10^{-8}]\ \text{C}, \tag{278}$$

$$W_{90}=[1+17.9(1.2)\times10^{-8}]\ \text{W}, \tag{279}$$

$$F_{90}=[1-1.765(23)\times10^{-8}]\ \text{F}, \tag{280}$$

$$H_{90}=[1+1.765(23)\times10^{-8}]\ \text{H}. \tag{281}$$

Equations (275) and (276) show that V_{90} exceeds V and Ω_{90} exceeds Ω, which means that measured voltages and resistances traceable to the Josephson effect and K_{J-90} and the quantum-Hall effect and R_{K-90}, respectively, are too small relative to the SI. However, the differences are well within the 40×10^{-8} uncertainty assigned to $V_{90}/$ V and the 10×10^{-8} uncertainty assigned to Ω_{90}/Ω by the Consultative Committee for Electricity and Magnetism (CCEM) of the International Committee for Weights and Measures (CIPM) (Quinn, 1989; Quinn, 2001).

2. Josephson and quantum-Hall effects

Watt-balance and XRCD-N_A advances have led to tests of the exactness of the quantum-Hall and Josephson effect relations $R_K=h/e^2$ and $K_J=2e/h$ that are less clouded by inconsistencies of the data. Indeed, based on the 2014 data as used in adjustment 2 summarized in Table XXVIII, Sec. XIII.B.2, the possible corrections ϵ_K and ϵ_J to the quantum-Hall and Josephson effect relations are $2.2(1.8)\times10^{-8}$ and $-0.9(1.5)\times10^{-8}$, respectively; see Table XXXI, Sec. XIII.B.3. Thus the exactness of these relations is experimentally confirmed within about 2 parts in 10^8. However, as Table XXXI indicates, some of the initial 2014 input data are not as supportive of the exactness of the relations, most notably the NIST-89 result for Γ'_{p-90}; on the other hand, its normalized residual in the adjustment that produced the above values of ϵ_K and ϵ_J is 2.3 and because of its low-weight it is omitted from the 2006 and 2010 final adjustments as well as the 2014 final adjustment.

3. The new SI

The impact of the new data that have become available for the 2014 adjustment on the establishment of the new SI by the CGPM is discussed in detail in the Introduction section of this report (see Sec. I.B.1) and need not be repeated here. Suffice it to say that the uncertainties of the 2014 recommended values of the four new defining constants h, e, k, and N_A, which in parts in 10^8 are 1.2, 0.61, 57, and 1.2, are already sufficiently small to meet the requirements deemed necessary by the CIPM and CGPM for the adoption of the new SI.

4. Proton radius

The severe disagreement of the proton rms charge radius r_p determined from the Lamb shift in muonic hydrogen with values determined from H and D transition frequencies and electron-proton scattering experiments present in the 2010 adjustment remain present in the 2014 adjustment. Although the uncertainty of the muonic hydrogen value is significantly smaller than the uncertainties of these other values, its negative impact on the internal consistency of the theoretically predicted and experimentally measured frequencies, as well as on the value of the Rydberg constant, was considered by the Task Group to be still so severe that the only recourse was to once again exclude it from the final adjustment.

5. Muon magnetic-moment anomaly

The long-standing significant difference between the theoretically predicted, standard-model value of a_μ and the experimentally determined value that led to the exclusion of the theoretical expression for a_μ from the 2010 adjustment remains; the difference is still at about the 3σ level depending on the way the all-important lowest-order hadronic vacuum polarization and hadronic light-by-light contributions are evaluated. Because of the continuing difficulty of reliably calculating these terms, the Task Group decided to omit the theory from the 2014 adjustment as in 2010. The 2014 recommended values of a_μ and those of other constants that depend on it are, therefore, based on experiment.

6. Electron magnetic-moment anomaly, fine-structure constant, and QED

A useful test of the QED theory of a_e is to compare two values of α: The first, with relative uncertainty 2.4×10^{-10}, is that obtained by equating the experimental value of a_e with its QED theoretical expression; the second, which is only weakly

RIGHTSLINK

dependent on QED theory and with relative uncertainty 6.2×10^{-10}, is that obtained from the measurement of $h/m(^{87}\mathrm{Rb})$ using atom interferometry. These two values (see the first and second rows in Table XX, Sec. XIII.A) differ by 1.8 times the uncertainty of their difference, or 1.8σ. Although this is acceptable agreement and supports the QED theory of a_e, the result of the same comparison in CODATA-10 based on the same experimental values of a_e and $h/m(^{87}\mathrm{Rb})$ is 0.4σ. The two main reasons for this rather significant change are the new and somewhat surprisingly large value of the $A_1^{(10)}$ coefficient in the theoretical expression for a_e which decreased the a_e value of α; and the decreased but highly accurate new value of $A_r(e)$ which increased the $h/m(^{87}\mathrm{Rb})$ value of α.

C. Suggestions for future work

As discussed, to deal with data inconsistencies the Task Group decided to (i) omit from the 2014 adjustment the value of r_p obtained from measurements of the Lamb shift in muonic hydrogen; (ii) omit the theory of the muon magnetic-moment anomaly a_μ; (iii) increase the initial uncertainties of the cyclotron frequency ratios $\omega_c(h)/\omega_c(^{12}C^{6+})$ and $\omega_c(HD^+)/\omega_c(^3He^+)$ relevant to the determination of $A_r(h)$ by an expansion factor of 2.8; and (iv) increase the initial uncertainties of the 14 values of G by an expansion factor of 6.3. Issues (i), (ii), and (iv) have been with us for some time and suggestions for their resolution were given in CODATA-10. Updated versions follow together with a suggestion regarding (iii).

As also discussed, the data now available provide values of the defining constants h, e, k, and N_A of the new SI with uncertainties sufficiently small for its adoption by the 26th CGPM in the fall of 2018 as planned. The final values are to be based on a special adjustment carried out by the Task Group during the summer of 2017. Because of its importance, the CIPM has decided that all the data to be used in that adjustment must have been published in an archival journal or be available in a preprint accepted for publication by 1 July 2017. Nevertheless, we include suggestions for work that will improve the robustness of the currently available data that determine these important constants.

(i) Work currently underway could solve the "proton radius puzzle" and should continue to be pursued as vigorously as possible. This includes the measurement of hydrogen transition frequencies, the analysis of μ-p and μ-d data, and possible new Lamb-shift measurements in μ-h and μ-α. New scattering data from experiments such as MUSE (Downie, 2014) and PRad (Gasparian, 2014) and improved methods to extract r_p from such data as well as verification of the theory of H, D, and muonic hydrogenlike energy levels could also help.

(ii) Because the disagreement between a_μ theory and experiment remains even after many years of effort devoted to improving the theory and the experimental results on which the theory relies, the solution to the problem may have to wait until the completion over the next 5 to 10 years of the two new experiments underway to remeasure a_μ (Mibe, 2011; Logashenko *et al.*, 2015). Improved measurements of cross sections for the scattering of e^+e^- into hadrons and better data on the decay of the τ into hadrons could also be useful.

(iii) The two cyclotron frequency ratios in question were obtained from experiments at the University of Washington and at Florida State University (FSU). A careful study of the University of Washington apparatus that might uncover an overlooked systematic effect is not possible because it is no longer available. However, the research program at FSU continues and the researchers are encouraged to search for a possible explanation of the disagreement. An experiment under way to measure the Q value of tritium at the Max-Planck Institut für Kernphysik, Heidelberg, Germany, could resolve the problem (Streubel *et al.*, 2014).

(iv) One or more measurements of G with an uncertainty of 1 part in 10^5 using new and innovative approaches might finally resolve some of the problems that have plagued the reliable determination of G over the past three decades. The possibliity of transferring the apparatus used by Quinn *et al.* (2014) and by Parks and Faller (2014) to other laboratories to be used there by new researchers in the hope of uncovering overlooked systematic effects could be helpful as well.

(v) Watt-balance and watt-balance-like measurements of h and the XRCD measurement of N_A currently under way should continue to be vigorously pursued with the goal of achieving uncertainties of no more than a few parts in 10^8. This also applies to experiments to determine R, k/h, and A_ϵ/R with an uncertainty goal of no more than a few parts in 10^6. An independent calculation of the $A_1^{(8)}$ and $A_1^{(10)}$ coefficients in the theoretical expression for a_e would increase confidence in the value of α from a_e. For this same reason, results from experiments currently under way to determine $h/m(X)$ with an uncertainty small enough to provide a value of α with an uncertainty of 5 parts in 10^{10} or less would be valuable.

List of Symbols and Abbreviations

ASD	NIST Atomic Spectra Database (online)
AMDC	Atomic Mass Data Center, transferred in 2013 to Institute of Modern Physics (IMP), Chinese Academy of Sciences, Lanzhou, PRC, from Centre de Spectrométrie Nucléaire et de Spectrométrie de Masse (CSNSM), Orsay, France
AME	Atomic mass evaluation from the AMDC (completed in year specified)
$A_r(X)$	relative atomic mass of X: $A_r(X)=m(X)/m_u$
A_{90}	conventional unit of electric current: $A_{90}=V_{90}/\Omega_{90}$
Å*	ångström star: $\lambda(\mathrm{WK}\alpha_1)=0.209\,010\,0$ Å*

RIGHTSLINK

a_e	electron magnetic-moment anomaly: $a_e = (\|g_e\| - 2)/2$
a_μ	muon magnetic-moment anomaly: $a_\mu = (\|g_\mu\| - 2)/2$
BIPM	International Bureau of Weights and Measures, Sèvres, France
BNL	Brookhaven National Laboratory, Upton, New York, USA
CERN	European Organization for Nuclear Research, Geneva, Switzerland
CGPM	General Conference on Weights and Measures
CIPM	International Committee for Weights and Measures
CODATA	Committee on Data for Science and Technology of the International Council for Science
CPT	combined charge conjugation, parity inversion, and time reversal
c	speed of light in vacuum
d	deuteron (nucleus of deuterium D, or ^{2}H)
d_{220}	{220} lattice spacing of an ideal crystal of naturally occurring silicon
$d_{220}(X)$	{220} lattice spacing of crystal X of naturally occurring silicon
e	symbol for either member of the electron-positron pair; when necessary, e^- or e^+ is used to indicate the electron or positron
e	elementary charge: absolute value of the charge of the electron
F	Faraday constant: $F = N_A e$
FSU	Florida State University, Tallahassee, Florida, USA
FSUJ	Friedrich-Schiller University, Jena, Germany
$\mathcal{F}_{90}$	$\mathcal{F}_{90} = (F/A_{90})$ A
G	Newtonian constant of gravitation
g	local acceleration due to gravity
g_d	deuteron g-factor: $g_d = \mu_d/\mu_N$
g_e	electron g-factor: $g_e = 2\mu_e/\mu_B$
g_p	proton g-factor: $g_p = 2\mu_p/\mu_N$
g'_p	shielded proton g-factor: $g'_p = 2\mu'_p/\mu_N$
g_t	triton g-factor: $g_t = 2\mu_t/\mu_N$
$g_X(Y)$	g-factor of particle X in the ground (1S) state of hydrogenic atom Y
g_μ	muon g-factor: $g_\mu = 2\mu_\mu/(e\hbar/2m_\mu)$
GSI	Gesellschaft für Schweironenforschung, Darmstadt, Germany
HD	HD molecule (bound state of hydrogen and deuterium atoms)
HT	HT molecule (bound state of hydrogen and tritium atoms)
HUST	Huazhong University of Science and Technology, Wuhan, PRC
h	helion (nucleus of ^{3}He)
h	Planck constant
$\hbar$	reduced Planck constant; $h/2\pi$
HarvU	Harvard University, Cambridge, Massachusetts, USA
IAC	International Avogadro Coordination
ILL	Institut Max von Laue-Paul Langevin, Grenoble, France
INRIM	Istituto Nazionale di Ricerca Metrologica, Torino, Italy
IRMM	Institute for Reference Materials and Measurements, Geel, Belgium
JILA	JILA, University of Colorado and NIST, Boulder, Colorado, USA
KRISS	Korea Research Institute of Standards and Science, Taedok Science Town, Republic of Korea
KR/VN	KRISS-VNIIM collaboration
K_J	Josephson constant: $K_J = 2e/h$
K_{J-90}	conventional value of the Josephson constant K_J: $K_{J-90} = 483\,597.9$ GHz V^{-1}
k	Boltzmann constant: $k = R/N_A$
LAMPF	Clinton P. Anderson Meson Physics Facility at Los Alamos National Laboratory, Los Alamos, New Mexico, USA
LANL	Los Alamos National Laboratory, Los Alamos, New Mexico, USA
LENS	European Laboratory for Non-Linear Spectroscopy, University of Florence, Italy
LKB	Laboratoire Kastler-Brossel, Paris, France
LK/SY	LKB and SYRTE collaboration
LNE	Laboratoire national de métrologie et d'essais, Trappes, France
MIT	Massachusetts Institute of Technology, Cambridge, Massachusetts, USA
METAS	Federal Institute for Metrology, Bern-Wabern, Switzerland
MPIK	Max-Planck-Institut für Kernphysik, Heidelberg, Germany
MPQ	Max-Planck-Institut für Quantenoptik, Garching, Germany
MSL	Measurement Standards Laboratory, Lower Hutt, New Zeland
$M(X)$	molar mass of X: $M(X) = A_r(X)M_u$
Mu	muonium (μ^+e^- atom)
M_u	molar mass constant: $M_u = 10^{-3}$ kg mol^{-1}
m_u	unified atomic mass constant: $m_u = m(^{12}\mathrm{C})/12$
m_X, $m(X)$	mass of X (for the electron e, proton p, and other elementary particles, the first symbol is used, i.e., m_e, m_p, etc.)
N_A	Avogadro constant
NIM	National Institute of Metrology, Beijing, PRC
NIST	National Institute of Standards and Technology, Gaithersburg, Maryland and Boulder, Colorado, USA
NMI	National Metrology Institute, Lindfield, Australia
NMIJ	National Metrology Institute of Japan, Tsukuba, Japan
NPL	National Physical Laboratory, Teddington, UK
NRC	National Research Council of Canada, Measurement Science and Standards, Ottawa, Ontario, Canada
n	neutron

RIGHTSLINK

PTB	Physikalisch-Technische Bundesanstalt, Braunschweig and Berlin, Germany
p	proton
QED	quantum electrodynamics
$p(\chi^2\|\nu)$	probability that an observed value of chi-square for ν degrees of freedom would exceed χ^2
R	molar gas constant
$\overline{R}$	ratio of muon anomaly difference frequency to free proton NMR frequency
R_B	Birge ratio: $R_B = (\chi^2/\nu)^{\frac{1}{2}}$
r_d	bound-state rms charge radius of the deuteron
R_K	von Klitzing constant: $R_K = h/e^2$
R_{K-90}	conventional value of the von Klitzing constant R_K: $R_{K-90} = 25\,812.807\ \Omega$
r_p	bound-state rms charge radius of the proton
R_∞	Rydberg constant: $R_\infty = m_e c\alpha^2/2h$
$r(x_i, x_j)$	correlation coefficient of estimated values x_i and x_j: $r(x_i, x_j) = u(x_i, x_j)/[u(x_i)u(x_j)]$
S_c	self-sensitivity coefficient
SI	Système international d'unités (International System of Units)
StPtrsb	various institutions in St. Petersburg, Russian Federation
StanfU	Stanford University, Stanford, California, USA
SUREC	Scottish Universities Environmental Research Centre, University of Glasgow, Glasgow, Scotland
SYRTE	Systèmes de référence Temps Espace, Paris, France
T	thermodynamic temperature
TR&D	Tribotech Research and Development Company, Moscow, Russian Federation
Type A	uncertainty evaluation by the statistical analysis of series of observations
Type B	uncertainty evaluation by means other than the statistical analysis of series of observations
t	triton (nucleus of tritium T, or ^{3}H)
UCI	University of California, Irvine, Irvine, California, USA
UMZ	Institut für Physik, Johannes Gutenberg Universität Mainz (or simply the University of Mainz), Mainz, Germany
USussex	University of Sussex, Brighton, UK
UWash	University of Washington, Seattle, Washington, USA
UWup	University of Wuppertal, Wuppertal, Germany
UZur	University of Zurich, Zurich, Switzerland
u	unified atomic mass unit (also called the dalton, Da): 1 u = $m_u = m(^{12}\mathrm{C})/12$
u_{diff}	standard uncertainty of the difference between two values (σ is sometimes used in place of u_{diff})
$u(x_i)$	standard uncertainty (i.e., estimated standard deviation) of an estimated value x_i of a quantity X_i (also simply u)
$u_r(x_i)$	relative standard uncertainty of an estimated value x_i of a quantity X_i: $u_r(x_i) = u(x_i)/\|x_i\|$, $x_i \neq 0$ (also simply u_r)
$u(x_i, x_j)$	covariance of estimated values x_i and x_j
$u_r(x_i, x_j)$	relative covariance of estimated values x_i and x_j: $u_r(x_i, x_j) = u(x_i, x_j)/(x_i x_j)$
$V_m(\mathrm{Si})$	molar volume of naturally occurring silicon
VNIIM	D. I. Mendeleyev All-Russian Research Institute for Metrology, St. Petersburg, Russian Federation
V_{90}	conventional unit of voltage based on the Josephson effect and K_{J-90}: $V_{90} = (K_{J-90}/K_J)$ V
WarsU	University of Warsaw, Warsaw, Poland
W_{90}	conventional unit of power: $W_{90} = V_{90}^2/\Omega_{90}$
XROI	combined x-ray and optical interferometer
xu(CuKα_1)	Cu x unit: $\lambda(\mathrm{CuK}\alpha_1) = 1\,537.400$ xu(CuKα_1)
xu(MoKα_1)	Mo x unit: $\lambda(\mathrm{MoK}\alpha_1) = 707.831$ xu(MoKα_1)
$x(X)$	amount-of-substance fraction of X
YaleU	Yale University, New Haven, Connecticut, USA
α	fine-structure constant: $\alpha = e^2/4\pi\epsilon_0\hbar c \approx 1/137$
α	alpha particle (nucleus of ^{4}He)
Γ'_{X-90}(lo)	$\Gamma'_{X-90}(\mathrm{lo}) = (\gamma'_X A_{90})$ A^{-1}, X = p or h
Γ'_{p-90}(hi)	$\Gamma'_{p-90}(\mathrm{hi}) = (\gamma'_p/A_{90})$ A
γ_p	proton gyromagnetic ratio: $\gamma_p = 2\mu_p/\hbar$
γ'_p	shielded proton gyromagnetic ratio: $\gamma'_p = 2\mu'_p/\hbar$
γ'_h	shielded helion gyromagnetic ratio: $\gamma'_h = 2\|\mu'_h\|/\hbar$
$\Delta E_B(^A X^{n+})$	energy required to remove n electrons from a neutral atom
$\Delta E_I(^A X^{i+})$	electron ionization energies, $i = 0$ to $n-1$
$\Delta\nu_{Mu}$	muonium ground-state hyperfine splitting
δ_C	additive correction to the theoretical expression for the electron ground-state g-factor in $^{12}\mathrm{C}^{5+}$
δ_e	additive correction to the theoretical expression for the electron magnetic-moment anomaly a_e
δ_{Mu}	additive correction to the theoretical expression for the ground-state hyperfine splitting of muonium $\Delta\nu_{Mu}$
δ_{Si}	additive correction to the theoretical expression for the electron ground-state g-factor in $^{28}\mathrm{Si}^{13+}$
$\delta_X(n\mathrm{L}_j)$	additive correction to the theoretical expression for an energy level of either hydrogen H or deuterium D with quantum numbers n, L, and j
ϵ_J	hypothetical correction to the Josephson effect relation: $K_J = (2e/h)(1+\epsilon_J)$
ϵ_K	hypothetical correction to the quantum-Hall-effect relation: $R_K = (h/e^2)(1+\epsilon_K)$
ϵ_0	electric constant (vacuum electric permittivity): $\epsilon_0 = 1/\mu_0 c^2$
$\doteq$	symbol used to relate an input datum to its observational equation
$\lambda(X\mathrm{K}\alpha_1)$	wavelength of Kα_1 x-ray line of element X
μ	symbol for either member of the muon-antimuon pair; when necessary, μ^- or μ^+ is used to indicate the negative muon or positive muon
μ_B	Bohr magneton: $\mu_B = e\hbar/2m_e$
μ_N	nuclear magneton: $\mu_N = e\hbar/2m_p$
$\mu_X(Y)$	magnetic moment of particle X in atom or molecule Y
μ_0	magnetic constant (vacuum magnetic permeability): $\mu_0 = 4\pi \times 10^{-7}$ N/A^2
μ_X, μ'_X	magnetic moment, or shielded magnetic moment, of particle X

RIGHTSLINK

ν	degrees of freedom of a particular adjustment
$\nu(f_p)$	difference between muonium hyperfine splitting Zeeman transition frequencies ν_{34} and ν_{12} at a magnetic flux density B corresponding to the free proton NMR frequency f_p
σ	Stefan-Boltzmann constant: $\sigma = 2\pi^5 k^4/(15h^3c^2)$
τ	symbol for either member of the tau-antitau pair; when necessary, τ^- or τ^+ is used to indicate the negative tau or positive tau
χ^2	the statistic "chi square"
Ω_{90}	conventional unit of resistance based on the quantum-Hall effect and R_{K-90}: $\Omega_{90} = (R_K/R_{K-90})\ \Omega$

Acknowledgments

As always, we gratefully acknowledge the help of our many colleagues throughout the world who provided the CODATA Task Group on Fundamental Constants with results prior to formal publication and for promptly and patiently answering our many questions about their work. We wish to thank our fellow Task Group members for their invaluable guidance and suggestions during the course of the 2014 adjustment effort.

XVI. References

Adikaram, D., *et al.*, 2015, Phys. Rev. Lett. **114**, 062003.
Adkins, G. S., M. Kim, C. Parsons, and R. N. Fell, 2015, Phys. Rev. Lett. **115**, 233401.
Aldrich, L. T., and A. O. Nier, 1948, Phys. Rev. **74**, 1590.
Aleksandrov, V. S., and Y. I. Neronov, 2011, Zh. Eksp. Teor. Fiz. **93**, 337 [JETP **93**, 305 (2011)].
Angeli, I., 2004, At. Data Nucl. Data Tables **87**, 185.
Antognini, A., F. Kottmann, F. Biraben, P. Indelicato, F. Nez, and R. Pohl, 2013a, Ann. Phys. (N.Y.) **331**, 127.
Antognini, A., *et al.*, 2013b, Science **339**, 417.
Aoyama, T., M. Hayakawa, T. Kinoshita, and M. Nio, 2012a, Phys. Rev. Lett. **109**, 111808.
Aoyama, T., M. Hayakawa, T. Kinoshita, and M. Nio, 2012b, Phys. Rev. Lett. **109**, 111807.
Aoyama, T., M. Hayakawa, T. Kinoshita, and M. Nio, 2014, arXiv:1412.8284.
Armstrong, T. R., and M. P. Fitzgerald, 2003, Phys. Rev. Lett. **91**, 201101.
Arnoult, O., F. Nez, L. Julien, and F. Biraben, 2010, Eur. Phys. J. D **60**, 243.
Arrington, J., 2015, J. Phys. Chem. Ref. Data **44**, 031203.
Arrington, J., and I. Sick, 2015, J. Phys. Chem. Ref. Data **44**, 031204.
ASD, 2015, "NIST Atomic Spectroscopy Database," http://pml.nist.gov/asd.
Audi, G., M. Wang, A. H. Wapstra, F. G. Kondev, M. MacCormick, X. Xu, and B. Pfeiffer, 2012, Chin. Phys. C **36**, 1287.
Azuma, Y., *et al.*, 2015, Metrologia **52**, 360.
Bagley, C. H., and G. G. Luther, 1997, Phys. Rev. Lett. **78**, 3047.
Baumann, H., F. Pythoud, D. Blas, S. Sibiryakov, A. Eichenberger, and E. E. Klingelé, 2015, Metrologia **52**, 635.
Beier, T., 2000, Phys. Rep. **339**, 79.
Beier, T., I. Lindgren, H. Persson, S. Salomonson, P. Sunnergren, H. Häffner, and N. Hermanspahn, 2000, Phys. Rev. A **62**, 032510.
Benayoun, M., P. David, L. DelBuono, and F. Jegerlehner, 2013, Eur. Phys. J. C **73**, 2453.
Bennett, G. W., *et al.*, 2006, Phys. Rev. D **73**, 072003.
Benz, S. P., A. Pollarolo, J. Qu, H. Rogalla, C. Urano, W. L. Tew, P. D. Dresselhaus, and D. R. White, 2011, Metrologia **48**, 142.
Berkeland, D. J., E. A. Hinds, and M. G. Boshier, 1995, Phys. Rev. Lett. **75**, 2470.
Bernauer, J. C., and M. O. Distler, 2016, arXiv:1606.02159v1.
Bernauer, J. C., *et al.*, 2014, Phys. Rev. C **90**, 015206.
Bich, W., 2013 (private communication).
BIPM, 2006, *International System of Units (SI)* (Bureau international des poids et mesures, Sèvres, France), 8th ed., supplement 2014: updates to the 8th edition (2006) of the SI Brochure.
Birge, R. T., 1929, Rev. Mod. Phys. **1**, 1.
Blaum, K., 2014 (private communication).
Blaum, K., *et al.*, 2009, J. Phys. B **42**, 154021.
Bouchendira, R., P. Cladé, S. Guellati-Khélifa, F. Nez, and F. Biraben, 2011, Phys. Rev. Lett. **106**, 080801.
Bourzeix, S., B. de Beauvoir, F. Nez, M. D. Plimmer, F. de Tomasi, L. Julien, F. Biraben, and D. N. Stacey, 1996, Phys. Rev. Lett. **76**, 384.
Breit, G., 1928, Nature (London) **122**, 649.
Carlson, C. E., 2015, Prog. Part. Nucl. Phys. **82**, 59.
Close, F. E., and H. Osborn, 1971, Phys. Lett. B **34**, 400.
Cohen, E. R., and B. N. Taylor, 1973, J. Phys. Chem. Ref. Data **2**, 663.
Cohen, E. R., and B. N. Taylor, 1987, Rev. Mod. Phys. **59**, 1121.
Colclough, A. R., T. J. Quinn, and T. R. D. Chandler, 1979, Proc. R. Soc. A **368**, 125.
Cox, M. G., C. Eiø, G. Mana, and F. Pennecchi, 2006, Metrologia **43**, S268.
Czarnecki, A., B. Krause, and W. J. Marciano, 1996, Phys. Rev. Lett. **76**, 3267.
Czarnecki, A., W. J. Marciano, and A. Vainshtein, 2003, Phys. Rev. D **67**, 073006; **73**, 119901(E) (2006).
Czarnecki, A., K. Melnikov, and A. Yelkhovsky, 2001, Phys. Rev. A **63**, 012509.
Davier, M., A. Hoecker, B. Malaescu, and Z. Zhang, 2011, Eur. Phys. J. C **71**, 1515; **72**, 1874(E) (2012).
Davier, M., and B. Malaescu, 2013, Eur. Phys. J. C **73**, 2597.
de Beauvoir, B., F. Nez, L. Julien, B. Cagnac, F. Biraben, D. Touahri, L. Hilico, O. Acef, A. Clairon, and J. J. Zondy, 1997, Phys. Rev. Lett. **78**, 440.
de Podesta, M., R. Underwood, G. Sutton, P. Morantz, P. Harris, D. F. Mark, F. M. Stuart, G. Vargha, and G. Machin, 2013, Metrologia **50**, 354.
de Podesta, M., I. Yang, D. F. Mark, R. Underwood, G. Sutton, and G. Machin, 2015, Metrologia **52**, S353.
Devoille, L., N. Feltin, B. Steck, B. Chenaud, S. Sassine, S. Djordevic, O. Séron, and F. Piquemal, 2012, Meas. Sci. Technol. **23**, 124011.
Diehl, C., K. Blaum, M. Höcker, J. Ketter, D. B. Pinegar, S. Streubel, and R. S. Van Dyck, Jr., 2011, Hyperfine Interact. **199**, 291.
DiSciacca, J., *et al.*, 2013, Phys. Rev. Lett. **110**, 130801.
Dorokhov, A. E., A. E. Radzhabov, and A. S. Zhevlakov, 2014a, JETP Lett. **100**, 133.
Dorokhov, A. E., A. E. Radzhabov, and A. S. Zhevlokov, 2014b, Int. J. Mod. Phys. Conf. Ser. **35**, 1460401.
Downie, E. J., 2014, EPJ Web Conf. **73**, 07005.
Eichenberger, A., H. Baumann, B. Jeanneret, B. Jeckelmann, P. Richard, and W. Beer, 2011, Metrologia **48**, 133.
Eides, M. I., 1996, Phys. Rev. A **53**, 2953.
Eides, M. I., 2015 (private communication).
Eides, M. I., and H. Grotch, 1997, Ann. Phys. (N.Y.) **260**, 191.
Eides, M. I., H. Grotch, and V. A. Shelyuto, 2001, Phys. Rep. **342**, 63.
Eides, M. I., H. Grotch, and V. A. Shelyuto, 2007, *Theory of Light Hydrogenic Bound States*, Springer Tracts in Modern Physics, Vol. 222 (Springer, Berlin).
Eides, M. I., and V. A. Shelyuto, 2004, Phys. Rev. A **70**, 022506.
Eides, M. I., and V. A. Shelyuto, 2007, Can. J. Phys. **85**, 509.
Eides, M. I., and V. A. Shelyuto, 2014, Phys. Rev. D **90**, 113002.
Eides, M. I., and V. A. Shelyuto, 2015, Phys. Rev. D **92**, 013010.
Erickson, G. W., 1977, J. Phys. Chem. Ref. Data **6**, 831.
Faustov, R., 1970, Phys. Lett. B **33**, 422.
Fellmuth, B., J. Fischer, C. Gaiser, O. Jusko, T. Priruenrom, W. Sabuga, and T. Zandt, 2011, Metrologia **48**, 382.
Gaiser, C., and B. Fellmuth, 2012, Metrologia **49**, L4.
Gaiser, C., T. Zandt, and B. Fellmuth, 2015, Metrologia **52**, S217.
Gaiser, C., T. Zandt, B. Fellmuth, J. Fischer, O. Jusko, and W. Sabuga, 2013, Metrologia **50**, L7.
Garbacz, P., K. Jackowski, W. Makulski, and R. E. Wasylishen, 2012, J. Phys. Chem. **116**, 11896.
Gasparian, A., 2014, EPJ Web Conf. **73**, 07006.
Gavioso, R. M., G. Benedetto, P. A. Giuliano Albo, D. Madonna Ripa, A. Merlone, C. Guianvarc'h, F. Moro, and R. Cuccaro, 2010, Metrologia **47**, 387.

RIGHTSLINK

Gavioso, R. M., D. Madonna Ripa, P. P. M. Steur, C. Gaiser, D. Truong, C. Guianvarc'h, P. Tarizzo, F. M. Stuart, and R. Dematteis, 2015, Metrologia **52**, S274.
Glazov, D. A., and V. M. Shabaev, 2002, Phys. Lett. A **297**, 408.
Gnendiger, C., D. Stöckinger, and H. Stöckinger-Kim, 2013, Phys. Rev. D **88**, 053005.
Godun, R. M., P. B. R. Nisbet-Jones, J. M. Jones, S. A. King, L. A. M. Johnson, H. S. Margolis, K. Szymaniec, S. N. Lea, K. Bongs, and P. Gill, 2014, Phys. Rev. Lett. **113**, 210801.
Goecke, T., C. S. Fischer, and R. Williams, 2013, Phys. Rev. D **87**, 034013.
Griffioen, K., C. Carlson, and S. Maddox, 2016, Phys. Rev. C **93**, 065207.
Grotch, H., 1970, Phys. Rev. Lett. **24**, 39.
Gundlach, J. H., and S. M. Merkowitz, 2000, Phys. Rev. Lett. **85**, 2869.
Gundlach, J. H., and S. M. Merkowitz, 2002 (private communication).
Hagiwara, K., R. Liao, A. D. Martin, D. Nomura, and T. Teubner, 2011, J. Phys. G **38**, 085003.
Hagley, E. W., and F. M. Pipkin, 1994, Phys. Rev. Lett. **72**, 1172.
Hanneke, D., S. Fogwell, and G. Gabrielse, 2008, Phys. Rev. Lett. **100**, 120801.
Higinbotham, W. D., A. A. Kabir, V. Lin, D. Meekins, B. Norum, and B. Sawatzky, 2016, Phys. Rev. C **93**, 055207.
Horbatsch, M., and E. A. Hessels, 2016, Phys. Rev. C **93**, 015204.
Hu, Z.-K., J.-Q. Guo, and J. Luo, 2005, Phys. Rev. D **71**, 127505.
Ishida, A., 2015, J. Phys. Chem. Ref. Data **44**, 031212.
Ivanov, V. G., S. G. Karshenboim, and R. N. Lee, 2009, Phys. Rev. A **79**, 012512.
Jackowski, K., 2015 (private communication).
Jackowski, K., M. Jaszuński, and M. Wilczek, 2010, J. Phys. Chem. A **114**, 2471.
Janssen, T. J. B. M., J. M. Williams, N. E. Fletcher, R. Goebel, A. Tzalenchuk, R. Yakimova, S. Lara-Avila, S. Kubatkin, and V. I. Fal'ko, 2012, Metrologia **49**, 294.
Jegerlehner, F., and A. Nyffeler, 2009, Phys. Rep. **477**, 1.
Jegerlehner, F., and R. Szafron, 2011, Eur. Phys. J. C **71**, 1632.
Jentschura, U. D., 2009, Phys. Rev. A **79**, 044501.
Jentschura, U. D., A. Czarnecki, K. Pachucki, and V. A. Yerokhin, 2006, Int. J. Mass Spectrom. **251**, 102.
Jentschura, U. D., S. Kotochigova, E.-O. Le Bigot, P. J. Mohr, and B. N. Taylor, 2005, Phys. Rev. Lett. **95**, 163003, http://pml.nist.gov/hdel.
Jentschura, U. D., A. Matveev, C. G. Parthey, J. Alnis, R. Pohl, T. Udem, N. Kolachevsky, and T. W. Hänsch, 2011, Phys. Rev. A **83**, 042505.
Karagioz, O. V., and V. P. Izmailov, 1996, Izmer. Tekh. **39**, 3 [Meas. Tech. **39**, 979 (1996)].
Karshenboim, S. G., 2000, Phys. Lett. A **266**, 380.
Karshenboim, S. G., 2014, Phys. Rev. D **90**, 053012.
Karshenboim, S. G., V. G. Ivanov, and V. M. Shabaev, 1999, Phys. Scr. **T80**, 491.
Karshenboim, S. G., V. G. Ivanov, and V. M. Shabaev, 2000, Zh. Eksp. Teor. Fiz. **117**, 67 [JETP **90**, 59 (2000)].
Karshenboim, S. G., V. G. Ivanov, and V. M. Shabaev, 2001a, Can. J. Phys. **79**, 81.
Karshenboim, S. G., V. G. Ivanov, and V. M. Shabaev, 2001b, Zh. Eksp. Teor. Fiz. **120**, 546 [JETP **93**, 477 (2001)].
Karshenboim, S. G., E. Y. Korzinin, V. A. Shelyuoto, and V. G. Ivanov, 2015, J. Phys. Chem. Ref. Data **44**, 031202.
Karshenboim, S. G., P. J. Mohr, and D. B. Newell, 2015, J. Phys. Chem. Ref. Data **44**, 031101.
Karshenboim, S. G., V. A. Shelyuto, and A. I. Vainshtein, 2008, Phys. Rev. D **78**, 065036.
Kibble, B. P., I. A. Robinson, and J. H. Belliss, 1990, Metrologia **27**, 173.
Kleinevoß, U., 2002, "Bestimmung der Newtonschen Gravitationskonstanten *G*," Ph.D. thesis, University of Wuppertal.
Kleinvoß, U., H. Meyer, H. Piel, and S. Hartmann, 2002 (private communication) (to be published).
Köhler, F., S. Sturm, A. Kracke, G. Werth, W. Quint, and K. Blaum, 2015, J. Phys. B **48**, 144032.
Korobov, V. I., L. Hilico, and J.-P. Karr, 2014, Phys. Rev. A **89**, 032511.
Kotochigova, S., 2006 (private communication).
Kraus, E., K. E. Mesick, A. White, R. Gilman, and S. Strauch, 2014, Phys. Rev. C **90**, 045206.
Kuramoto, N., Y. Azuma, H. Inaba, F.-L. Hong, and K. Fujii, 2015, IEEE Trans. Instrum. Meas. **64**, 1650.
Kuroda, K., 1995, Phys. Rev. Lett. **75**, 2796.
Kurz, A., T. Liu, P. Marquard, and M. Steinhauser, 2014a, Nucl. Phys. B **879**, 1.
Kurz, A., T. Liu, P. Marquard, and M. Steinhauser, 2014b, Phys. Lett. B **734**, 144.
Lan, S.-Y., P.-C. Kuan, B. Estey, D. English, J. M. Brown, M. A. Hohensee, and H. Müller, 2013, Science **339**, 554.
Lee, G., J. R. Arrington, and R. J. Hill, 2015, Phys. Rev. D **92**, 013013.
Lee, J.-Y., K. Marti, J. P. Severinghaus, K. Kawamura, H.-S. Yoo, J. B. Lee, and J. S. Kim, 2006, Geochim. Cosmochim. Acta **70**, 4507.
Lee, R. N., A. I. Milstein, I. S. Terekhov, and S. G. Karshenboim, 2005, Phys. Rev. A **71**, 052501.
Lees, J. P., *et al.*, 2012, Phys. Rev. D **86**, 032013.
Liard, J. O., C. A. Sanchez, B. M. Wood, A. D. Inglis, and R. J. Silliker, 2014, Metrologia **51**, S32.
Lin, H., X. J. Feng, K. A. Gillis, M. R. Moldover, J. T. Zhang, J. P. Sun, and Y. Y. Duan, 2013, Metrologia **50**, 417.
Liu, J., D. Sprecher, C. Jungen, W. Ubachs, and F. Merkt, 2010, J. Chem. Phys. **132**, 154301.
Liu, W., *et al.*, 1999, Phys. Rev. Lett. **82**, 711.
Logashenko, I., *et al.*, 2015, J. Phys. Chem. Ref. Data **44**, 031211.
Lorenz, I. T., U.-G. Meißner, H. W. Hammer, and Y.-B. Dong, 2015, Phys. Rev. D **91**, 014023.
Lundeen, S. R., and F. M. Pipkin, 1986, Metrologia **22**, 9.
Luo, J., Q. Liu, L.-C. Tu, C.-G. Shao, L.-X. Liu, S.-Q. Yang, Q. Li, and Y.-T. Zhang, 2009, Phys. Rev. Lett. **102**, 240801.
Luther, G. G., and W. R. Towler, 1982, Phys. Rev. Lett. **48**, 121.
Mana, G., *et al.*, 2015, J. Phys. Chem. Ref. Data **44**, 031209.
Mariam, F. G., 1981, "High Precision Measurement of the Muonium Ground State Hyperfine Interval and the Muon Magnetic Moment," Ph.D. thesis, Yale University.
Mariam, F. G., *et al.*, 1982, Phys. Rev. Lett. **49**, 993.
Marsman, A., M. Horbatsch, and E. A. Hessels, 2015a, J. Phys. Chem. Ref. Data **44**, 031207.
Marsman, A., M. Horbatsch, and E. A. Hessels, 2015b, Phys. Rev. A **91**, 062506.
Massa, E., C. P. Sasso, G. Mana, and C. Palmisano, 2015, J. Phys. Chem. Ref. Data **44**, 031208.
Matveev, A., *et al.*, 2013, Phys. Rev. Lett. **110**, 230801.
Melnikov, K., and A. Vainshtein, 2004, Phys. Rev. D **70**, 113006.
Mibe, T., 2011, Nucl. Phys. B, Proc. Suppl. **218**, 242.
Milton, M. J. T., R. Davis, and N. Fletcher, 2014, Metrologia **51**, R21.
Miyazaki, A., Y. Yamazaki, T. Suehara, T. Namba, S. Asai, T. Kobayashi, H. Saito, Y. Tatematsu, I. Ogawa, and T. Idehara, 2015, Prog. Theor. Exp. Phys. **2015**, 011C01.
Mizushima, S., N. Kuramoto, K. Ueda, and K. Fujii, 2015, IEEE Trans. Instrum. Meas. **64**, 1527.
Mohr, P. J., and B. N. Taylor, 2000, Rev. Mod. Phys. **72**, 351.
Mohr, P. J., and B. N. Taylor, 2005, Rev. Mod. Phys. **77**, 1.
Mohr, P. J., B. N. Taylor, and D. B. Newell, 2008a, Rev. Mod. Phys. **80**, 633.
Mohr, P. J., B. N. Taylor, and D. B. Newell, 2008b, J. Phys. Chem. Ref. Data **37**, 1187.
Mohr, P. J., B. N. Taylor, and D. B. Newell, 2012a, Rev. Mod. Phys. **84**, 1527.
Mohr, P. J., B. N. Taylor, and D. B. Newell, 2012b, J. Phys. Chem. Ref. Data **41**, 043109.
Moldover, M., 2015 (private communication).
Moldover, M. R., R. M. Gavioso, J. B. Mehl, L. Pitre, M. de Podesta, and J. T. Zhang, 2014, Metrologia **51**, R1.
Moldover, M. R., R. M. Gavioso, and D. B. Newell, 2015, Metrologia **52**, S376.
Moldover, M. R., J. P. M. Trusler, T. J. Edwards, J. B. Mehl, and R. S. Davis, 1988, J. Res. Natl. Bur. Stand. **93**, 85.
Mondéjar, J., J. H. Piclum, and A. Czarnecki, 2010, Phys. Rev. A **81**, 062511.
Mooser, A., H. Kracke, K. Blaum, S. A. Bräuninger, K. Franke, C. Leiteritz, W. Quint, C. C. Rodegheri, S. Ulmer, and J. Walz, 2013, Phys. Rev. Lett. **110**, 140405.
Mooser, A., S. Ulmer, K. Blaum, K. Franke, H. Kracke, C. Leiteritz, W. Quint, C. C. Rodegheri, C. Smorra, and J. Walz, 2014, Nature (London) **509**, 596.
Mooser, A., *et al.*, 2013, Phys. Lett. B **723**, 78.
Müller, H., 2015 (private communication).
Myers, E., 2015 (private communication).
Myers, E. G., A. Wagner, H. Kracke, and B. A. Wesson, 2015, Phys. Rev. Lett. **114**, 013003.
Nakamura, K., *et al.*, 2010, J. Phys. G **37**, 075021.
Narukawa, T., A. Hioki, N. Kuramoto, and K. Fujii, 2014, Metrologia **51**, 161.
Neronov, Y. I., 2015 (private communication).

RIGHTSLINK

Neronov, Y. I., and V. S. Aleksandrov, 2011, Pis'ma Zh. Eksp. Teor. Fiz. **94**, 452 [JETP Lett. **94**, 418 (2011)].
Neronov, Y. I., and N. N. Seregin, 2012, Zh. Eksp. Teor. Fiz. **115**, 777 [JETP **142**, 883 (2012)].
Neronov, Y. I., and N. N. Seregin, 2014, Metrologia **51**, 54.
Newman, R., M. Bantel, E. Berg, and W. Cross, 2014, Phil. Trans. R. Soc. A **372**, 20140025.
Newton, G., D. A. Andrews, and P. J. Unsworth, 1979, Phil. Trans. R. Soc. A **290**, 373.
Nomura, D., and T. Teubner, 2013, Nucl. Phys. B **867**, 236.
Nyffeler, A., 2009, Phys. Rev. D **79**, 073012.
Nyffeler, A., 2014, Int. J. Mod. Phys. Conf. Ser. **35**, 1460456.
Olive, K. A., *et al.* (Particle Data Group), 2014, Chin. Phys. C **38**, 090001.
Pachucki, K., A. Czarnecki, U. D. Jentschura, and V. A. Yerokhin, 2005, Phys. Rev. A **72**, 022108.
Pachucki, K., U. D. Jentschura, and V. A. Yerokhin, 2004, Phys. Rev. Lett. **93**, 150401; **94**, 229902(E) (2005).
Parks, H. V., and J. E. Faller, 2010, Phys. Rev. Lett. **105**, 110801.
Parks, H. V., and J. E. Faller, 2014, Phil. Trans. R. Soc. A **372**, 20140024.
Parthey, C. G., A. Matveev, J. Alnis, R. Pohl, T. Udem, U. D. Jentschura, N. Kolachevsky, and T. W. Hänsch, 2010, Phys. Rev. Lett. **104**, 233001.
Parthey, C. G., *et al.*, 2011, Phys. Rev. Lett. **107**, 203001.
Piszczatowski, K., M. Puchalski, J. Komasa, B. Jeziorski, and K. Szalewicz, 2015, Phys. Rev. Lett. **114**, 173004.
Pitre, L., 2015 (private communication).
Pitre, L., C. Guianvarc'h, F. Sparasci, A. Guillou, D. Truong, Y. Hermier, and M. E. Himbert, 2009, C.R. Phys. **10**, 835.
Pitre, L., L. Risegari, F. Sparasci, M. D. Plimmer, M. E. Himbert, and P. A. Giuliano Albo, 2015, Metrologia **52**, S263.
Pitre, L., F. Sparasci, D. Truong, A. Guillou, L. Risegari, and M. E. Himbert, 2011, Int. J. Thermophys. **32**, 1825.
Pohl, R., *et al.*, 2010, Nature (London) **466**, 213.
Prades, J., E. de Rafael, and A. Vainshtein, 2010, in *Lepton Dipole Moments*, edited by B. L. Roberts and W. J. Marciano, Advanced Series on Directions in High Energy Physics, Vol. 20 (World Scientific, Singapore), Chap. 9, pp. 303–317.
Pramann, A., K.-S. Lee, J. Noordmann, and O. Rienitz, 2015, Metrologia **52**, 800.
Prevedelli, M., L. Cacciapuoti, G. Rosi, F. Sorrentino, and G. M. Tino, 2014, Phil. Trans. R. Soc. A **372**, 20140030.
Puchalski, M., J. Komasa, and K. Pachucki, 2015, Phys. Rev. A **92**, 020501.
Qu, J., S. P. Benz, A. Pollarolo, H. Rogalla, W. L. Tew, R. White, and K. Zhou, 2015, Metrologia **52**, S242.
Quinn, T., H. Parks, C. Speake, and R. Davis, 2013, Phys. Rev. Lett. **111**, 101102; Phys. Rev. Lett.**113**, 039901(E) (2014).
Quinn, T., C. Speake, H. Parks, and R. Davis, 2014, Phil. Trans. R. Soc. A **372**, 20140032.
Quinn, T. J., 1989, Metrologia **26**, 69.
Quinn, T. J., 2001, Metrologia **38**, 89.
Quinn, T. J., C. C. Speake, S. J. Richman, R. S. Davis, and A. Picard, 2001, Phys. Rev. Lett. **87**, 111101.
Ribeiro-Palau, R., *et al.*, 2015, Nat. Nanotechnol. **10**, 965.
Robinson, I. A., 2012, Metrologia **49**, 113.
Rodegheri, C. C., K. Blaum, H. Kracke, S. Kreim, A. Mooser, W. Quint, S. Ulmer, and J. Walz, 2012, New J. Phys. **14**, 063011.
Rosi, G., F. Sorrentino, L. Cacciapuoti, M. Prevedelli, and G. M. Tino, 2014, Nature (London) **510**, 518.
Rothleitner, C., T. M. Niebauer, and O. Francis, 2014, Metrologia **51**, L9.
Rudziński, A., M. Puchalski, and K. Pachucki, 2009, J. Chem. Phys. **130**, 244102.
Sanchez, C. A., and B. M. Wood, 2014, Metrologia **51**, S42.
Sanchez, C. A., B. M. Wood, R. G. Green, J. O. Liard, and D. Inglis, 2014, Metrologia **51**, S5.
Sanchez, C. A., B. M. Wood, R. G. Green, J. O. Liard, and D. Inglis, 2015, Metrologia **52**, L23.
Sanchez, C. A., B. M. Wood, D. Inglis, and I. A. Robinson, 2013, IEEE Trans. Instrum. Meas. **62**, 1506.
Sano, Y., H. Wakita, and C.-W. Huang, 1986, Nature (London) **323**, 55.
Sapirstein, J. R., and D. R. Yennie, 1990, in *Quantum Electrodynamics*, edited by Kinoshita T. (World Scientific, Singapore), Chap. 12, pp. 560–672.
Schabinger, B., S. Sturm, A. Wagner, J. Alonso, W. Quint, G. Werth, and K. Blaum, 2012, Eur. Phys. J. D **66**, 71.
Scherer, H., and B. Camarota, 2012, Meas. Sci. Technol. **23**, 124010.
Schlamminger, S., D. Haddard, F. Seifert, L. S. Chao, D. B. Newell, R. Liu, R. L. Steiner, and J. R. Pratt, 2014, Metrologia **51**, S15.
Schlamminger, S., E. Holzschuh, W. Kündig, F. Nolting, R. E. Pixley, J. Schurr, and U. Straumann, 2006, Phys. Rev. D **74**, 082001.
Schlamminger, S., R. L. Steiner, D. Haddad, D. B. Newell, F. Seifert, L. S. Chao, R. Liu, E. R. Williams, and J. R. Pratt, 2015, Metrologia **52**, L5.
Schmidt, J. W., R. M. Gavioso, E. F. May, and M. R. Moldover, 2007, Phys. Rev. Lett. **98**, 254504.
Schwob, C., L. Jozefowski, B. de Beauvoir, L. Hilico, F. Nez, L. Julien, F. Biraben, O. Acef, and A. Clairon, 1999, Phys. Rev. Lett. **82**, 4960; Phys. Rev. Lett. **86**, 4193(E) (2001).
Shabaev, V. M., and V. A. Yerokhin, 2002, Phys. Rev. Lett. **88**, 091801.
Sick, I., 2008, in *Precision Physics of Simple Atoms and Molecules*, edited by Karshenboim S. G., Lecture Notes in Physics, Vol. 745 (Springer, Berlin/Heidelberg), pp. 57–77.
Sick, I., 2015, J. Phys. Chem. Ref. Data **44**, 031213.
Sprecher, D., J. Liu, C. Jungen, W. Ubachs, and F. Merkt, 2010, J. Chem. Phys. **133**, 111102.
Steele, A. G., J. Meija, C. A. Sanchez, L. Yang, B. M. Wood, R. E. Sturgeon, Z. Mester, and A. D. Inglis, 2012, Metrologia **49**, L8.
Steiner, R. L., E. R. Williams, R. Liu, and D. B. Newell, 2007, IEEE Trans. Instrum. Meas. **56**, 592.
Stock, M., P. Barat, R. S. Davis, A. Picard, and M. J. T. Milton, 2015, Metrologia **52**, 310.
Streubel, S., T. Eronen, M. Höcker, J. Ketter, M. Schuh, R. S. Van Dyck, Jr., and K. Blaum, 2014, Appl. Phys. B **114**, 137.
Sturm, S., 2015 (private communication).
Sturm, S., K. Blaum, B. Schabinger, A. Wagner, W. Quint, and G. Werth, 2010, J. Phys. B **43**, 074016.
Sturm, S., F. Köhler, J. Zatorski, A. Wagner, Z. Harman, G. Werth, W. Quint, C. H. Keitel, and K. Blaum, 2014, Nature (London) **506**, 467.
Sturm, S., F. Köhler, J. Zatorski, A. Wagner, Z. Harman, G. Werth, W. Quint, C. H. Keitel, and K. Blaum, 2015 (private communication).
Sturm, S., A. Wagner, M. Kretzschmar, W. Quint, G. Werth, and K. Blaum, 2013, Phys. Rev. A **87**, 030501.
Sturm, S., A. Wagner, B. Schabinger, and K. Blaum, 2011, Phys. Rev. Lett. **107**, 143003.
Sturm, S., A. Wagner, B. Schabinger, J. Zatorski, Z. Harman, W. Quint, G. Werth, C. H. Keitel, and K. Blaum, 2011, Phys. Rev. Lett. **107**, 023002.
Sutton, G., R. Underwood, L. Pitre, M. de Podesta, and S. Valkiers, 2010, Int. J. Thermophys. **31**, 1310.
Taylor, B. N., and P. J. Mohr, 2001, IEEE Trans. Instrum. Meas. **50**, 563.
Thomas, M., P. Espel, D. Ziane, P. Pinot, P. Juncar, F. Pereira Dos Santos, S. Merlet, F. Piquemal, and G. Genevès, 2015, Metrologia **52**, 433.
Tu, L.-C., Q. Li, Q.-L. Wang, C.-G. Shao, S.-Q. Yang, L.-X. Liu, Q. Liu, and J. Luo, 2010, Phys. Rev. D **82**, 022001.
Udem, T., 2014 (private communication).
Ulmar, S., K. Blaum, H. Kracke, A. Mooser, W. Quint, C. C. Rodegheri, and J. Walz, 2013, Nucl. Instrum. Methods Phys. Res., Sect. A **705**, 55.
Ulmer, S., K. Blaum, H. Kracke, A. Mooser, W. Quint, C. C. Rodegheri, and J. Walz, 2011, Phys. Rev. Lett. **107**, 103002.
Ulmer, S., C. Rodegheri, K. Blaum, H. Kracke, A. Mooser, W. Quint, and J. Walz, 2011, Phys. Rev. Lett. **106**, 253001.
Valkiers, S., D. Vendelbo, M. Berglund, and M. de Podesta, 2010, Int. J. Mass Spectrom. **291**, 41.
Van Dyck, R., Jr., 2015 (private communication).
Van Dyck, R. S., Jr., D. B. Pinegar, S. V. Liew, and S. L. Zafonte, 2006, Int. J. Mass Spectrom. **251**, 231.
Van Dyck, R. S., Jr., P. B. Schwinberg, and H. G. Dehmelt, 1987, Phys. Rev. Lett. **59**, 26.
Wang, M., G. Audi, A. H. Wapstra, F. G. Kondev, M. MacCormick, X. Xu, and B. Pfeiffer, 2012, Chin. Phys. C **36**, 1603.
Waseda, A., H. Fujimoto, X. W. Zhang, N. Kuramoto, and K. Fujii, 2015, IEEE Trans. Instrum. Meas. **64**, 1692.
Weitz, M., A. Huber, F. Schmidt-Kaler, D. Leibfried, W. Vassen, C. Zimmermann, K. Pachucki, T. W. Hänsch, L. Julien, and F. Biraben, 1995, Phys. Rev. A **52**, 2664.
Wicht, A., J. M. Hensley, E. Sarajlic, and S. Chu, 2002, Phys. Scr. **T102**, 82.
Williams, E. R., R. L. Steiner, D. B. Newell, and P. T. Olsen, 1998, Phys. Rev. Lett. **81**, 2404.
Wood, B., 2013 (private communication).
Xu, J., *et al.*, 2016, Metrologia **53**, 86.

RIGHTSLINK

Yang, I., L. Pitre, M. R. Moldover, J. Zhang, X. Feng, and J. S. Kim, 2015, Metrologia **52**, S394.
Yang, L., Z. Mester, R. E. Sturgeon, and J. Meija, 2012, Anal. Chem. **84**, 2321.
Yerokhin, V. A., A. N. Artemyev, V. M. Shabaev, and G. Plunien, 2005, Phys. Rev. A **72**, 052510.
Yerokhin, V. A., and Z. Harman, 2013, Phys. Rev. A **88**, 042502.
Yerokhin, V. A., P. Indelicato, and V. M. Shabaev, 2002, Phys. Rev. Lett. **89**, 143001.
Yerokhin, V. A., P. Indelicato, and V. M. Shabaev, 2004, Phys. Rev. A **69**, 052503.
Yerokhin, V. A., and U. D. Jentschura, 2008, Phys. Rev. Lett. **100**, 163001.
Yerokhin, V. A., and U. D. Jentschura, 2010, Phys. Rev. A **81**, 012502.
Zafonte, S. L., and R. S. Van Dyck, Jr., 2015, Metrologia **52**, 280.
Zhang, J. T., H. Lin, X. J. Feng, J. P. Sun, K. A. Gillis, M. R. Moldover, and Y. Y. Duan, 2011, Int. J. Thermophys. **32**, 1297.
Zhang, L., Y. Azuma, A. Kurokawa, N. Kuramoto, and K. Fujii, 2015, IEEE Trans. Instrum. Meas. **64**, 1509.

RIGHTSLINK